Bioconjugation Strategies Through Thiol-Alkylation of Peptides and Proteins

Kantner, Terrence

Award date:
2015

Awarding institution:
University of Bath

Bioconjugation Strategies Through Thiol-Alkylation of Peptides and Proteins

Terrence Kantner

A thesis submitted for the degree of Doctor of Philosophy
University of Bath
Department of Pharmacy and Pharmacology
June 2015

This research has been carried out under the supervision of
Dr. Andrew G. Watts

Signed
Date

Abstract

Bioconjugation chemistry generally refers to the covalent derivatisation of biomolecules. Derivatisation of cysteine's thiol of peptides and proteins is a common method in bioconjugation chemistry as the thiolate is an excellent nucleophile in aqueous conditions.

The propensity for thiols to oxidise in an aqueous environment necessitates the need for a disulfide reduction step prior to the addition of ligands derivatised with thiol alkylating linkers. Disulfide reducing agents such as tris(2-carboxyethyl)phosphine (TCEP) and tris(3-hydroxypropyl)phosphine (THPP) are disulfide reducing agents that are often marketed as being non-reactive with thiol alkylating reagents. The reaction of TCEP and THPP with thiol alkylation linkers was therefore investigated. Characterisation of reaction products and mechanistic studies revealed that TCEP and THPP both react with thiol alkylation reagents. A novel protocol was, therefore, developed utilising the Staudinger reaction to oxidise excess TCEP and THPP prior to the addition of thiol alkylating reagents. The protocol offers a simple "one-pot" method for effecting conjugate production *via* thiol alkylation, without the need for an intermediate purification step for the removal of excess disulfide reducing agents.

4-Vinyl pyridine (4-VP) derivatives were developed and explored as an alternative Michael acceptor class for thiol alkylation of peptides and proteins. The 4-VP derivatives exhibited high reactivity and specificity for thiol alkylation between pH = 7 and pH = 8. A selection of 4-VP linkers were subsequently functionalised with either carbohydrates or polyethylene glycol (PEG) and successfully utilised to produce peptide or protein conjugates *via* thiol alkylation reactions.

Acknowledgements

I would like to thank Dr. Andrew G. Watts for the opportunity to pursue research towards a PhD in his laboratory. I was provided with an environment to learn new techniques and mature as a scientist. I am also grateful for the freedom to explore research avenues which I deemed interesting during the PhD program. The University of Bath has been instrumental in making my PhD a possibility. I am very grateful for their funding through the University Research Scholarship (URS) program. I would also like to extend my appreciation for the support I received from our collaborator, Dr. Jean van den Elsen as well as my group members Dr. Ricardo Resende and Mr. Yi Yang.

Finally I would like to thank my family for all their support and encouragement to pursue my passion for science.

Table of Contents

List of Figures

List of Tables

List of Graphs

Abbreviations

Abbreviation : Full Description

α	Alpha
&	And
Å	Angstrom
B	Beta
°C	Degree Celsius
ε	Epsilon
δ	Delta
>	Greater than
<	Less than
4-VP	4-Vinyl pyridine
AcOH	Acetic acid
ADA	Adenosine deaminase
ADC	Antibody drug conjugate
amu	Atomic mass unit
Ar	Aromatic
Arg	Arginine
Asp	Aspartic acid
BC	B cell receptor
BIS-TRIS	Bis(2-hydroxyethyl)-amino-tris(hydroxymethyl)-methane
BME	β-mercaptoethanol
Boc	*tert*-Butyloxycarbonyl
br.	Broad
BSA	Bovine serum albumin
BST	Biotin switch technique
Bt-HPDP	Biotin-(N-[6-(biotinamido)hexyl]-3'-(2'-pyridyldithio)propionamide
C-18	Octadecyl carbon chain
CFP	Cyan fluorescent protein
cGK	Cyclic guanosine monophosphate-dependant kinase
cGMP	Cyclic guanosine monophosphate
cm	Centimetre
CRM_{197}	Cross reacting material-197
Cu	Copper
Cys	Cysteine
CysNO	S-nitrosocysteine
DBU	1,8-Diazabicyclo[5.4.0]undec-7-ene
DCM	Dichloromethane
dd	Doublet of doublets
DEANONOate	Diethylamine/nitric oxide complex sodium salt hydrate
DMF	Dimethyl formamide
DMSO	Dimethyl sulfoxide

DNA	Deoxyribonucleic acid
DTE	Dithioerythritol
DTT	Dithiothreitol
EDTA	Ethylenediaminetetraacetic acid
e.g.	*Exempli gratia*
e.q.	Equivalent
ELISA	Enzyme-linked immunosorbent assay
eNOS	Endothelial nitric oxide synthase
ESI-HRMS	Electrospray ionisation-high resolution mass spectrometry
EtOAc	Ethyl acetate
FDA	Federal Drug Administration
FRET	Förster resonance energy transfer
FT-IR	Fourier transform-infrared
g	Gram
Gd(III)	Gadolinium(III)
GalNAc	*N*-Acetylgalactosamine
GlcNAc	*N*-Acetylglucosamine
Glu	Glutamic acid
GSNO	S-nitrosoglutathione
GSK	GlaxoSmithKline
GTP	Guanosine triphosphate
HATU	1-[Bis(dimethylamino)methylene]-1*H*-1,2,3-triazolo [4,5-*b*]pyridinium 3-oxid hexafluorophosphate
HC2	Hybrid Capture 2
His	Histidine
HPLC	High performance liquid chromatography
HPV	Human papilloma virus
HRMS	High resolution mass spectrometry
HRP	Horseradish peroxidase
Hz	Hertz
IAM	Iodoacetamide
IgG	Immunoglobulin G
iNOS	Inducible nitric oxide synthase
IPA	Isopropyl alcohol
ISV	Ion source voltage
kDa	Kilo Dalton
KF	Potassium fluoride
KLH	Keyhole limpet hemocyanin
kV	Kilo volt
L	Levorotatory
Lys	Lysine
m	Multiplet
M	Molar
MALDI-MS	Matrix assisted laser desorption mass spectrometry
m-CPBA	*meta*-Chloroperbenzoic acid
mbar	Millibar

MDa	Mega Dalton
MeCN	Acetonitrile
MeOH	Methanol
mg	Milligram
MHC II	Major histocompatibility complex II
MHz	Mega Hertz
min.	Minute
mL	Millilitre
mm	Millimetre
mM	Millimolar
mmol	Millimole
MMTS	Methyl methanethiosulfate
mol	Mole
MOPS	3-(N-morpholino)propanesulfonic acid
MRI	Magnetic Resonance Imaging
m/z	Mass-to-charge ratio
N	Asparagine
N-	Nitrogen linked
ng	Nanogram
NEM	N-Ethyl maleimide
nm	Nanometre
NMR	Nuclear magnetic resonance
nNOS	Neuronal nitric oxide synthase
NO	Nitric oxide
NOS	Nitric oxide synthase
O-	Oxygen linked
PD-10	Polydextran 10 kilo Dalton cut-off
PDE	Phosphodiesterase
PEG	Polyethylene glycol
pH	$-\log[H^+]$
PET	Positron emission tomography
Pet. ether	Petroleum ether
Ph	Phenyl
pKa	$-\log K_a$
Pn6B	Pneumococcal serotype 6B
PTM	Post translational modification
q	Quartet
R	*Rectus*
$t_{1/2}$	Half-life
TFA	Trifluoroacetic acid
RNA	Ribonucleic acid
RP	Reverse phase
RSNO	Nitrosated thiol derivative
R.T.	Room temperature
s	Seconds
s	Singlet

S	*Sinister*
S/T	Serine/Threonine
Sbi	*Staphylococcus* binder of immunoglobulins
SDS	Sodium dodecyl sulphate
SEB	*Staphylococcus enterotoxin* B
sGC	Soluble guanylyl cyclase
sLe^a	Sialyl Lewis a
SLe^x	Sialyl Lewis x
SNO-alb	S-nitroso albumin
SNO-RAC	S-nitroso-resin assisted capture
SNO-SID	S-nitroso-site identification
sTn	Sialyl-Thomsen-nouvelle
t	Triplet
$t_{1/2}$	Time required for 50 % consumption of substrate
TACA's	Tumor associated carbohydrate antigens
TBP	Tributylphosphine
T cell	Thymus cell
TCEP	Tris(2-carboxyethyl)phosphine
TFA	Trifluoroacetic acid
THF	Tetrahydrofuran
THPP	Tris(3-hydroxypropyl)phosphine
TLC	Thin layer chromatography
Tris	Tris(hydroxymethyl)aminomethane
S→N	Sulfur to nitrogen transfer
SDS-PAGE	Sodium dodecyl sulphate polyacrylamide gel electrophoresis
µL	Microlitre
µM	Micromolar
US	United States
V	Volts
vs	Versus
v/v	Volume/Volume
w/w	Weight/Weight
YFP	Yellow fluorescent protein

Chapter 1: Introduction

1.0) History and Development of Bioconjugation Chemistry

The early application of chemistry for the modification of proteins relied mostly on empirical evidence, with a minimal understanding of the chemistry behind the outcomes. An example was the use of formaldehyde in the tanning industry. Formaldehyde was utilised for the hardening of leather products, which was due to the cross-linking of proteins and at the time was not clearly understood [1]. The early use of formalin to convert toxic proteins into non-toxic (toxoid) products was also not clearly understood but was essential for the progress of vaccination experiments [1]. The formalin-treated toxoid protein products retained much of their antigenic determinants and provided a safer method for inoculating patients. It was during the 1920's when formalin induced toxoid variants of diphtheria toxin were developed for immunisation studies and is a method still utilised for the production of toxoid protein products [2]. Over the following two decades more detailed research was conducted into characterising the chemistry of modification of proteins by chemical reagents, which culminated in an review by Olcott and Fraenkel-Conrat in 1947 [3]. The accumulated evidence over this period provided the foundations for chemical techniques utilised to modify proteins today.

The evolution of protein modification chemistry has been accelerated by the accumulating evidence that the vast majority of eukaryotic proteins undergo some form of chemical modification after ribosomal synthesis. The protein modifications are generally achieved through hydrolytic cleavage by proteases or the attachment of a ligand to the side chain of an amino acid [4]. These modifications are termed post-translational modifications (PTM) and may be transient or permanent alterations to the protein's structure. The chemical alteration of the protein, which is usually a specific modification is regulated by enzymes and serves to impart specific physiological and/or functional properties to the protein: including the

protein's structure, function, stability and cellular localisation. PTM's of proteins include glycosylation, phosphorylation, nitrosation, acylation, methylation and ubiquitylation amongst many others and are essential for diverse biological processes (**Figure 1.1**). The ability of biological processes to specifically modify biomolecules such as proteins to impart a particular physiological and/or functional property is an idea that has sparked much scientific interest in replicating or inventing new methods for the chemical modification of biomolecules, which has resulted in the flourishing field of bioconjugate chemistry.

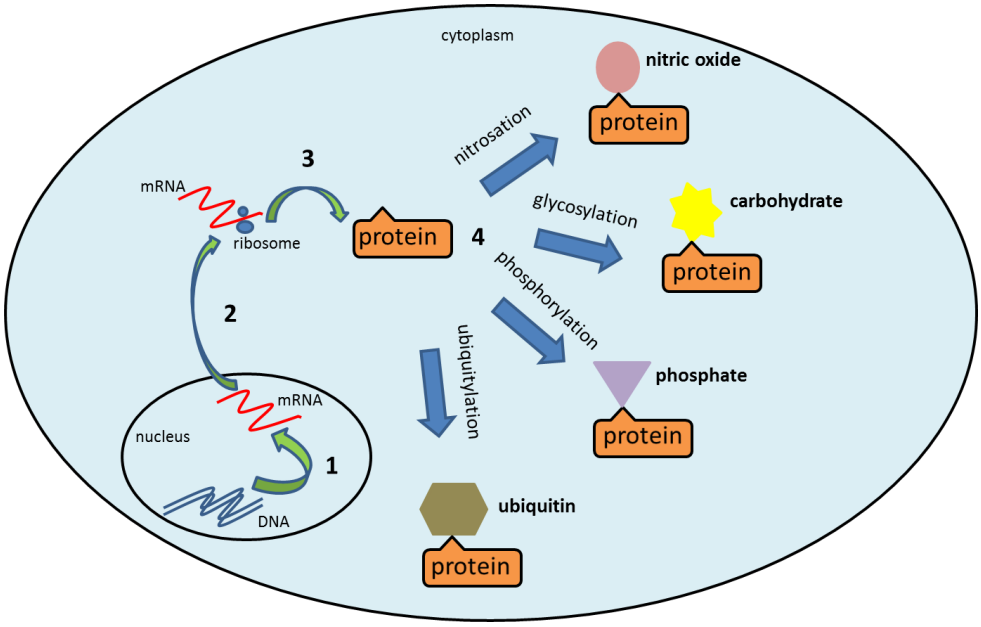

Figure 1.1: Illustration of a number of potential protein PTMs which can affect the localisation and function of a protein.

Bioconjugate chemistry involves the covalent attachment of appropriate ligands functionalised with suitable linker functional groups to biomolecules such as proteins. The linker functional group which is attached to the ligand is usually chosen to effect a chemoselective and stable chemical reaction with the biomolecule. Linkers are chosen with respect to the type of functional group targeted on the biomolecule (**Figure 1.2**). Linker derivatised ligands may be synthetic or biological and vary from polyethylene glycol (PEG) [5], nanoparticles [6], carbohydrates [7], fluorescent probes [8], peptides [9], proteins [10], RNA [11] and DNA [12]. The biomolecule may be a peptide, protein, RNA or DNA. The

development of specialised chemical coupling methods to achieve site-specific, covalent modifications has had major contributions in areas such as diagnostics, imaging, drug delivery, drug stability and biopharmaceutical production such as antibody drug conjugates (ADC's) and conjugate vaccines [13-16].

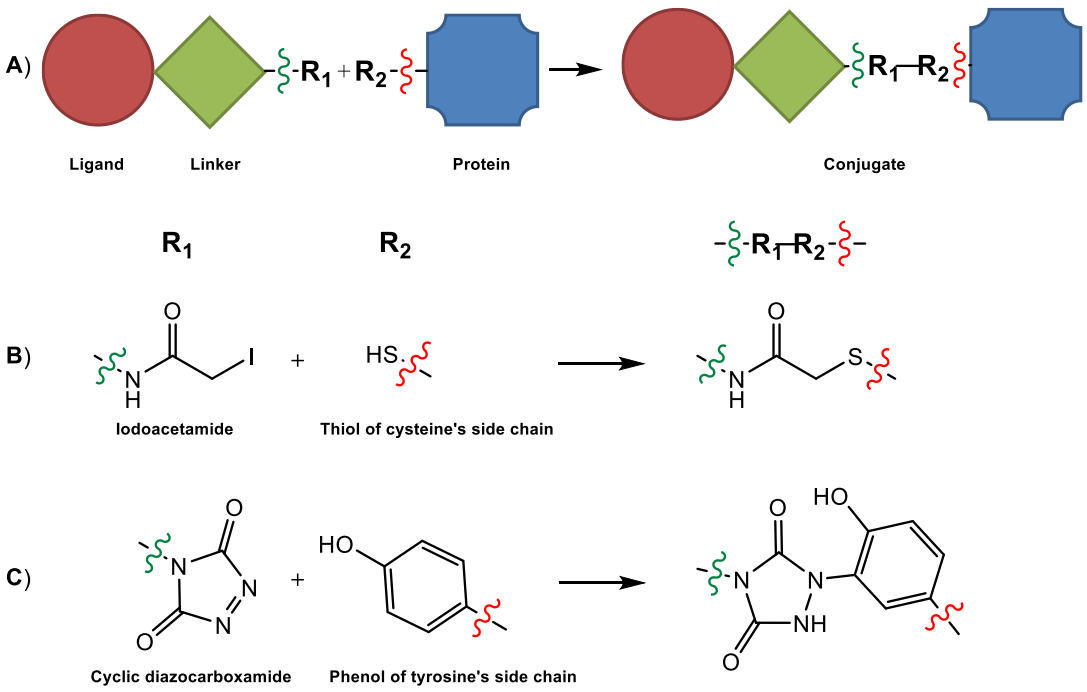

Figure 1.2: **A**) Ligands can be derivatised with a variety of linkers to effect a chemoselective linkage on biomolecules. **B**) An iodoacetamide functionalised ligand can react selectively with a thiol functional group [17, 18]. **C**) A cyclic diazocarboxamide can be used to selectively functionalise the phenol ring of tyrosine [19].

1.1) Applications of Bioconjugation Chemistry

1.1.1) Diagnostics and Imaging

The physiological concentration of most biomolecules such as DNA, RNA and proteins are often only present in μM levels in cells. The low concentration of most biomolecules *in vivo*, therefore, requires highly sensitive diagnostic tools to ensure detection in assays. A biodiagnostic often utilises bioconjugate chemistry to generate products that are able to improve screening and detection of low abundance analytes present in a heterogeneous sample. An example of such a biodiagnostic tool is the covalent attachment of a ligand with high affinity (e.g., biotin) for an affinity matrix (e.g. streptavidin) to a biomolecular probe (e.g. antibody) which exhibits specific binding potential to an analyte in a sample (**Figure 1.3**) [20]. Incubation of the bioconjugate in a complex sample solution results in the binding of the biomolecular probe to a specific analyte. The bound analyte is enriched for detection by the elution of the sample solution through an affinity matrix, specific for binding the affinity tag to which the probe and analyte are attached (**Figure 1.3**). This principle has been utilised to develop a microfluidic immunosensor for the detection of the food-borne pathogen *Staphylococcus enterotoxin* B (SEB) [21] as well as the enzyme-linked immunosorbent assay (ELISA). ELISA is an analytical assay that is utilised for the detection and quantification of peptides, proteins, antibodies and hormones, which are often present at low concentrations [22].

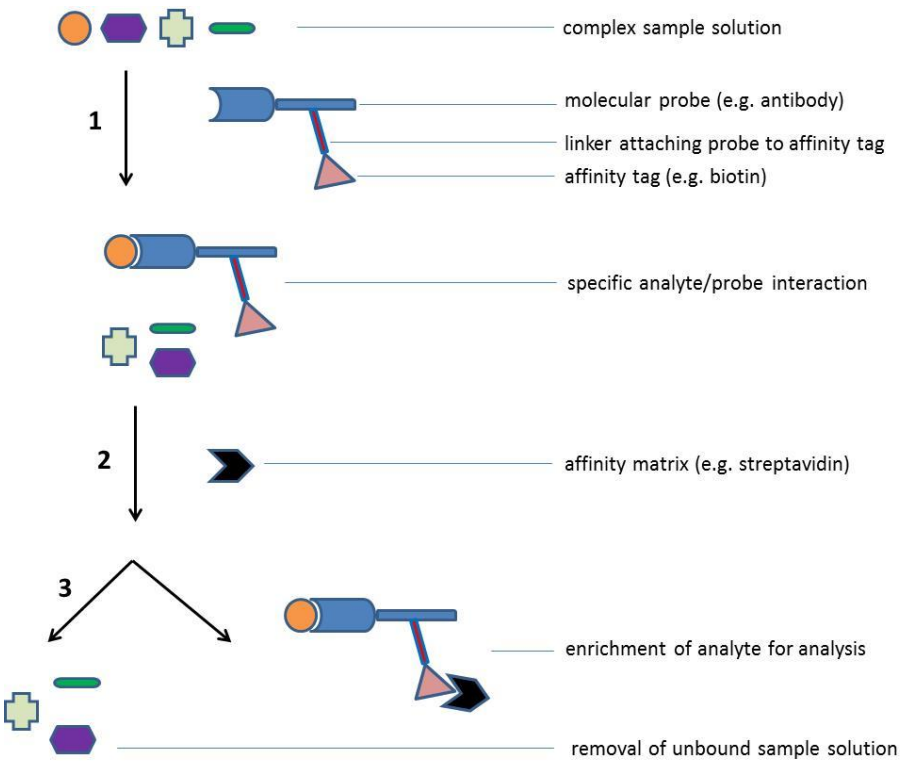

Figure 1.3: Bioconjugates comprised of molecular probes and affinity tags are useful tools for enriching a sample for specific analyte detection. **1**) Incubation of the conjugate with a sample results in specific analyte-conjugate complex formation. **2**) Incubation with an affinity matrix "captures" the conjugate-analyte complex. **3**) A washing step removes all unbound compounds from the affinity matrix.

An example of a Federal Drug Administration (FDA) approved biodiagnostic is the Hybrid Capture 2 (HC2) assay for the diagnosis of 5 low-risk and 13 high-risk Human Papilloma virus (HPV) types (**Figure 1.4**) [23]. The HC2 assay utilises an RNA probe to bind complementary DNA sequences in a sample that originate from the HPV virus. The RNA/DNA hybrids are subsequently captured by a RNA/DNA hybrid-specific antibody that is usually coated on a microtitre plate. After a washing procedure to remove the unbound analytes from the sample, a second RNA/DNA-specific antibody is added, which has been synthetically conjugated to an alkaline phosphatase enzyme. A chemiluminescent substrate for the alkaline phosphatase enzyme is subsequently added as a method to indirectly confirm the presence of HPV DNA in the sample (**Figure 1.4**) [23, 24].

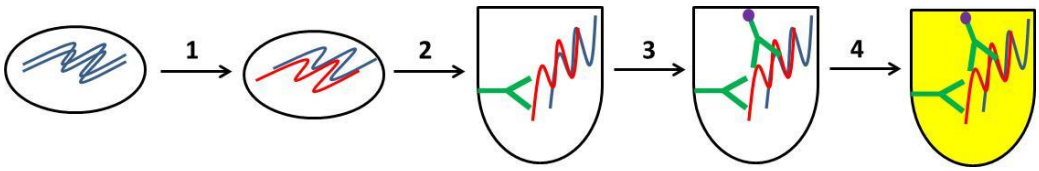

Figure 1.4: Illustration of the HC2 assay for detection of HPV DNA. **1**) Denature DNA in sample and hybridise HPV DNA with complementary RNA probe. **2**) Capture of DNA/RNA by antibody attached to microtitre plate. **3**) A second RNA/DNA hybrid-specific antibody is added that is conjugated to the enzyme alkaline phosphatase. **4**) A chemiluminescent substrate for alkaline phosphatase is added. Substrate consumption results in the emission of light, which provides indirect evidence for the presence of HPV DNA.

In some cases sample preparation for imaging or diagnosis is not possible and analysis needs to be performed *in vivo* using techniques such as magnetic resonance imaging (MRI) and positron emission tomography (PET). MRI is a non-invasive method for the internal imaging of an organism by detecting radiofrequencies emitted by excited hydrogen nuclei (**Figure 1.5**, **A**). Relaxation rates of these excited nuclei vary according to their location which allows tissue differentiation during image construction (**Figure 1.5**, **A**). The use of contrast agents in MRI such as Gd(III) greatly improves the sensitivity of the technique. Contrast agents such as Gd(III) function by increasing the relaxation rate of water protons in the surrounding tissue due to their paramagnetic properties [25]. The covalent attachment of contrast agents to molecular probes such as antibodies enhances the *in vivo* targeting of the contrast agents to specific areas of disease requiring evaluation [26].

PET imaging is a technique utilised to produce internal images of patients by using radiopharmaceuticals (**Figure 1.5**, **B**). PET imaging reagents are compounds that have been functionalised with a positron-emitting radionuclide. Positron emitters are neutron deficient and achieve stability by transmutation of a proton to a neutron with subsequent emission of a neutrino and a positron. The positron undergoes annihilation through contact with an electron to emit gamma rays that can be detected to generate an internal image of the patient (**Figure 1.5**, **B**) [27]. Positron emitters such as ^{18}F are currently incorporated into compounds such as

deoxyglucose and administered to the patient. The radioactive drug enters the circulatory system and is subsequently metabolised and incorporated into various tissues within the body which can then be imaged. Radionuclides used usually have very short half-lives (^{18}F = 109.8 minutes), therefore the synthesis of the radiopharmaceutical needs to be rapid and followed by immediate administration and detection procedures. Improved imaging can be achieved by the conjugation of the radionuclide to antibodies to improve targeting [28].

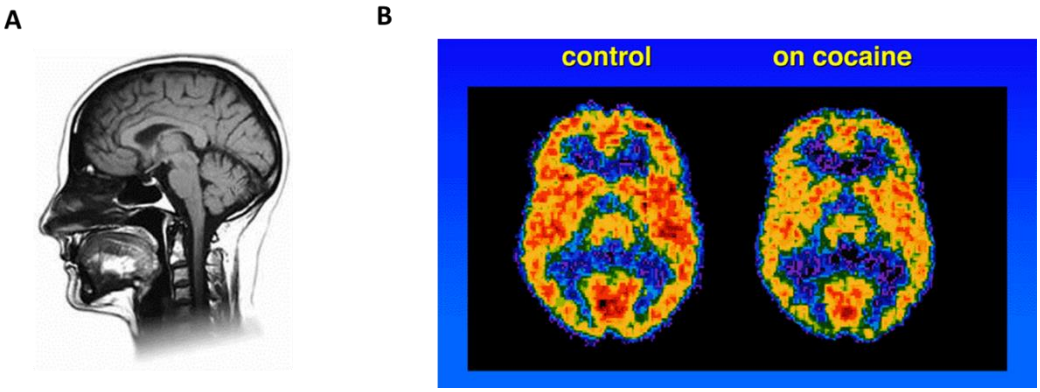

Figure 1.5: Images generated using MRI and PET imaging techniques. **A**) MRI image of a human head. Taken from [29]. **B**) PET image of a human brain. Taken from [30].

Bioconjugate techniques have also been developed for the structural characterisation of protein, DNA and RNA, as well as investigating biomolecular interactions (**Figure 1.6**). Förster resonance energy transfer (FRET) is a technique that utilises a pair of fluorescent molecules that are covalently attached to different locations of the biomolecule. A donor fluorophore transfers energy to an acceptor fluorophore, which subsequently emits radiation at a characteristic emission frequency. FRET experiments can serve as a nanoscale ruler, where distances between the fluorophores can be determined. A variety of fluorophores have been developed for this area of research including synthetic fluorophores, quantum dots and fluorescent proteins [31-33].

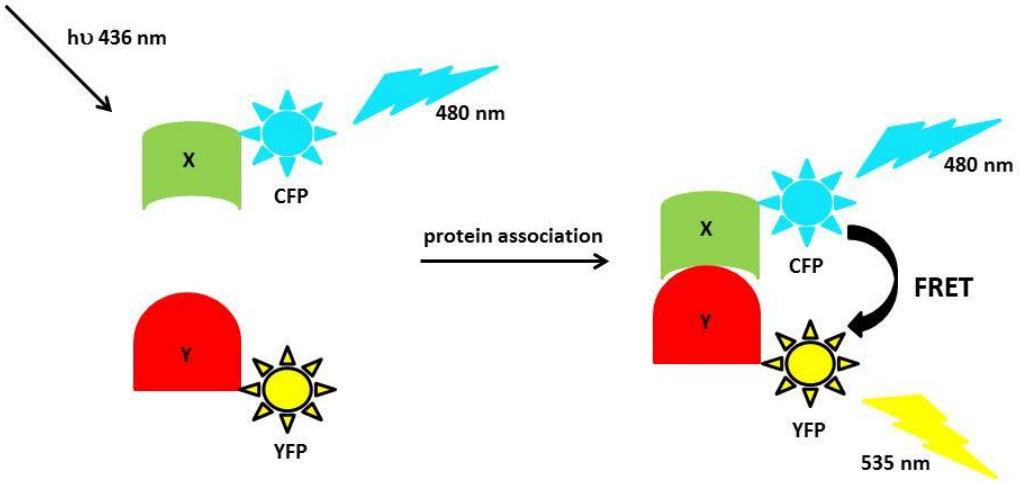

Figure 1.6: FRET imaging to detect protein-protein interactions. The association of protein x-cyan fluorescent protein (CFP) conjugate with protein Y-yellow fluorescent protein (YFP) conjugate results in a transfer of energy from CFP to YFP, resulting in a FRET emission at 535 nm [34].

1.1.2) PEGylation

PEGylation, first developed by Abuchowski *et al.* refers to the covalent attachment of one or more polyethylene glycol (PEG) chains (**Figure 1.7, A**) to a biomolecule or particle surface (**Figure 1.7**, **B**) [35, 36]. PEGylation with respect to biopharmaceutical manufacture often offers many advantages over non-PEGylated products. PEG is hydrophilic, non-immunogenic, available as linear or branched derivatives, available as a variety of molecular weights and is FDA approved [37]. PEGylation imparts a number of improved pharmacodynamics and pharmacokinetic properties to the derivatised biomolecule. It improves solubility, hinders proteolytic degradation, improves circulatory half-life and improves stability of the biomolecule. In 1990 Adagen® became the first FDA approved PEGylated biopharmaceutical to appear on the market. Adagen® is a PEGylated form of the enzyme adenosine deaminase (ADA). ADA is responsible for the conversion of deoxyadenosine from DNA breakdown and is toxic to leucocytes to non-toxic deoxyinosine. ADA deficiency, therefore, results in the toxic build-up of deoxyadenosine resulting in a diminished lymphocyte population and greater susceptibility to infection [29]. Administration of Adagen® provides patients with adenosine deaminase to ensure clearance of deoxyadenosine. PEGylation of ADA

improves the half-life of the enzyme's circulation from 2.8 hours to 50 hours, which offers the advantage of a reduced dosing regime [38].

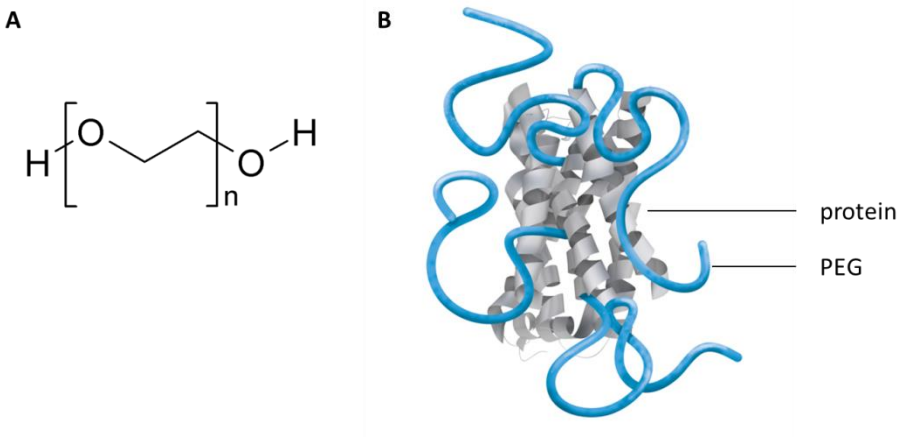

Figure 1.7: PEGylation of proteins offers improved stability and longer circulation times *in vivo.* **A**) Repeat unit of a PEG chain. **B**) Illustration of a PEGylated protein.

1.1.3) Glycosylation

Glycosylation of proteins is a common post translational modification performed in eukaryotic cells. It is an enzyme mediated process occurring in the endoplasmic reticulum (ER) and Golgi apparatus of cells, whereby oligosaccharides are covalently attached to the side chains of ether asparagine (N-linked) or serine/threonine (O-linked), as shown in (**Figure 1.8**) [39]. Glycosylation of proteins has been implicated in aiding protein folding, protein trafficking, ligand recognition, protein stabilisation, regulation of serum half-life and regulation of proteins biological activity [40]. It is, therefore, often crucial that protein based therapeutics are glycosylated to potentiate the functional activity and stability of the drug. Eukaryotic expression systems have the necessary cellular machinery to glycosylate proteins and can be used for large scale production of glycosylated protein-based therapeutics [39]. There are, however, a few problems associated with the utilisation of eukaryotic expression systems to glycosylate proteins, including the introduction of non-human glycoforms and batchwise variation in glycoform production [39]. Chemical conjugation of synthetic oligosaccharides to the protein is an alternative approach

for the production of glycosylated protein-based therapeutics. Reductive amination is the most common technique to achieve chemical coupling of carbohydrates to proteins [41]. The chemical attachment of carbohydrates to proteins is utilised in the production of carbohydrate based cancer vaccines [42] and conjugate vaccines towards pathogens [43].

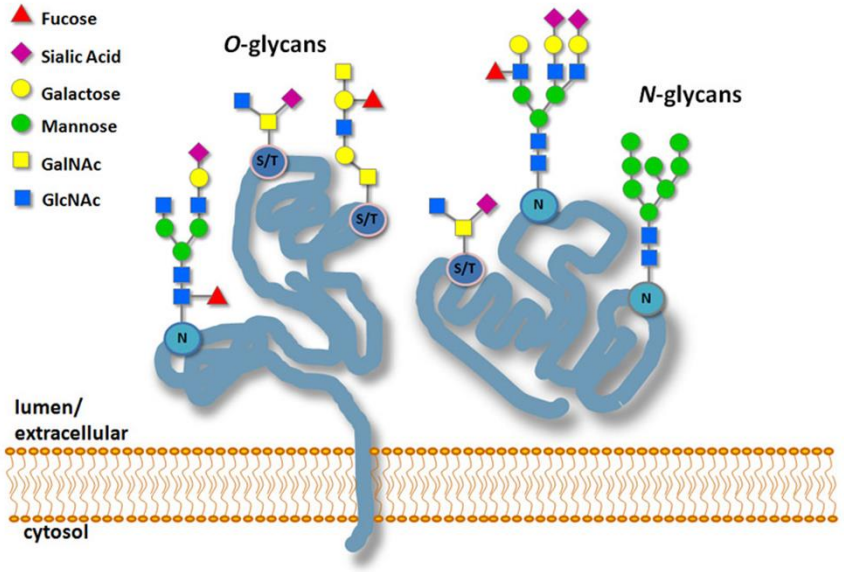

Figure 1.8: Illustration of O and N-linked oligosaccharides attached to a protein. Taken from [44].

1.1.4) Biotherapeutics

Biotherapeutics are medicinal products that are manufactured utilising biological sources. Numerous biotherapeutics have been developed which also require bioconjugation chemistry during production. An example is antibody drug conjugates (ADC's), which are generated through the covalent attachment of cytotoxic drugs to antibodies for the treatment of cancer (**Figure 1.9**). The highly selective delivery of the cytotoxic drug by the antibody offers the potential of improved efficacy and tolerability of the treatment. A number of factors contribute to the effectiveness of the ADC. The antibody should possess selectivity for antigens expressed on tumor cells, the linker chemistry and payload should not affect the activity of the antibody and the linker should be stable during circulation and only release the cytotoxic payload at the targeted site. ADC's have been produced with

cleavable (hydrazone, disulfide and peptide-based) and non-cleavable (thioether) linkers [14]. Both strategies rely on tumor localisation, internalisation and lysosomal processing to release the payload to effect cell death. The first FDA approved ADC was in 2000 for Mylotarg®, towards treatment for acute myeloid leukaemia. It was voluntarily removed from the U.S. market in 2010 due to its unacceptable toxicity. This was largely attributed to the labile hydrazone linkage coupling the antibody to the cytotoxic payload [14, 45]. This proved a valuable lesson regarding the manufacture of stable ADC's. In 2013 the FDA approved Kadcyla™, an ADC for the treatment of metastatic breast cancer. The projected annual sales for this particular ADC are in the region of US$ 2-5 billion per anum [46].

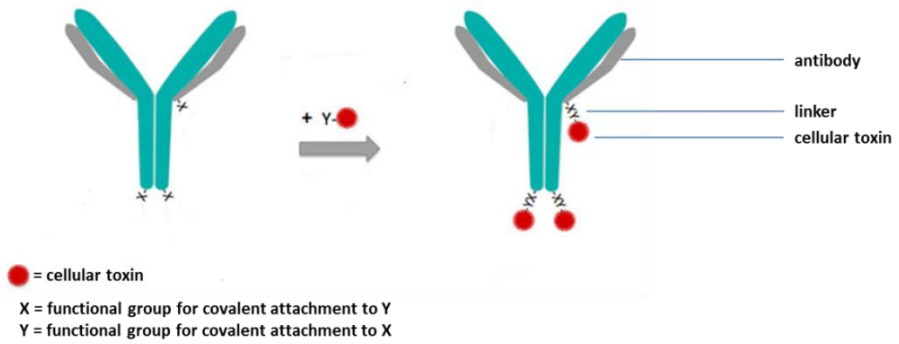

Figure 1.9: Representation of an ADC. An ADC is produced by the covalent attachment of a cellular toxin to an antibody. Adapted from [47].

1.1.5) Vaccines

A vaccine is a prophylactic formulation that consists of antigen derived from a pathogen or an epitope specific to an unhealthy cell such as a tumor cell. Administration of the vaccine enables the immune system to generate long-lived memory cells and plasma cells, capable of producing protective antibodies against the antigenic material (**Figure 1.10**). Priming the immune system with antigen enables a rapid and specific immune response to either the development of the epitope-expressing tumor cell or the infection by the antigen-expressing pathogen.

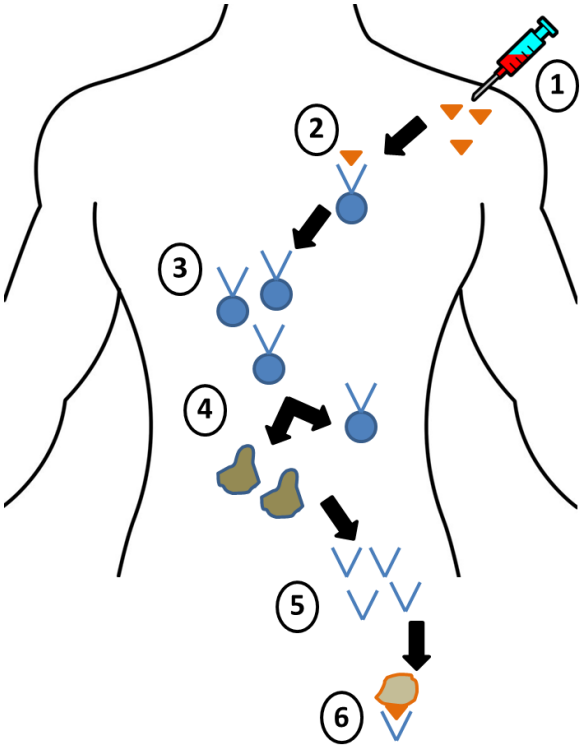

Figure 1.10: Illustration of how a vaccine functions. **1**) Vaccination with a formulation containing antigen from a pathogen, **2**) Recognition of antigen by a specific B-lymphocyte population, **3**) Proliferation of the B-lymphocyte population specific for antigen recognition, **4**) Maturation of B-lymphocytes to memory cells and antibody producing plasma cells, **5**) Plasma cells produce antibodies specific for antigen binding, **6**) Antibodies bind to pathogen-specific antigen to effect clearance from the host. Adapted from [48].

The identification and characterisation of tumor-associated antigens provides specific targets for cancer vaccine design (**Figure 1.11**). Carbohydrate-based cancer vaccines are a potential class of prophylactics requiring the use of bioconjugate techniques. Many tumor cells have been identified to express cancer-specific carbohydrate epitopes on the cell surface. Research has characterised many of these tumor associated carbohydrate antigens (TACA's), particularly in breast cancer, where the overexpression sLe^a, sLe^x and sTn epitopes (**Figure 1.11**) are indicative of tumor progression [49]. Priming the immune system with a vaccine formulated from TACA's offers could result in the clearance of any developing TACA expressing carcinoma cells.

Carbohydrates, however, are poorly immunogenic and lead to a T-cell independent immune response. T-cell participation in an immune response is necessary for the development of long-lived plasma cells which are capable of generating antigen specific antibodies [50]. A T-cell independent immune response implies only transient protection to antigenic epitopes. An effective strategy to generate long-lived memory to antigens is *via* covalent coupling of the TACA's to antigenic carrier proteins. The glycoprotein conjugates are engulfed by B-cells and hydrolysed into smaller glycopeptide fragments. The glycopeptides are presented to T-helper cells, which subsequently produce cytokines that promote the maturation of B-cells into antibody producing plasma cells capable of targeting the carcinogenic epitopes [51]. An example of a carbohydrate-based vaccine is Theratope® (Biomira Inc.). Theratope® is a vaccine produced by the covalent attachment of the breast cancer associated sTn antigen to the carrier protein keyhole limpet hemocyanin (KLH). Theratope® initially showed promising results in phase 1 and phase 2 clinical trials for the treatment of breast cancer. The much anticipated phase 3 trials however, were disappointing. Although high antigen-specific antibody titres were detected, there was no significant difference in median survival time between treatment and control groups [52, 53].

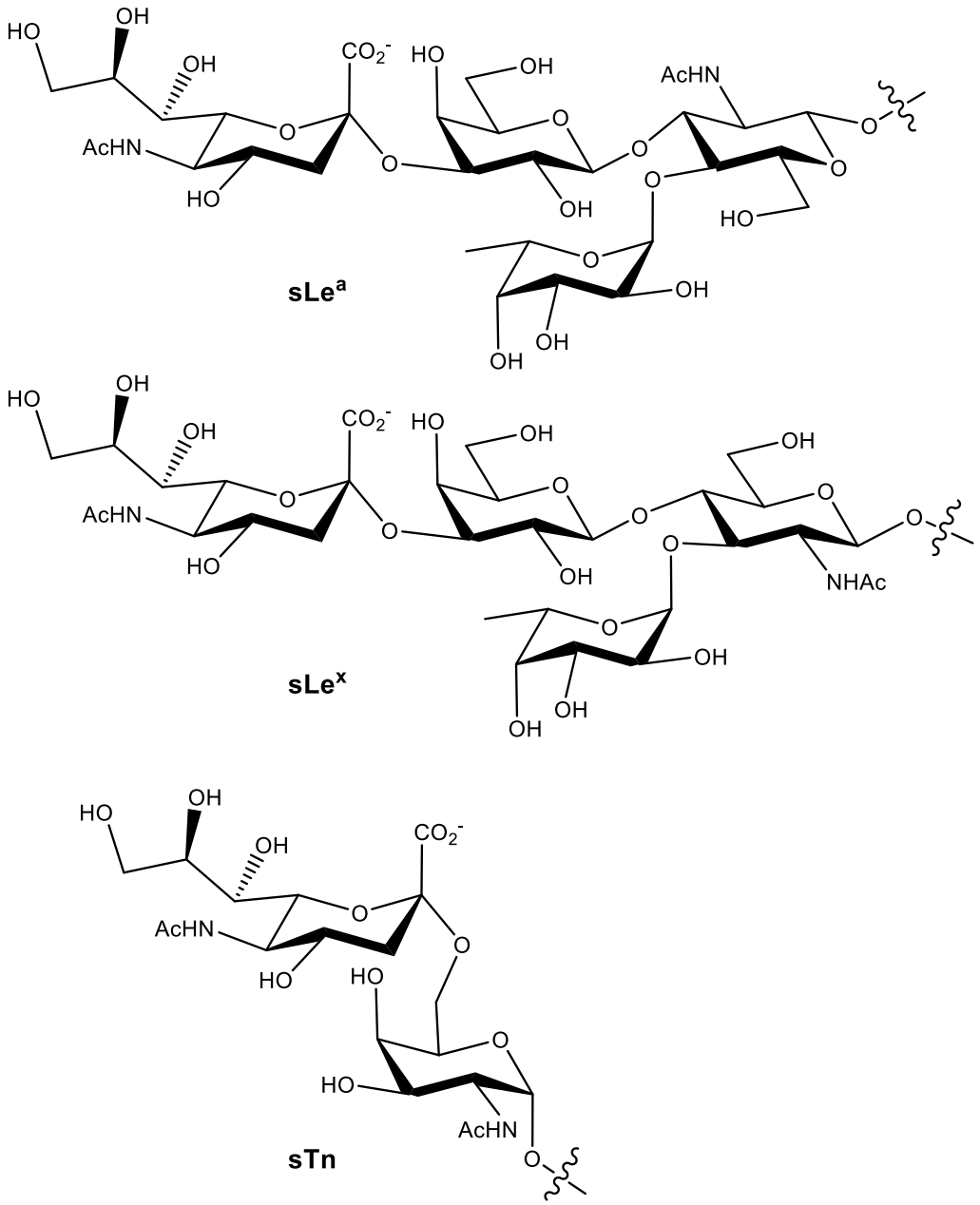

Figure 1.11: Structures of the cancer-associated glycans, sLe^a, sLe^x and sTn.

The conjugation of pathogen associated carbohydrates to antigenic carrier proteins has proven successful in the development of conjugate vaccines towards *Neisseria meningitis* (Menactra® and Menveo®), *Streptococcus pneumonia* (Synflorix® and Prevnar-13®) and *Haemophilus influenza* type B (Hiberix® and ActHIB®). The above mentioned pathogens are often epidemic in developing countries with infants, elderly and immunocompromised individuals being the most susceptible to infection. Conjugate vaccines are manufactured through the covalent attachment

of pre-purified oligosaccharides derived from the cellular membranes of the most virulent pathogen strains to antigenic carrier proteins such as toxoid diphtheria and tetanus protein and antigenic outer membrane proteins [54]. The conjugate vaccines induce a T cell dependant immune response, which results in long term protection and memory to the administered pathogen derived carbohydrate-based epitopes [55, 56].

1.2) Chemical Linkages used in Bioconjugation

A variety of linkages have been explored to effect bioconjugation between an appropriate ligand and a biomolecule.

1.2.1) Amide Bond Conjugation

Bioconjugation through the generation of an amide bond is a common and useful strategy due to the stability of the amide bond at neutral pH. The amide bond is usually generated between an amine-containing molecule and a reagent possessing an activated ester. Targeting amine-containing amino acids on peptides and proteins to generate bioconjugates *via* amide bond formation can generate heterogeneous products due to the general abundance of primary and secondary amines present in the amino acid sequence. Amide bond formation can occur at the side chain of lysine amino acids, the amine present on the amino acid at the N-terminus of the of the peptide/protein sequence and the imidazole side chain of histidine that may be present in the amino acid sequence. The multiple sites for potential amide bond formation can complicate purification protocols and increase the cost of the conjugate production.

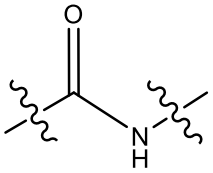

amide bond

Native chemical ligation offers another route to amide bond generation between peptide and proteins [57] and has been utilised for the site specific attachment of fluorescent molecules to proteins (**Figure 1.12**) [58]. The thiol of a terminal cysteine-containing peptide is reacted with a thioester-containing peptide in a trans-thioesterification reaction. A subsequent S→N acyl transfer generates an amide bond (**Figure 1.12**). Native chemical ligation method, however, also generates a free thiol functional group after amide bond formation. The presence of a thiol may be advantageous, offering an additional functional group for subsequent bioconjugation reactions. The presence of a thiol may also be disadvantageous as it could offer a site for unwanted side reactions and dimerisation of the bioconjugate by disulfide bond formation. Chemical desulfurisation offers a solution to the problem if the peptide or protein does not contain addition cysteine residues necessary for its structure or function [59].

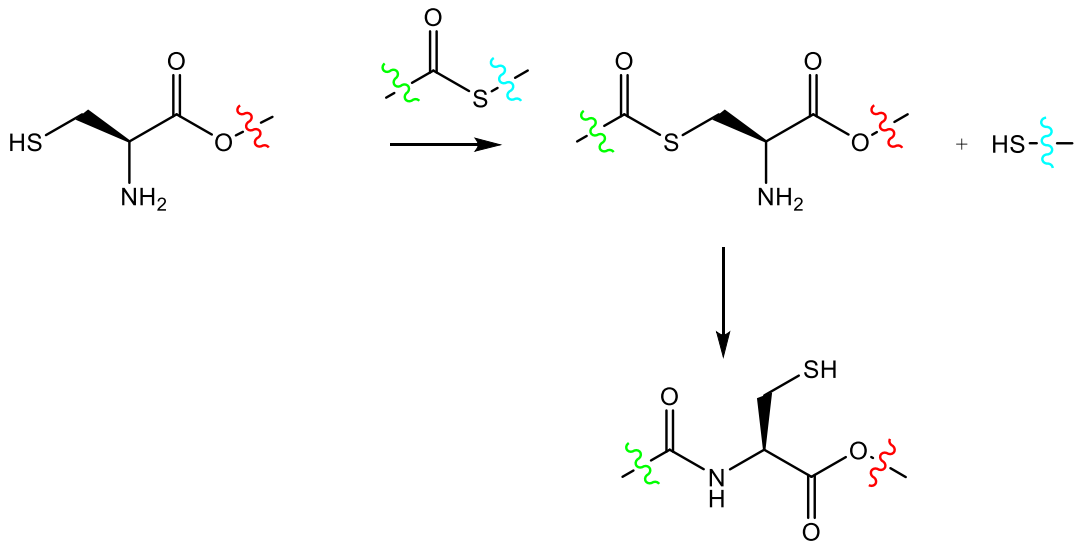

Figure 1.12: Amide bond formation using the native chemical ligation method.

Staudinger ligation offers an alternative route to generating bioconjugates *via* amide bond formation. Staudinger ligation is based on the original Staudinger reaction where an azide is reduced to the amine through the use of a phosphine [60]. The Staudinger ligation method of amide bond formation is achieved by conjugating a ligand derivatised with an azide functional group to a second ligand

containing a phosphine functional group and an acyl donor, which is necessary for the amide bond generation [61]. Staudinger ligation can been used to generate both non-traceless (presence of a phosphine oxide derivative in the product, **Figure 1.13, A**) and traceless (absence of phosphine oxide derivative in the product, **Figure 1.13, B**) bioconjugates. Staudinger ligation has been previously utilised to introduce glycans onto cell surfaces [61, 62]. Staudinger ligation provides an opportunity for a very specific reaction to produce homogenous bioconjugates that can simplify purification and characterisation of the products. A potential disadvantage of this method is the incorporation of non-natural azide-containing amino acids or carbohydrates into the cellular structure.

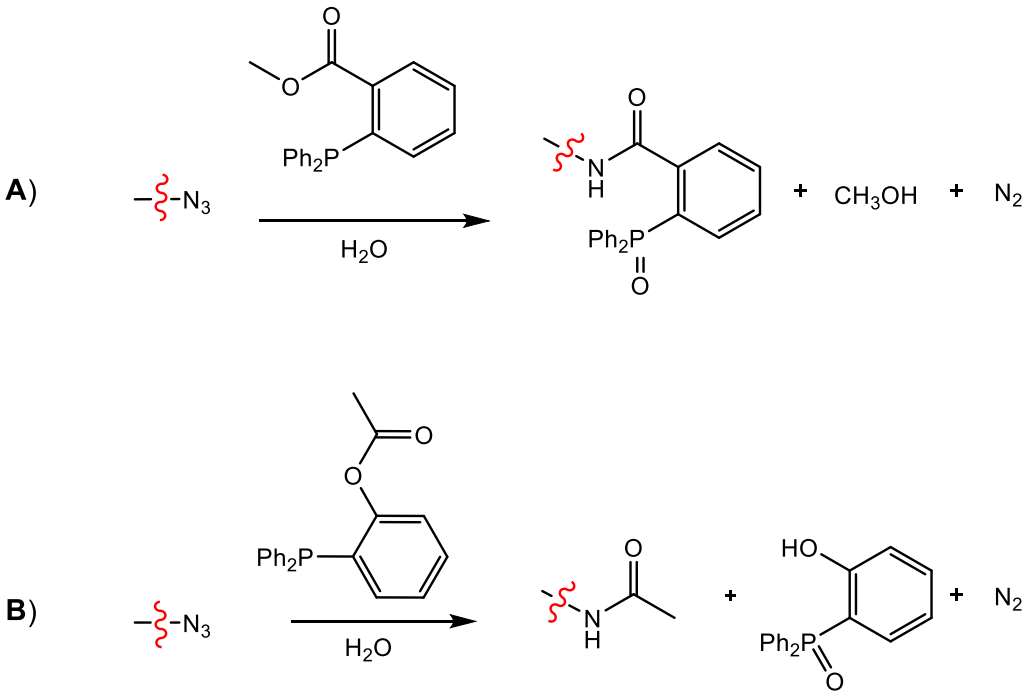

Figure 1.13: (**A**) Non-traceless Staudinger ligation and (**B**) Traceless Staudinger ligation to generate amide bonds. Adapted from [63].

1.2.2) C-N Double Bond Conjugation

The generation of a carbon-nitrogen double bond can be achieved in an aqueous environment which is attractive for bioconjugation chemistry. The linkage is generated by reaction of an amine with either an aldehyde or ketone functional group to generate an imine bond. The reaction is reversible, rendering the bond fairly labile. The imine is can be reduced to render a more stable linkage and is a strategy that has been utilised to link carbohydrates to proteins [64].

Hydrazone (C=N-N) and oxime (C=N-O) linkages can be generated by the reaction of hydrazine or alkoxyamine functional groups with an aldehyde or ketone functional group. Hydrazones and oximes are more stable than imine linkages but are also prone to hydrolysis. They have, however, found applicability in bioconjugation chemistry, especially were long term stability is not a concerning priority. Hydrazone and oxime linkages have been utilised to attach peptides to glass slides to generate microarrays for the detection of antibodies in blood samples and cell-adhesion assays [65, 66].

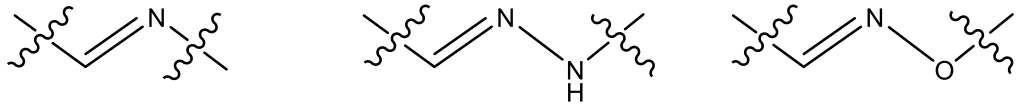

imine bond **hydrazone bond** **oxime bond**

1.2.3) Linkages by Cycloaddition

The Cu(I) accelerated Huisgen azide-alkyne 1,3-dipolar cycloaddition (“click”) reaction to generate a stable 1,4-disubstituted(1,2,3)triazole linkage has become a very useful reaction to generate bioconjugates (**Figure 1.14, A**). The click reaction is a versatile, reaction, tolerant to a wide range of temperatures, a variety of solvents, a wide pH range and often purified by simple product filtration [67]. The azide and alkyne functional groups are unreactive to most functional groups, which aids in the production of homogenous conjugates. The triazole linkage is water soluble and rigid, which minimises interaction of the connected ligands, minimising aggregation

and any potential reaction between the two ligands. The presence Cu(I) can be cytotoxic which can limit the use of click chemistry *in vivo* [63]. Catalyst free click reactions are, however, possible with the use of a ring strained alkyne such as cyclooctyne (**Figure 1.14, B**). The click reaction has been utilised in a diverse range of bioconjugations including labelling of peptides, proteins and DNA [68].

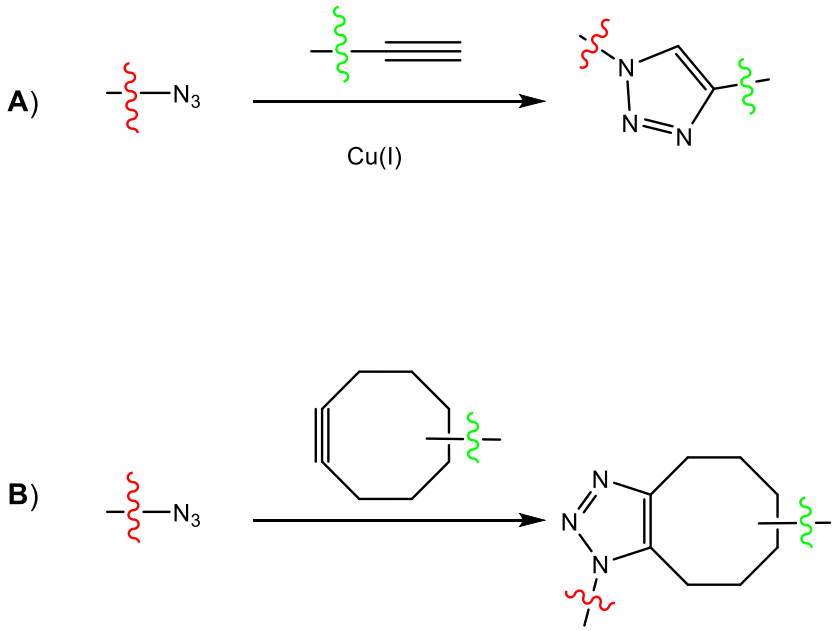

Figure 1.14: (**A**) Cu(I)-catalysed Huisgen 1,3-dipolar azide-alkyne cycloaddition and (**B**) strain-induced Huisgen 1,3-dipolar azide-alkyne cycloaddition.

The Diels-Alder reaction between a diene and a dienophile is an alternative cycloaddition reaction utilised in bioconjugation chemistry. Diene derivatised peptides have been successfully immobilised onto dienophile functionalised glass slides for peptide chip production [69]. Diene derivatised proteins have also been functionalised with a dienophile functionalised carbohydrates [70].

1.2.4) Thioether Linkages

The thiol functional group is naturally present in peptides and proteins as the terminal functional group of cysteine's side chain. The hydrogen bonding interactions within a protein can greatly affect the pKa of the thiol, with a range of 4-10 reported [71]. Deprotonation of the thiol generates a thiolate, which is an excellent nucleophile for thioether bond formation. Generally, cysteine accounts for 3 % of a proteins constitution [72]. The low thiol abundance provides a possibility of producing a small number of bioconjugate derivatives, which can simplify purification protocols and decrease production costs of the bioconjugate.

There are some important considerations to address before performing bioconjugations based on thioether formation. Thiols are important functional groups in the mechanism of catalysis for enzymes such as cysteine proteases [73]. Covalent modification of the thiol at the catalytic site may affect the activity of bioconjugate. Thiol functional groups also exist in peptides and proteins as disulfide bonds. Disulfide bonds play an important role in the tertiary structure, and hence, function of the peptide or protein [74]. If thiols are not available for bioconjugation due to their functional roles within the peptide or protein, it is possible to biochemically or chemically introduce thiol functional groups. Site directed mutagenesis is a biochemical method for the introduction of a cysteine residue into a protein [75]. Synthetic methods are also possible through functionalisation of a pre-existing amino acid residue to display a thiol. Cystamine (**Figure 1.15 A**, **1.3**) is utilised to introduce a thiol (existing as a disulfide) through derivatisation of carboxylic acids (**Figure 1.15 A**) or phosphates. As an example, a general carboxylic acid is initially reacted with a water soluble carbodiimide **1.1** to yield an activated ester **1.2**. The intermediate is then incubated with cystamine (**1.3**), which yields a urea by-product **1.4** and a disulfide derivative **1.5**. Incubation of derivative **1.5** with a thiol-containing biomolecule can generate a mixed disulfide product. The disulfide bond of **1.5** can also be reduced to access the thiol functional group for conjugation to a biomolecule derivatised with a thiol-alkylating reagent.

The ε-amino group of lysine may also be derivatised to display a thiol functional group through the use of 2-iminothiolane (**1.6**, **Figure 1.15 B**) [76, 77].

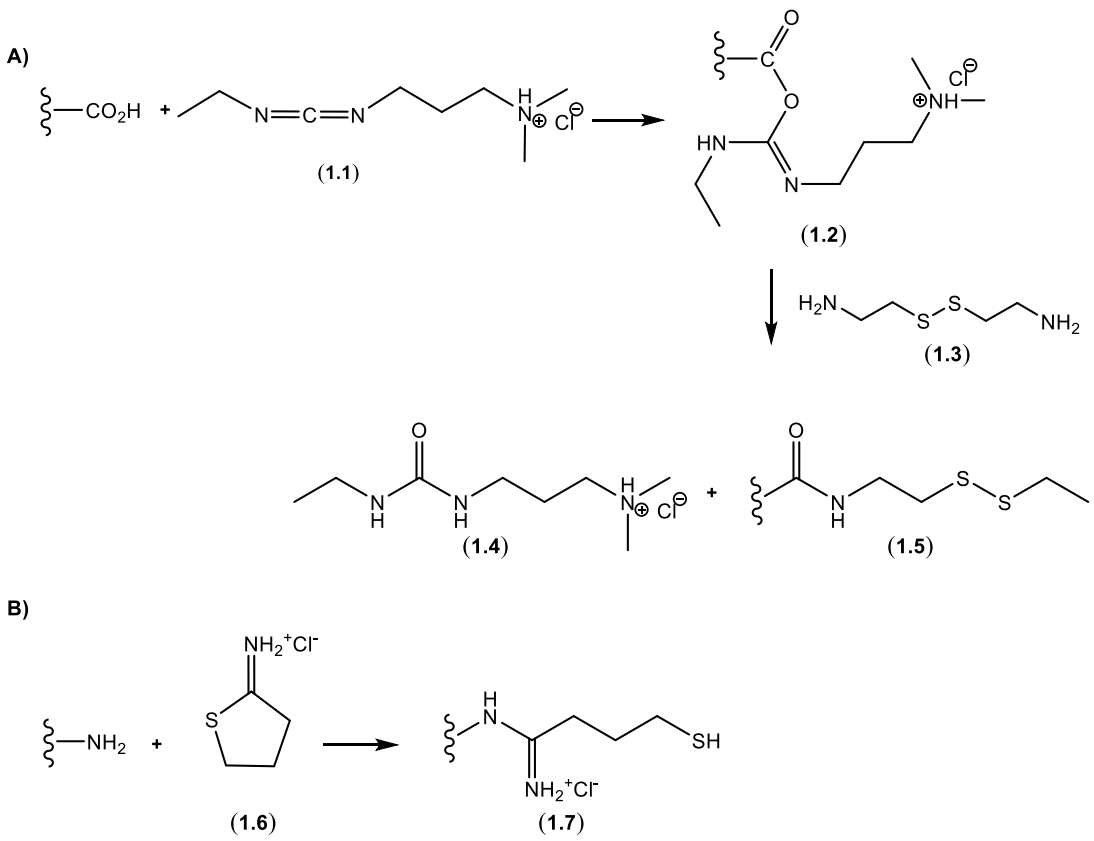

Figure 1.15: Functionalisation of amino acid side chains to introduce a thiol functional group. **A**) Introduction of a thiol *via* derivatisation of a carboxylic acid. **B**) Introduction of a thiol *via* derivatisation of a primary amine.

The attachment of ligands to thiols on peptides or proteins is often performed under aqueous conditions. There is a tendency for free thiols under aqueous conditions to oxidise and form disulfide bonds. A prerequisite regarding conjugations utilising the thiol functional group is the necessary step of pre-reduction of disulfide bonds to thiol functional groups. A number of reducing agents have been developed for the reduction of disulfides under aqueous conditions and are either alkyl-thiols or trialkylphosphines [18]. Alkyl-thiol reducing agents need to be removed from the solution prior to bioconjugation reactions since the thiol-based reducing agents have the capacity to compete with the thiols present on the peptide or protein for the thiol-reactive ligands. Reducing agent

removal requires rapid and efficient protocols by dialysis or gel filtration chromatography, under oxygen depleted conditions to avoid re-oxidation of the thiols to disulfide bonds. The process of removing the excess reducing agent can contribute significantly to reducing the yield of bioconjugation reactions.

Commercial sources for the trialkylphosphine-based disulfide reducing agent tris(2-carboxyethyl)phosphine (TCEP) report that TCEP does not need to be removed from solution after the disulfide reduction step and prior to the addition of thiol-selective modification reagents [78, 79]. The potential to leave the trialkylphosphine in solution and subsequently add a thiol-alkylating reagent offers a simple "one-pot" protocol to generate conjugates, while minimising the exposure of the thiols to oxidative conditions during a reducing agent removal step. There is, however, some reports claiming that TCEP does react with thiol alkylating reagents and can reduce conjugate yields if not removed post disulfide reduction [8, 80].

Post disulfide reduction, a ligand derivatised with a thiol-alkylating linker is generally added to effect a conjugation reaction. There are a variety of reagents currently available that will alkylate a thiol functional group rapidly and fairly selectively, though each reagent possesses individual strengths and limitations.

1.2.4.1) α-Halocarbonyls

Alkyl halides based on iodoacetic acid or iodoacetamide (**Figure 1.16**) are often used for the alkylation of sulfhydryls [18, 81]. α-Halocarbonyls are fairly unstable compounds that require careful storage and are also light sensitive. α-Halocarbonyls irreversibly alkylate thiols through a nucleophilic substitution reaction, which is optimal at alkaline pH, where the thiolate is an excellent nucleophile towards the alkyl halide [18]. The α-halocarbonyls may also react, in a pH dependant manner, with the hydroxyl group of tyrosine, the ε-amino group of lysine, the imidazole group of histidine and the N terminus of proteins. Generally, the thiolate on the cysteine side chain reacts much faster with the α-halocarbonyl than the functional groups of tyrosine, lysine and imidazole [18]. The alkylating

reagent is often required in high concentration to ensure sufficient conjugation which may promote the non-specific modification of other amino acid functional groups. The alkaline conditions necessary for optimal alkylation may also be detrimental to the stability of the protein.

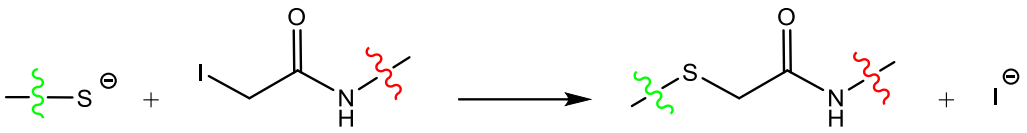

Figure 1.16: Thiol alkylation *via* an iodoacetamide derivative.

1.2.4.2) Michael Acceptors

Maleimide is by far the most common reagent used for thiol alkylation of a cysteine residue. Ligands can be functionalised with maleimide using a maleimido-N-hydroxysuccinimide ester. Maleimide-based alkylation is achieved through the conjugate addition of the thiolate at the activated alkene of the maleimide ring and results in a diastereomeric mixture of thioether derivatives (**Figure 1.17**). This may be problematic in terms of meeting potential purity standards in some therapeutic applications [82]. Maleimide is specific for thiols between pH = 6.5 and pH = 7.5 and at pH = 7 is 1000 more reactive towards thiols than amines [83]. Reactions with amines are more prevalent at a pH greater than 7 [18]. Maleimide is about 20 fold more reactive than iodoacetic acid or iodoacetamide derivatives and also has membrane permeability capacity [18]. The alkylation can be followed spectrophotometrically at 300 nm, with conjugation resulting in the disappearance of double bond absorbance [18, 83].

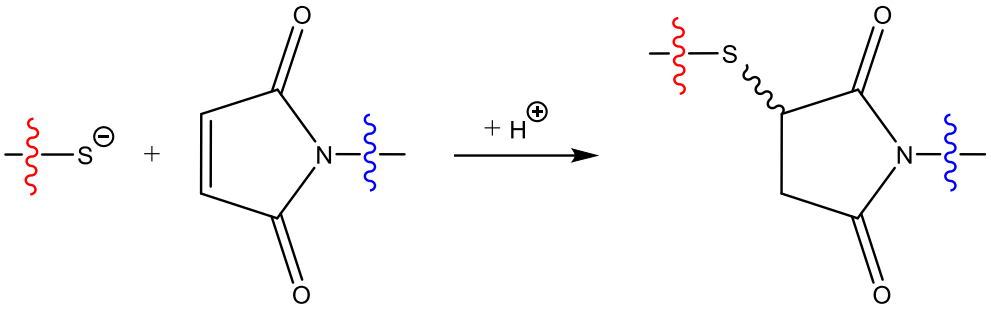

Figure 1.17: Thiol alkylation *via* a maleimide derivative.

Maleimide derivatives are fairly stable at or below pH = 6. At pH = 7, they exhibit a half-life of 45 hours yet at pH = 9 it decreases to less than 1 hour [18]. The shortened stability is attributed to the hydrolysis of the maleimide ring to yield maleamic acid (**Figure 1.18**, **A**). A similar ring opening reaction may occur to a thiol-maleimide adduct, which may be unfavourable when producing therapeutics requiring prolonged storage in an aqueous environment. The alkene of maleimide is highly electrophilic and is susceptible to nucleophilic attack from amines. This is a major disadvantage when considering the potential purification complexity. At alkaline pH the maleimide addition products can undergo transamidation reactions to form a cyclic compound, which can complicate product purification and characterisation (**Figure 1.18**, **B**) [18]. There is the added potential of hydrolysis of the maleimide-thioconjugate to regenerate the free thiol (**Figure 1.18**, **C**). The limitations of the maleimide functional group must be considered before being utilised for the production of conjugates.

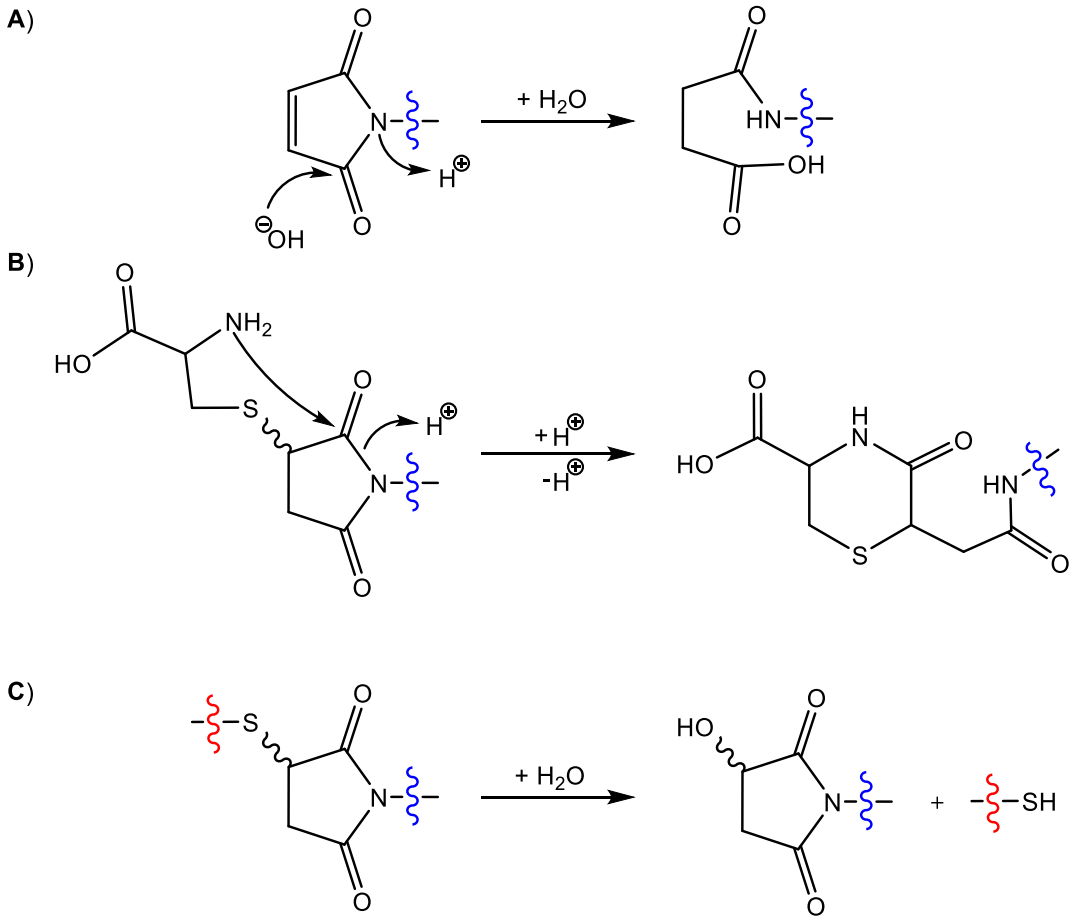

Figure 1.18: Potential limitations associated with the use of maleimide as a thiol alkylating reagent. (**A**) Alkaline conditions can cause ring opening of the maleimide ring to generate maleamic acid derivatives. (**B**) Transamidation reaction on the maleimide ring. (**C**) Hydrolysis of the thioether linkage on the maleimide ring. Adapted from [18].

Vinyl sulfone is an additional Michael acceptor utilised in the production of bioconjugates *via* thioether bond formation (**Figure 1.19**). Vinyl sulfone offers an advantage over the use of maleimide due to irreversible formation of an achiral thioether bond. Vinyl sulfone is predominantly used for the alkylation of thiols but is also reactive towards amine nucleophiles, which can potentially lead to the production of heterogeneous conjugates, which can complicate purification protocols and reduce yields of the desired products. [84]. Vinyl sulfone has been utilised to attach various ligands to thiol containing biomolecules such as PEG, fluorophores and affinity tags [84].

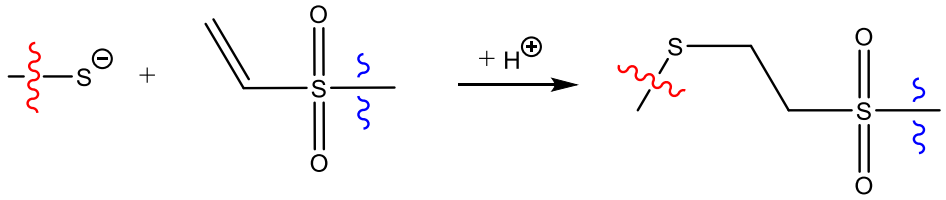

Figure 1.19: Thiol alkylation *via* a vinyl sulfone derivative

1.3) Aims and Objectives

This thesis seeks to utilise the thiolate of cysteine present in peptides and proteins for the attachment of ligands *via* suitable linker chemistry towards the production of bioconjugates. Key areas of optimisation include the reduction of disulfide bonds to generate free thiols in the biomolecule and developing protocols suited for high yielding bioconjugation reactions between the biomolecule and the linker-functionalised ligand. An additional area of optimisation is the development of linkers chemoselective for thiol alkylation for generating high yielding, homogenous bioconjugate products.

Chapter 2 describes the reaction of trialkylphosphine reducing agents with thiol-alkylating reagents. Water soluble trialkylphosphines such as TCEP and THPP have emerged as popular and very effective disulfide reducing agents. Chapter 2 aims to investigate the reaction of the trialkylphosphine reducing agents with the Michael acceptor thiol alkylating reagents: maleimide and vinyl sulfone through product characterisation and mechanistic studies. The aim is to provide some clear conclusions regarding the potential reaction between TCEP/THPP and maleimide/vinyl sulfone in the hope of standardising the necessary reduction protocol prior to synthesis of bioconjugates *via* thiol alkylation.

Chapter 3 describes the development of a novel, “one-pot” method for effecting thiol-alkylation reactions after a reduction step by trialkylphosphines. Reductant removal is usually possible using techniques such as dialysis, gel filtration and spin filtration, but may lead to the reoxidation of the thiols to disulfide bonds and lead to loss in conjugate yield. It also adds extra time and cost into the production of the

conjugate. The aim is, therefore, to remove the excess reducing agent *in situ* in the hope of developing a "one-pot" method for the production of conjugates utilising thiol alkylation chemistry. The addition of a water soluble alkyl azide offers a possible route to achieve this objective. The addition of a water soluble alkyl azide to quench excess TCEP or THPP should yield products (phosphine oxide, alkyl-amine and nitrogen gas) compatible with the subsequent conjugation step. The protocol offers the potential of a simple and novel method for the production of conjugates and is validated through the derivatisation of cysteine containing amino acids and peptides by maleimide functionalised ligands.

Chapter 4 describes the development of 4-vinyl pyridine (4-VP) derivatives as linkers for thiol-alkylation as an alternative to popular maleimide-based chemistry. Maleimide offers excellent reactivity and sufficient selectivity for thiols at neutral pH. Disadvantages, however, include potential reactions with amines, production of a diastereomeric mixtures, reversibility of the reaction and maleimide ring instability at an alkaline pH. The aim is to develop an alternative class of thiol alkylating reagents to overcome some of the pitfalls of maleimide chemistry. 4-Vinyl pyridine has been previously used to exclusively alkylate thiols of peptides and proteins prior to mass spectrometric analysis. The aim is to utilise the selectivity of 4-VP for broader applications in bioconjugate chemistry. It was envisaged to synthesise suitably derivatised 4-VP derivatives to facilitate the covalent attachment to ligands such as PEG and carbohydrates. The development of 4-VP as a thiol alkylating reagent involved the synthesis of a variety of 4-VP derivatives, characterisation of the reactions between the 4-VP derivatives and thiol containing peptides, pH-rate determination for the 4-VP derivatives and investigating the potential for derivatising thiol-containing proteins by glycation and PEGylation.

Chapter 5 describes the development of a novel method for thiol alkylation of S-nitrosated (SNO) proteins. Nitrosation of cysteinyl thiols of peptides and proteins is a transient post translational modification that is implicated in many biological processes such as vasodilation and cell signalling. A number of techniques have

been developed for the identification of the nitrosation sites, the most common being the biotin switch technique (BST). There are some pitfalls associated with this technique, which can lead to low yielding isolates or the isolation of false positives. The key to functionalising and identifying correct nitrosation sites are mild sample preparation protocols and a chemoselective reaction with the thio-nitroso functional group. The research aim is to develop a novel, one-step method that allows for the selective functionalisation of a thio-nitroso group, followed by sample enrichment using biotin affinity tag chemistry. There is precedence in the literature of 4-VP reacting with a nitrosated thiol to generate an oxime product, although no product characterisation was published. The method was repeated to validate the chemistry. The chemistry proved successful but an additional product *via* Michael addition of thiols was also isolated, rendering the method unsuitable for the specific targeting of nitrosated thiols. The allyl functional group was subsequently explored as method for specifically reacting with a nitrosated thiol. The method was successfully validated. The technique, however, proved to be low yielding but was successful in identifying nitrosated thiols in a model protein.

Appendix 1 describes the reduction of α,β-unsaturated 1,4-dicarbonyl substrates by THPP. The discovery of rapid maleimide reduction to succinimide by THPP under aqueous conditions prompted the investigation of THPP as a potential general reductant of α,β-unsaturated 1,4-dicarbonyls. Characterisation and mechanistic studies of the reduction reaction were performed on a variety of α,β-unsaturated 1,4-dicarbonyls, proving that THPP can be utilised as an effective reducing agent for α,β-unsaturated 1,4-dicarbonyl substrates.

Appendix 2 explores the potential of a TCEP-maleimide ylene adduct, isolated in Chapter 2, to react with Selctflour, an electrophilic fluorine source. This was pursued to validate the hypothesis of a TCEP-maleimide ylene adduct. The ylene was predicted to react with Selectfluor, analogous to the Wittig reaction where an ylide derivative reacts with an electrophilic carbonyl function group.

Chapter 2: Reaction of Trialkylphosphine Reducing Agents with Thiol-Alkylating Reagents

2.0) Disulfide Reducing Agents

The thiol functional group of cysteine's side chain in peptides and proteins is usually oxidised and exists predominantly as a disulfide bond. The disulfide bond is not reactive towards most reagents designed for thiol alkylation. A prerequisite, therefore, for thiol alkylation strategies on proteins is the necessary step of pre-reduction of disulfides to thiol functional groups.

A number of reducing agents have been developed for the reduction of disulfides under aqueous conditions. The choice of reducing agent is often dictated by the limitations of the reducing agent as well as the biomolecule of choice. A particular limitation of a biomolecule is typified by the requirement to often only partially reduce disulfides of antibodies prior to bioconjugation to necessitate the maintenance of tertiary structure of the protein, which is facilitated by the numerous disulfide bridges [83].

2.0.1) Mono Thiol Containing Disulfide Reductants

β-Mercapatoethanol (BME, **2.1**) is a water soluble liquid that is often utilised as a disulfide reducing agent. BME requires use in a ventilated hood because of its very strong odour and toxicity, which are principle reasons for its decline in use. BME is a powerful disulfide reducing agent and can be used if complete disulfide reduction within the protein is required. BME is often used to aid in protein denaturation for sodium dodecyl polyacrylamide gel electrophoresis (SDS-PAGE) of proteins [85]. BME is utilised in bioconjugation protocols, for example, to reduce disulfides in proteins and reduce mixed disulfides of ligands prior to attachment to gold nanoparticles [86, 87]. BME has also been utilised to react with excess maleimidyl groups after a bioconjugation reaction to prevent the attachment of potential nucleophiles to the synthesised conjugate [88].

β-Mercaptoethylamine hydrochloride (BMEA, **2.2**) is a weaker disulfide reducing agent compared to BME. BMEA is a water soluble solid that can be used for the partial disulfide reduction of antibodies for the production of antibody-ligand conjugates [89]. BMEA has also been used to introduce thiols into biomolecules to enable the synthesis of conjugate vaccines by thiol alkylation [90].

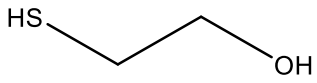

BME

(2.1)

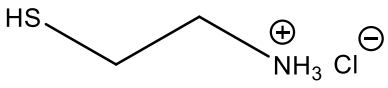

BMEA

(2.2)

The mechanism of disulfide reduction by mono thiol-containing reductants is a 2 step process, with an intermediate mixed disulfide existing before complete reduction of the target disulfide (**Figure 2.1**). The rate of disulfide reduction is relatively slow due to the rate of mixed disulfide exchange being approximately equal to the rate of the target disulfide reduction. Mono thiol-containing reducing agents are, therefore, needed in large excesses, require long incubation periods and, importantly, need to be removed prior to bioconjugation reactions.

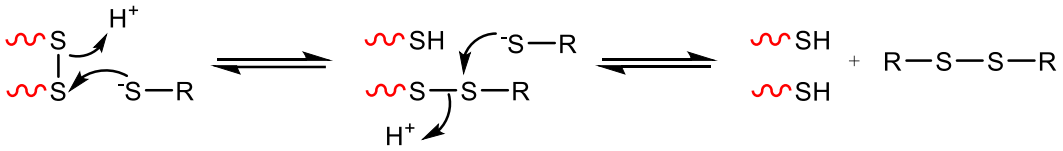

Figure 2.1: Mechanism of disulfide reduction by a mono thiol-containing disulfide reductant such as BME (R = $(CH_2)_2OH$) and BMEA (R = $(CH_2)_2NH_2$).

2.0.2) Dithiol Containing Disulfide Reductants

The use of dithiothreitol (DTT, **2.3**) and dithioerythritol (DTE, **2.4**) as disulfide reducing agents was first described by Cleland in 1964 [91]. DTT and DTE are water soluble compounds, have a reduced offensive odour and are stronger disulfide reducing agents compared to BME and BMEA and so quickly replaced the mono-thiol reductants as disulfide reducing agents of proteins.

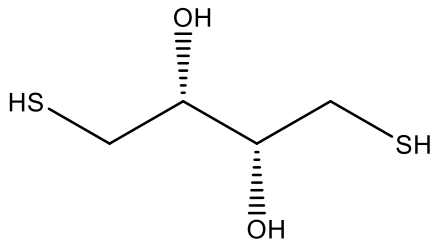

DTT

(**2.3**)

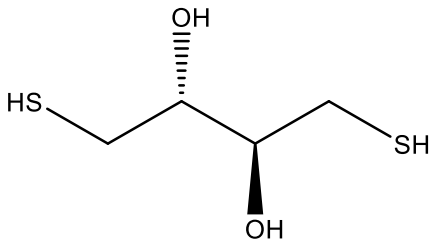

DTE

(**2.4**)

The driving force for disulfide reduction in proteins is the ability of DTT and DTE to form intramolecular ring structures (4,5-dihydroxy-1,2-dithiane) [92]. The reducing agent initially acts as a nucleophile on the disulfide of the protein, reducing one of the target sulfur atoms and generating a mixed disulfide intermediate on the second sulfur atom of the protein. The remaining free thiol of DTT or DTE nucleophilically attacks the mixed disulfide bond to reduce the second target sulphur atom, and in the process, generating a disulfide-containing 6-membered ring. The generation of a disulfide containing cyclic by-product drives the equilibrium towards disulfide reduction in the protein (**Figure 2.2**). DTT and DTE are able to reduce most solvent accessible disulfides in proteins [83]. In the absence of denaturants such a SDS or urea, DTT and DTE are often not able to reduce all disulfides in the protein as they are unable to access the core of the protein's folded structure due to steric hindrance [93]. Very rarely a DTT mixed disulfide may be formed with the biomolecule. The two sulfur atoms of DTT may also form disulfide bonds to two different sulfur atoms. This prevents the DTT molecule from cyclising and may complicate purification of the biomolecule and reduce yields during the bioconjugation reaction [93]. It is essential to remove DTT and DTE from the reaction before conjugation chemistry is pursued as the thiol-based reducing agents have the capacity to react with thiol-alkylating reagents, reducing yields of alkylation at the target thiol. This class of disulfide reductant has been successfully utilised in many bioconjugation protocols, including the reduction of antibodies [77], reduction of cytokines prior to PEGylation [94], activation of nanoparticles [95] and production of conjugate vaccines [96].

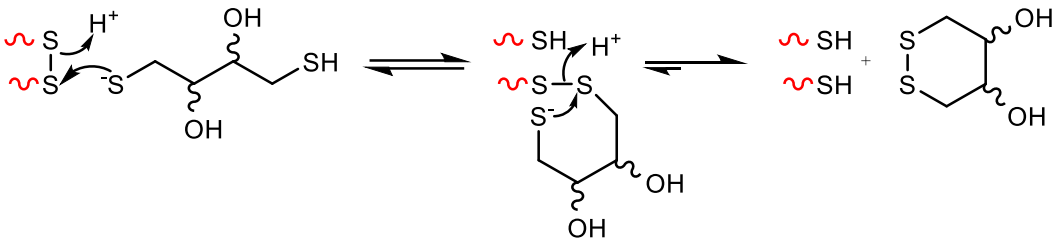

Figure 2.2: Mechanism of disulfide reduction by DTT or DTE.

2.0.3) Water Soluble Trialkylphosphines

Triphenylphosphine was the first phosphine-based reagent utilised for the reduction of simple disulfide-containing compounds in the presence of water and was reported in 1935 [97]. A more water soluble phosphine: tris(hydroxymethyl) phosphine was later developed and utilised to reduce the disulfides of immunoglobulins [98].

Trialkylphosphine reducing agents do possess a few advantages over thiol-based disulfide reducing agents. The phosphorus atom of commercial water-soluble phosphines have pKa's of 7-8. This is a common pH range to perform bioconjugations, therefore, the trialkylphosphines are more effective nucleophiles than thiol-based reducing agents to effect disulfide reduction within this pH range. Disulfide reduction utilising trialkylphosphines is irreversible, unlike the reversible mechanism of disulfide reduction observed with thiol-containing reducing agents. The driving force for the irreversible reduction of disulfides by trialkyphosphines is the generation of the strong P-O bond as the trialkylphosphine is oxidised to trialkylphosphine oxide (**Figure 2.3**). Trialkylphosphines, therefore, do not need to be utilised in vast excess as required by thiol-based reducing agents. Optimised conditions theoretically allow for stoichiometric use of trialkylphosphines in disulfide reduction, however, trialkylphosphines are susceptible to oxidation to trialkylphosphine oxides in the presence of molecular oxygen and so need to be handled in oxygen depleted environments.

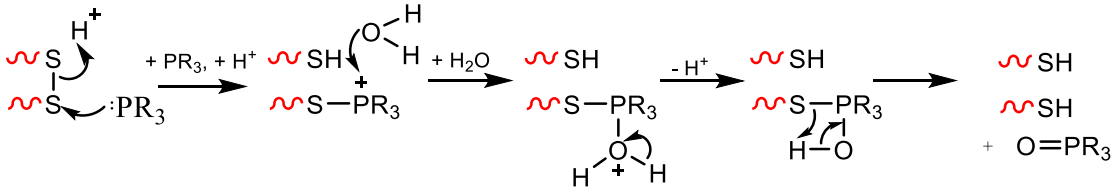

Figure 2.3: Mechanism of disulfide reduction by trialkylphosphines. R = alkyl.

Tributylphosphine (TBP, **2.5**) has a pKa of 8.43 (phosphorus atom) and has been utilised for the reduction of protein disulfides for many decades [92, 99-102]. TBP is very sensitive to oxidation and, therefore, needs to be utilised as a fresh solution and stored under inert conditions. There is also the added disadvantages of TBP possessing a foul odour and poor water solubility, which tends to limit its use in bioconjugation chemistry, although it is still a commercially available product marketed for biological applications [103, 104]. TBP has generally been replaced by less odorous, more stable and water soluble derivatives such as tris(2-carboxyethy)phosphine (TCEP, **2.6**) to reduce disulfides in proteins.

The first use of TCEP for disulfide reduction was reported in 1969 for the reduction of immunoglobulins [98] and eventually became commercially available in 1992 [80, 105]. The use of TCEP has gained in popularity since its introduction as a biological disulfide reducing agent. TCEP offers many advantages over DTT. TCEP has a pKa of 7.68 (phosphorus atom), is an odourless and water soluble crystalline solid that is relatively stable to oxidation and is stable in an aqueous environment over a wide pH range [106, 107]. TCEP is a weaker chelator of metal ions than DTT so, therefore, has less potential to interfere in bioinorganic systems [107]. TCEP does not form mixed disulfides during disulfide reduction, which is especially favourable when producing therapeutics which require strict characterisation protocols, for example, antibody-drug conjugates [108]. There are, however, a few potential limitations to be considered. Co-elution of TCEP with peptides and proteins during gel filtration purification has been reported, which can complicate purification protocols [109]. TCEP is fairly impermeable to the hydrophobic protein core so may only cause selective reduction of proteins [110]. TCEP has the potential to cause

desulfurisation of cysteine [111] and cleave cysteine containing peptide bonds [112]. The cost of TCEP is also generally 2-3 times more than DTT. Despite the potential disadvantages, TCEP has been successfully utilised in bioconjugate production, including the reduction of disulfides in RNA [113], peptides[114] and proteins [80, 115].

Tris(3-hydroxypropyl)phosphine (THPP, **2.7**) is a relatively new commercially available, water soluble phosphine that is emerging as an alternative disulfide reducing agent to TCEP [116]. THPP is a viscous liquid of relatively low odour. The phosphorus atom of THPP has a pKa of 7.22, is stable to oxygen dependant oxidation over a wide pH range and has shown superior reducing qualities when compared to TCEP [18, 117, 118]. THPP and has been utilised in bioconjugation chemistry for reducing plasma proteins [119].

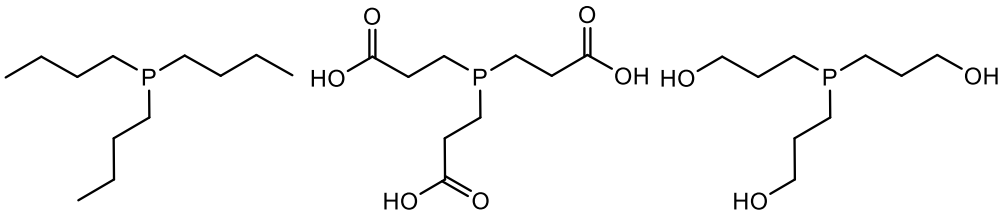

TBP (**2.5**) **TCEP** (**2.6**) **THPP** (**2.7**)

2.1) Reaction of TCEP with the Thiol-Alkylating Reagent Maleimide

The maleimide functional group is a Michael acceptor and is the most widely used thiol-alkylating reagent in bioconjugation chemistry due to its specificity for sulfhydryl nucleophiles at neutral pH [18]. There is conflicting data in the literature with regards to the potential for reaction of the maleimide functional group with TCEP during bioconjugation reactions. The debate has not been completely resolved and needs to be addressed to ensure high bioconjugation yields and prevent unwanted side reactions that may compromise the purity of bioconjugates.

A number of commercial sources for TCEP report that TCEP does not react with maleimide and, therefore, does not need to be removed before introduction of the

maleimide functionalised ligand to alkylate the reduced disulfides of the biomolecule [120, 121]. Literature protocols have also been published where TCEP is claimed to be non-reactive towards maleimide when TCEP is not removed prior to addition of maleimide-based reagents [108, 122]. The potential reaction of TCEP with maleimide can be overlooked if the maleimide functionalised ligand is used in significant excess to TCEP [108].

There is, however, also literature claiming that TCEP does react with maleimide and therefore, needs to be removed in a similar manner to thiol-based disulfide reducing agents before the maleimide-based bioconjugation chemistry is pursued [8, 80, 109]. The presence of TCEP in bioconjugation reactions between maleimide and cysteinyl proteins has been reported to reduce conjugation yields [8]. TCEP was, therefore, proposed to compete with thiols for addition to maleimide, however, no product characterisation has been performed [8, 80, 109, 123]. Mass spectrometry of bioconjugation reactions where maleimide and TCEP have been utilised have identified a potential phosphonium ion adduct between TCEP and maleimide as the likely product [124, 125], which is consistent with earlier literature reporting a phosphonium ion adduct between a trisubstituted phosphine and maleimide [126]. There is also additional literature where triphenylphosphine has been used to reduce maleimide to succinimide under reflux conditions [127].

As such, we first sought to investigate the ambiguity in the literature regarding the reaction of TCEP with Michael acceptors such as maleimide. The possible reaction between THPP and maleimide was also investigated. The possible reaction of trialkylphosphines TCEP or THPP with the Michael acceptor vinyl sulfone is also included in the investigation. It is envisaged to provide evidence that may standardise protocols utilising trialkylphosphines to reduce disulfide bonds and Michael acceptors to effect bioconjugation by thiol alkylation.

2.1.1) Characterisation of the Reaction Product between TCEP and Maleimide

The reaction of TCEP (**2.6**) and the maleimide functional group was initially investigated by incubation of TCEP with N-ethyl maleimide (**2.8**) in aqueous sodium phosphate (0.1 M, pH = 7) for 1 hour (**Figure 2.4**). Purification of the reaction by reverse phase (C-18) chromatography yielded a TCEP-maleimide adduct in a 73 % yield, which could exist as a resonance hybrid of an ylene **2.9** or an ylide **2.10**. NMR and MS spectroscopy could not aid in distinguishing the TCEP-maleimide product as either **2.9** or **2.10**. Infrared spectroscopy was more useful in postulating the structure for the TCEP-maleimide adduct as being N-ethyl-3-(tris(carboxyethyl)phosphorylidene)pyrrolidine-2,5-dione (**2.9**). The identification of a band at 1229 cm^{-1} in the infrared spectrum could be indicative of a P=C bond as a P=C bond stretching frequency is expected in the region 1180-1230 cm^{-1} [128]. The isolation of product **2.9** in good yield is clear evidence that TCEP does react with maleimide. The ylene adduct **2.9** has not been reported in the literature, although a phosphonium ion adduct has been previously proposed based on mass spectrometry methods [124, 125].

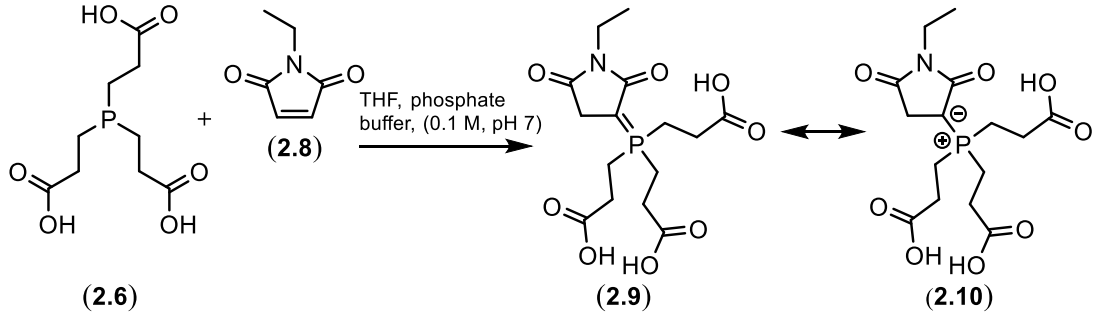

Figure 2.4: Reaction of TCEP (**2.6**) with N-ethyl maleimide (**2.8**) to form a covalent adduct **2.9**.

The reaction between TCEP and a maleimide-functionalised amino acid was subsequently investigated. The reaction was performed to isolate and characterise any potential reaction products in a model system that more closely resembled a bioconjugation reaction. TCEP was incubated with the maleimide functionalised amino acid N^6-[3-(2,5-dioxo-2,5-dihydro-1*H*-pyrrol-1-yl)propanoyl]-L-lysine (**2.11**) in

aqueous sodium phosphate (0.1 M, pH = 7) for 1 hour (**Figure 2.5**). Purification of the reaction by reverse phase (C-18) chromatography yielded a TCEP-maleimide adduct in 70 % yield, which could exist as a resonance hybrid of the ylene product **2.12** or the ylide **2.13**. Unfortunately NMR and MS spectroscopy could not aid in distinguishing the TCEP-maleimide product as either **2.12** or **2.13**. Infrared red spectroscopy was utilised to suggest the structure for the TCEP-maleimide adduct as the ylene derivative **2.12**. The identification of a band at 1164 cm^{-1} in the infrared spectrum could be indicative of a P=C bond. The ylene structure is, therefore, postulated as the product from the reaction of TCEP with **2.12**. Results suggest that trialkylphosphines are likely to react with maleimide functionalised biomolecules under typical conditions used for bioconjugation.

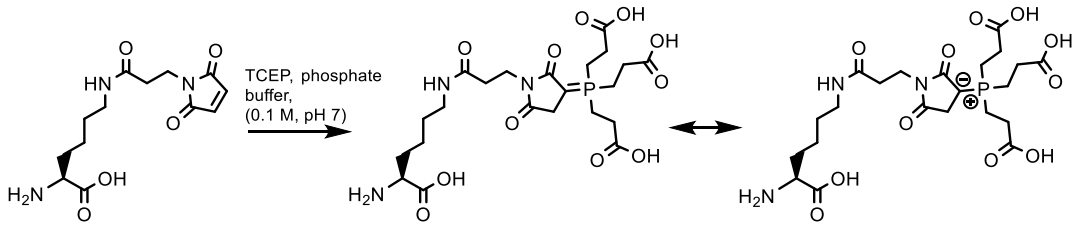

(**2.11**) (**2.12**) (**2.13**)

Figure 2.5: Reaction of maleimide derivatised lysine (**2.11**) with TCEP to form a covalent adduct.

2.1.2) Mechanism of the Reaction between TCEP and Maleimide

We next sought to investigate the mechanism of reaction for TCEP-maleimide adduct formation by repeating the original reaction of TCEP (**2.6**) with N-ethyl maleimide (**2.8**), this time using a deuterated buffer (**Figure 2.6**). NMR and MS analysis of deuterated products aids in determining the sites on the substrates where hydrogen atoms may have been added or lost during the reaction. This can assist in the formulation of a mechanism for the reaction. A racemic deuterium containing TCEP-maleimide ylene adduct **2.14** was isolated as the major product of the reaction after reverse phase (C-18) chromatography in a 79 % yield. The ylene structure was suggested through analysis of the infrared spectrum. The

identification of a band at 1233 cm^{-1} in the infrared spectrum could be indicative of a P=C bond stretching frequency.

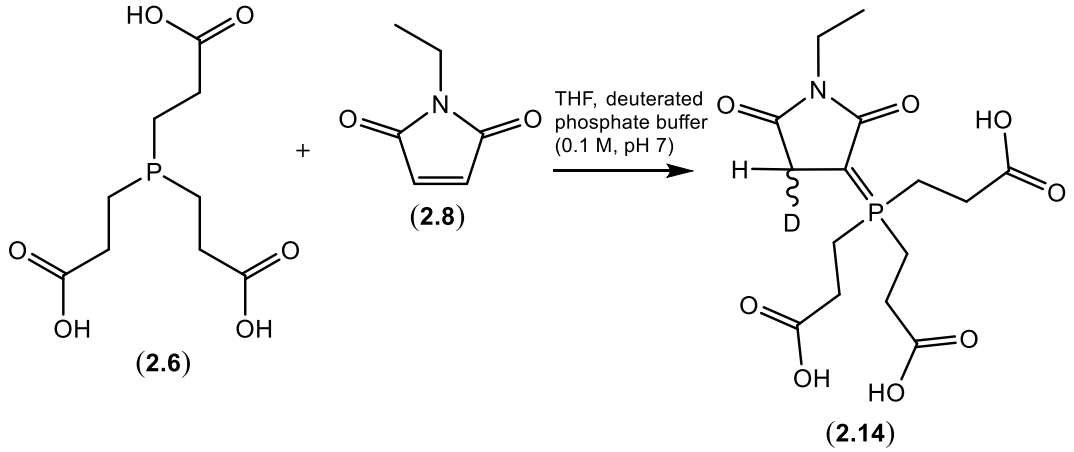

Figure 2.6: Reaction of TCEP (**2.6**) with N-ethyl maleimide (**2.8**) in a deuterated buffer to yield the product **2.14**.

The isolation and characterisation of **2.14** allowed postulation of a mechanism for the formation of the product (**Figure 2.7**). Nucleophilic attack of the phosphorus atom of TCEP at the conjugated alkene of maleimide initially forms a phosphonium ion adduct. The acidic α-proton attached to the carbon atom bearing the phosphonium cation is lost to neutralise the positive charge of the phosphonium ion intermediate, resulting in an ylene product. It is postulated that the three electron withdrawing 2-carboxyethyl groups attached to the phosphorus atom of TCEP destabilises the phosphonium ion associated with an ylide and instead favour the formation of a neutral ylene product.

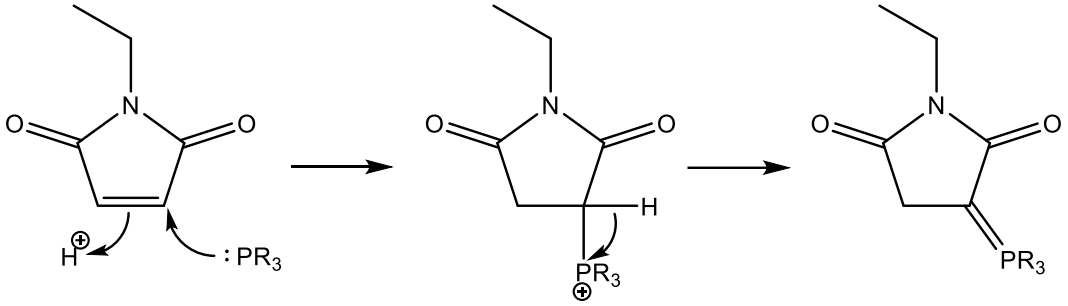

Figure 2.7: A proposed mechanism for TCEP-maleimide adduct formation. R = $(CH_2)_2CO_2H$

2.2) Reaction of THPP with the Thiol-Alkylating Reagent Maleimide

THPP is a relatively new commercial disulfide reducing agent that can be utilised as a substitute for TCEP. The above observation of a reaction between TCEP and maleimide derivatives (**Figure 2.4**-**Figure 2.6**) prompted an investigation into the potential reaction of THPP with maleimide derivatives.

2.2.1) Characterisation of the Reaction Product between THPP and Maleimide

The potential for reaction between THPP (**2.7**) and maleimide was investigated by incubating THPP with N-ethyl maleimide (**2.8**) for 1 hour in a buffered solution (phosphate, 0.1 M, pH = 7). Purification of the reaction by silica gel chromatography yielded the product N-ethyl succinimide (**2.15**) in 61 % yield (**Figure 2.8**). This was a surprising result as we initially anticipated ylide or ylene products analogous to the TCEP reactions with maleimide derivatives (**Figure 2.4** and **Figure 2.5**). There is, however, evidence in the literature of triphenylphosphine reducing maleimide to succinimide, although reflux conditions were utilised [127]. Here, THPP appears to have the capacity to rapidly reduce α,β-unsaturated 1,4-dicarbonyl substrates under very mild, aqueous conditions.

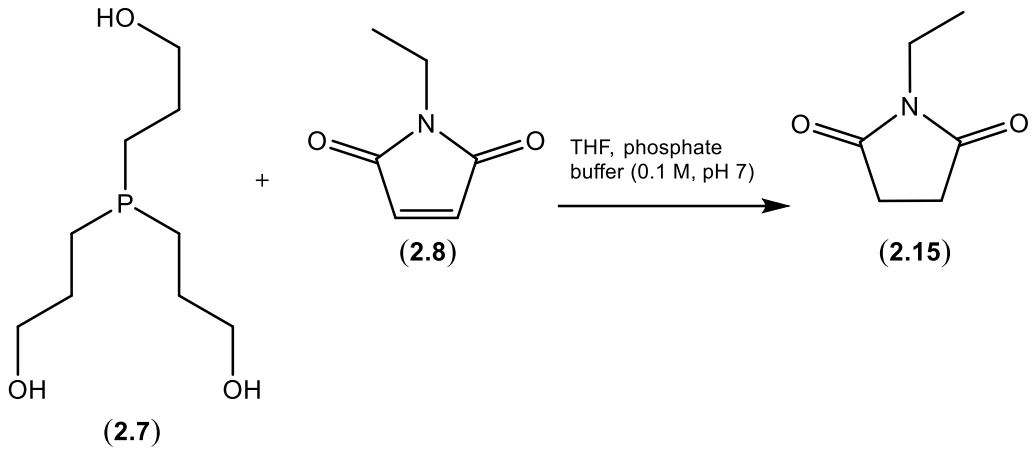

Figure 2.8: Reaction of THPP (**2.7**) with N-ethyl maleimide (**2.8**).

The reaction between THPP and a maleimide-functionalised amino acid was subsequently investigated. The reaction was performed to isolate and characterise any potential reaction products in a model system that more closely resembled a typical bioconjugation reaction. As such, THPP (**2.7**) was incubated with the maleimide functionalised amino acid N^6-[3-(2,5-dioxo-2,5-dihydro-1*H*-pyrrol-1-yl)propanoyl]-L-lysine (**2.11**) in aqueous sodium phosphate (0.1 M, pH = 7) for 1 hour. The reduced product N^6-[3-(2,5-dioxopyrrolidin-1-yl)propanoyl]-L-lysine (**2.16**) was successfully isolated by reverse phase (C-18) chromatography in a 59 % yield (**Figure 2.9**).

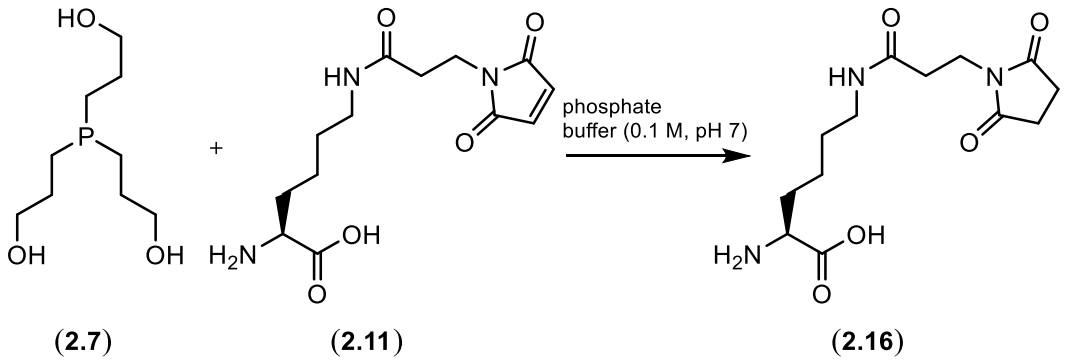

(**2.7**) (**2.11**) (**2.16**)

Figure 2.9: Reaction of maleimide derivatised lysine (**2.11**) with THPP (**2.7**) to yield the succinimide-lysine derivative (**2.16**).

2.2.2) Mechanism of the Reaction between THPP and Maleimide

The mechanism of maleimide reduction by THPP was investigated by repeating the reaction of THPP (**2.7**) with N-ethyl maleimide (**2.8)** in deuterated aqueous sodium phosphate (0.1 M, pH = 7) for 1 hour. A racemic mixture of 1-ethyl-3-dideutero-(4*R*,*S*)-deutero-pyrrolidine-2,5-dione (**2.17**), which was confirmed by NMR and HRMS analysis, was isolated by silica gel chromatography in a 52 % yield (**Figure 2.10**).

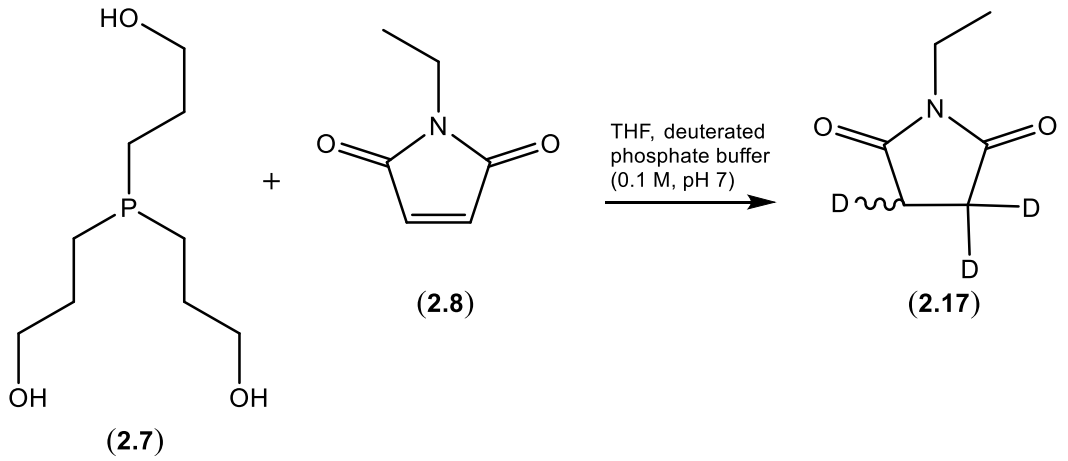

(**2.7**) (**2.8**) (**2.17**)

Figure 2.10: Reaction of THPP (**2.7**) with N-ethyl maleimide (**2.8**) in deuterated buffer to yield the deuterated succinimide product **2.17**.

The deuterated succinimide product **2.17** allowed postulation of a mechanism for the reduction of maleimide by THPP. Nucleophilic attack by the phosphorus atom of THPP at the alkene carbon of maleimide results in a phosphonium cation adduct as an intermediate. The acidic α-proton attached to the carbon atom bearing the phosphonium cation is lost to neutralise the positive charge of the phosphonium ion intermediate, which results in a resonance hybrid of an ylene and an ylide intermediate. The ylide intermediate and aqueous conditions facilitate oxidation of the phosphorus atom of the ylide intermediate to generate THPP oxide and N-ethyl succinimide (**Figure 2.11**).

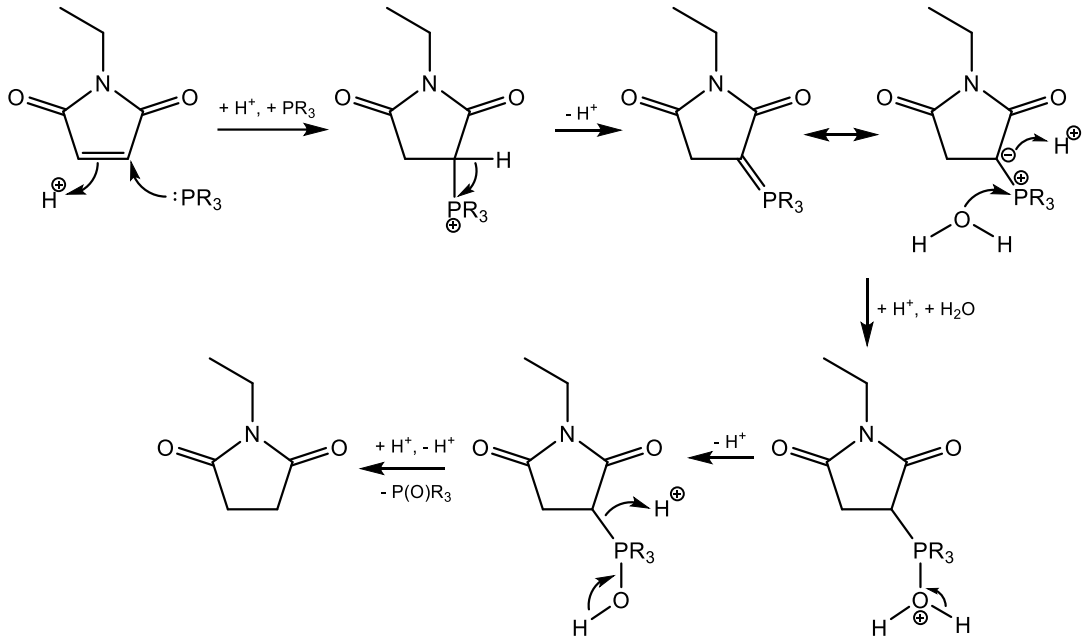

Figure 2.11: Proposed mechanism for THPP reduction of maleimide to succinimide. R = $(CH_2)_3OH$.

2.3) Reaction of TCEP with Vinyl Sulfone: a Thiol-Alkylating Functional group

Vinyl sulfone is an alternative Michael acceptor thiol alkylating reagent which has been developed and used successfully in bioconjugation reactions. The vinyl sulfone functional group has been functionalised with poly(ethylene)glycol (PEG) for generating PEGylated biomolecules *via* thiol alkylation [129]. A variety of different ligands such as fluorophores and affinity tags have also been functionalised with vinyl sulfone for bioconjugate applications [84].

The reaction of TCEP with vinyl sulfone has not been previously explored and requires investigation, especially in light of our previous findings that the ylene product **2.9** is generated by the reaction of TCEP with maleimide. Vinyl sulfone, similar to maleimide, is a Michael acceptor so it is very probable that a reaction between TCEP and vinyl sulfone may occur.

As such, phenyl vinyl sulfone (**2.18**) was incubated with TCEP (**2.6**) in aqueous sodium phosphate (0.1 M, pH = 7) for 1 hour (**Figure 2.12**). Purification of the reaction by reverse phase (C-18) chromatography yielded a TCEP-vinyl sulfone-adduct in 84 % yield. NMR spectroscopy was ineffective in distinguishing the product as either the phosphonium ion adduct **2.19** or the penta co-ordinate phosphorus product **2.20**. However, the identification of a peak at 1153 cm^{-1} (P-O-ethyl = 1155-1165 cm^{-1}) in the infrared spectrum suggests the penta co-ordinate derivative **2.20** as the product [130]. This product may be generated by the nucleophilic attack of TCEP at the vinylic terminal carbon of phenyl vinyl sulfone to yield a phosphonium cation. The charged intermediate may be neutralised by the formation of a five membered ring *via* attack of one of the carboxylate functional groups of TCEP on the phosphonium cation. The isolation of **2.20** confirms that TCEP does react with vinyl sulfone and, therefore, should be removed prior to addition of vinyl sulfone derivatised ligands to effect thiol alkylation reactions.

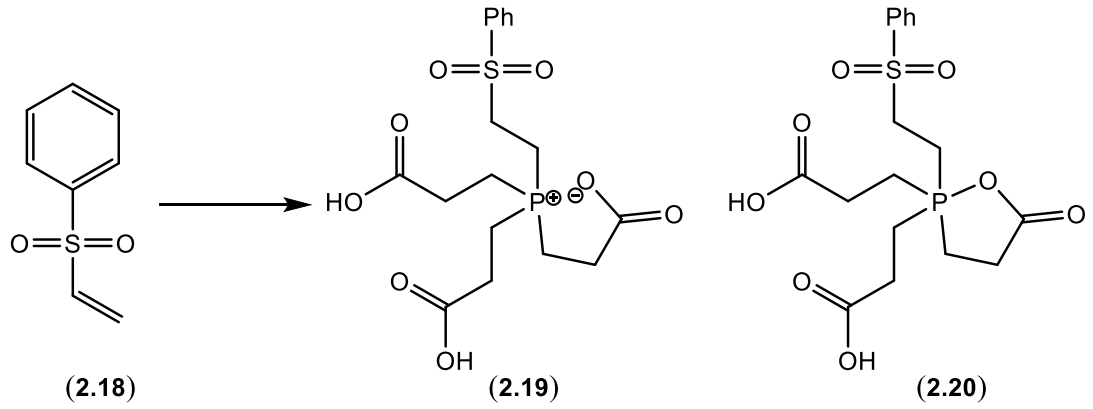

Figure 2.12: Reaction of TCEP (**2.6**) with phenyl vinyl sulfone (**2.18**).

2.4) Reaction of THPP with Vinyl Sulfone: a Thiol-Alkylating Functional Group

The evidence of TCEP's reaction with a vinyl sulfone functional group also prompted an investigation into the reaction of THPP with a vinyl sulfone functional group (**Figure 2.13**). THPP (**2.7**) was incubated with phenyl vinyl sulfone (**2.18**) for 1 hour at neutral pH. The reaction resulted in a large number of products and it was not possible to isolate anything from the mixture. On the basis of these results it is suggested to avoid THPP when using vinyl sulfone chemistry in bioconjugation reactions or ensure the complete removal of THPP prior to the use of vinyl sulfone derivatised ligands.

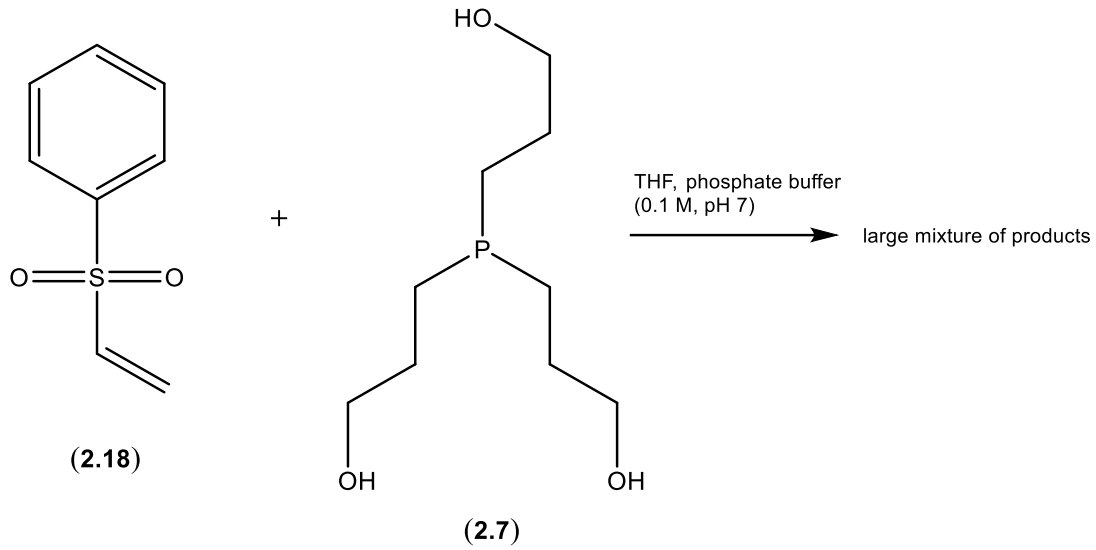

Figure 2.13: Reaction of THPP (**2.7**) with phenyl vinyl sulfone (**2.18**) yielded a complex mixture of products.

2.5) Reaction of the TCEP-Maleimide Adduct 2.9 with Thiols

The aim of the following investigation was to investigate the potential of the product **2.9** to react with a thiol functional group. The investigation was performed to test if the TCEP-maleimide adduct **2.9** could still be a potentially productive intermediate and facilitate thiol alkylation in bioconjugation protocols.

The potential turnover of the TCEP-maleimide ylene adduct **2.9** by thiols was investigated over a wide pH range and monitored by either ^{31}P NMR spectroscopy or high resolution mass spectrometry (**Figure 2.14**). The phosphorus signal in the ^{31}P NMR spectrum of TCEP displays a characteristic peak between δ -15 and -20 ppm compared to the ylene adduct (δ -35 to -40 ppm) and TCEP oxide (δ -55 to -60 ppm). ^{31}P NMR spectroscopy, therefore, provides a rapid method for monitoring the potential reaction of **2.9** with a thiol functional group.

The adduct **2.9** was synthesised in conditions mentioned previously and confirmed by ^{31}P NMR spectroscopy against an authentic sample. Reduced glutathione (**2.21**), a thiol-containing tripeptide, was subsequently added and the reaction was left at room temperature overnight in a buffered solution (pH = 7). The reaction was

subsequently analysed by ^{31}P NMR and HRMS. No change was observed by ^{31}P NMR and the HRMS only detected unreacted glutathione and **2.9**. The absence of a glutathione-maleimide product demonstrated that the ylene **2.9** is stable at neutral pH, in the presence of nucleophilic thiols. The same experiment was performed at pH = 8 to increase the nucleophilic thiolate anion concentration. Again, no change was observed by NMR or HRMS spectroscopy. The results confirmed the inability of a thiolate to turnover the ylene **2.9** under neutral or basic conditions and at ambient temperature. The same reaction was performed in an acidic environment (pH = 4) to access the stability of the ylene. Reduced glutathione was, again, unable to turnover the maleimide-TCEP adduct **2.9**. The above evidence demonstrated the stability of **2.9** towards thiol-based nucleophiles over a wide pH range and is, therefore, a non-productive species when considering nucleophilic orientated chemical bioconjugations. These results would suggest, therefore, that TCEP should be removed prior to the introduction of maleimide functionalised ligands, to prevent the consumption of the thiol alkylating reagent.

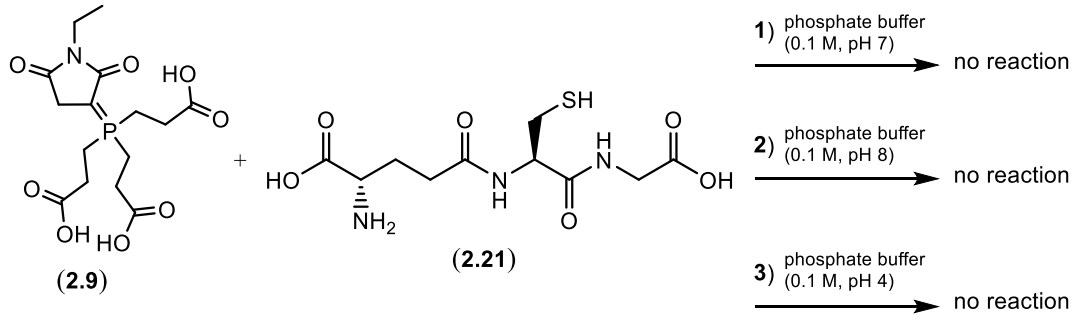

Figure 2.14: Incubation of **2.9** with glutathione (**2.21**) over a pH range. The reactions were monitored by either NMR or HRMS spectroscopy for any potential reactions of **2.9** with glutathione (**2.21**).

2.6) Impact of the TCEP-Maleimide Reaction in Bioconjugations

The discovery of the adducts between TCEP and maleimide (**2.9**, **2.12** & **2.14**) and the reduction of maleimide derivatives by THPP (**2.15**, **2.16** & **2.17**) have implications with regards to bioconjugation chemistry. If the reducing agents (TCEP or THPP) are not removed prior to the addition of a maleimide-functionalised ligand, the yield for the bioconjugation process may be reduced. Conjugate-TCEP adducts may also be generated, which may be problematic during the synthesis of conjugate vaccines.

2.6.1) The Effect of Not Removing TCEP or THPP Prior to Maleimide PEGylation of a Model Protein

The effect of not removing the reducing agents TCEP or THPP from bioconjugation reactions utilising a protein relying on thiol alkylation by maleimide-derivatised ligands was initially investigated.

Yeast enolase was used as a model protein to investigate the effect of reducing agents on thiol alkylation by maleimide functionalised ligands. Yeast enolase (47 kDa) is a commercially available protein containing a single cysteine (Cys248) residue and is, therefore, an excellent model protein to perform thiol alkylation experiments. The cysteine residue, however, is buried in the core of the protein's structure and so it is first necessary to denature the protein (8 M urea) to expose the cysteine to facilitate thiol alkylation.

Yeast enolase (1 mg/mL) was initially denatured in argon purged Tris buffer (0.5 M, pH = 7.2) containing 5 mM EDTA and 8 M urea. Varying concentrations of TCEP or THPP (1-10 eq.) were added to aliquots of protein and incubated for 45 minutes at 25 °C. Maleimide-PEG2kDa (1 eq.) was subsequently added and the reaction was incubated at 37 °C for 18 hours. The reactions were analysed by SDS-PAGE (**Figure 2.15**).

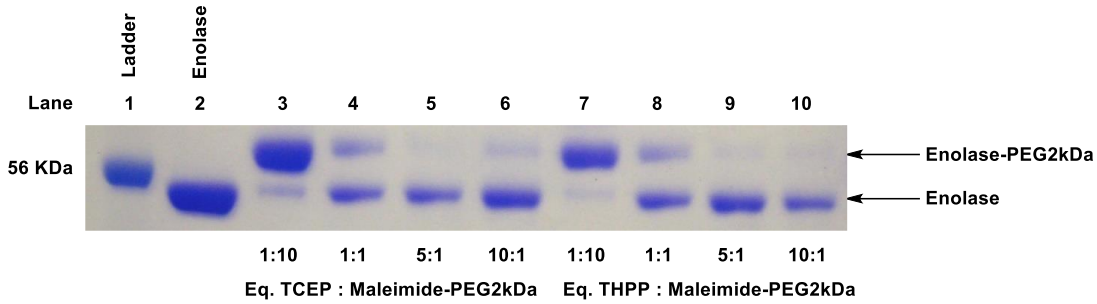

Figure 2.15: SDS-PAGE analysis of PEGylation (1 eq.) experiments on yeast enolase with varying TCEP/THPP concentrations (1-10 eq.). **Lane 1:** ladder, **Lane 2:** enolase, **Lane 3:** enolase + TCEP (1 eq.) + maleimide-PEG2kDa (10 eq.), **Lane 4:** enolase + TCEP (1 eq.) + maleimide-PEG2kDa (1 eq.), **Lane 5:** enolase + TCEP (5 eq.) + maleimide-PEG2kDa (1 eq.), **Lane 6:** enolase + THPP (10 eq.) + maleimide-PEG2kDa (1 eq.), **Lane 7:** enolase + THPP (1 eq.) + maleimide-PEG2kDa (10 eq.), **Lane 8:** enolase + THPP (1 eq.) + maleimide-PEG2kDa (1 eq.), **Lane 9:** enolase + THPP (5 eq.) + maleimide-PEG2kDa (1 eq.), **Lane 10:** enolase + THPP (10 eq.) + maleimide-PEG2kDa (1 eq.). The SDS-PAGE gel was stained with Coomassie solution and analysed utilising Image Studio Lite software.

The phosphorus atom of TCEP and THPP competes with the cysteine thiol of yeast enolase for nucleophilic addition to maleimide-PEG2kDa, which results in very poor yields of PEGylated protein (**Figure 2.15**, **Lanes 4-6 & 8-10**). The electrophoresis results clearly demonstrates the need to consume or remove both TCEP and THPP prior to maleimide-based bioconjugation reactions.

2.6.2) The Effect of Not Removing TCEP when Utilising Maleimide for Conjugate Vaccine Production

There is an additional important implication regarding the reaction of TCEP with maleimide, particularly regarding the production of conjugate vaccines. The production of conjugate vaccines *via* thiol alkylation by methods utilising maleimide are well documented [131, 132]. The assembly of conjugate vaccines is generally achieved *via* coupling of a carrier protein to an antigen and may be achieved through two different strategies. The carrier protein may provide the nucleophilic thiol either *via* synthetic introduction or a naturally occurring cysteine residue, while the antigen may be functionalised with the electrophilic thiol alkylating reagent such as maleimide [133]. Conversely, it is also possible to functionalise the

carrier protein with maleimide while the antigen provides the nucleophilic thiol [134].

Regardless of the strategy employed, it is important that TCEP is completely removed prior to maleimide-dependant conjugation due to the potential for TCEP to covalently link to the maleimide functional group. If the maleimide is attached to either the antigen (**Figure 2.16**, **A**) or the carrier protein (**Figure 2.16**, **B**) there is a risk of forming heterogeneous products consisting of carrier protein, antigen and TCEP. The covalent attachment of TCEP to the bioconjugate presents an additional antigen to the host during vaccination and this may result in the production of non-productive antibodies to the TCEP ligand attached to the bioconjugate.

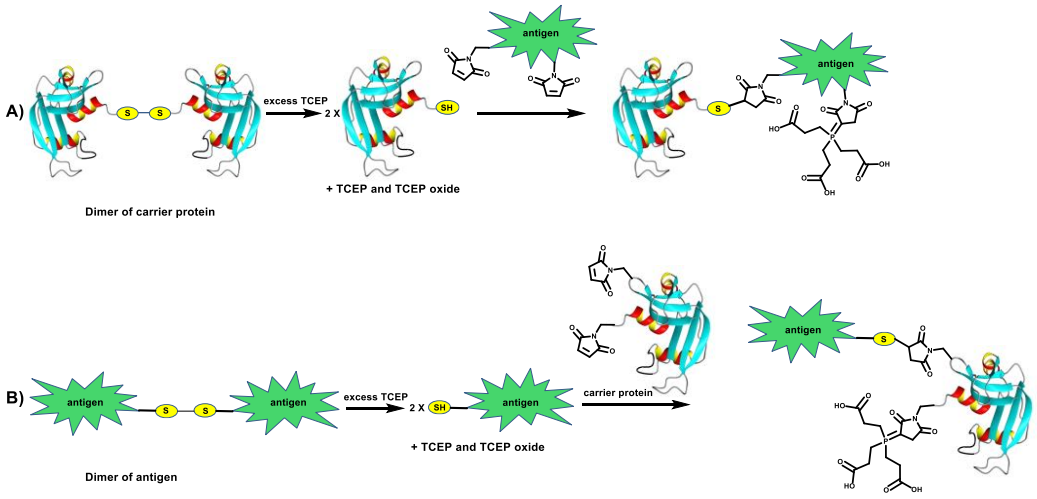

Figure 2.16: Illustration of the potential for TCEP addition to conjugate vaccine products. **A)** If the excess TCEP is not removed prior to the addition of a maleimide-functionalised antigen, the resulting bioconjugate could be composed of carrier protein, antigen and TCEP. **B)** If the excess TCEP is not removed prior to the addition of a maleimide-functionalised carrier protein, the resulting bioconjugate could be composed of carrier protein, antigen and TCEP.

As such, the potential attachment of TCEP to maleimide functionalised ligands utilised for conjugate vaccine production was investigated. The antigenic polysaccharide (Pn6B) from the outer protective capsule of the pathogen *Streptococcus pneumoniae* was chosen as the ligand for maleimide functionalisation as it is a common antigen utilised in vaccine production to prevent

infection from *S. pneumoniae* [135]. The Pn6B is a 0.9-1.5 MDa carbohydrate and consists of a repeat unit of (→2-α-D-Galactopyranose-(1→3)-α-D-Glucopyranose-(1→3)-α-L-rhamnopyranose-(1→4)-D-ribitol-5-phosphate→) (**Figure 2.17**).

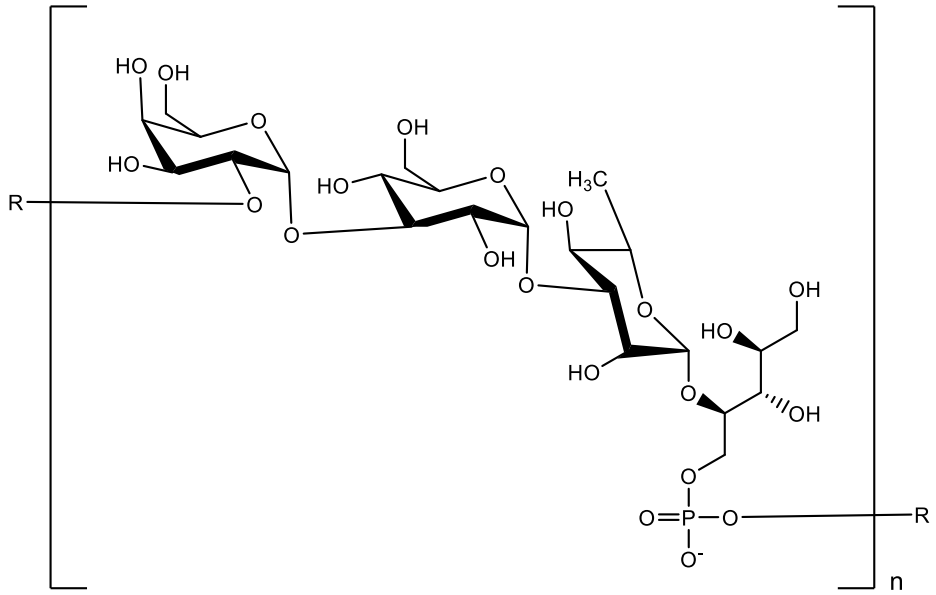

Figure 2.17: Repeat unit of the Pn6B polysaccharide, n>1000.

The maleimide-isocyanate linker N-(5-isocyanatopentyl)maleimide (**2.23**) was prepared for the functionalisation of Pn6B (**2.24**, **Figure 2.18**). 6-Maleimidohexanoic acid (0.25 g, **2.22**) was dissolved in anhydrous THF (4 mL) containing triethylamine (0.3 mL). Diphenylphosphoryl azide (0.38 mL) was added and the reaction was stirred at room temperature for 2 hours. Anhydrous toluene (100 mL) was subsequently added and the solution was concentrated to a volume of 5 mL. The solution was heated at 70 °C for 2 hours and then allowed to cool back to room temperature, followed by a silica gel chromatography purification step to produce N-(5-isocyanatopentyl)maleimide (**2.23**) in a 51 % yield (**Figure 2.18**).

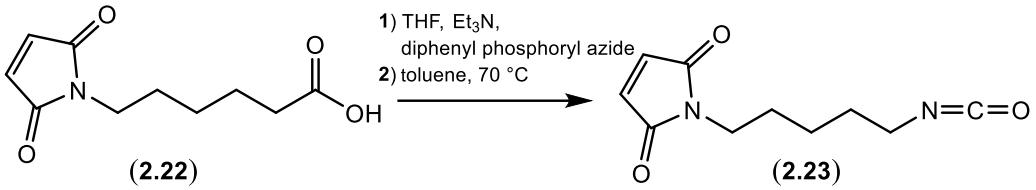

Figure 2.18: Synthesis of N-(5-isocyanatopentyl)maleimide (**2.23**).

Pn6B (10 mg) was added to 2 mL of water and stirred at room temperature until the carbohydrate dissolved. The viscous solution was then loaded onto an ion exchange column (tetrabutylammonium form) and incubated for 30 minutes before elution. The fractions containing carbohydrate as a tetrabutylammonium salt were pooled and subsequently lyophilised to yield a white solid (9.4 mg). The white solid was added to 4 mL of anhydrous DMSO and stirred at 30 °C under N_2 overnight to dissolve the carbohydrate.

An anhydrous DMSO solution (0.5 mL) containing **2.23** (3 mg) was added to a solution of Pn6B (9.4 mg) in anhydrous DMSO (4 mL) and allowed to stir for 2 hours at room temperature. The solution was transferred to a dialysis bag (12-14 kDa cut-off) and dialysed against 5 litres of 0.1 M sodium phosphate buffer (pH = 7), followed by 5 litres of 0.01 M sodium phosphate buffer (pH = 7), 3) and finally 5 litres of water. The solution within the dialysis bag was frozen and lyophilised to yield 6 mg of white solid (**2.24**, **Figure 2.19**). A portion of product (0.5 mg) was analysed by NMR spectroscopy to determine the maleimide/carbohydrate ratio. The amount of maleimide incorporated was estimated as being 2 % by comparing the integrals representing the maleimide alkene protons to the methyl protons of the rhamnose moiety of the carbohydrate.

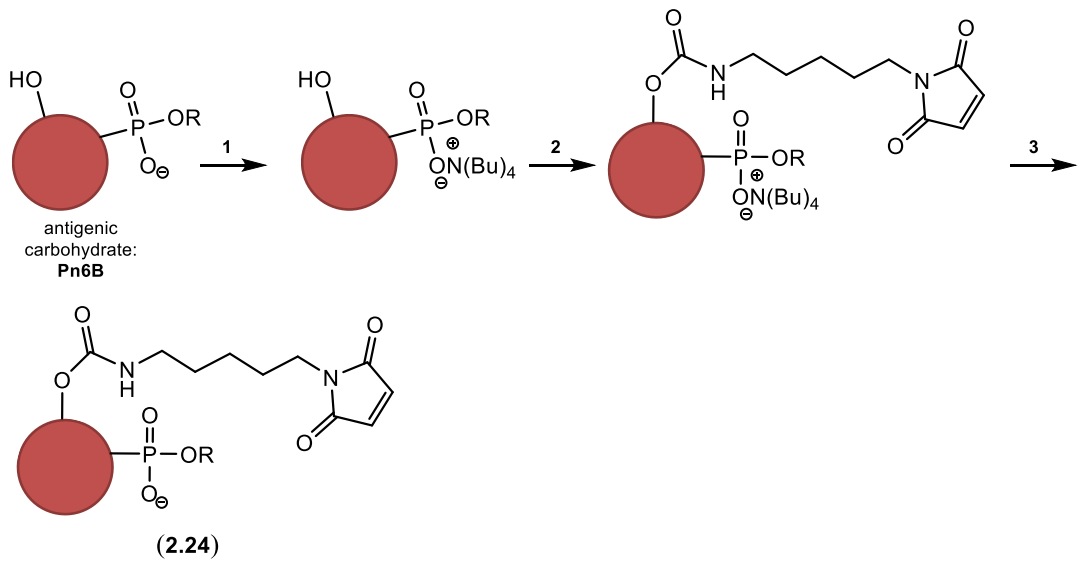

(**2.24**)

Figure 2.19: Maleimide functionalisation of Pn6B (**2.24**). **1**) Dowex 50X4-200 (tBu_4N+), **2**) (**2.23**), DMSO, **3**) dialysis **a**) 0.1 M sodium phosphate buffer, pH = 7, **b**) 0.01 M sodium phosphate buffer, pH =7, **c**) water, **d**) lyophilisation.

The maleimide-functionalised polysaccharide was dissolved in deuterium oxide for the acquisition of a ^{31}P NMR spectrum. A characteristic peak for the phosphate functional group of the Pn6B repeat unit was identified at δ -0.08 ppm in the ^{31}P NMR spectrum. A sample of maleimide functionalised Pn6B polysaccharide was subsequently dissolved in water containing TCEP and incubated at room temperature for 1 hour. The polysaccharide was then extensively purified using gel filtration chromatography and subsequently lyophilised. The product was resuspended in deuterium oxide and analysed by ^{31}P NMR spectroscopy. The peak representing the phosphate functional group within the repeat unit of Pn6B was still identifiable, along with the appearance of a new peak at δ 38.4 ppm, which is a characteristic chemical shift for the ylene product observed previously between maleimide and TCEP. This result provides clear evidence for the necessity of TCEP removal prior to addition of maleimide-functionalised ligands, especially in the context of conjugate vaccine production.

2.7) Conclusions

Trialkylphosphines such as TCEP and THPP are effective disulfide reducing agents but are reactive with Michael acceptors such as maleimide and vinyl sulfone. TCEP and THPP have been found to react with maleimide to produce different products. TCEP reacts with maleimide to produce a stable ylene adduct that is resistant to nucleophilic attack by thiols. THPP reduces maleimide to succinimide which could significantly reduce yields during the bioconjugation process. TCEP reacts with vinyl sulfone to generate a speculated penta co-ordinate phosphorus product, while THPP reacts with vinyl sulfone to produce a complex mixture of products. These reactions may also lower yields during bioconjugate production and may also complicate purification protocols. It is clearly evident that both the reducing agents need to be completely removed before the alkylating reagents are added to the reaction. Towards this aim, a method for '*in situ*' removal of phosphine reducing agents prior to addition of alkylating reagents is explored in Chapter 3.

Chapter 3: A Novel Method for Thiol-Alkylation Reactions Involving *in situ* Reduction of Trialkylphosphines

3.0) Introduction

Our previous work demonstrated that both TCEP and THPP react with Michael acceptor thiol alkylating reagents such as maleimide and vinyl sulfone (**Chapter 2**), which clearly indicates the need for complete consumption or removal of TCEP or THPP prior to the bioconjugation reactions being performed. Currently, the consumption or removal of the TCEP or THPP is achieved using a number of methods.

The use of an excess of alkylating reagent with respect to amount of TCEP or THPP present in the reaction ensures consumption of the reducing agent, while still enabling a successful alkylation reaction [108]. The addition of excess alkylating reagent offers a simple protocol to consume the disulfide reducing agent prior to thiol-alkylation reactions. The method does, however, require consumption of thiol-alkylating ligands that may be expensive to synthesise or purchase, which would be the case for ADC production. The previous addition of excess alkylating reagent by other groups may be a reason why the reaction of TCEP (or THPP) with thiol-alkylating reagents are often overlooked [123].

Another potential problem with not removing the reducing agent is the possibility of the trialkylphosphine forming a covalent adduct with a biomolecule derivatised with an alkylating functional group such as maleimide. The covalent adduct may compromise the bioconjugate's structure or function. **Chapter 2** demonstrated this pitfall within the context of conjugate vaccine production, where an adduct between TCEP and a maleimide derivatised antigenic carbohydrate (Pn6B) was observed.

Excess reducing reagents may also be removed using purification techniques such as dialysis or gel filtration, however, the inclusion of a purification step to remove the reducing agent may affect the time and cost of production, especially when applied to a commercial scale. This purification step can contribute to a decrease in yields, as the freshly reduced disulfide of the biomolecule is potentially exposed to oxidising conditions. Exposure to oxygen is especially applicable to dialysis, which often requires an extensive incubation period for effective dialytic removal of the reducing agent. Gel filtration potentially offers a more rapid approach for reducing agent removal, therefore, minimising exposure of the thiols to oxidative conditions, however, gel filtration is not always effective in removing reducing agents such as TCEP. TCEP is reported to form high molecular weight oligomers, which co-elute with the proteins of interest during gel filtration [109].

Commercially available TCEP on solid support potentially offers a strategy for the effective reduction of disulfides, followed by rapid removal of the solid support by centrifugation or filtration prior to addition of thiol alkylating reagents. The potential to rapidly remove TCEP on solid support can minimise exposure of the reduced disulfides to oxidative conditions, therefore, promoting high yielding thiol alkylation reactions. There is, however, literature which claims a low recovery of peptides after utilising TCEP on solid support to reduce disulfides. The low peptide recovery is attributed to binding of the peptides to the solid support [136].

The methods mentioned above to remove excess disulfide reducing agents have been shown to possess some limitations. As such we sought to develop an alternative method to consume excess TCEP or THPP *in situ*, which does not interfere with thiol alkylation reactions. Here, the Staudinger reaction is explored as a potential protocol to oxidise excess TCEP or THPP prior to the addition of maleimide or vinyl sulfone ligands to alkylate thiols.

The use of the Staudinger reaction could provide a protocol that eliminates dialysis or gel filtration to remove TCEP or THPP, therefore minimising the exposure of reduced disulfides to oxidative conditions.

TCEP has already been previously shown to react through a Staudinger mechanism with azides under aqueous conditions. [137, 138]. The Staudinger reaction was, therefore, utilised to develop a novel 'one-pot' protocol to oxidise excess TCEP or THPP followed by a thiol alkylation reaction.

3.1) Addition of a Water Soluble Alkyl Azide to Oxidise Excess TCEP or THPP after the Reduction of Disulfides

The Staudinger reaction was first reported by Staudinger, H. and Meyer J. in 1919, where a reaction between phenyl azide and triphenylphoshine was found to generate an iminophosphorane and nitrogen gas [60]. The iminophosphorane, under aqueous conditions, can be hydrolysed to generate phosphine oxide and an alkyl amine (**Figure 3.1**).

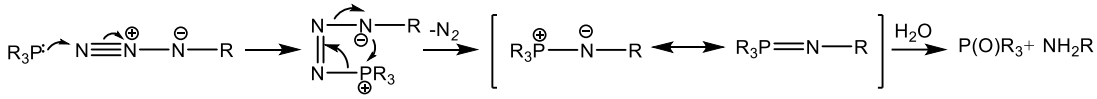

Figure 3.1: Mechanism for the Staudinger reaction. A tri-substituted phosphine reacts with an alkyl azide to generate a phosphazide, which loses N_2 to form an iminophosphorane intermediate. An aqueous work-up results in an alkyl amine and a trisubstituted phosphine oxide derivative. R = alkyl or aryl.

We considered that the addition of a water soluble alkyl azide, following the reduction of disulfides by trialkylphosphine reducing agents (TCEP or THPP) should facilitate oxidation of the excess trialkylphosphine to trialkylphosphine oxide, generating nitrogen gas and an alkyl amine as products. The trialkylphosphine oxide should no longer react with alkylating reagents such as maleimide and vinyl sulfone. The alkyl amine product should also not react with alkylating reagents such as maleimide and vinyl sulfone providing the reactions are performed at pH < 8.5.

It was envisaged to test the ability of a water soluble alkyl azide to oxidise excess TCEP or THPP after a disulfide reduction step of cysteine derivatives, followed by the addition of a maleimide derivative to effect thiol alkylation. Derivatives of

cysteine were initially chosen for ease of purification, with the hope to quantify yields of the thiol alkylated products.

Commercially available L-cysteine ethyl ester hydrochloride salt, which can exist as a dimer **3.1a**, was dissolved in phosphate buffer at neutral pH, containing excess (3 eq.) TCEP (**2.6**) to reduce any potential disulfides (**Figure 3.2**, **A**), generating the monomeric form of the amino acid **3.2a**. The reaction was left for 30 minutes at room temperature. Initially, 1,14-diazido-3,6,9,12-tetraoxatetradecane (**3.3**) was not added to oxidise excess TCEP to TCEP oxide (**3.4**). N-ethyl maleimide (**2.8**) was added and the reaction incubated at room temperature for 30 minutes (**Figure 3.2**, **C**). Purification of the reaction by either silica gel or C-18 chromatography proved unsuccessful due to the polarity of reagents and products. The reaction was therefore analysed by HRMS. The negative ion mass spectrum revealed the presence of a number of compounds, including unreacted TCEP (**2.6**), TCEP oxide (**3.4**) and the ylene adduct between TCEP and N-ethyl maleimide (**Chapter 2**, **2.9**). The positive ion mass spectrum revealed the presence of the intended product, ethyl S-[(3*R,S*)-1-ethyl-2,5-dioxopyrrolidin-3-yl]-L-cysteinate (**3.7a**). The HRMS data provided clear evidence of nucleophilic competition between TCEP (**2.6**) and cysteine thiol of **3.2** for the alkene of N-ethyl maleimide (**2.8**).

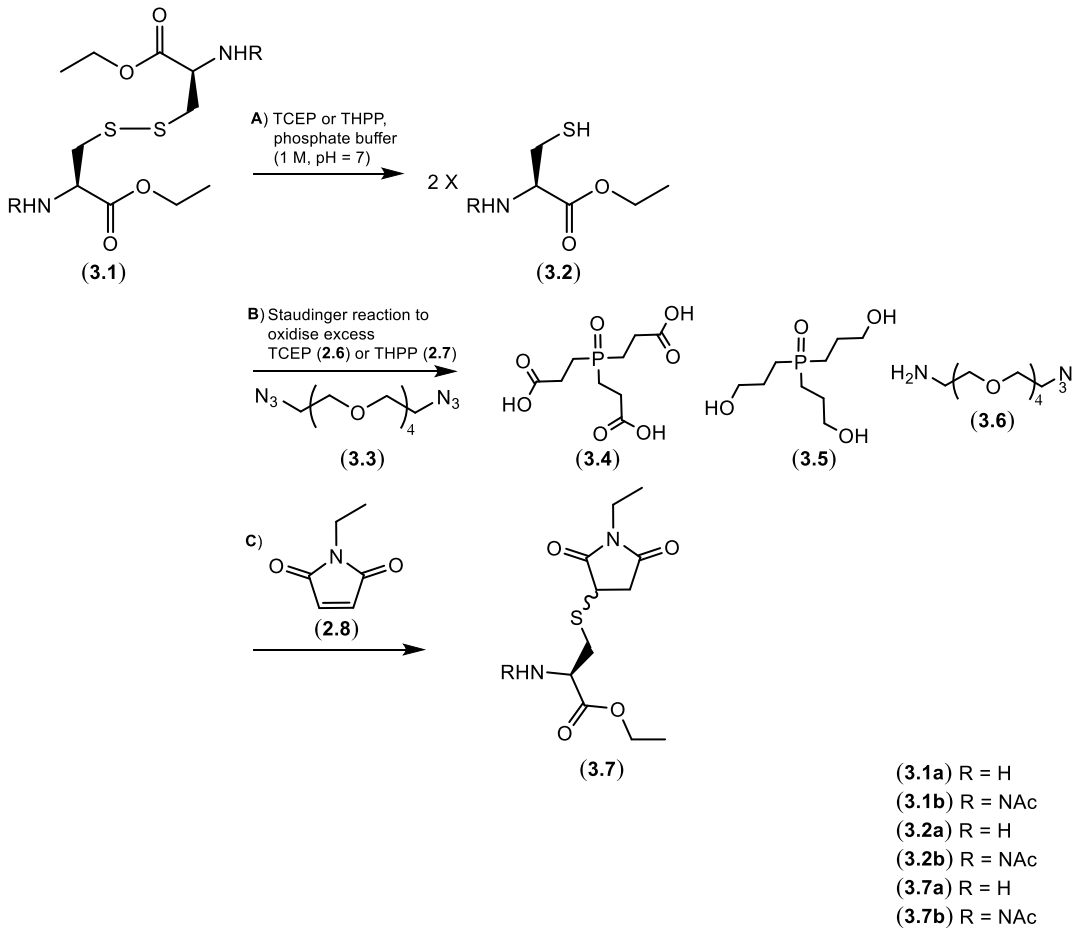

Figure 3.2: Assessment of the ability of the water soluble alkyl azide **3.3** to oxidise excess reducing agents (TCEP or THPP) prior to thiol alkylation of L-cysteine derivatives **3.2a** & **3.2b** by N-ethyl maleimide (**2.8**). **A**) The oxidised amino acid **3.1** was reduced to monomers **3.2a** or **3.2b** by the addition of either TCEP or THPP. **B**) The alkyl azide **3.3** was added to oxidise excess TCEP or THPP. **C**) N-ethyl maleimide (**2.8**) was added to thiol alkylate **3.2a** or **3.2b**, generating **3.7a** & **3.7b**.

The above reaction was repeated, this time, with the addition of 3 equivalents of alkyl azide **3.3** (**Figure 3.2 B**) to oxidise excess TCEP (**2.6**) to TCEP oxide (**3.4**) prior to the addition of N-ethyl maleimide (**2.8**, **Figure 3.2 C**). The reaction was subsequently investigated by HRMS and analysis of the negative ion mass spectrum confirmed the complete oxidation of TCEP (**2.6**) to TCEP oxide (**3.4**). There was also no detection of TCEP-maleimide ylene adduct **2.9**. The mass spectrum confirmed the presence of intended product **3.7a**, the mono-reduced azide **3.6** and unreacted azide **3.3**. This experiment proved the potential of a water soluble azide to

completely oxidise TCEP (**2.6**) to TCEP oxide (**3.4**), resulting in a thiol alkylated amino acid **3.7a** and no detection of a TCEP-maleimide adduct **2.9**.

The water soluble azide **3.3** was subsequently tested to potentially oxidise excess THPP (**2.7**) to THPP oxide (**3.5**) prior to maleimide alkylation of L-cysteine ethyl ester (**3.2a**). L-Cysteine ethyl ester hydrochloride salt (**3.1**) was dissolved in phosphate buffer at neutral pH containing excess (3 eq.) THPP (**2.7**) to reduce any potential disulfides and incubated at room temperature for 30 minutes (**Figure 3.2, A**). Initially the alkyl azide **3.3** was not added to oxidise excess THPP (**2.7**) to THPP oxide (**3.5**). N-Ethyl maleimide (**2.8**) was added and the reaction was incubated at room temperature for 30 minutes (**Figure 3.2**, **C**). Purification of the reaction by either silica gel or C-18 chromatography proved unsuccessful due to the polarity of reagents and products. The reaction was, therefore, analysed by HRMS. The positive ion mass spectrum revealed the presence of unreacted THPP (**2.7**) and THPP oxide (**3.5**). The unwanted reduction of N-ethyl maleimide to N-ethyl succinimide (**2.15**, **Chapter 2**) by THPP was also observed. The intended product **3.7a** was also observed in the HRMS. The experiment provides clear evidence of nucleophilic competition between THPP (**2.7**) and cysteine thiol of **3.2a** for the alkene of N-maleimide (**2.8**).

The reaction described was repeated, this time, with the addition of 3 equivalents of alkyl azide (**3.3**, **Figure 3.2**, **B**) to oxidise excess THPP (**2.7**) prior to the addition of N-ethyl maleimide (**2.8**, **Figure 3.2 C**). The reaction was subsequently analysed by HRMS. The positive ion mass spectrum confirmed the presence of THPP oxide (**3.5**), the intended product **3.7a** and mono-reduced azide **3.6**. No reduction of N-ethyl maleimide to N-ethyl succinimide (**2.15**) or excess THPP (**2.7**) was observed in the HRMS. The HRMS experiment proved the ability of a water soluble alkyl azide to completely oxidise THPP to THPP oxide, resulting in a thiol alkylated amino acid and no detection of maleimide reduction to succinimide by THPP.

We sought to quantify yields of a maleimide alkylated amino acid with and without the use of the alkyl azide **3.3** to oxidise excess TCEP or THPP in the reaction. N-acetyl-L-cysteine methyl ester (**3.1b**, **Figure 3.2**) was therefore chosen as a substrate for thiol alkylation as it is more amenable to silica gel purification due to the derivatisation of both its amino and carboxylic acid functional groups.

The experiments involved the dissolution of N-acetyl-L-cysteine methyl ester dimer (**3.1b**) in THF and Tris buffer (0.5 M, pH = 7.2), containing excess (5 eq.) TCEP (**2.6**) or THPP (**2.7**) and incubation for 30 minutes at room temperature. Initially, the excess reducing agents were not oxidised to phosphine oxides by the alkyl azide **3.3** prior to addition of N-ethyl maleimide (**2.8**). N-Ethyl maleimide (**2.8,** 1.1 eq.) was added and the reactions were incubated at room temperature for 1 hour. The reactions were subsequently purified by silica gel chromatography to access the yields of methyl *N*-acetyl-S-[(3*R,S*)-1-ethyl-2,5-dioxopyrrolidin-3-yl]-L-cysteinate (**3.7b**) formation (**Table 3.1**, **No. 1 & 2**). Poor yields of **3.7b** were observed for both reactions carried out in the absence of alkyl azide **3.3**. The reaction where TCEP was utilised, and the excess was not oxidised by the addition of **3.3**, resulted in a low yield of **3.7b** of 27 %, following the addition of N-ethyl maleimide. A similarly low yield of **3.7b** of 21 % was achieved following purification of the reaction where excess THPP was not oxidised by addition of **3.3** prior to the addition of N-ethyl maleimide.

The reactions were subsequently repeated, but with the addition of excess (10 eq.) alkyl azide **3.3** to oxidise TCEP or THPP prior to the addition of N-ethyl maleimide (**2.8**). Purification of both the reactions and quantification of **3.7b** was performed. Significant yield improvements were observed for both reactions, with a 74 % yield of **3.7b** for the reaction utilising TCEP and a 69 % yield of **3.7b** for the reaction utilising THPP (**Table 3.1, No. 3** & **4**). The experiments suggested that TCEP and THPP can be oxidised to trialkylphosphine oxides *in situ* through the addition of a water soluble alkyl azide **3.3**. Maleimide can, subsequently, be added directly to the

azide-treated reaction, resulting in significantly improved yields of thiol alkylated products.

Reaction	Reducing Agent	Alkyl Azide (3.3)	Yield of (3.7b) (%)
1	TCEP	-	27
2	THPP	-	21
3	TCEP	+	74
4	THPP	+	69

Table 3.1: Summary of yields for **3.7b** with and without trialkylphosphine (TCEP or THPP) oxidation by alkyl azide **3.3**.

3.2) Investigating the Potential Reaction of Maleimide with Alkyl Azide 3.3

Although the addition of a water soluble azide to oxidise excess TCEP or THPP proved to be an effective method for effecting high yields of maleimide-alkylated products, it was also considered necessary to investigate the possibility of a reaction between maleimide and the alkyl azide **3.3**, as it could potentially lead to reduced yields of conjugate.

N-Ethyl maleimide (**2.8,** 5 mg) was incubated with equimolar alkyl azide **3.3** in deuterium oxide and monitored by ^{1}H NMR spectroscopy. After 16 hours incubation at room temperature, the ^{1}H NMR spectrum exhibited signs of product formation

by the appearance of doublets at δ 4.68 and 5.61 ppm with coupling constants of 11 Hz. The appearance of these signals was an indication of a potential reaction between N-ethyl maleimide (**2.8**) and alkyl azide **3.3**.

The observation was further investigated by scaling up the reaction and monitored by thin layer chromatography (TLC). The alkyl azide **3.3** (50 mg) was dissolved in phosphate buffer (0.1 M, pH = 7, 2 mL) containing N-ethyl maleimide (**2.8**, 1.5 eq., 32.6 mg) and left to stir at room temperature. The appearance of product was extremely slow and so the reaction was left to stir for 2.5 days. After 2.5 days a second product was detectable by TLC. Purification of the reaction by silica gel chromatography resulted in the isolation of triazoline derivatives 1-(14-azido-3,6,9,12-tetraoxatetradec-1-yl)-5-ethyl-3a,6a-dihydropyrrolo[3,4-d][1,2,3]triazole-4,6(1H,5H)-dione (**3.8**) in 42 % yield and 1,1'-(3,6,9,12-tetraoxatetradecane-1,14-diyl)bis(5-ethyl-3a,6a-dihydropyrrolo[3,4-*d*][1,2,3]triazole-4,6(1*H*,5*H*)-dione) (**3.9**) in 25 % yield (**Figure 3.3**). The formation of the two products **3.8** and **3.9** appears to occur *via* a [3+2] cycloaddition between the maleimide and azide functional groups. The cycloaddition reaction between an alkyl azide and a maleimide functional group is reported in the literature, although it was performed in an organic solvent and under reflux conditions [139].

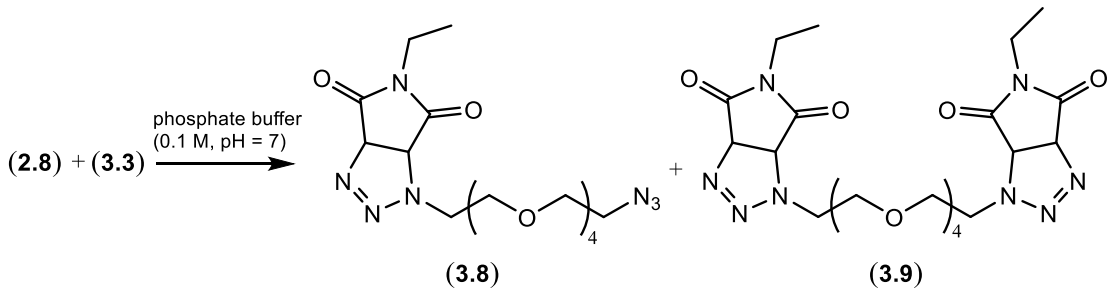

Figure 3.3: Reaction of N-ethyl maleimide (**2.8**) with the alkyl azide **3.3** to generate triazoline derivatives **3.8** and **3.9**.

The low rate of triazoline formation is advantageous as it minimises potential interference with the reaction between the alkyl azide **3.3** and the trialkylphosphines TCEP and THPP prior to maleimide-based thiol alkylation reactions. The reaction between thiols and maleimide is extremely rapid hence thiols should out-compete the azide for addition to maleimide. This was confirmed by the absence of triazoline derivatives in the experiments performed in previous **section 3.1**, but required further validation through additional experiments. NMR and MS spectrometry experiments were designed to confirm that a thiol addition to maleimide would outcompete any possible triazoline formation through the reaction of the alkyl azide **3.3** with N-ethyl maleimide (**2.8**).

Initially N-ethyl maleimide (**2.8**, 1 mM) was dissolved in deuterated phosphate buffer (0.5 M, pH = 7.2) and analysed by ^{1}H NMR spectroscopy to verify the detection of the signature singlet at δ ~7 ppm representing the alkene protons of the maleimide ring. The experiment was also performed to test the sensitivity of the NMR instrument to analyse the dilute solution. Analysis of the ^{1}H NMR spectrum did confirm the presence of the singlet of the alkene protons at δ 6.75 ppm. Reduced glutathione (**2.21**, 1 mM), a tripeptide containing a cysteine residue, was added to the solution of N-ethyl maleimide (**2.8**) and immediately analysed by ^{1}H NMR spectroscopy. The ^{1}H NMR spectrum showed complete disappearance of the singlet representing the maleimide alkene protons, which was confirmation of a rapid reaction between N-ethyl maleimide (**2.8**) and glutathione (**2.21**). The thiol

alkylated peptide **3.10** was also confirmed by HRMS (**Figure 3.4,** *m/z* 433.1381 ($M\text{-}H^+$)).

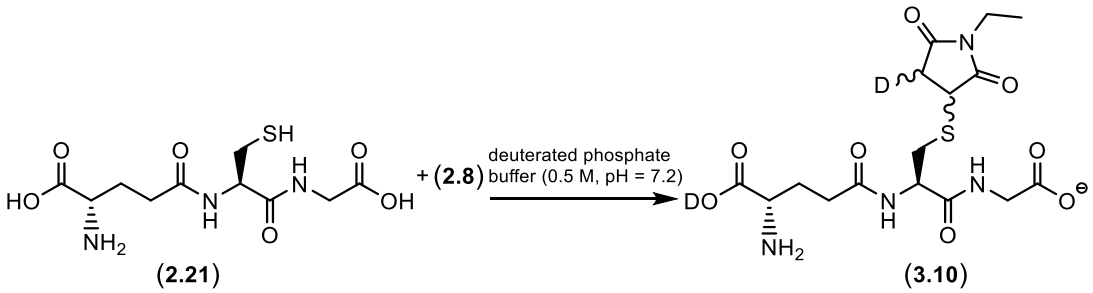

Figure 3.4: Reaction of glutathione (**2.21**) with N-ethyl maleimide (**2.8**) in a deuterated buffer to yield **3.10**.

An experiment was subsequently performed to prove the superior reaction rate of a thiol addition to maleimide over the [3+2] cycloaddition of the alkyl azide **3.3** to maleimide. Reduced glutathione (**2.21**, 1 eq.) was dissolved in deuterated phosphate buffer (0.5 M, pH = 7.2), containing alkyl azide **3.3** (50 eq.). N-Ethyl maleimide (**2.8**, 1 eq.) was subsequently added and the reaction was immediately analysed by ^{1}H NMR spectroscopy. The ^{1}H NMR spectrum showed complete disappearance of the singlet representing the maleimide alkene protons, which confirmed the consumption of N-ethyl maleimide. There was no evidence in the ^{1}H NMR spectrum of a pair of doublets at $\delta \sim 4.68$ and ~ 5.61 ppm with coupling constants of 11 Hz, which would have been a positive indication of triazoline formation. The above observations proved that reduced thiols react much more rapidly with maleimide than the water soluble alkyl azide, even when the alkyl azide is at a 50 fold excess to the thiol. The evidence was further validated by HRMS analysis. The identification of a maleimide derivatised peptide **3.10** (*m/z* 433.1375 ($M\text{-}H^+$)) and the absence of any peaks in the HRMS spectrum representing triazoline derivatives supported the evidence provided by the ^{1}H NMR data (**Figure 3.5**).

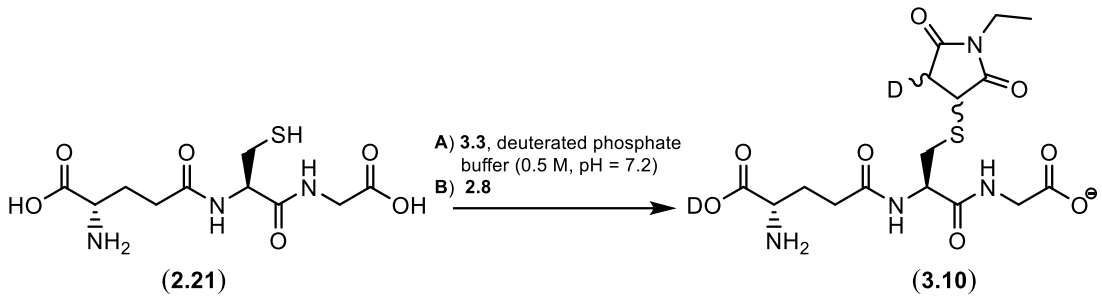

Figure 3.5: **A**) Glutathione (**2.21**) and alkyl azide **3.3** were initially dissolved in deuterated buffer. **B**) N-ethyl maleimide (**2.8**) was added to the solution and the reaction was subsequently analysed by NMR spectroscopy and MS. The thiol alkylated peptide **3.10** was confirmed by MS, while no reaction between N-ethyl maleimide (**2.8**) and alkyl azide **3.3** was observed by either NMR spectroscopy or MS.

NMR experiments were subsequently performed to determine the rate of triazoline formation between maleimide derivatives and the alkyl azide **3.3**. Either N-ethyl maleimide (**2.8**, 1 eq.) or maleimide-PEG2kDa (1 eq.) was dissolved in deuterated phosphate buffer (0.5 M, pH = 7.2) containing the alkyl azide **3.3** (100 eq.). The reactions were monitored by ^{1}H NMR spectroscopy at room temperature (**Graph 3.1**), through the consumption of maleimide (diminishing singlet representing the alkene protons of the maleimide ring) and the appearance of triazoline product (increasing appearance of doublets representing the bridgehead protons). A plot of the data revealed a 50 % consumption of N-ethyl maleimide (**2.8**) after 11.3 hours and 50 % consumption of maleimide-PEG2kDa after 10.7 hours (**Graph 3.1**). Analysis of the experiment indicated that triazoline formation is very slow, when comparing to a reaction between maleimide and thiols, which is too rapid to be analysed by NMR spectroscopy. The potential triazoline formation should not interfere with the rapid thiol alkylation reaction utilising maleimide chemistry.

The accumulated NMR and MS data has indicated that triazoline formation does not interfere with bioconjugation between a thiol and a maleimide functional group, even with the water soluble alkyl azide present in a vast excess to the thiol functional group. The addition of a water soluble alkyl azide, therefore, offers a

simple solution to oxidising excess phosphine-based disulfide reducing agents prior to alkylation using maleimide chemistry.

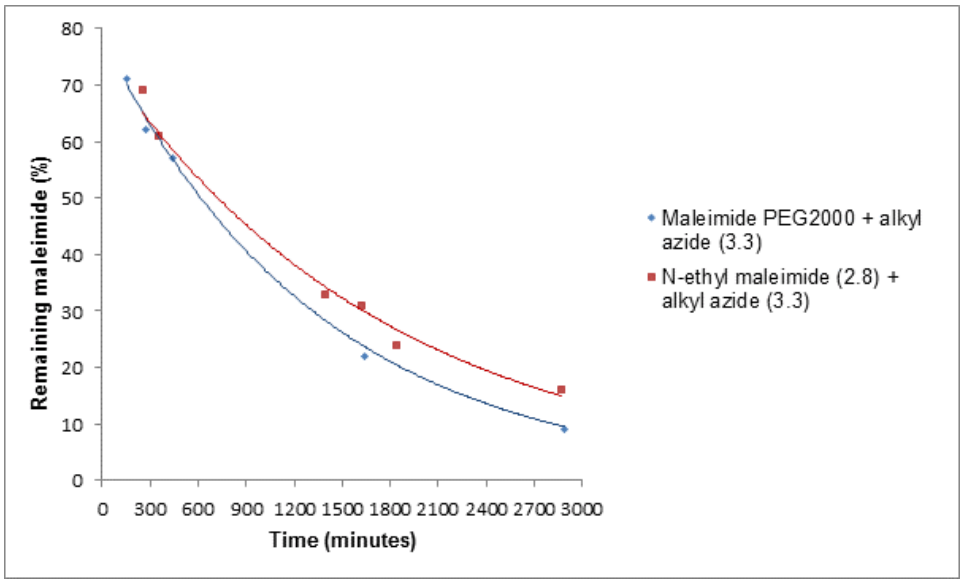

Graph 3.1: Consumption of maleimide derivatised ligands through triazoline formation with the alkyl azide **3.3**.

3.3) Reaction of a Vinyl Sulfone Functional Group with the Alkyl Azide 3.3

As discussed earlier, vinyl sulfone derivatives are also utilised as Michael acceptors for the alkylation of thiol-containing molecules. As such, we next investigated the potential reaction of the alkyl azide **3.3** with a vinyl sulfone functional group, following the earlier observation that the Michael acceptor, N-ethyl maleimide (**2.8**) reacted with **3.3** to form triazoline derivatives **3.8** and **3.9**. The possible reaction of **3.3** with vinyl sulfone was explored because it was envisaged to potentially use **3.3** as a reagent to oxidise excess TCEP or THPP prior to addition vinyl sulfone derivatives to alkylate thiols.

The alkyl azide **3.3** (110 mg) was dissolved in THF (2 mL) and water (8 mL), containing phenyl vinyl sulfone (**2.18**, 2 eq., 128 mg) and stirred at room temperature (**Figure 3.6**). The appearance of a product (TLC analysis) was extremely slow and so the reaction was allowed to stir for 4 days. Purification of the reaction

by silica gel chromatography resulted in the isolation of the triazoline derivative 1-(14-azido-3,6,9,12-tetraoxatetradecan-1-yl)-4-(benzenesulfonyl)-4,5-dihydro-1H-1,2,3-triazole (**3.11**) in 59 % yield (**Figure 3.7**). However, unlike the analogous reaction with N-ethyl maleimide, here no di-triazoline derivative was isolated.

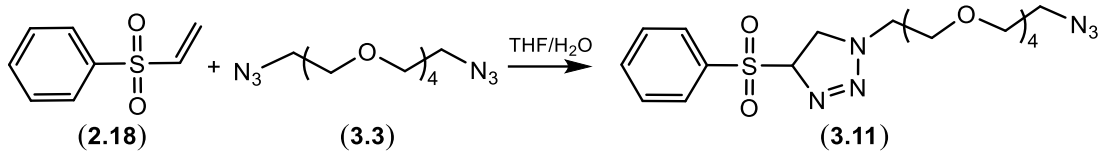

Figure 3.6: Reaction of phenyl vinyl sulfone (**2.18**) with the alkyl azide **3.3** to generate the triazoline derivative **3.11**.

The [3+2] cycloaddition reaction of phenyl vinyl sulfone (**2.18**) with the alkyl azide **3.3** appeared to be much slower than that of N-ethyl maleimide with the alkyl azide **3.3**. The slower rate implied that utilisation of the alkyl azide **3.3** for trialkylphosphine oxidation should also be compatible to vinyl sulfone-based chemistry, with little chance of triazoline formation occurring, given the rate difference.

To demonstrate this, glutathione (**2.21**, 1 eq.) was incubated with the alkyl azide **3.3** (50 eq.) in deuterated phosphate buffer (0.5 M, pH = 7.2), followed by the addition of phenyl vinyl sulfone (**2.18**, 1 eq.). The reaction was monitored by ^{1}H NMR spectroscopy and HRMS. Analysis of the ^{1}H NMR spectra revealed the absence of peaks representing the vinyl protons, which indicated that phenyl vinyl sulfone had undergone a reaction, possibly to glutathione, which was confirmed by HRMS (**3.12**, **Figure 3.7**). There was no evidence of triazoline formation in the ^{1}H NMR spectrum or HRMS spectrum. The alkyl azide **3.3**, therefore, can be added to a conjugation reaction to oxidise excess TCEP or THPP when utilising vinyl sulfone derivatised ligands to alkylate thiols.

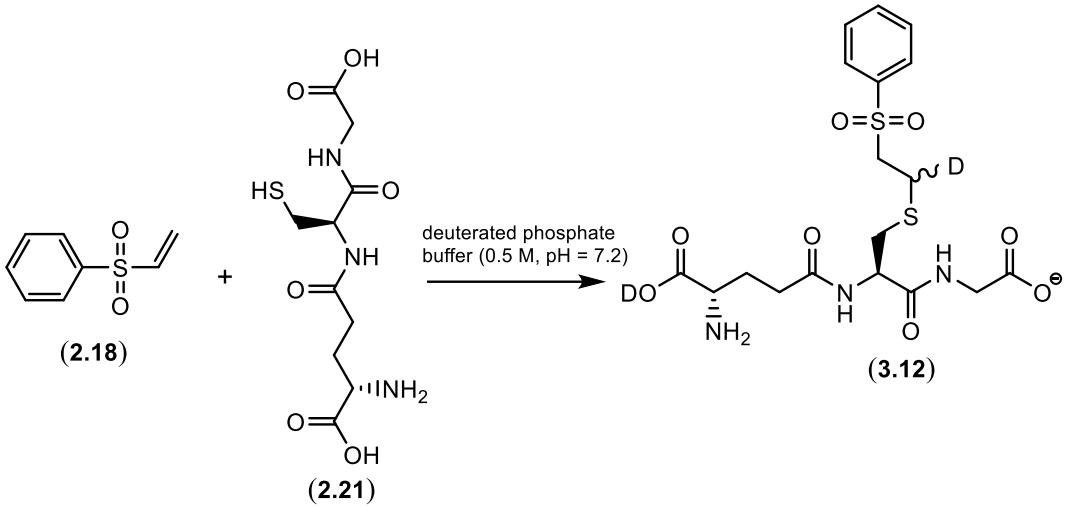

Figure 3.7: Reaction of phenyl vinyl sulfone (**2.18**) with glutathione (**2.21**) to generate the thiol alkylated peptide **3.12**.

3.4) Addition of the Water Soluble Alkyl Azide 3.3 to Oxidise Excess TCEP or THPP in Bioconjugation Reactions

The addition of a water soluble alkyl azide could prove a useful technique to achieve the goal of trialkyphosphine oxidation in bioconjugation reactions, without resorting to traditional purification techniques such as dialysis or gel filtration.

3.4.1) TCEP and THPP Oxidation by the Alkyl Azide 3.3 in Bioconjugation Reactions

The incubation time of **3.3** (100 eq.) necessary to oxidise excess TCEP or THPP (10 eq.) prior to addition of maleimide derivatised ligands was explored.

Initially, ^{31}P NMR spectroscopy was utilised to follow the reaction of TCEP (10 eq.) with **3.3** (100 eq.) in Tris buffer (0.5 M, pH = 7.2) by monitoring the disappearance of the peak representing the phosphorus atom of trialkylphosphine and the appearance of the peak representing the phosphorus of trialkylphosphine oxide. ^{31}P NMR spectroscopy proved ineffective in accurately monitoring the reaction due to the poor signal-to-noise ratio of the phosphorus peak of the trialkylphosphine.

HRMS proved an excellent alternative method to monitor the oxidation of trialkylphosphine to trialkylphosphine oxide. TCEP or THPP (10 mM) was incubated with **3.3** (100 mM) in Tris buffer (0.5 M, pH = 7.2) at 37 °C. After 30 minutes the reactions were analysed by HRMS and indicated the complete oxidation of both TCEP and THPP to the corresponding trialkylphosphine oxide products. Incubation of **3.3** (10 eq.) with either TCEP or THPP for 30 minutes at 37 °C was sufficient to oxidise both the reducing agents.

3.4.2) Use of Alkyl Azide 3.3 to Oxidise Excess TCEP or THPP to Ensure High Protein-Maleimide-Fluorescein Conjugate Yields

Protein labelling by maleimide derivatised fluorescent probes has previously been shown by SDS-electrophoresis to significantly decreases as the TCEP concentration increases relative to the fluorescent probe [8] and similar results are presented in **Chapter 2, Figure 2.15**. Yeast enolase was utilised as a model protein for both investigations. It was, therefore, envisaged to utilise yeast enolase and maleimide-fluorescein in experiments where either excess TCEP or THPP would be oxidised by the addition of alkyl azide **3.3** prior to the addition of maleimide-fluorescein to alkylate yeast enolase.

Varying amounts of TCEP (1-10 eq.) were added to aliquots of yeast enolase and incubated for 45 minutes at 25 °C. Commercially available maleimide-fluorescein (1 eq.) was subsequently added and the reactions were incubated at 37 °C for 18 hours (**Figure 3.8**, **lanes 1-3**). In parallel experiments the alkyl azide **3.3** (100 eq.) was added to aliquots of yeast enolase containing varying amounts of TCEP (1-10 eq.). The samples were incubated for 1 hour at 37 °C prior to addition of maleimide-fluorescein (1 eq.) followed by incubation at 37 °C for 18 hours (**Figure 3.8**, **lanes 4-6**).

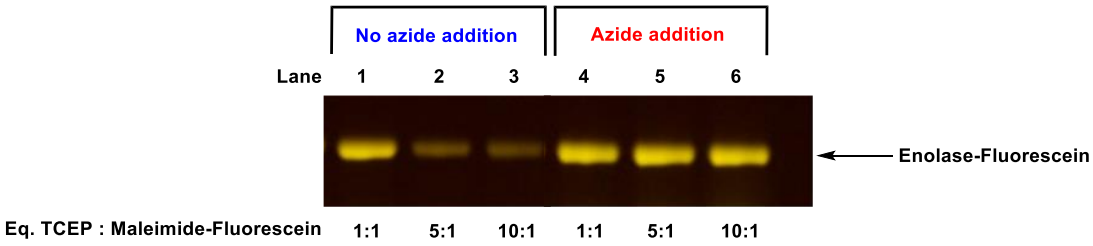

Figure 3.8: SDS-PAGE analysis of reactions between maleimide-fluorescein (1 eq.) and yeast enolase in the presence of varying TCEP amounts (1-10 eq.), in the presence or absence of the alkyl azide **3.3** (100 eq.). **Lane 1:** enolase + TCEP (1 eq.) + maleimide-fluorescein (1 eq.), **Lane 2:** enolase + TCEP (5 eq.) + maleimide-fluorescein (1 eq.), **Lane 3:** enolase + TCEP (10 eq.) + maleimide-fluorescein (1 eq.), **Lane 4:** enolase + TCEP (1 eq.) + **3.3** (100 eq.) + maleimide-fluorescein (1 eq.), **Lane 5:** enolase + TCEP (5 eq.) + **3.3** (100 eq.) + maleimide-fluorescein (1 eq.), **Lane 6:** enolase + TCEP (10 eq.) + **3.3** (100 eq.) + maleimide-fluorescein (1 eq.). The SDS-PAGE gel was analysed utilising Image Studio Lite software.

The SDS gel shows that there is a progressive decrease in the amount of fluorescent bioconjugate as the concentration of TCEP increases relative to the concentration of maleimide-fluorescein as a result of the reaction between TCEP and the maleimide functionalised fluorescent probe (**Figure 3.8**, **Lanes 1-3**). In contrast, the addition of alkyl azide **3.3** results in consistent levels of conjugation (**Figure 3.8**, **Lanes 4-6**). The effectiveness of **3.3** in oxidising TCEP is illustrated in **Graph 3.2** by quantification of the fluorescent bands representing the enolase-fluorescein conjugate. Quantification of the fluorescent bands was achieved by utilising a Licor ODYSSEY® CLx scanner and Image Studio Lite software, which is capable of determining the intensity of the selected bands on the gel. **Graph 3.2** illustrates a consistent level of fluorescent protein conjugate by the addition of alkyl azide **3.3**, regardless of the initial TCEP concentration relative to the concentration of maleimide-fluorescein added. The addition of **3.3** is, therefore, an effective strategy to oxidise TCEP prior to addition of thiol reactive fluorescent probes.

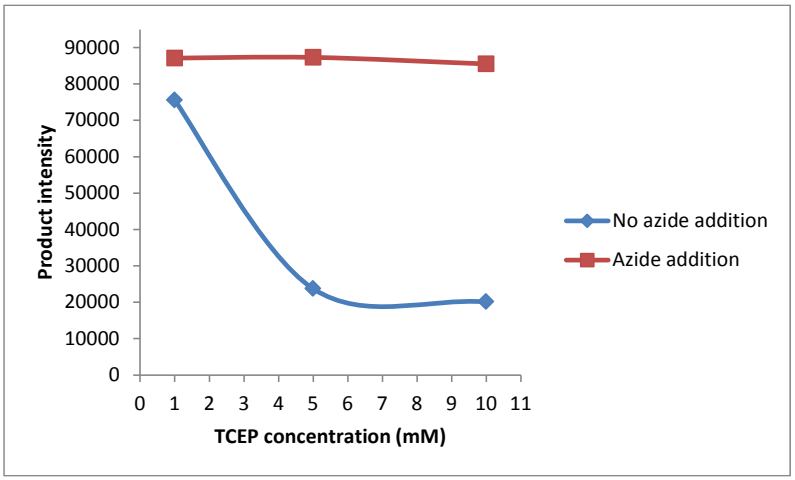

Graph 3.2: Enolase-fluorescein conjugate production with and without the addition of the alkyl azide **3.3** to oxidise TCEP.

The addition of alkyl azide **3.3** to oxidise THPP was investigated using maleimide-fluorescein as the ligand to attach to the thiol-containing yeast enolase protein. Varying concentrations of THPP (1-10 eq.) were added to aliquots of yeast enolase and incubated for 45 minutes at 25 °C. Maleimide-fluorescein (1 eq.) was subsequently added and the reactions were incubated at 37 °C for 18 hours (**Figure 3.9**, **lanes 1**-**3**). In parallel experiments **3.3** (100 eq.) was added to aliquots of enolase containing varying amounts of THPP (1-10 eq.). The samples were incubated for 1 hour at 37 °C prior to addition of maleimide-fluorescein (1 eq.) followed by incubation at 37 °C for 18 hours (**Figure 3.9**, **lanes 4**-**6**).

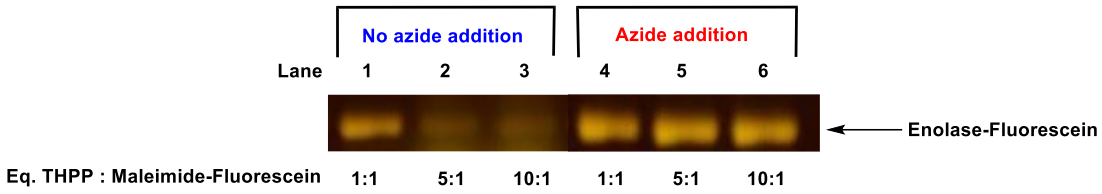

Figure 3.9: SDS-PAGE analysis of reactions between maleimide-fluorescein (1 eq.) and yeast enolase in the presence of varying THPP amounts (1-10 eq.), in the presence or absence of the alkyl azide **3.3** (100 eq.). **Lane 1:** enolase + THPP (1 eq.) + maleimide-fluorescein (1 eq.), **Lane 2:** enolase + THPP (5 eq.) + maleimide-fluorescein (1 eq.), **Lane 3:** enolase + THPP (10 eq.) + maleimide-fluorescein (1 eq.), **Lane 4:** enolase + THPP (1 eq.) + **3.3** (100 eq.) + maleimide-fluorescein (1 eq.), **Lane 5:** enolase + THPP (5 eq.) + **3.3** (100 eq.) + maleimide-fluorescein (1 eq.), **Lane 6:** enolase + THPP (10 eq.) + **3.3** (100 eq.) + maleimide-fluorescein (1 eq.). The SDS-PAGE gel was analysed utilising Image Studio Lite software.

The SDS gel shows that there is a progressive decrease in the amount of fluorescent conjugate as the concentration of THPP increases relative to the concentration of maleimide-fluorescein as a result of the reaction between THPP and the maleimide functionalised probe (**Figure 3.9**, **Lanes 1**-**3**). In contrast, the addition of the alkyl azide **3.3** results in consistent levels of conjugation (**Figure 3.9**, **Lanes 4**-**6**). The effectiveness of **3.3** in oxidising THPP is illustrated in **Graph 3.3**, showing a consistent level of fluorescent protein conjugate, regardless of the initial THPP concentration relative to concentration of the maleimide-fluorescein added. The addition of **3.3** is, therefore, an effective strategy to oxidise THPP prior to addition of thiol reactive fluorescent probes.

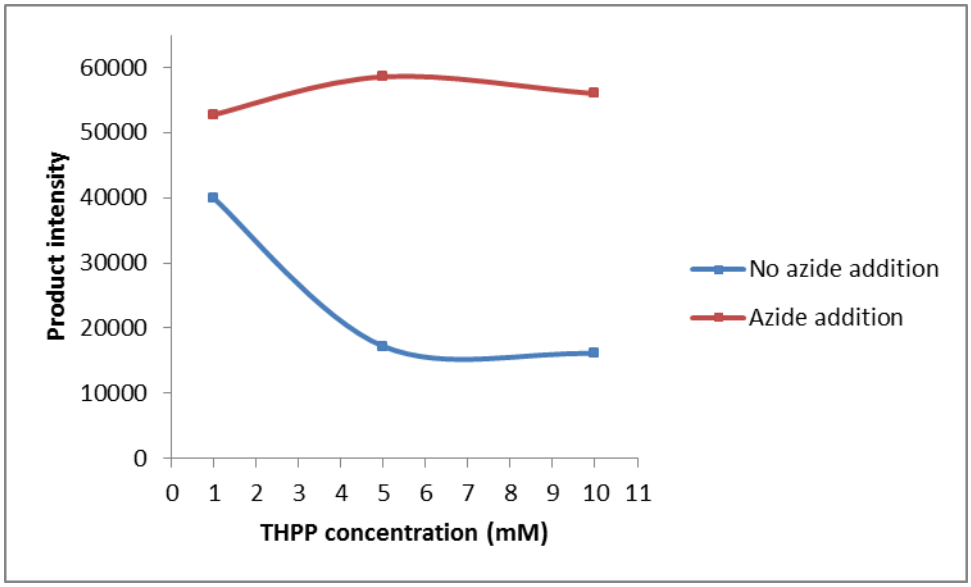

Graph 3.3: Enolase-fluorescein conjugate production with and without the addition of the alkyl azide **3.3** to oxidise excess THPP.

Here we have shown that the presence of TCEP or THPP in solution with maleimide functionalised ligands reduces the yields of conjugate production. The addition of a water alkyl azide oxidises these disulfide reducing agents, which no longer react with maleimide, enabling consistent conjugation to the denatured protein.

The addition of alkyl azide **3.3** to oxidise TCEP or THPP prior to thiol alkylation of a folded protein was subsequently investigated. The experiments were pursued to illustrate the usefulness of the method for trilakylphosphine oxidation in non-denaturing conditions, and the potential of the method to facilitate the production of high yielding, folded protein conjugates.

Experiments were performed on the folded protein, Staphylococcus aureus binder of immunoglobulins ($Sbi_{3,4\text{-}Cys}$). $Sbi_{3,4\text{-}Cys}$ is a 15 kDa protein with a single C-terminal cysteine residue. The thiol of the cysteine residue is solvent-exposed, therefore, denaturing conditions are not required to effect bioconjugations *via* thiol-alkylation. Pre-reduction of the protein is, however, necessary to reduce the disulfide bonds that can form dimers of the protein.

Varying amounts of TCEP (1-10 eq.) were added to aliquots of $Sbi_{3,4\text{-}Cys}$ and incubated for 45 minutes at 25 °C. Maleimide-fluorescein (1 eq.) was subsequently added and the reactions were incubated at 37 °C for 18 hours (**Figure 3.10**, **lanes 1-3**). In parallel experiments **3.3** (100 eq.) was added to aliquots of $Sbi_{3,4\text{-}Cys}$ containing varying amounts of TCEP (1-10 eq.). The samples were incubated for 1 hour at 37 °C prior to addition of maleimide-fluorescein (1 eq.) followed by incubation at 37 °C for 18 hours (**Figure 3.10**, **lanes 4-6**).

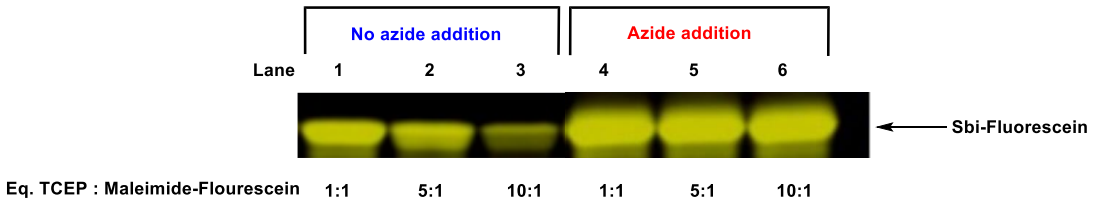

Figure 3.10: SDS-PAGE analysis of reactions between maleimide-fluorescein (1 eq.) and Sbi in the presence of varying TCEP amounts (1-10 eq.) and in the presence or absence of the alkyl azide **3.3** (100 eq.). **Lane 1**: Sbi + TCEP (1 eq.) + maleimide-fluorescein (1 eq.), **Lane 2**: Sbi + TCEP (5 eq.) + maleimide-fluorescein (1 eq.), **Lane 3**: Sbi + TCEP (10 eq.) + maleimide-fluorescein (1 eq.), **Lane 4**: Sbi + TCEP (1 eq.) + **3.3** (100 eq.) + maleimide-fluorescein (1 eq.), **Lane 5**: Sbi + TCEP (5 eq.) + **3.3** (100 eq.) + maleimide-fluorescein (1 eq.), **Lane 6**: Sbi + TCEP (10 eq.) + **3.3** (100 eq.) + maleimide-fluorescein (1 eq.). The SDS-PAGE gel was analysed utilising Image Studio Lite software.

There is a progressive decrease of fluorescent conjugate as the concentration of TCEP increases relative to the amount of maleimide-fluorescein (**Figure 3.10**, **Lanes 1-3**). The addition of **3.3**, however, results in consistent yields of fluorescent protein conjugate (**Figure 3.10**, **Lanes 4-6**). **Graph 3.4** illustrates a consistent level of fluorescent protein conjugate production by the addition of alkyl azide **3.3**, regardless of the initial TCEP concentration relative to the concentration of maleimide-fluorescein. There is, however a progressive loss of fluorescent conjugate without the addition of **3.3** and as the TCEP concentration increase relative to the maleimide-fluorescein concentration. The addition of **3.3** is, therefore, an effective strategy to oxidise TCEP prior to addition of thiol reactive fluorescent probes, facilitating the production of fluorescent conjugates in consistent yields.

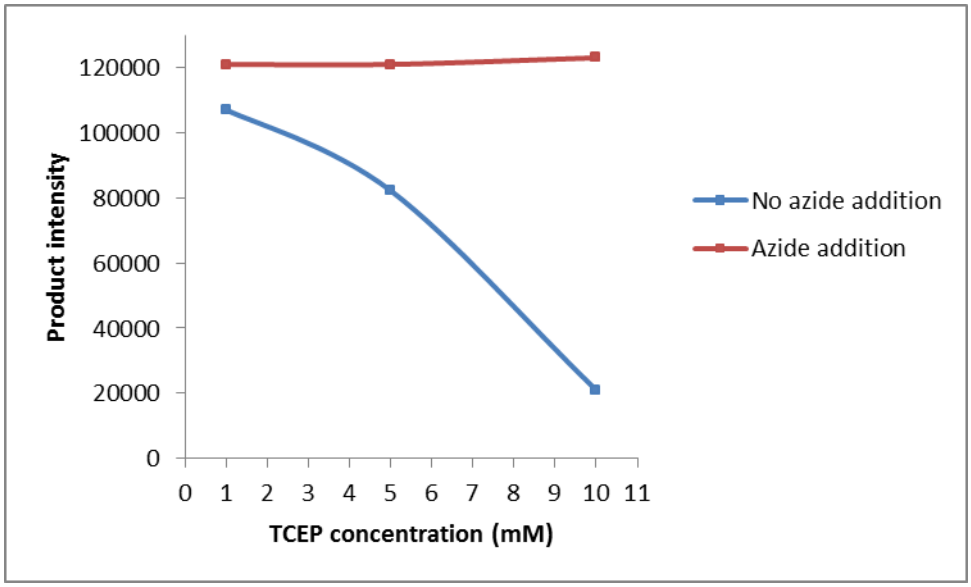

Graph 3.4: Sbi-fluorescein conjugate production with and without the addition of the alkyl azide **3.3** to oxidise TCEP.

The addition of alkyl azide **3.3** to oxidise THPP was subsequently investigated, using maleimide-fluorescein as the ligand to attach to the folded thiol-containing protein $Sbi_{3,4\text{-}Cys}$. Varying concentrations of THPP (1-10 eq.) were added to aliquots of protein and incubated for 45 minutes at 25 °C. Maleimide-fluorescein (1 eq.) was subsequently added and the reaction was incubated at 37 °C for 18 hours (**Figure 3.11**, **lanes 1-3**). In parallel experiments **3.3** (100 eq.) was added to aliquots of $Sbi_{3,4\text{-}Cys}$ containing varying amounts of THPP (1-10 eq.). The samples were incubated for 1 hour at 37 °C prior to addition of maleimide-fluorescein (1 eq.), followed by incubation at 37 °C for 18 hours (**Figure 3.11**, **lanes 4-6**).

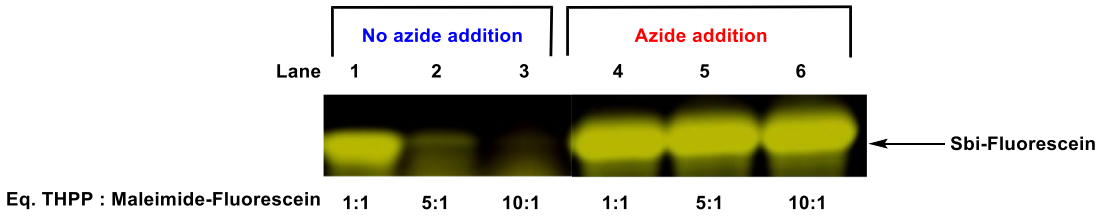

Figure 3.11: SDS-PAGE analysis of reactions between maleimide-fluorescein (1 eq.) and Sbi in the presence of varying THPP amounts (1-10 eq.) and in the presence or absence of the alkyl azide **3.3** (100 eq.). **Lane 1:** Sbi + THPP (1 eq.) + maleimide-fluorescein (1 eq.), **Lane 2:** Sbi + THPP (5 eq.) + maleimide-fluorescein (1 eq.), **Lane 3:** Sbi + THPP (10 eq.) + maleimide-fluorescein (1 eq.), **Lane 4:** Sbi + THPP (1 eq.) + **3.3** (100 eq.) + maleimide-fluorescein (1 eq.), **Lane 5:** Sbi + THPP (5 eq.) + **3.3** (100 eq.) + maleimide-fluorescein (1 eq.), **Lane 6:** Sbi + THPP (10 eq.) + **3.3** (100 eq.) + maleimide-fluorescein (1 eq.). The SDS-PAGE gel was analysed utilising Image Studio Lite software.

There is decrease of fluorescent conjugate as the amount of THPP increases relative to the amount of maleimide-fluorescein (**Figure 3.11**, **Lanes 1**-**3**). There is, however, consistent conjugate production following the oxidation of THPP by the addition of **3.3** (**Figure 3.11**, **Lanes 4**-**6**). The effectiveness of excess THPP oxidation by addition of **3.3** is illustrated in **Graph 3.5**. The **Graph 3.5** illustrates a consistent level of fluorescent protein conjugate production by the addition of alkyl azide **3.3**, regardless of the initial THPP concentration relative to the concentration of maleimide-fluorescein. There is, however a progressive loss of fluorescent conjugate without the addition of **3.3** and as the THPP concentration increases relative to the maleimide-fluorescein concentration. The addition of **3.3** is, therefore, an effective strategy to oxidise THPP prior to addition of thiol reactive fluorescent probes, facilitating the production of fluorescent conjugates in consistent yields.

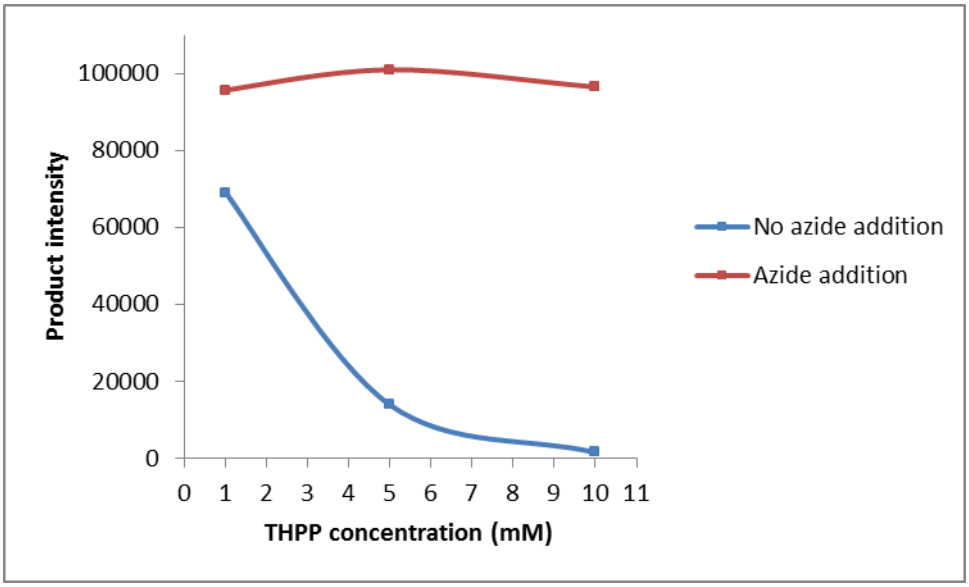

Graph 3.5: Sbi-fluorescein conjugate production with and without the addition of the alkyl azide **3.3** to oxidise THPP.

The utilisation of a low molecular weight thiol-reactive fluorescent probe (maleimide-fluorescein) to functionalise unfolded and folded proteins has so far been useful in analysing trends in functionalisation when in the presence or absence of excess TCEP or THPP.

The experiments, however, have not been useful in quantifying yields of conjugate production as there is insufficient molecular weight gain of the fluorescent conjugate relative to the native protein to visualise both proteins bands by SDS-PAGE. The experiments were, therefore, repeated using maleimide-PEG2kDa to thiol alkylate the proteins. PEGylation of the proteins would result in a sufficient molecular weight gain relative to the native proteins to be resolved by SDS-PAGE. PEGylation experiments should allow quantification of conjugation reactions where excess TCEP or THPP is present in the conjugation reactions compared to the utilisation of an alkyl azide to oxidise excess reducing agents prior to the conjugation reactions.

3.4.3) Addition of the Alkyl Azide 3.3 to Oxidise TCEP/THPP to Ensure High Yeast Enolase-Maleimide-PEG2kDa Conjugate Yields

Quantification of PEGylation experiments by SDS-PAGE were initially performed on yeast enolase, a denatured protein. Yeast enolase was denatured in argon purged Tris buffer (0.5 M, pH = 7.2) containing 5 mM EDTA and 8 M urea. Varying amounts of TCEP (1-10 eq.) were added to aliquots of protein and incubated for 45 minutes at 25 °C. Maleimide-PEG2kDa (1 eq.) was subsequently added and the reactions were incubated at 37 °C for 18 hours (**Figure 3.12**, **lanes 3**-**5**). In parallel experiments **3.3** (100 mM) was added to aliquots of yeast enolase containing varying amounts of TCEP (1-10 eq.). The samples were incubated for 1 hour at 37 °C prior to addition of maleimide-PEG2kDa (1 eq.), followed by incubation at 37 °C for 18 hours (**Figure 3.12**, **lanes 6**-**8**).

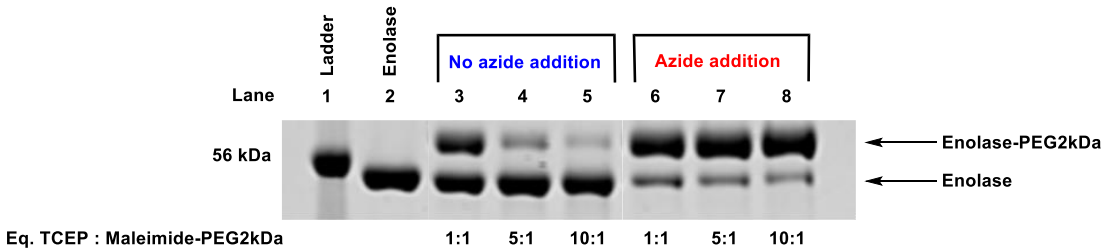

Figure 3.12: SDS-PAGE analysis of reactions between maleimide-PEG2kDa (1 eq.) and yeast enolase in the presence of varying TCEP amounts (1-10 eq.) and in the presence or absence of the alkyl azide **3.3** (100 eq.). **Lane 1:** ladder, **Lane 2:** enolase, **Lane 3:** enolase + TCEP (1 eq.) + maleimide-PEG2kDa (1 eq.), **Lane 4:** enolase + TCEP (5 eq.) + maleimide-PEG2kDa (1 eq.), **Lane 5:** enolase + TCEP (10 eq.) + maleimide-PEG2kDa (1 eq.), **Lane 6:** enolase + TCEP (1 eq.) + **3.3** (100 eq.) + maleimide-PEG2kDa (1 eq.), **Lane 7:** enolase + TCEP (5 eq.) + **3.3** (100 eq.) + maleimide-PEG2kDa (1 eq.), **Lane 8:** enolase + TCEP (10 eq.) + **3.3** (100 eq.) + maleimide-PEG2kDa (1 eq.). The SDS-PAGE gel was stained with Coomassie solution and analysed utilising Image Studio Lite software.

There is a significant and progressive decrease in protein conjugation as the amount of TCEP increases relative to the amount of maleimide-PEG2kDa (**Figure 3.12**, **Lanes 3-5)**. The addition of the alkyl azide **3.3** (**Figure 3.12**, **Lanes 6-8**) was successful in oxidising excess TCEP to facilitate high conjugate yields. The experiment has proved that the addition of **3.3** is an effective strategy to quench TCEP, resulting in high yields (**Table 3.2**) of PEGylated proteins, without necessity for intermediate purification protocols.

The ability of the alkyl azide **3.3** to quench the alternative reducing agent (THPP) and effect high PEGylated yeast enolase yields was subsequently investigated. Yeast enolase was denatured in argon purged Tris buffer (0.5 M, pH = 7.2), containing 5 mM EDTA and 8 M urea. Varying amounts of THPP (1-10 eq.) were added to aliquots of protein and incubated for 45 minutes at 25 °C. Maleimide-PEG2kDa (1 eq.) was subsequently added and the reactions were incubated at 37 °C for 18 hours (**Figure 3.13**, **lanes 3-5**). In parallel experiments the alkyl azide **3.3** (100 eq.) was added to aliquots of enolase containing varying amounts of THPP (1-10 eq.). The samples were incubated for 1 hour at 37 °C prior to addition of maleimide-

PEG2kDa (1 eq.) followed by incubation at 37 °C for 18 hours (**Figure 3.13**, **lanes 6-8**).

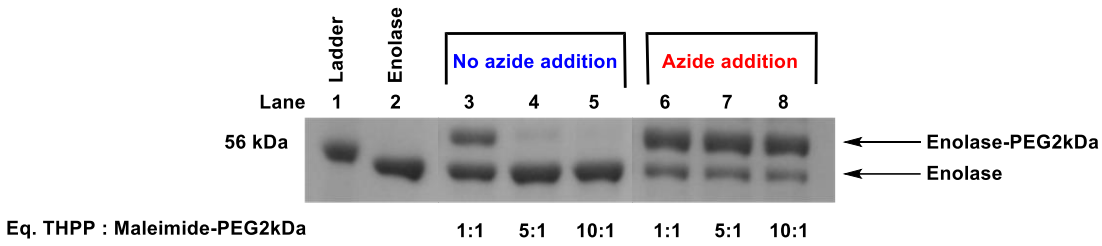

Figure 3.13: SDS-PAGE analysis of reaction between maleimide-PEG2kDa (1 eq.) and yeast enolase in the presence of varying THPP amounts (1-10 eq.) and in the presence or absence of the alkyl azide **3.3** (100 eq.). **Lane 1:** ladder, **Lane 2:** enolase, **Lane 3:** enolase + THPP (1 eq.) + maleimide-PEG2kDa (1 eq.), **Lane 4:** enolase + THPP (5 eq.) + maleimide-PEG2kDa (1 eq.), **Lane 5:** enolase + THPP (10 eq.) + maleimide-PEG2kDa (1 eq.), **Lane 6:** enolase + THPP (1 eq.) + **3.3** (100 eq.) + maleimide-PEG2kDa (1 eq.), **Lane 7:** enolase + THPP (5 eq.) + **3.3** (100 eq.) + maleimide-PEG2kDa (1 eq.), **Lane 8:** enolase + THPP (10 eq.) + **3.3** (100 eq.) + maleimide-PEG2kDa (1 eq.). The SDS-PAGE gel was stained with Coomassie solution and analysed utilising Image Studio Lite software.

There is a significant and progressive decrease in protein conjugation as the amount of THPP increases relative to the amount of maleimide-PEG2kDa (**Figure 3.13**, **Lanes 3-5**). The addition of an alkyl azide (**Figure 3.13**, **Lanes 6-8**) was successful in oxidiing excess THPP, facilitating high conjugate yields. The addition of **3.3** is an effective strategy to quench THPP and produce PEGylated proteins in high yields.

Quantification of PEGylated yeast enolase yields in the presence or absence of excess TCEP or THPP was achieved utilising Image Studio Lite version 4.0 software. The results are presented in **Table 3.2**. The presence of TCEP in the conjugation reactions significantly lowered PEGylated protein yields from 42 % when present in equimolar amounts relative to maleimide-PEG2kDa to as low as 11 % when the TCEP was in a tenfold excess relative to the maleimide-PEG2kDa. However, fairly consistent yields of 76-85 % of PEGylated protein were achieved when TCEP was oxidised by alkyl azide **3.3** prior to addition of maleimide-PEG2kDa. A similar trend was observed with the experiments utilising THPP. The presence of THPP produced

low PEGylated protein yields, from 37 % when present in equimolar amounts relative to maleimide-PEG2kDa to 3 % when the THPP was in a tenfold excess relative to the maleimide-PEG2kDa. Fairly consistent yields of 68-76 % of PEGylated protein were achieved when THPP was oxidised by alkyl azide **3.3** prior to addition of maleimide-PEG2kDa. **Table 3.2** also illustrates the superior reactivity of THPP compared to TCEP. When there is no addition of alkyl azide **3.3** to oxidise either TCEP or THPP, there are consistently lower conjugate yields when utilising THPP compared to TCEP. The trishydroxypropyl substituents of THPP are less electron withdrawing than the 2-carboxyethyl substituents of TCEP. The phosphorus atom of THPP is, therefore, more nucleophilic than the phosphorus atom of TCEP and reacts more rapidly with maleimide-PEG2kDa than TCEP, resulting in comparably lower conjugate yields. The addition of **3.3** to oxidise TCEP or THPP, however, offers an excellent strategy to ensure consistent and high yields of conjugation when utilising maleimide derivatised ligands.

		Eq. Reducing Agent : Maleimide-PEG2kDa		
		1:1	5:1	10:1
Reducing Agent	Alkyl Azide 3.3	Yield (%) of PEGylated yeast enolase		
TCEP	-	42.3 +/- 0.7	16.6 +/- 1.8	10.5 +/- 0.04
TCEP	+	76.4 +/- 3.6	82.4 +/- 2.9	84.7 +/- 1.3
THPP	-	37.0 +/- 4.4	6.7 +/- 1.4	3.1 +/- 0.6
THPP	+	68.0 +/- 6.0	73.4 +/- 5.0	75.8 +/- 3.2

Table 3.2: Yields of yeast enolase PEGylation by maleimide-PEG2kDa when in the presence or absence of reducing agents (TCEP or THPP), with and without the addition of the alkyl azide **3.3**.

3.4.4) Addition of an Alkyl Azide to Oxidise TCEP/THPP to Ensure High $Sbi_{3,4\text{-}Cys}$-Maleimide-PEG2kDa Conjugate Yields

Quantification of PEGylation yields on the folded protein $Sbi_{3,4\text{-}Cys}$ was subsequently pursued, in a similar fashion to that achieved for the PEGylation of the unfolded yeast enolase experiments in **section 3.4.3**.

$Sbi_{3,4\text{-}Cys}$ was suspended in argon purged Tris buffer (0.5 M, pH = 7.2), containing 5 mM EDTA. Varying amounts of TCEP (1-10 eq.) were added to aliquots of the protein and incubated for 45 minutes at 25 °C. Maleimide-PEG2kDa (1 eq.) was subsequently added and the reaction was incubated at 37 °C for 18 hours (**Figure 3.14**, **lanes 3**-**5**). In parallel experiments **3.3** (100 eq.) was added to aliquots of $Sbi_{3,4\text{-}Cys}$ containing varying amounts of TCEP (1-10 eq.). The samples were incubated for 1 hour at 37 °C prior to addition of maleimide-PEG2kDa (1 eq.), followed by incubation at 37 °C for 18 hours (**Figure 3.14**, **lanes 6**-**8**).

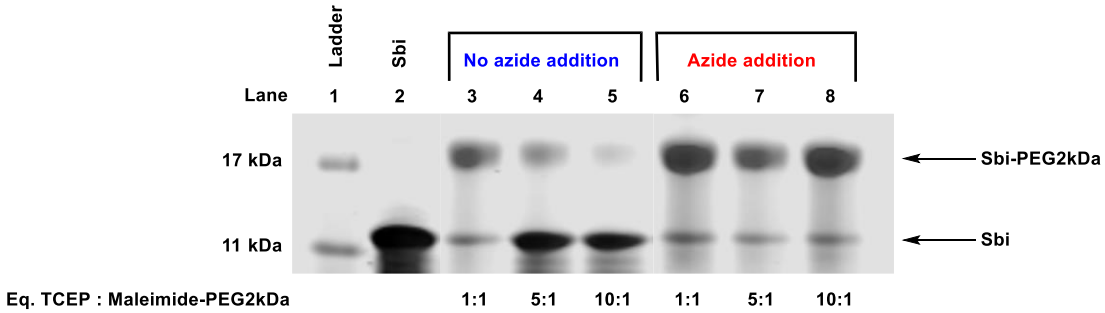

Figure 3.14: SDS-PAGE analysis of reactions between maleimide-PEG2kDa (1 eq.) and Sbi in the presence of varying TCEP amounts (1-10 eq.) and in the presence or absence of the alkyl azide **3.3** (100 eq.). **Lane 1:** ladder, **Lane 2:** Sbi, **Lane 3:** Sbi + TCEP (1 eq.) + maleimide-PEG2kDa (1 eq.), **Lane 4:** Sbi + TCEP (5 eq.) + maleimide-PEG2kDa (1 eq.), **Lane 5:** Sbi + TCEP (10 eq.) + maleimide-PEG2kDa (1 eq.), **Lane 6:** Sbi + TCEP (1 eq.) + **3.3** (100 eq.) + maleimide-PEG2kDa (1 eq.), **Lane 7:** Sbi + TCEP (5 eq.) + **3.3** (100 eq.) + maleimide-PEG2kDa (1 eq.), **Lane 8:** Sbi + TCEP (10 eq.) + **3.3** (100 eq.) + maleimide-PEG2kDa (1 eq.). The SDS-PAGE gel was stained with Coomassie solution and analysed utilising Image Studio Lite software.

There is a decrease of PEGylated protein as the amount of TCEP increases relative to the amount of maleimide-PEG2kDa (**Figure 3.14**, **Lanes 3**-**5**). There is, however, production of consistent amounts of PEGylated protein following the oxidation of excess TCEP (**Figure 3.14**, **Lanes 6**-**8**) by the addition of the alkyl azide **3.3**.

The ability of the alkyl azide **3.3** to quench THPP and effect high bioconjugations yields between the folded protein ($Sbi_{3,4\text{-}Cys}$) and maleimide-derivatised ligands was also investigated.

$Sbi_{3,4\text{-}Cys}$ was suspended in argon purged Tris buffer (0.5 M, pH = 7.2), containing 5 mM EDTA. Varying amounts of THPP (1-10 eq.) were added to aliquots of the protein and incubated for 45 minutes at 25 °C. Maleimide-PEG2kDa (1 eq.) was subsequently added and the reaction was incubated at 37 °C for 18 hours (**Figure 3.15**, **lanes 3**-**5**). In parallel experiments **3.3** (100 eq.) were added to aliquots of $Sbi_{3,4\text{-}Cys}$ containing varying amounts of THPP (1-10 eq.). The samples were incubated for 1 hour at 37 °C prior to addition of maleimide-PEG2kDa (1 eq.) followed by incubation at 37 °C for 18 hours (**Figure 3.15**, **lanes 6**-**8**).

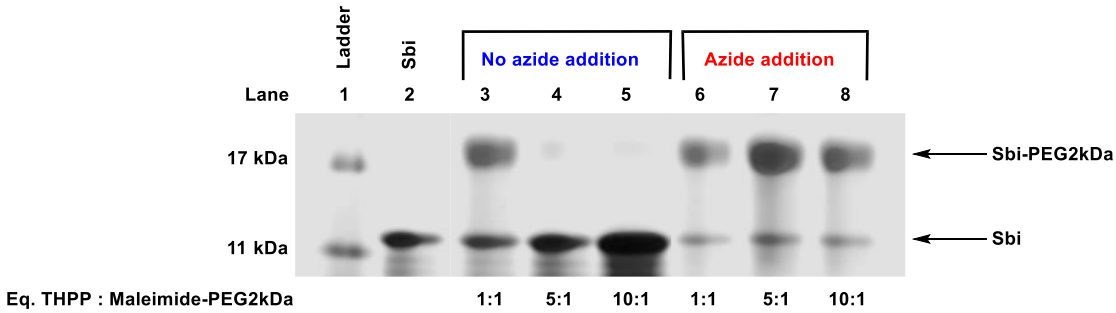

Figure 3.15: SDS-PAGE analysis of reactions between maleimide-PEG2kDa (1 eq.) and Sbi in the presence of varying THPP amounts (1-10 eq.) and in the presence or absence of the alkyl azide **3.3** (100 eq.). **Lane 1:** ladder, **Lane 2:** Sbi, **Lane 3:** Sbi + THPP (1 eq.) + maleimide-PEG2kDa (1 eq.), **Lane 4:** Sbi + THPP (5 eq.) + maleimide-PEG2kDa (1 eq.), **Lane 5:** Sbi + THPP (10 eq.) + maleimide-PEG2kDa (1 eq.), **Lane 6:** Sbi + THPP (1 eq.) + **3.3** (100 eq.) + maleimide-PEG2kDa (1 eq.), **Lane 7:** Sbi + THPP (5 eq.) + **3.3** (100 eq.) + maleimide-PEG2kDa (1 eq.), **Lane 8:** Sbi + THPP (10 eq.) + **3.3** (100 eq.) + maleimide-PEG2kDa (1 eq.). The SDS-PAGE gel was stained with Coomassie solution and analysed utilising Image Studio Lite software.

There is a decrease in bioconjugate yields as the amount of THPP increases relative to the amount of maleimide-PEG2kDa (**Figure 3.15**, **Lanes 3**-**5**). There is, however, production of consistent yields of PEGylated protein following the oxidation of excess THPP (**Figure 3.15**, **Lanes 6**-**8**) by the addition of **3.3**.

Quantification of PEGylated $Sbi_{3,4\text{-}Cys}$ yields in the presence or absence of excess TCEP or THPP are presented in **Table 3.3**. The presence of TCEP significantly lowered PEGylated protein yields to 36 % and 27 % when present in fivefold or tenfold excess relative to the maleimide-PEG2kDa respectively. However, fairly consistent yields of 70 % of PEGylated protein were achieved when TCEP was oxidised by alkyl azide **3.3** prior to addition of maleimide-PEG2kDa. A similar trend was observed with the experiments utilising THPP. The presence of THPP significantly lowered PEGylated protein yields to 19 % and 10 % when present in fivefold or tenfold excess relative to the maleimide-PEG2kDa respectively. Fairly consistent yields of 67-70 % of PEGylated protein were achieved when THPP was oxidised by alkyl azide **3.3** prior to addition of maleimide-PEG2kDa.

		Reducing Agent : Maleimide-PEG2kDa		
		1:1	5:1	10:1
Reducing Agent	Alkyl Azide 3.3	Yield (%) of PEGylated Sbi		
TCEP	-	70.1 +/- 3.9	35.7 +/- 8.1	27.1 +/- 15.2
TCEP	+	70.5 +/- 4.8	71.7+/- 5.3	69.9 +/- 10.0
THPP	-	56.8 +/- 8.2	19.4 +/- 14.5	9.7 +/- 7.5
THPP	+	67.4 +/- 6.8	69.5 +/- 7.6	70.1 +/- 10.4

Table 3.3: Yields of $Sbi_{3,4\text{-}Cys}$ PEGylation by maleimide-PEG2kDa when in the presence or absence of reducing agents (TCEP or THPP), with and without the addition of alkyl azide **3.3**.

3.5) Conclusion

TCEP and THPP are disulfide reducing agents that react with Michael acceptor thiol alkylating reagents such as maleimide and vinyl sulfone. They, therefore, need to be removed prior to performing the bioconjugation reaction between the Michael acceptor derivatised reagent and a thiol-containing biomolecule. The addition of a water soluble alkyl azide is able to oxidise excess TCEP or THPP to the corresponding phosphine oxides. The phosphine oxide products are not reactive with the alkylating reagents, which allows for a 'one-pot' protocol for performing bioconjugations using thiol-alkylation chemistry. The method was initially validated during functioanlisation of cysteine amino acid derivatives and was subsequently utilised during the functionslisation of both folded and unfolded folded proteins. The method proved successful in oxidising excess reducing agents to facilitate high protein conjugate yields when using either a maleimide-derivatised PEG or fluorophore.

Chapter 4: 4-Vinyl Pyridine Derivatives as Reagents for Thiol-Alkylation

4.0) Introduction

4-Vinyl pyridine (4-VP) has been utilised as a reagent for thiol-alkylation, which has been reported to be 300 times faster compared to alkylation of amines at pH greater than 7 [18]. Previously 4-VP has primarily been used for the alkylation of cysteine-containing peptides and proteins for mass spectrometric analysis [81, 140]. 4-VP has not been extensively explored as a reagent for bioconjugation chemistry, predominantly as a consequence of the success of maleimide-derivatised products. As such, we sought to investigate the application of 4-VP in bioconjugation reactions by synthesising a variety of 4-VP derivatives as potential linkers for the attachment of ligands to thiol-containing peptides and proteins.

Thiol-alkylation by 4-VP proceeds *via* conjugate addition of the thiolate at the terminal carbon of the vinyl functional group, resulting in a thio-ether bond (**Figure 4.1**), which is stable towards hydrolysis [141]. The use of 4-VP for thiol alkylation also offers the advantage of utilising UV analysis for the detection and monitoring of thiol-alkylated products. However, the conjugate addition of 4-VP to thiols is reported to be much slower ($x10^3$) in rate when compared to maleimide-derived conjugate additions [18]. As such, reaction conditions for thiol alkylation of peptides and proteins by 4-VP would require optimisation, largely to minimise reoxidation of thiols to disulfides as a consequence of the reduced reaction rates.

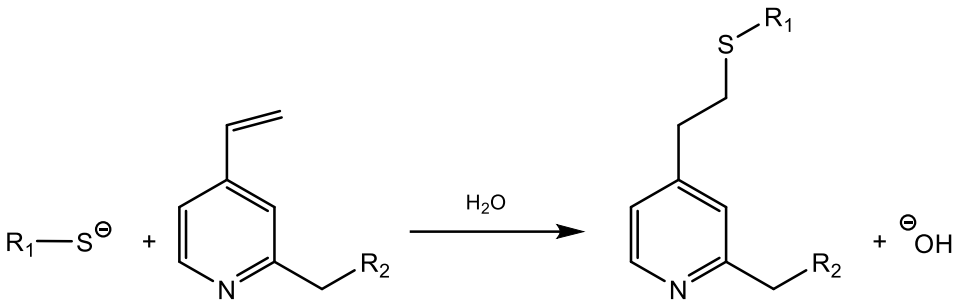

Figure 4.1: General scheme for thiol-alkylation using a 4-VP linker. R_1 = peptide or protein, R_2 = alkyl or aryl ligand.

The development of 4-VP derivatives as potential linkers for thiol alkylation requires functionalisation of the pyridine ring (**Figure 4.1**), with functional groups such as hydroxyls, amines or carboxylic acids for the attachment of ligands through ester or amide bond formation. The investigation, therefore, aimed to develop suitable 4-VP derivatives for the attachment of ligands, followed by rapid and specific thiol alkylation of peptides and proteins. There were, however, a number of factors that required prior consideration.

The pKa of the nitrogen atom of the pyridine ring is a key determinant of reactivity for 4-VP derivatives. Protonation of the nitrogen atom increases the electrophilicity of the vinyl group, which promotes nucleophilic attack at the terminal carbon of the vinyl group by a thiolate. The substituents on the pyridine ring, which are required for the attachment of ligands to the aromatic ring will affect the pKa of the ring nitrogen, ultimately influencing the rate of thiol alkylation. The pKa of the thiol functional group attached to the peptide or protein is also an important factor. It is the deprotonated thiol, the thiolate anion, which acts as a nucleophile towards the vinyl group to generate a thioether bond. Hence, the pH of the reaction will also influence the rate of alkylation. Additional reaction variables also need to be considered. Reactions should ideally be performed in an oxygen depleted and metal ion free environment to minimise oxidation of thiols, which might render the thiol unreactive towards the vinyl group. As such, we first sought to investigate the impact of the above mentioned factors on the ability of the 4-VP derivatives to react with thiols.

4.1) pKa Prediction of the Nitrogen Atom for Selected 4-VP Derivatives

The experimentally determined pKa of 4-VP is 5.62 [142]. Ideally, reactions should be performed at a pH lower than the pKa to promote protonation of nitrogen atom of the pyridine ring to increase the reactivity of 4-VP. However, this would also promote protonation of the sulfur atom to generate a thiol functional group instead of a nucleophilic thiolate. Additionally, performing conjugations under acidic conditions may also be unsuitable for the stability of some proteins. Hence, our initial aim was to develop 4-VP linkers where the pyridine nitrogen atom exhibits a pKa closer to neutral pH. Raising the nitrogen's pKa closer towards that of a general thiol was predicted to result in increased reaction rates at neutral pH, since optimal conjugation rates should occur at a pH which is the average of the 4-VP derivative and the thiol pKa values [141].

The inductive effects of functional groups on the pyridine ring can raise or lower the pKa value of the pyridine ring nitrogen. When considering raising the pKa of the nitrogen atom of a derivatised 4-VP reagent from a value of around 5.6 to a value closer to 7, the effect of substituents in the *ortho* position of the aromatic ring on the nitrogen's pKa were investigated. The pKa of four selected 4-VP derivatives as potential linker precursors, **4.1**-**4.4**, were calculated using REAXYS® software and are illustrated in **Figure 4.2** [143]. The 4-VP derivatives were chosen where the substituent at C-2 of the aromatic ring could be chemically transformed to generate functional groups such as hydroxyls or carboxylic acids for the subsequent attachment of ligands through ester or amide bond formation.

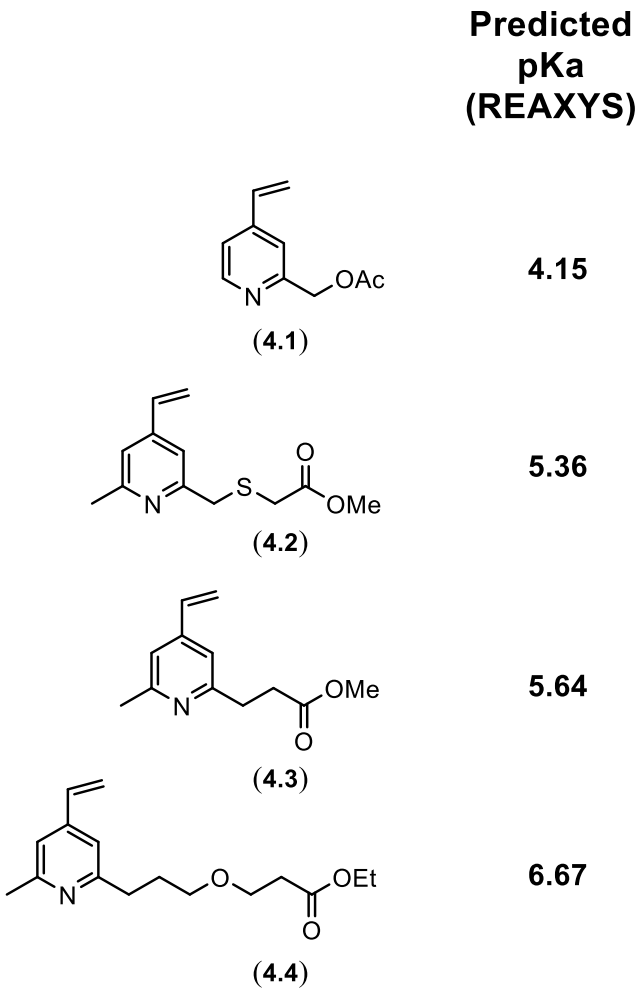

Figure 4.2: Predictions of the pKa of 4-VP derivatives **4.1-4.4** using REAXYS® software.

The accuracy of the pKa predictions by the REAXYS® software was initially tested by comparing the predicted pKa of 4-VP to the experimentally derived pKa of 4-VP. The REAXYS® software predicted a pKa of 5.46 for 4-VP, which is a close approximation to the reported literature value of 5.62 [142]. The software was subsequently utilised to predict the pKa values of 4-VP derivatives **4.1**-**4.4**. The pKa of compound **4.1** was predicted to be 4.15. Hence, alkylation at the *ortho* position of the nitrogen is predicted to result in a considerable decrease in pKa relative to 4-VP. This decrease in pKa is attributed to the inductive effect of the electronegative oxygen atom of the methyl acetate substituent. The pKa of compound **4.2** was predicted to be 5.36, which is a significant increase in pKa compared to **4.1**, though still not as high as the parent 4-VP itself. The electron donating effect of the methyl

group at C-6 of the pyridine ring of **4.2** improves the availability of the nitrogen atoms lone pair for protonation. The close proximity of the electronegative sulfur atom of the methyl (methylsulfanyl)acetate substituent to the ring nitrogen may, however, decrease the pKa of the ring nitrogen. The 4-VP derivative **4.3** has a predicted pKa of 5.64, a marginal increase in pKa compared to derivative **4.2**. The 2 carbon atom separation between the electron withdrawing ester functionality and the pyridine ring increases the basicity of the ring nitrogen in addition to the electron donating effect of the methyl group at C-6 of the pyridine ring. The 4-VP derivative **4.4**, however, has a predicted pKa of 6.67, a significant increase over the pKa of derivative **4.3**. The three carbon-atom separation between the electron withdrawing oxygen atom of the ethyl 3-propoxypropanoate substituent and the pyridine ring further increases the basicity of the ring nitrogen, in addition to the electron donating effect of the methyl group at C-6 of the pyridine ring. The 4-VP derivatives **4.1**-**4.4** were deemed valuable synthetic targets for comparing their potential as thiol alkylation reagents.

4.2) Synthesis of 4-VP Derivatives 4.1-4.4

The chemical synthesis of the 4-VP derivative (4-ethenylpyridin-2-yl)methyl acetate (**4.1**) was achieved in four steps in an overall yield of 34 % (**Figure 4.3**). The synthesis of **4.1** began with the bromination of commercially available 2-methyl-4-nitropyridine 1-oxide (**4.5**), which generated 4-bromo-2-methylpyridine 1-oxide (**4.6**) in 59 % yield [144, 145]. The oxygen atom of **4.6** was acylated utilising trifluoracetic anhydride, which underwent base catalysed rearrangement to (4-bromopyridin-2-yl)methyl trifluoroacetate as an intermediate. The basic conditions employed subsequently hydrolysed the acetate group to produce (4-bromopyridin-2-yl)methanol (**4.7**) in 77 % yield [144, 145]. The hydroxyl functional group was reacylated utilising acetic anhydride in pyridine, which yielded (4-bromopyridin-2-yl)methyl acetate (**4.8**) in 92 % yield. The vinyl functional group was introduced through a palladium catalysed cross coupling reaction (Stille reaction), which yielded the target compound **4.1** in 82% yield (**Figure 4.3**) [146].

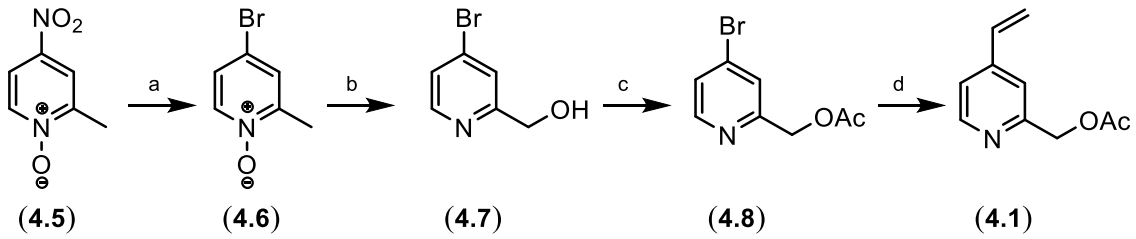

Figure 4.3: Synthesis of **4.1** **a**) AcBr, AcOH, 120 °C, **b**) 1) TFAA, 2) NaOH, **c**) Ac_2O, pyridine, **d**) $Bu_3SnC_2H_3$, tetrakis(triphenylphosphine)Pd(0), toluene, 85 °C.

The chemical synthesis of the 4-VP derivative methyl {[(4-ethenyl-6-methylpyridin-2-yl)methyl]sulfanyl}acetate (**4.2**) was achieved in five steps in an overall yield of 27 % (**Figure 4.4**). The synthesis of **4.2** started with the bromination of commercially available 2,6-dimethylpyridine 1-oxide (**4.9**), which generated 4-bromo-2,6-dimethylpyridine 1-oxide (**4.10**) in 72 % yield [144, 145]. The oxygen atom of **4.10** was acylated utilising trifluoracetic anhydride, which underwent base catalysed rearrangement to (4-bromo-6-methylpyridin-2-yl)methyl trifluoroacetate as an intermediate. The basic conditions employed subsequently hydrolysed the acetate group to produce (4-bromo-6-methylpyridin-2-yl)methanol (**4.11**) in 64 % yield [144, 145]. Tosylation of the hydroxyl functional group of **4.11**, resulted in (4-bromo-6-methylpyridin-2-yl)methyl 4-methylbenzenesulfonate (**4.12**) in 94 % yield, which was subsequently treated with methyl thioglycolate, resulting in methyl 2-(((4-bromo-6-methylpyridin-2-yl)methyl)thio)acetate (**4.13**) in 72 % yield [147]. The vinyl functional group was introduced in a palladium catalysed cross coupling reaction (Stille reaction), which yielded the target compound **4.2** in 86 % yield (**Figure 4.4**) [146].

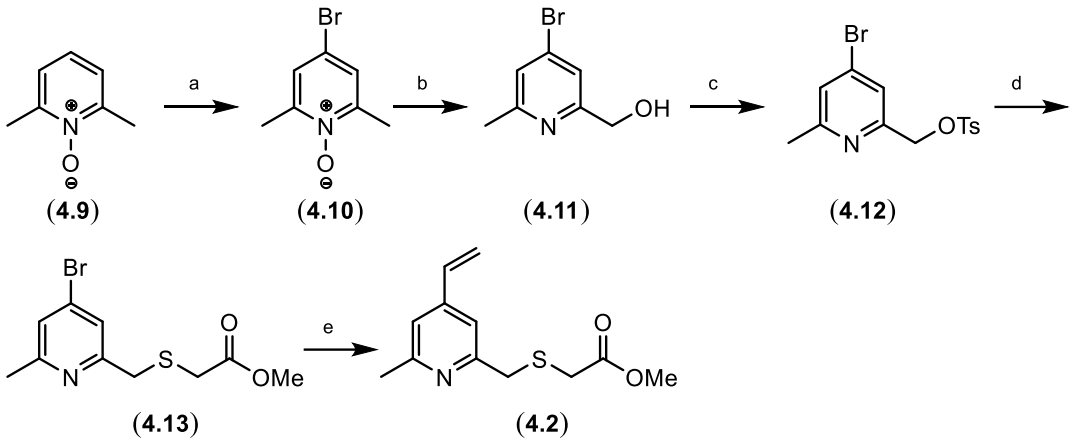

Figure 4.4: Synthesis of **4.2** **a**) Br_2, AcOH, 85 °C, **b**) 1) TFAA, 2) NaOH, **c**) TsCl, NaOH, **d**) methyl thioglycolate, **e**) $Bu_3SnC_2H_3$, tetrakis(triphenylphosphine)Pd(0), toluene, 85 °C.

The chemical synthesis of the 4-VP derivative methyl 3-(4-ethenyl-6-methylpyridin-2-yl)propanoate (**4.3**) was achieved in five steps in an overall yield of 14 % (**Figure 4.5**). The synthesis of **4.3** began with the oxidation of commercially available 3-(6-methylpyridin-2-yl)propan-1-ol (**4.14**), generating 3-(6-methylpyridin-2-yl)propanoic acid (**4.15**), which was subsequently esterified, to give methyl 3-(6-methylpyridin-2-yl)propanoate (**4.16**) in 55 % yield [148]. The nitrogen atom of **4.16** was then oxidised using *m*-CPBA, to give 2-(3-methoxy-3-oxopropyl)-6-methylpyridine 1-oxide (**4.17**) in 67 % yield [149]. Compound **4.17** was subsequently brominated to give 4-bromo-2-(3-methoxy-3-oxopropyl)-6-methylpyridine 1-oxide (**4.18**) in 52 % yield [144, 145]. The nitrogen atom of **4.18** was reduced using phosphorus tribromide, to give methyl 3-(4-bromo-6-methylpyridin-2-yl)propanoate (**4.19**) in 87 % yield [150]. The 4-vinyl functional group was introduced through a palladium catalysed cross coupling reaction (Stille reaction) which yielded the target compound **4.3** in 86 % yield (**Figure 4.5**) [146].

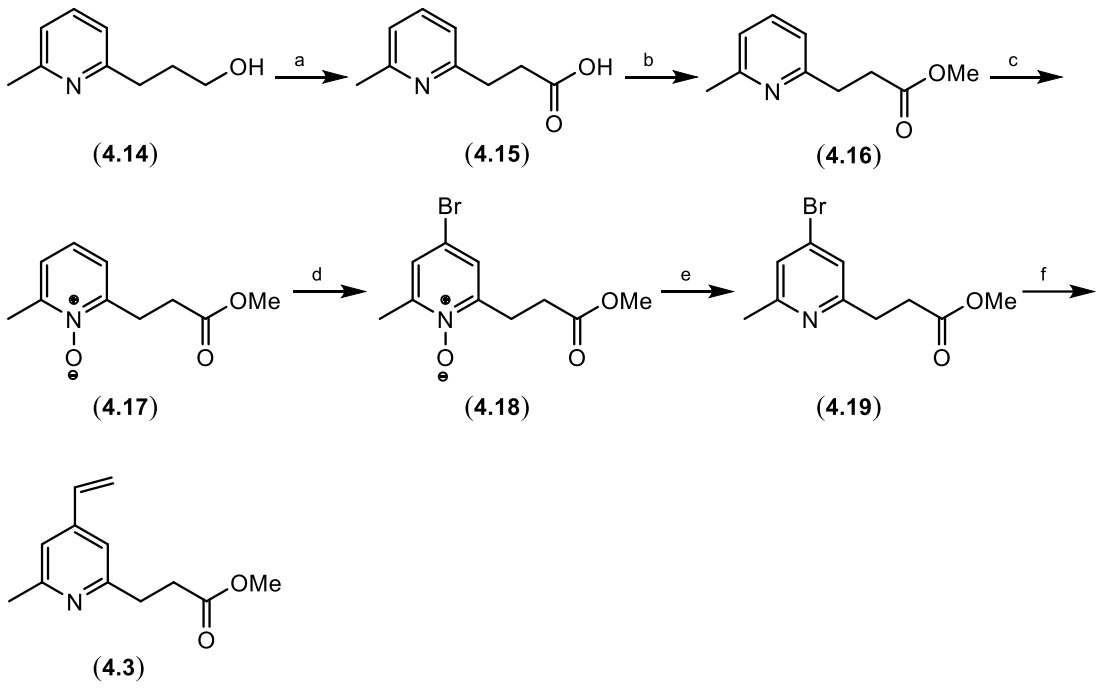

Figure 4.5: Synthesis of **4.3** **a**) $RuCl_3$, $NaIO_4$, **b**) H_2SO_4, MeOH, reflux, **c**) m-CPBA, CH_2Cl_2, **d**) Br_2, AcOH, 85 °C, **e**) PBr_3, toluene, **f**) $Bu_3SnC_2H_3$, tetrakis(triphenylphosphine)Pd(0), toluene, 85 °C.

The chemical synthesis of the 4-VP derivative ethyl 3-[3-(4-ethenyl-6-methylpyridin-2-yl)propoxy]propanoate (**4.4**) was achieved in seven steps in an overall yield of 9 % (**Figure 4.6**). The synthesis of **4.4** started with the acylation of commercially available 3-(6-methylpyridin-2-yl)propan-1-ol (**4.14**), generating 3-(6-methylpyridin-2-yl)propyl acetate (**4.20**) in 95 % yield. The nitrogen atom of **4.20** was oxidised using *m*-CPBA, to give 2-(3-acetoxypropyl)-6-methylpyridine 1-oxide (**4.21**) in 79 % yield, which was subsequently brominated to give 2-(3-acetoxypropyl)-4-bromo-6-methylpyridine 1-oxide (**4.22**) in 56 % yield [144, 145, 149]. The nitrogen atom of **4.22** was reduced using phosphorus tribromide to give 3-(4-bromo-6-methylpyridin-2-yl)propyl acetate (**4.23**) in 85 % yield [150]. The intermediate **4.23** was deacetylated using sodium methoxide in methanol to give 3-(4-bromo-6-methylpyridin-2-yl)propan-1-ol (**4.24**) in 94 % yield. Michael addition of **4.24** to ethyl acrylate, resulted in 3-(3-(4-bromo-6-methylpyridin-2-yl)propoxy)propanoate (**4.25**) in 34 % yield [151]. The vinyl functional group was then introduced using a

palladium catalysed cross coupling reaction (Stille reaction) to yield the target compound **4.4** in 75 % yield (**Figure 4.6**) [146].

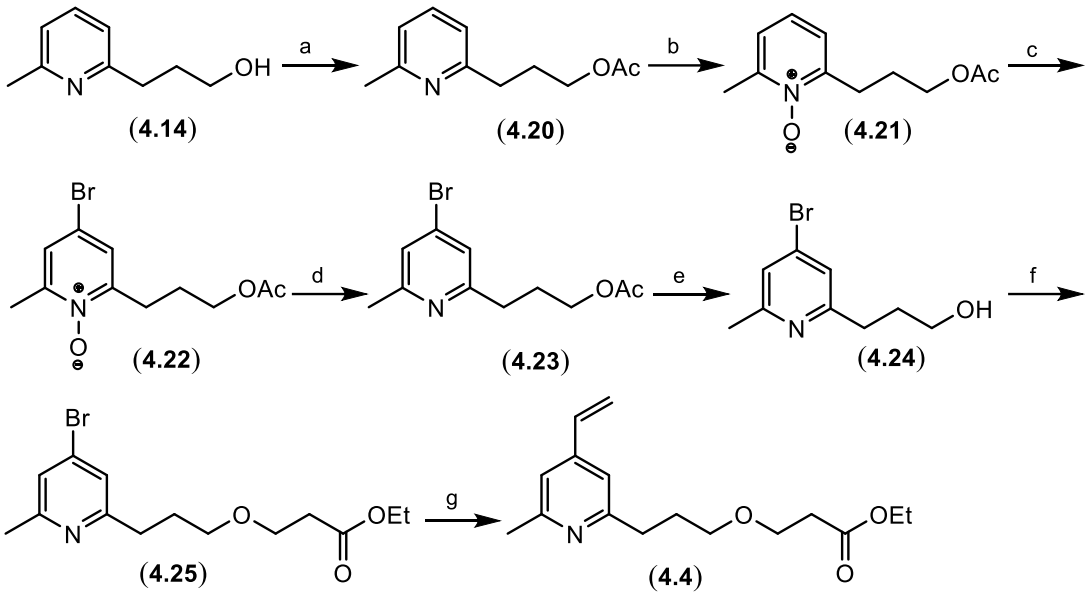

Figure 4.6: Synthesis of **4.4** **a**) Ac_2O, pyridine, **b**) m-CPBA, CH_2Cl_2, **c**) Br_2, AcOH, 85 °C, **d**) PBr_3, toluene, **e**) NaOMe, MeOH, **f**) $(Bu)_4NOH$, ethyl acrylate, **g**) $Bu_3SnC_2H_3$, tetrakis(triphenylphosphine)Pd(0), toluene, 85 °C.

4.3) Experimental Determination of the pKa of the Pyridine Ring for Compounds 4.1-4.4

Following the successful synthesis of 4-VP derivatives **4.1**-**4.4**, the pKa values for each of the respective ring nitrogen atoms were experimentally determined.

The 4-VP derivatives **4.1**-**4.4** were titrated against a dilute sodium hydroxide (NaOH) solution, followed by titration against a dilute hydrochloric acid (HCl) solution, with the continual monitoring of the pH of the solution. The pKa values of the 4-VP derivatives **4.1**-**4.4** were determined by the intersection of the two titration curves. Intersections occurred at inflection points of individual titration curves. The results of the titration experiments are illustrated in **Figure 4.7**.

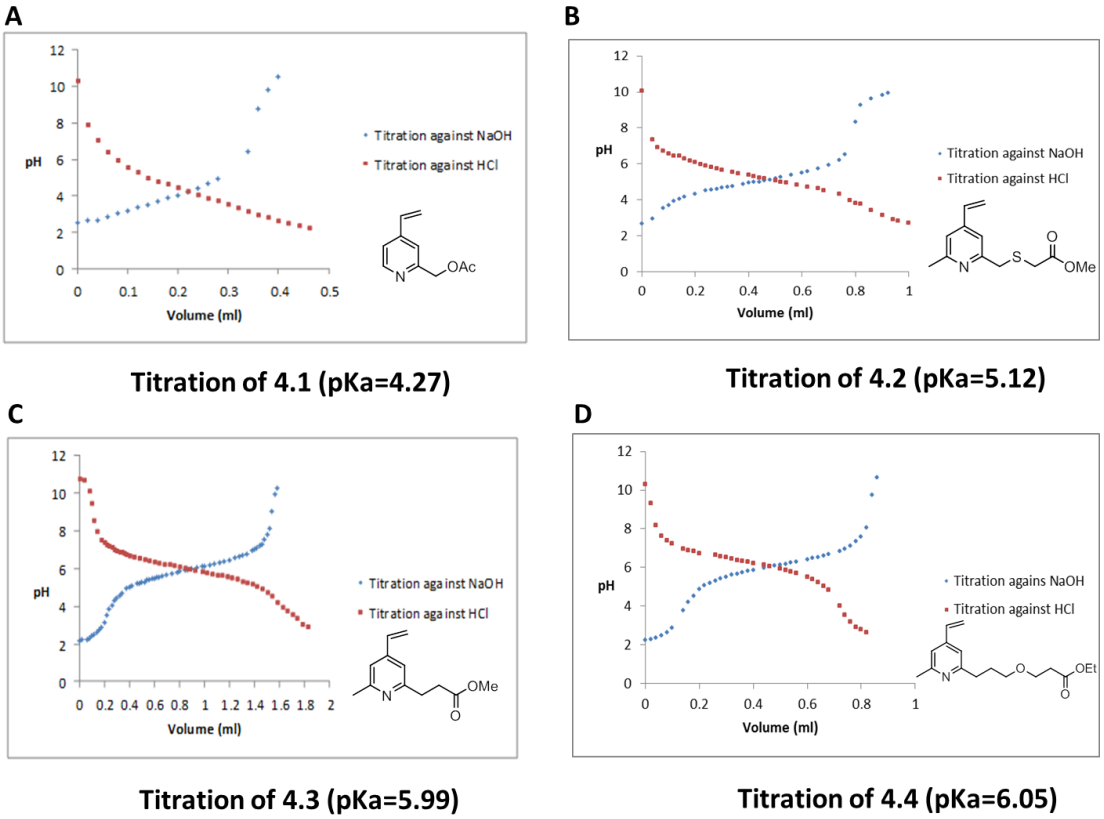

Figure 4.7: Titration curves to determine the pKa values for derivatives **4.1**-**4.4**. Derivatives **4.1**-**4.4** were titrated against acid (HCl) and base (NaOH). The pKa values were determined by the intersection points of the acid/base titration curves.

The REAXYS® software proved to be a reasonably accurate method for predicting the pKa values of 4-VP derivatives **4.1**-**4.4** when compared to the values that were experimentally determined (**Table 4.1**). The titration experiments confirmed the effectiveness of the introduction of the electron donating methyl group at C-6 of the pyridine ring in raising the pKa of the ring nitrogen. The increased length of the alkyl chain of **4.4** compared to **4.3** to separate electron withdrawing groups from the pyridine ring imparted only a small increase in the pKa value to **4.4** relative to **4.3**. The titration experiments have predicted that **4.3** and **4.4** should exhibit similar reactivity towards thiolates on the basis of their similar pKa values.

4-VP derivative	Predicted pKa (REAXYS)	Experimentally determined pKa
4.1	4.15	4.27
4.2	5.36	5.12
4.3	5.64	5.99
4.4	6.67	6.05

Table 4.1: A comparison between predicted (REAXYS) and experimentally determined pKa values for 4-VP derivatives **4.1**-**4.4**.

4.4) Investigation of the Reactions between the 4-VP Derivatives 4.1-4.4 and the Thiol-Containing Peptide Glutathione

We next sought to investigate the reaction of 4-VP derivatives **4.1**-**4.4** with the thiol containing peptide glutathione (**2.21**) to determine the impact of pKa on reaction rate. Each of the derivatives **4.1**-**4.4** were reacted in a THF/phosphate buffer solution (0.1 M, pH = 7) with glutathione (0.9 eq.), followed by purification of the reaction mixtures by reverse phase (C-18) chromatography and characterisation of the products by NMR spectroscopy. All four 4-VP derivatives were found to undergo a reaction with glutathione, successfully alkylating the thiol of the peptide. The identity of the isolated products **4.26**-**4.29** are summarised in **Figure 4.8**.

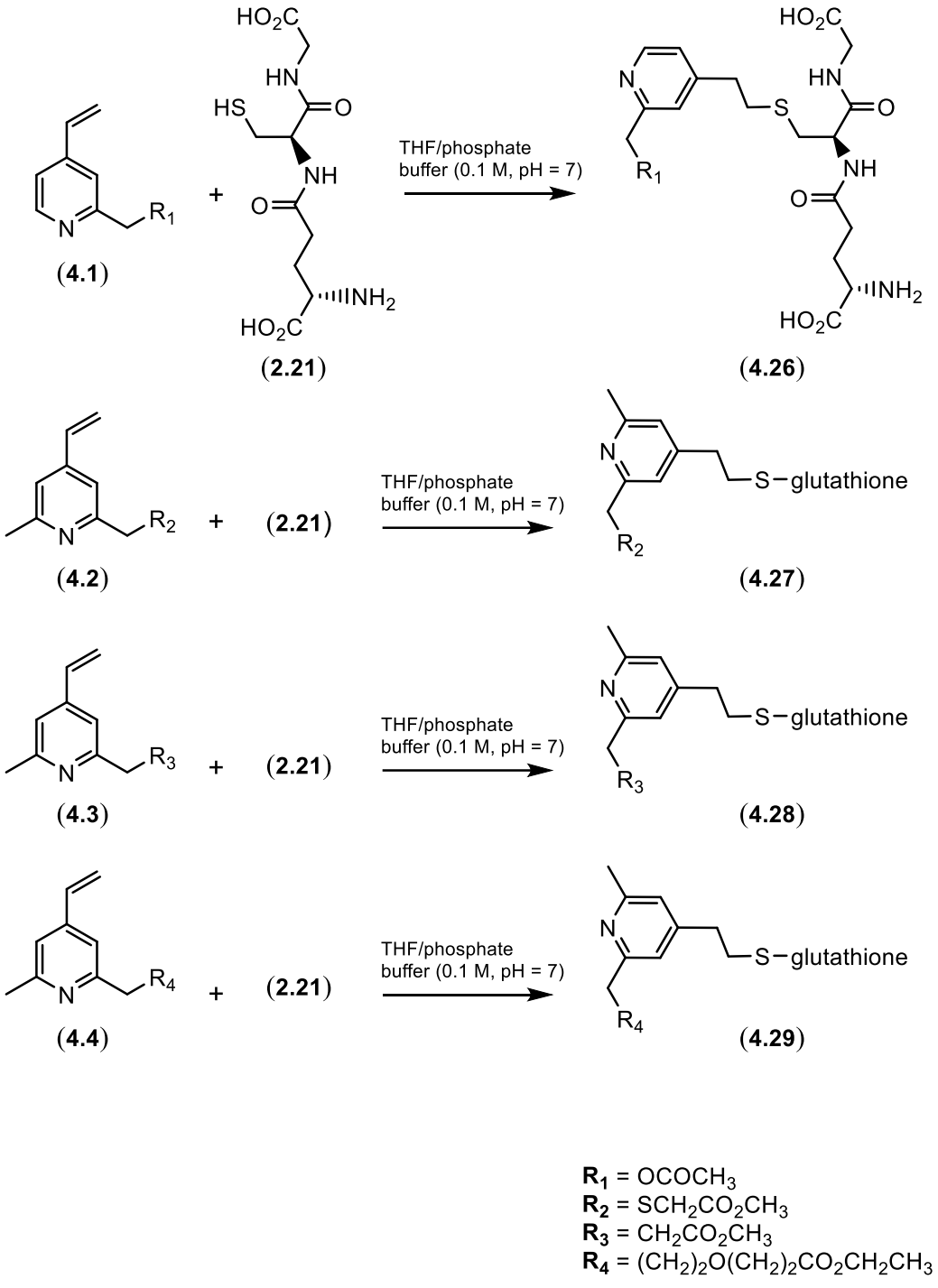

Figure 4.8: Reaction of 4-VP derivatives **4.1**-**4.4** with reduced glutathione (**2.21**) to yield thiol-alkylated products **4.26**-**4.29**.

Following the successful synthesis of alkylated glutathione derivatives **4.26**-**4.29**, we next sought to investigate the rate of formation of **4.26**-**4.29** as a function of pH. These experiments were performed to determine the pH optimum for performing

thiol alkylation conjugations for each of the 4-VP derivatives **4.1**-**4.4**. The rates of alkylation of glutathione were determined using NMR spectroscopy (**Figure 4.9**).

The 4-VP derivatives **4.1**-**4.4** were individually incubated with glutathione (**2.21**) in deuterated dimethyl sulfoxide (DMSO-$_{d6}$, 10 %) and deuterated aqueous sodium phosphate (0.1 M, pH = 7) within a NMR tube and vortexed vigorously before being continuously monitored by NMR spectroscopy over 90 minutes at 25 °C. The reactions were monitored through consumption of the 4-VP derivatives (represented by the gradual decrease of the vinyl proton peaks and shift of the H-3 and H-5 aromatic proton peaks) and the appearance of thiol alkylated peptide (represented by the increase in product peaks of H-3' and H-5' aromatic proton peaks) over the time interval (**Figure 4.9**).

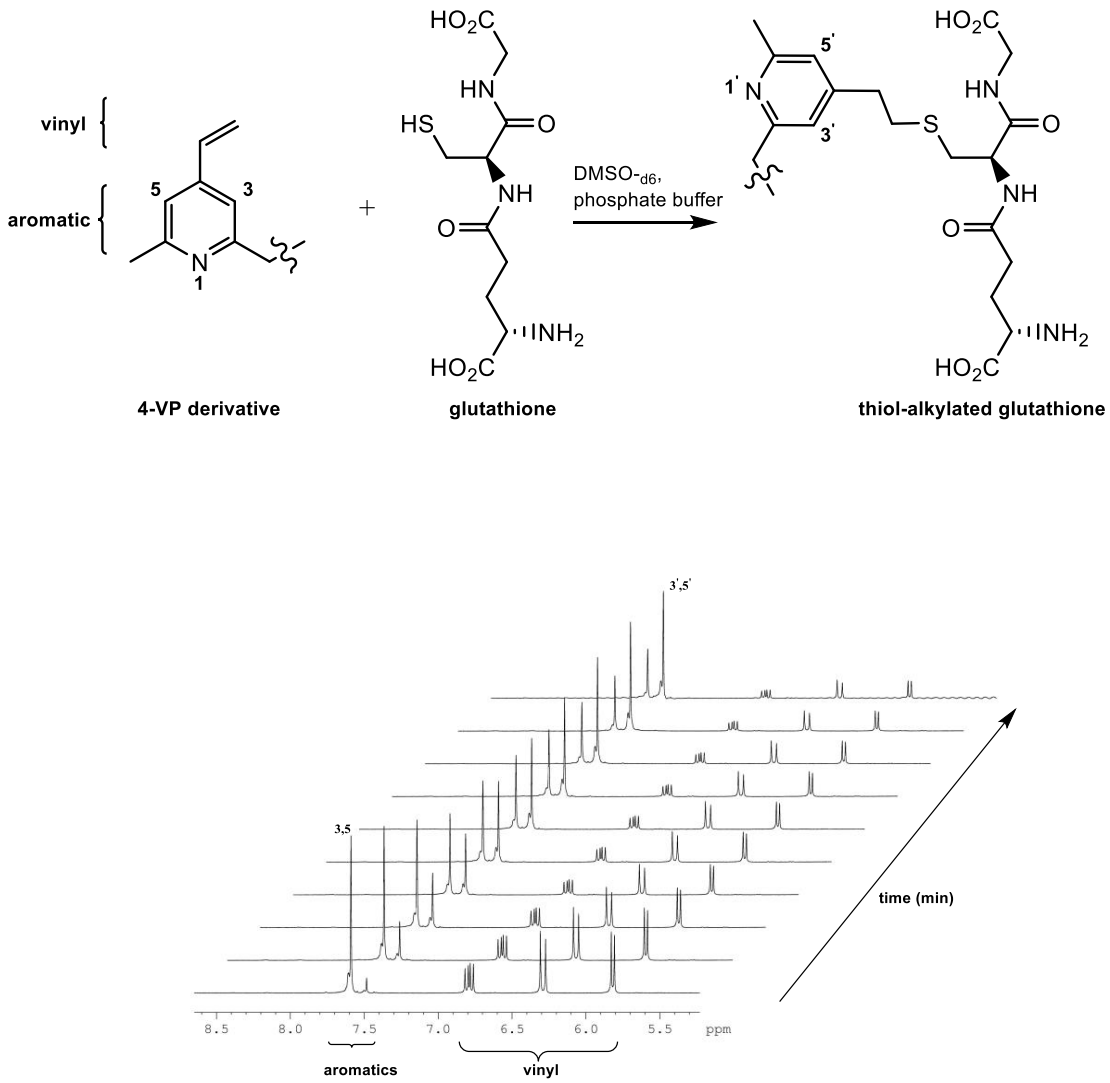

Figure 4.9: An example of using NMR to monitor the time-course of thiol-alkylation of glutathione by a 4-VP derivative.

The relative rates of thiol-alkylation of glutathione by 4-VP derivatives **4.1**-**4.4** at pH = 7 were plotted from which a time for 50 % consumption ($t_{1/2}$) of 4-VP could be obtained and is illustrated in **Figure 4.10**.

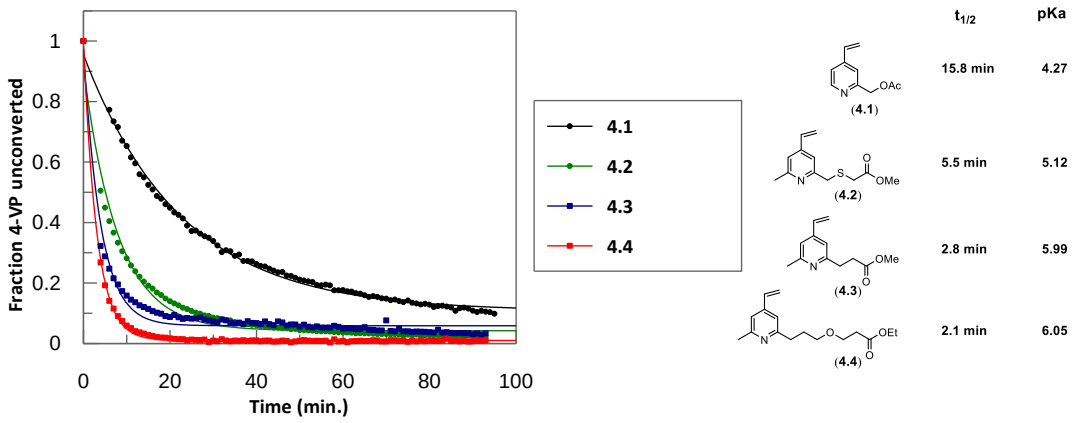

Figure 4.10: Relative rates, pKa values and half-life of thiol-alkylation of glutathione (**2.21**) by 4-VP derivatives **4.1**-**4.4** at pH = 7. NMR spectroscopy was utilised to monitor the reaction of 4-VP derivatives **4.1**-**4.4** with **2.21**. The graphical data was utilised to obtain a time at which 50 % of the alkylating reagent was consumed.

Linker **4.1** proved to be the least reactive ($t_{1/2}$ = 15.8 mins.) of the four alkylating reagents utilised to functionalise glutathione at pH = 7. The ring nitrogen of **4.1** is mostly unprotonated at pH = 7 due to its low pKa value (pKa = 4.27), which decreases the electrophilic potential of the vinyl group and leads to a relatively slow thiol alkylation reaction. Linker **4.2** was almost 3 times more reactive ($t_{1/2}$ = 5.5 mins.) than derivative **4.1**, consistent with the higher pKa of the ring nitrogen (pKa = 5.12). The 4-VP linkers **4.3** & **4.4** displayed similar reactivity and proved to be the most reactive linkers at pH = 7. The 4-VP linkers **4.3** & **4.4** possess pKa values that are closest to the pH of the reaction and, therefore, exhibited superior thiol-alkylation kinetics ($t_{1/2}$ = 2.8 mins. & 2.1 mins. respectively) compared to 4-VP derivatives **4.1** & **4.2**. Similar pKa's reflected in similar rates further supported the suggestion that the pKa of the pyridine ring is an important factor influencing reactivity with regards to thiol alkylation.

The pH of the reactions were subsequently varied (pH = 6 & pH = 8) for the reaction between **4.3** or **4.4** and reduced glutathione (**2.21**) to determine the relative rate changes of thiol-alkylation as a function of reaction pH. The reactions were monitored by NMR spectroscopy, similar to that performed previously, to yield reaction rates as a function of the pH of the reaction (**Figure 4.11**).

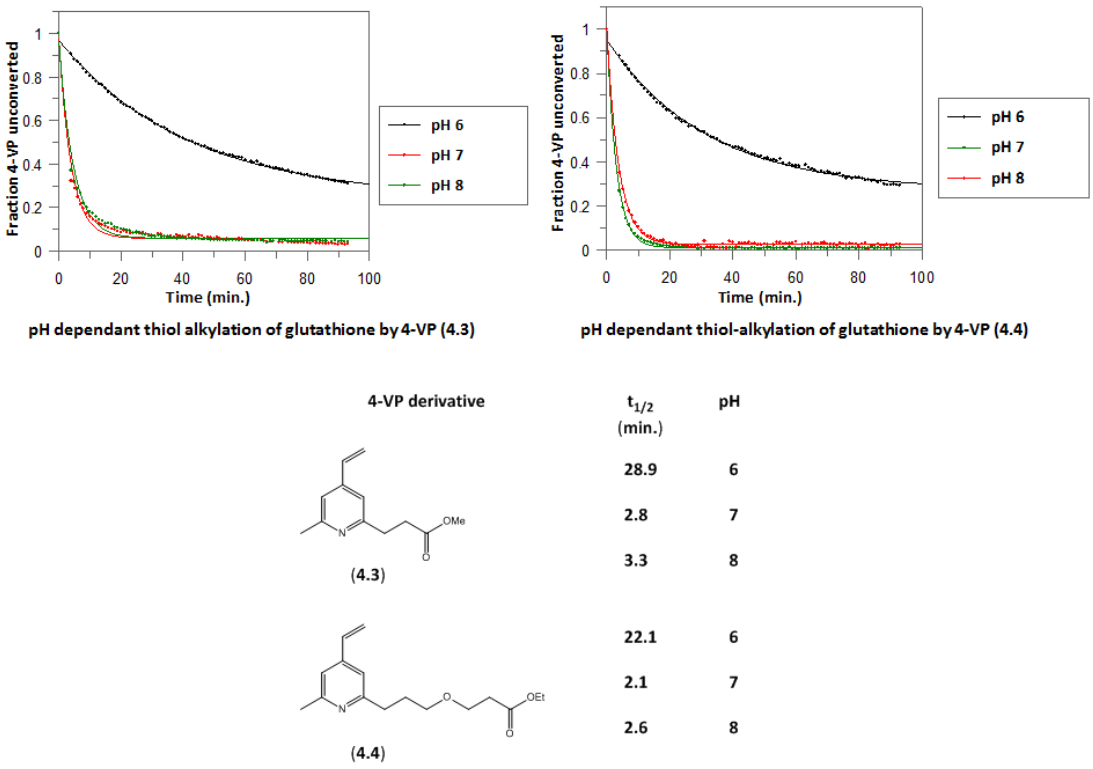

Figure 4.11: Relative rates and half-life of thiol-alkylation of glutathione (**2.21**) by 4-VP derivatives **4.3** & **4.4** as a function of the pH of the reaction. NMR spectroscopy was utilised to monitor the reaction of 4-VP derivatives **4.3** & **4.4** with **2.21**. The graphical data was utilised to obtain a time at which 50 % of the alkylating reagent was consumed ($t_{1/2}$).

An insignificant rate change for thiol alkylation was observed for both linkers **4.3** and **4.4** when raising the pH from pH = 7 to pH = 8 (**Figure 4.11**). The alkaline pH favours deprotonation of the thiol to form a nucleophilic thiolate, which may compensate for a decreased concentration of protonated 4-VP species. An approximate ten-fold drop in the rate of alkylation was, however, observed for both linkers **4.3** and **4.4** when decreasing the pH from pH = 7 to pH = 6. The reduction in pH may favour the protonated form of the 4-VP derivatives, but this does not seem to be the significant factor with regards to the rate of the reaction. The concentration of the thiolate seems to be the critical determinant.

The most effective pH range for thiol-alkylation of thiols by **4.3** and **4.4** is between pH = 7 and pH = 8, a compromise between the pKa of the nitrogen of the pyridine ring of the 4-VP derivatives and the pKa of the thiol of glutathione.

4.5) Specificity of 4-VP Derivatives 4.2 and 4.3 for Thiol Alkylation

The specificity of a selection of 4-VP derivatives for alkylation of thiol nucleophiles over amine nucleophiles as a function of pH was investigated.

The specificity of 4-VP **4.2** towards thiol alkylation over amine alkylation was tested at pH = 7 and pH = 8 (**Figure 4.12**). N-acetyl-L-cysteine (**3.9**) and benzyl amine (**4.30**, 1 eq.) were dissolved in argon purged 10 % THF in aqueous sodium phosphate (0.9 mL, 0.1 M, pH = 7). A solution of 4-VP (**4.2**, 1 eq.) in THF (0.1 mL) was added and the reaction was rapidly stirred at room temperature for three hours. The reaction was initially investigated by mass spectrometry. The thiol-alkylated product **4.31** was detected in the mass spectrum, however, no alkylation of benzyl amine by the 4-VP derivative **4.2** was observed. Purification of the reaction by silica gel chromatography confirmed the observations by mass spectrometry. The thiol alkylated amino acid **4.31** was isolated in 76 % yield while no amine-alkylated product was isolated.

The above reaction was repeated at pH = 8 and initially investigated by mass spectrometry. The thiol alkylated product **4.31** was again observed, however no amine alkylated product was detected. Purification of the reaction by silica gel chromatography yielded the thiol alkylated product **4.31** in 79 % yield, while no amine-alkylated product was isolated.

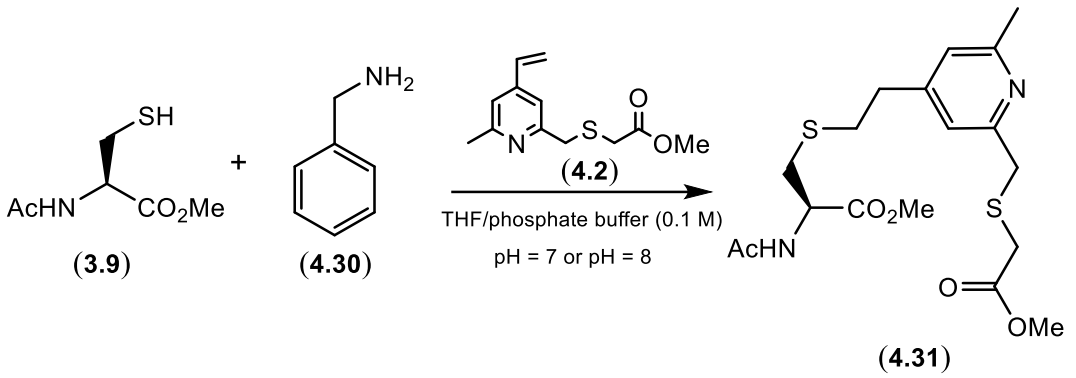

Figure 4.12: 4-VP derivative **4.2** reacts specifically with the thiol derivative **3.9** instead of the amine derivative **4.30** at both pH = 7 and pH = 8.

The specificity of 4-VP derivative **4.3** towards thiol alkylation over amine alkylation was also tested at pH = 7 and pH = 8 (**Figure 4.13**). N-acetyl-L-cysteine (**3.9**) and benzyl amine (**4.30**, 1 eq.) were dissolved in argon purged 10 % THF in aqueous sodium phosphate (0.9 mL, 0.1 M, pH = 7). A solution of 4-VP (**4.3**, 1 eq.) in THF (0.1 mL) was added and the reaction was rapidly stirred at room temperature for three hours and subsequently investigated by mass spectrometry. The thiol-alkylated product **4.32** was observed in the mass spectrum, however, no alkylation of benzyl amine was observed. Purification of the reaction by silica gel chromatography yielded the thiol alkylated product **4.32** in 75 % yield, while no amine alkylated product was isolated.

The above reaction was repeated at pH = 8 and initially investigated by mass spectrometry. The thiol alkylated product **4.32** was again observed, however no amine alkylated product was detected. Purification of the reaction by silica gel chromatography yielded the thiol alkylated product **4.32** in 81 % yield, while no amine alkylated product was isolated.

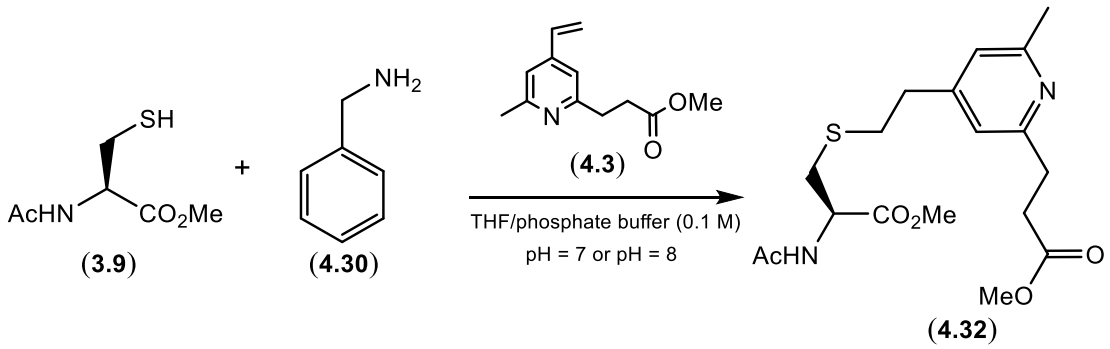

Figure 4.13: 4-VP derivative **4.3** reacts specifically with the thiol derivative **3.9** instead of the amine derivative **4.30** at both pH = 7 and pH = 8.

The above experiments have indicated that a selection of 4-VP derivatives for bioconjugation purposes are reagents that can be specific for thiol alkylation. The specificity for thiol alkylation at an alkaline pH offers a significant advantage over α-halo-carbonyl and maleimide linkers, which have been reported to react with thiols and amines at pH $>$ 7 [18].

4.6) Reaction of TCEP (2.6) and THPP (2.7) with 4-VP (4.33)

4-VP is a Michael-like acceptor similar to maleimide and vinyl sulfone and, therefore, may exhibit similar reaction trends with TCEP (**2.6**) and THPP (**2.7**) to those observed for maleimide and vinyl sulfone in **Chapter 2**. It has been reported that tributylphosphine is compatible with 4-VP but there is no evidence for the potential reaction of TCEP or THPP with 4-VP derivatives [152]. TCEP or THPP could potentially be used as disulfide reducing agents of peptides or proteins prior to the addition of 4-VP derivatives to effect thiol alkylation. As such, an assessment of a potential reaction between TCEP or THPP and 4-VP was deemed necessary.

4-VP (**4.33**, 20 mg) was first incubated with TCEP (**2.6**, 49 mg) in THF (2 mL) and aqueous sodium phosphate (0.1 M, pH = 7, 8 mL) for three hours at room temperature. Purification of the reaction by C-18 chromatography yielded a 4-VP-TCEP adduct in 64 % yield that could not be distinguished by NMR spectroscopy as either **4.34** or **4.35** (**Figure 4.14**). However, the isolation of an adduct between 4-VP

and TCEP demonstrated that the reducing agent should be removed before addition of 4-VP derivatised ligands into bioconjugation reactions.

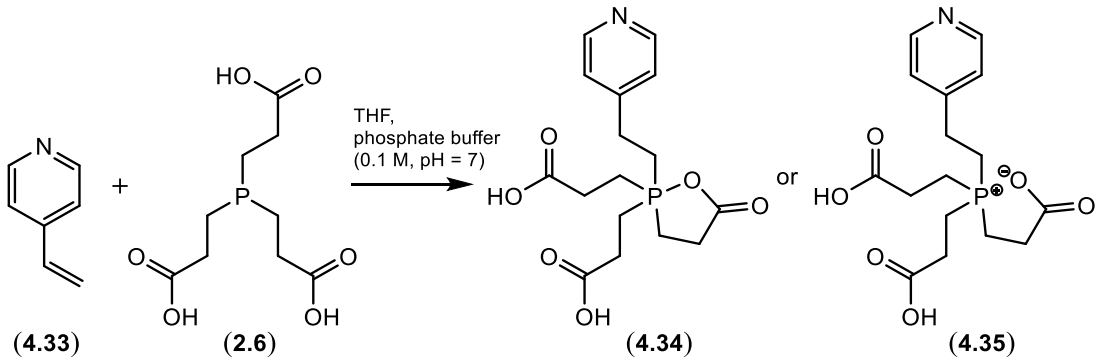

Figure 4.14: Reaction of 4-VP (**4.33**) with TCEP (**2.6**).

4-VP (**4.33**, 15.0 mg) was subsequently incubated with THPP (**2.7**, 26.7 mg) in THF (2 mL) and aqueous sodium phosphate (0.1 M, pH = 7, 8 mL) for three hours at room temperature. Purification of the reaction by C-18 chromatography yielded a 4-VP-THPP adduct in 61 % yield that could not be distinguished by NMR spectroscopy as either **4.36** or **4.37** (**Figure 4.15**). Again, the isolation of an adduct between 4-VP and THPP, similar to TCEP, suggested that the reducing agent should be removed prior to addition of 4-VP derivatised ligands into bioconjugation reactions.

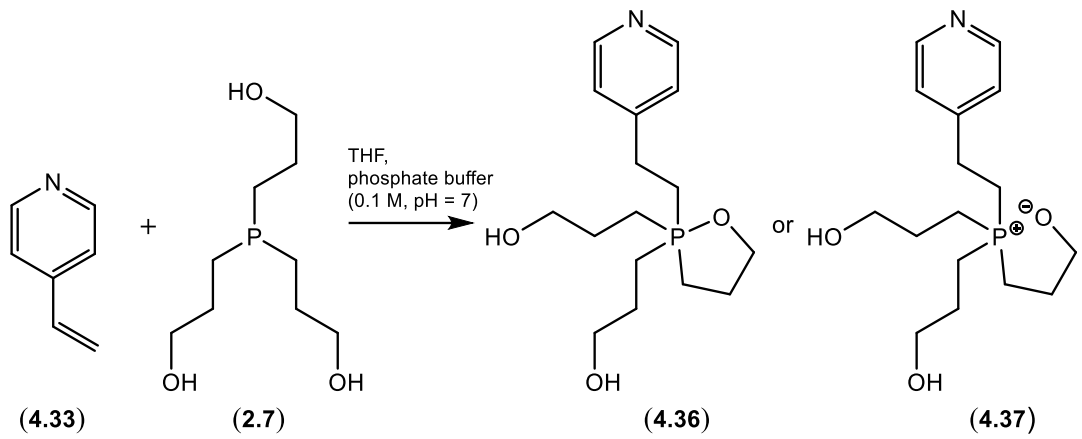

Figure 4.15: Reaction of 4-VP (**4.33**) with THPP (**2.7**).

4.7) Investigating a Possible Reaction of 4-VP with Alkyl Azide 3.3

It was envisaged to utilise the water soluble alkyl azide **3.3** (discussed in **Chapter 3**) to oxidise excess TCEP or THPP after reduction of disulfides and before the addition of 4-VP derivatised ligands for alkylation of thiols. A [3+2] cycloaddition reaction of alkyl azide **3.3** was characterised with both Michael acceptors N-ethyl maleimide (**2.8**) and phenyl vinyl sulfone (**2.18**). 4-VP is also a Michael acceptor and so the possible reaction between **3.3** and 4-VP (**4.33**) was investigated.

4-VP (**4.33**) was dissolved in THF (1.5 mL) and aqueous sodium phosphate (0.25 M, pH = 7, 1.5 mL) containing alkyl azide **3.3** (1 eq.). The reaction was rapidly stirred at room temperature and monitored by TLC and HRMS. After 2 days no evidence of triazoline formation was evident by either TLC or HRMS. This investigation indicated that the addition of **3.3** for excess phosphine oxidation can be used in a reaction containing thiol alkylating reagents based on 4-VP.

A selection of 4-VP derivatives were subsequently functionalised with ligands such as carbohydrates and PEG to investigate bioconjugation reactions with thiol-containing peptides and proteins.

4.8) A 4-VP Derivatised Carbohydrate for the Conjugation of Carbohydrates to Peptides and Proteins

A 4-VP-carbohydrate derivative was explored as a novel method for the site-specific addition of glycans to thiol-containing peptides and proteins. The 4-VP acceptor **4.39** was synthesised in 68 % yield for subsequent glycosylation to a carbohydrate containing donor (**Figure 4.16**). The acceptor **4.39** was based on the 4-VP derivative **4.4** due to its favourable reactivity at neutral pH.

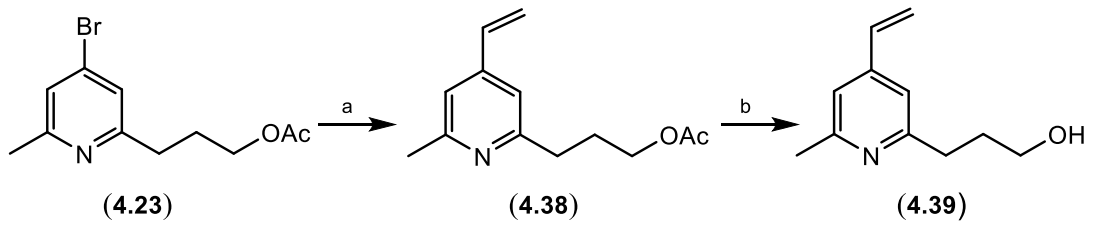

(**4.23**) (**4.38**) (**4.39**)

Figure 4.16: Synthesis of the 4-VP derivative **4.39**. **a**) $Bu_3SnC_2H_3$, tetrakis(triphenylphosphine)Pd(0), toluene, 85 °C, **b**) NaOMe, MeOH.

Lactose, a disaccharide consisting of β-D-galactopyranosyl-(1→4)-D-glucose (**4.40**) was chosen as a model carbohydrate for attachment to the 4-VP linker **4.39**. Lactose is a cheap and commercially available starting material. It was readily available in our laboratory, which was the main reason for its choice as the carbohydrate ligand. The lactose donor **4.43** was synthesised using standard protection/deprotection strategies employed in synthetic carbohydrate chemistry in an overall 51 % yield (**Figure 4.17**). The final 4-VP-lactose derivative **4.45** was generated through a glycosylation step between the 4-VP acceptor **4.39** and the lactosyl donor **4.43** followed by a deacetylation reaction of **4.44** in an overall yield of 52 %.

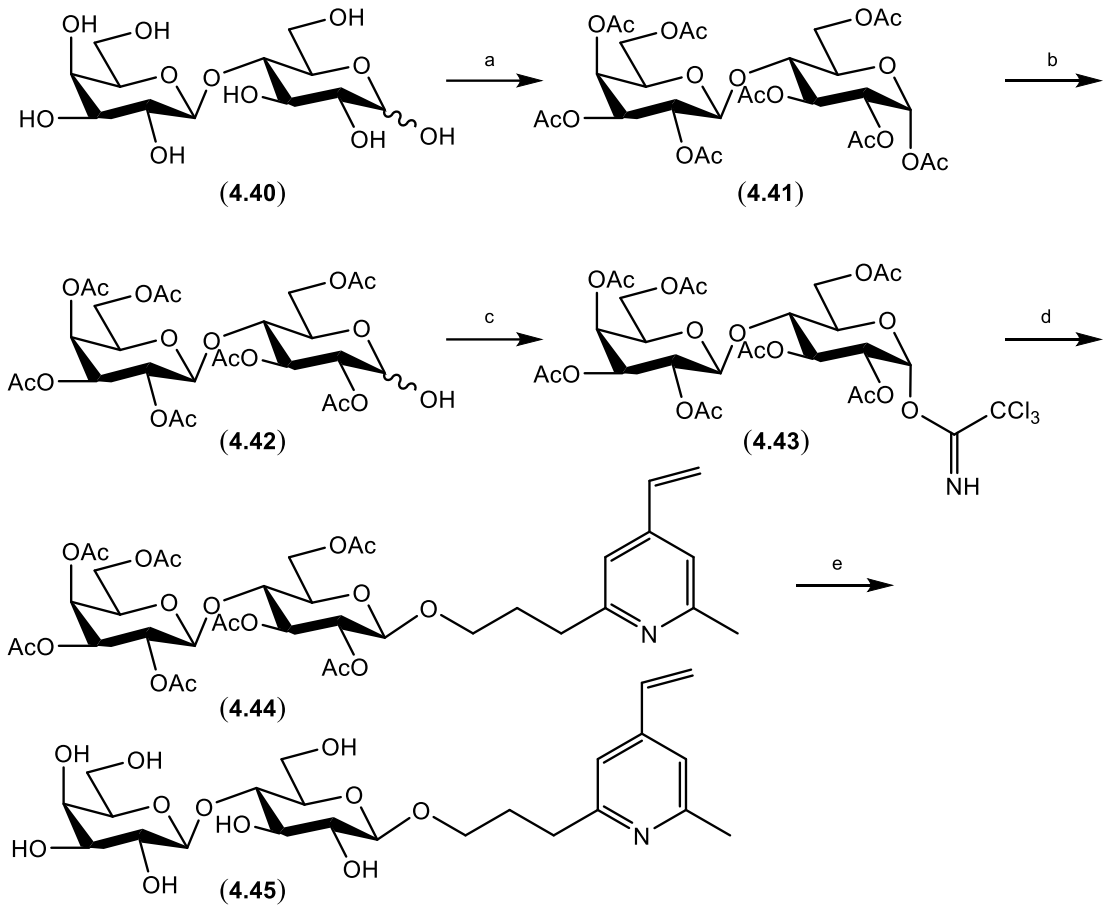

Figure 4.17: Synthesis of the 4-VP-lactose derivative **4.45**. **a**) Ac_2O, pyridine, **b**) $NH_2NH_2{\cdot}AcOH$, $MeOH/CH_2Cl_2$, **c**) CCl_3CN, DBU, CH_2Cl_2, **d**) **4.39**, TMSOTf, DCM, **e**) NaOMe, MeOH.

The reaction of the 4-VP-lactose derivative **4.45** with a thiol-containing peptide was initially performed on glutathione (**2.21**). The 4-VP-lactose derivative (**4.45**, 10 mg) was dissolved a solution of THF (1 mL) and aqueous sodium phosphate (0.1 M, pH = 7, 3 mL). Glutathione (**2.21**, 5.5 mg) was added and the reaction was left to stir for three hours at room temperature. Purification of the reaction by reverse phase chromatography resulted in the isolation of the thiol alkylated peptide **4.46** in 65 % yield, which was characterised by NMR spectroscopy (**Figure 4.18**). The characterisation of product **4.46** confirmed the ability of utilising a 4-VP linker to chemically glycosylate peptides *via* thiol alkylation of a cysteine residue.

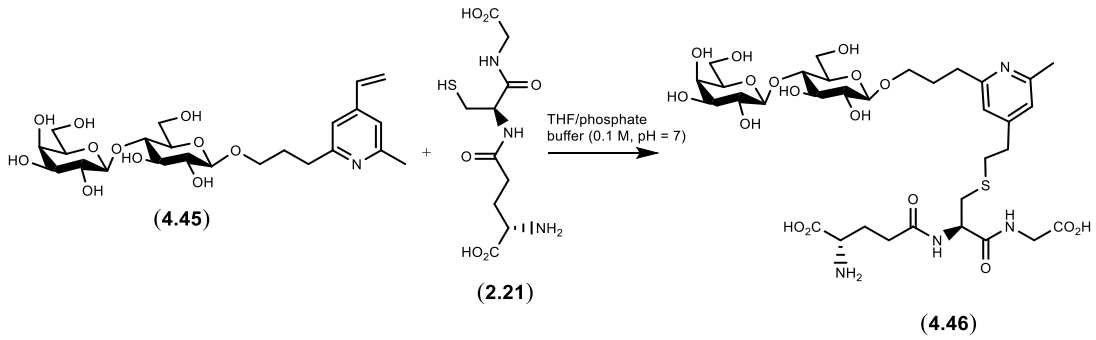

(**4.45**) (**2.21**) (**4.46**)

Figure 4.18: Thiol alkylation of glutathione (**2.21**) using the 4-VP-lactose derivative **4.45**.

The 4-VP-lactose derivative **4.45** was subsequently utilised for the glycosylation of a longer peptide sequence possessing a single cysteine residue. The final 20 amino acid sequence at the carboxy terminal end from the protein, Staphylococcus aureus binder of immunoglobulins ($Sbi_{3,4\text{-}Cys}$), which was in utilised in **Chapter 3**, was outsourced for synthesis to Thermo Fisher Scientific (**4.47**). The synthesised peptide consists of the following amino acid sequence:

NH_2-WQKQLDALVAQKDAEKKVA **C**-CO_2H

(**4.47**)

The glycosylation of the 20 amino acid peptide by *via* thiol-alkylation of the C-terminal cysteine residue was monitored by high performance liquid chromatography (HPLC). The reaction of the peptide (0.37 mM) with **4.45** (1.1 mM) was performed in aqueous sodium phosphate (0.1 M, pH = 7). The native peptide sequence eluted at 12.8 minutes, while the glycosylated peptide eluted at 12.2 minutes under the conditions developed on the HPLC instrument. The adequate resolution of the reactant and product peaks permitted the monitoring of the glycosylation reaction over a time course. A plot of the glycosylation reaction was performed through analysis of the integrals associated with the diminishing reactant peak and increasing product peak over the time course (**Graph 4.1**). HPLC analysis revealed that 50 % of glycosylated peptide product was achieved after 3.3 hours. The product eluting at 12.2 minutes was subsequently collected and analysed by mass spectrometry. The product was identified by MS (*m/z* 2773.43),

which was expected for the glycosylated product (expected for $C_{123}H_{202}N_{29}O_{41}S_1$ $(M+H^+) = 2773.43$).

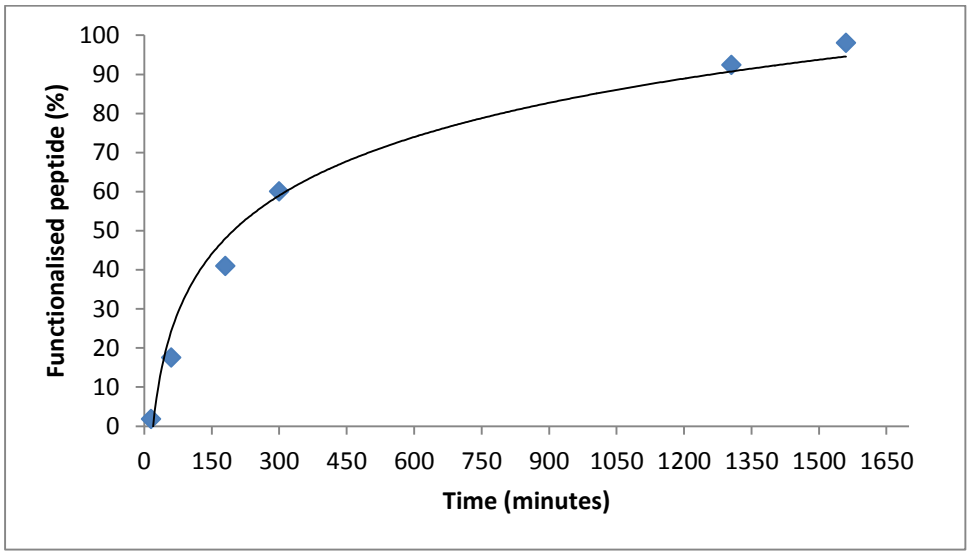

Graph 4.1: Thiol alkylation of a cysteine-containing peptide utilising the 4-VP-lactose derivative **4.45**.

The potential of the 4-VP-lactose derivative **4.45** to alkylate a protein was subsequently investigated using the full $Sbi_{3,4\text{-}Cys}$ protein and analysed by mass spectrometry. $Sbi_{3,4\text{-}Cys}$ (1 mg/mL) was incubated with TCEP (5 mM) for 1 hour then desalted using a PD-10 column. Mass spectrometry analysis of the unfunctionalised $Sbi_{3,4\text{-}Cys}$ revealed a mass of *m/z* 14832.29 for the protein. Reaction of the $Sbi_{3,4\text{-}Cys}$ protein(33 μM) with the 4-VP-lactose derivative **4.45** (0.5 mM) was performed in aqueous sodium phosphate (0.1 M, pH = 7) for 6 hours, desalted using a PD-10 column and analysed by mass spectrometry. A peak of *m/z* 15334.16 was identified which was expected for the glycosylated protein $(M+H^+)$.

In summary, a 4-VP linker has been successfully utilised to attach a carbohydrate to peptides and a protein *via* thiol alkylation. A selection of 4-VP linkers were subsequently derivatised with polyethylene glycol (PEG) to demonstrate that 4-VP can be functionalised with a variety of ligands, followed by alkylation experiments on thiol-containing proteins.

4.9) 4-VP Derivatised PEG's as Reagents for Protein PEGylation

4-VP derivatives **4.2** and **4.3** were chosen as linkers for the functionalisation of commercially available methoxy-PEG-amine-2kDa, due to the availability of suitable intermediates for their synthesis and their favourable rates of alkylation of a peptide at neutral pH (**Figure 4.10**). The synthesis of both the 4-VP-PEG derivatives **4.48** and **4.49** are illustrated in **Figure 4.19**.

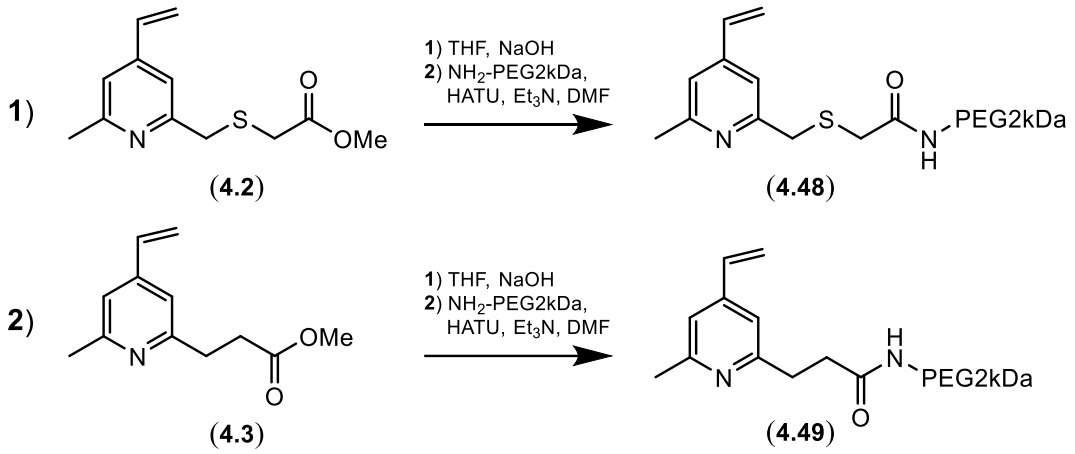

Figure 4.19: Synthesis of 4-VP-PEG derivatives **4.48** and **4.49**.

The ability of 4-VP-PEG derivatives **4.48** and **4.49** to alkylate a thiol containing protein was tested on yeast enolase, a 47 kDa protein with a single cysteine residue, which was previously utilised in **Chapter 3**. The effect of excess TCEP or THPP present in reactions with 4-VP-PEG derivatives on PEGylation yields was also investigated. Further, the addition of the water soluble alkyl azide **3.3** was pursued as a method to oxidise excess TCEP or THPP prior to addition of **4.48** or **4.49** for thiol alkylation of the protein. The reactions between yeast enolase and 4-VP derivatives **4.48** and **4.49** were analysed by SDS-PAGE.

Yeast enolase was denatured in argon purged Tris buffer (0.5 M, pH = 7.2), containing 5 mM EDTA and 8 M urea. Varying amounts of TCEP (1-10 eq.) were added to aliquots of protein and incubated for 45 minutes at 25 °C. The 4-VP-PEG2kDa **4.48** (1 eq.) was subsequently added and the reaction was incubated at 37 °C for 18 hours (**Figure 20**, **lanes 3**-**5**). In parallel experiments, the alkyl azide **3.3**

(100 eq.) was added to aliquots of yeast enolase containing varying amounts of TCEP (1-10 eq.). The samples were incubated for 1 hour at 37 °C prior to addition of 4-VP-PEG2kDa **4.48** (1 eq.), followed by incubation at 37 °C for 18 hours (**Figure 4.20**, **lanes 6**-**8**).

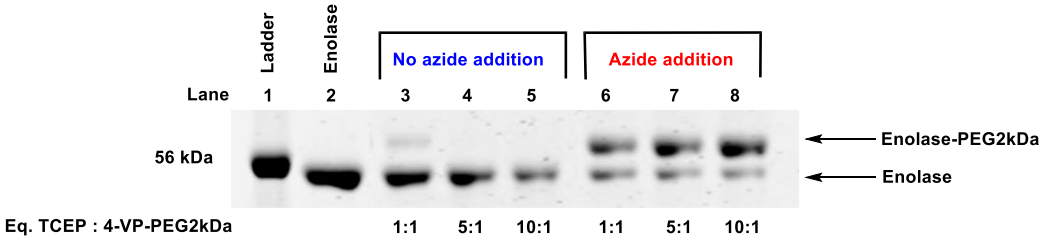

Figure 4.20: SDS-PAGE of reactions between **4.48** (1 eq.) and yeast enolase in the presence of varying TCEP amounts (1-10 eq.) and in the presence or absence of the alkyl azide **3.3** (100 eq.). **Lane 1**: ladder, **Lane 2**: enolase, **Lane 3**: enolase + TCEP (1 eq.) + **4.48** (1 eq.), **Lane 4**: enolase + TCEP (5 eq.) + **4.48** (1 eq.), **Lane 5**: enolase + TCEP (10 eq.) + **4.48** (1 eq.), **Lane 6**: enolase + TCEP (1 eq.) + **3.3** (100 eq.) + **4.48** (1 eq.), **Lane 7**: enolase + TCEP (5 eq.) + **3.3** (100 eq.) + **4.48** (1 eq.), **Lane 8**: enolase + TCEP (10 eq.) **3.3** (100 eq.) + **4.48** (1 eq.). The SDS-PAGE gel was stained with Coomassie solution and analysed utilising Image Studio Lite software.

The presence of TCEP in the conjugation reactions with 4-VP-PEG2kDa **4.48** results in extremely low yields (calculated using Image Studio Lite version 4.0) of PEGylated protein (**Figure 20**, **Lanes 3**-**5**). Much lower yields (0-11 %, **Table 4.2**) were obtained when comparing to similar experiments utilising maleimide-PEG2kDa to PEGylate yeast enolase (11-42 %, **Chapter 3**, **Table 3.2** and included in **Table 4.2**) in the presence of TCEP. The 4-VP-PEG2kDa derivative **4.48** appears to be less reactive than maleimide-PEG2kDa with regards to thiol alkylation and reacts with the TCEP present in the reaction, resulting in low PEGylation yields. The addition of the alkyl azide **3.3** (**Figure 4.20**, **Lanes 6**-**8**) was successful in oxidising TCEP, which resulted in higher yields of PEGylated yeast enolase when utilising 4-VP-PEG2kDa derivative **4.48** (62-79 %, **Table 4.2**). Similar yields (76-85 %, **Chapter 3**, **Table 3.2** and included in Table **4.2**) were obtained in experiments utilising maleimide-PEG2kDa, illustrating that 4-VP derivatives can produce conjugate yields comparable to established reagents, such as maleimide derivatives.

The addition of the alkyl azide **3.3** to oxidise excess TCEP present in solution improved PEGylation of yeast enolase by **4.48.** High Pegylation yields were achieved without the necessity for intermediate purification protocols.

The effect of the reducing agent THPP (**2.7**) on PEGylation of a protein by 4-VP-PEG2kDa derivative **4.48** was subsequently investigated. The ability of the alkyl azide **3.3** to oxidise THPP prior to PEGylation by 4-VP-PEG2kDa derivative **4.48** was also explored. Yeast enolase was denatured in argon purged Tris buffer (0.5 M, pH = 7.2), containing 5 mM EDTA and 8 M urea. Varying amounts of THPP (1-10 eq.) were added to aliquots of protein and incubated for 45 minutes at 25 °C. 4-VP-PEG2kDa **4.48** (1 eq.) was subsequently added and the reactions were incubated at 37 °C for 18 hours (**Figure 4.21**, **lanes 3**-**5**). In parallel experiments the alkyl azide **3.3** (100 eq.) was added to aliquots of enolase containing varying amounts of THPP (1-10 eq.). The samples were incubated for 1 hour at 37 °C prior to addition of 4-VP-PEG2kDa **4.48** (1 eq.) followed by incubation at 37 °C for 18 hours (**Figure 4.21**, **lanes 6**-**8**).

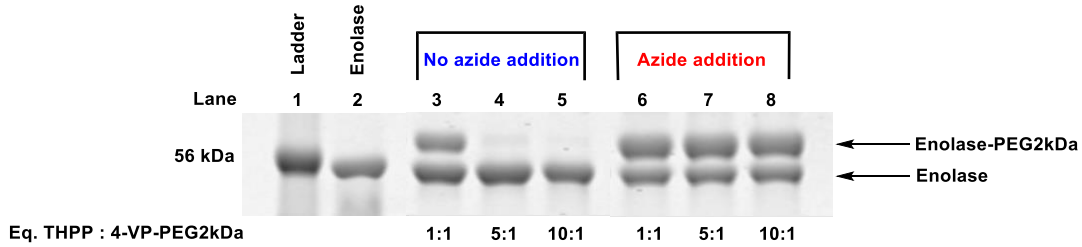

Figure 4.21: SDS-PAGE of reactions between **4.48** (1 eq.) and yeast enolase in the presence of varying THPP amounts (1-10 eq.) and in the presence or absence of the alkyl azide **3.3** (100 eq.). **Lane 1**: ladder, **Lane 2**: enolase, **Lane 3**: enolase + THPP (1 eq.) + **4.48** (1 eq.), **Lane 4**: enolase + THPP (5 eq.) + **4.48** (1 eq.), **Lane 5**: enolase + THPP (10 eq.) + **4.48** (1 eq.), **Lane 6**: enolase + THPP (1 eq.) + **3.3** (100 eq.) + **4.48** (1 eq.), **Lane 7**: enolase + THPP (5 eq.) + **3.3** (100 eq.) + **4.48** (1 eq.), **Lane 8**: enolase + THPP (10 eq.) + **3.3** (100 eq.) + **4.48** (1 eq.). The SDS-PAGE gel was stained with Coomassie solution and analysed utilising Image Studio Lite software.

The presence of THPP with 4-VP-PEG derivative **4.48** in the reactions results in low yields of PEGylated protein (**Figure 21**, **Lanes 3**-**5**). The yields (0-38 %) are, however, comparable (**Table 4.2**) with similar experiments utilising maleimide-PEG2kDa to

PEGylate yeast enolase (3-37 %) in the presence of THPP (**Chapter 3**, **Table 3.2** and included in **Table 4.2**). It appears that THPP is a very nucleophilic phosphine derivative and reacts rapidly with both maleimide and 4-VP derivatives before the low concentration of thiolates are alkylated.

The addition of the alkyl azide **3.3** (**Figure 4.21**, **Lanes 6**-**8**) was successful in oxidising excess THPP, which resulted in higher yields (56-57 %) of PEGylated yeast enolase (**Table 4.2**) when utilising 4-VP-PEG2kDa derivative **4.48**. The yields are lower than the yields (68-76 %) achieved in similar experiments utilising maleimide-PEG2kDa (**Chapter 3**, **Table 3.2** and included in **Table 4.2**). The slower rates of thiol alkylation exhibited by 4-VP derivatives compared to maleimide derivatives may result in the oxidation of the thiols before alkylation is effected by the 4-VP derivatives.

The addition of the alkyl azide **3.3** proved to be an effective strategy to oxidise THPP present in solution, which allows PEGylation of yeast enolase by **4.48** in consistently yields, without necessity for intermediate purification protocols.

		Eq. Reducing Agent : 4-VP-PEG2kDa (4.48)			Eq. Reducing Agent : Maleimide-PEG2kDa		
		1:1	5:1	10:1	1:1	5:1	10:1
Reducing Agent	Alkyl Azide (3.3)	Yield of PEGylated Yeast Enolase (%)			Yield of PEGylated Yeast Enolase (%)		
TCEP	-	11.1	0	0	42.3	16.6	10.5
TCEP	+	61.7	71.2	78.6	76.4	82.4	84.7
THPP	-	37.9	3.0	0	37.0	6.7	3.1
THPP	+	57.0	57.8	56.1	68.0	73.4	75.8

Table 4.2: Comparison of PEGylated yeast enolase yields achieved by 4-VP-PEG2kDa derivative **4.48** and maleimide-PEG2kDa, with and without the use of the alkyl azide **3.3** to oxidise reducing agents TCEP (**2.6**) or THPP (**2.7**).

The PEGylation yields of yeast enolase when utilising 4-VP-PEG2kDa derivative **4.49** in the presence or absence of TCEP or THPP was subsequently explored. Yeast enolase was denatured in argon purged Tris buffer (0.5 M, pH = 7.2) containing 5 mM EDTA and 8 M urea. Varying amounts of TCEP (1-10 eq.) were added to aliquots

of protein and incubated for 45 minutes at 25 °C. The 4-VP-PEG2kDa derivative **4.49** (1 eq.) was subsequently added and the reactions were incubated at 37 °C for 18 hours (**Figure 22**, **lanes 3**-**5**). In parallel experiments the alkyl azide **3.3** (100 eq.) was added to aliquots of yeast enolase containing varying amounts of TCEP (1-10 eq.). The samples were incubated for 1 hour at 37 °C prior to addition of 4-VP-PEG2kDa derivative **4.49** (1 eq.), followed by incubation at 37 °C for 18 hours (**Figure 4.22**, **lanes 6**-**8**).

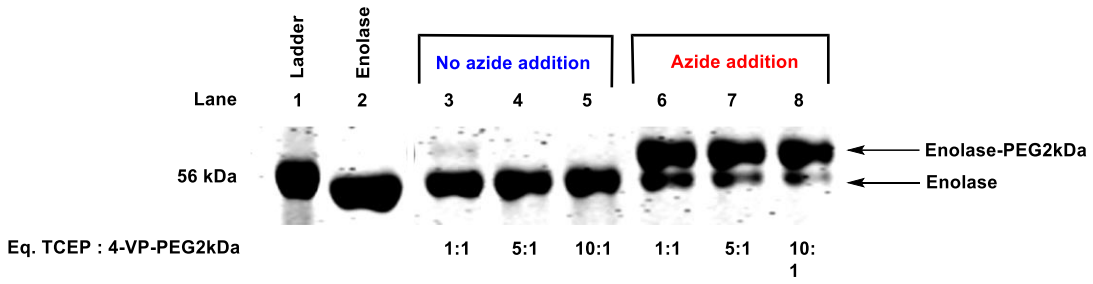

Figure 4.22: SDS-PAGE analysis of reactions between **4.49** (1 eq.) and yeast enolase in the presence of varying TCEP amounts (1-10 eq.) and in the presence or absence of the alkyl azide **3.3** (100 eq.). **Lane 1**: ladder, **Lane 2**: enolase, **Lane 3**: enolase + TCEP (1 eq.) + **4.49** (1 eq.), **Lane 4**: enolase + TCEP (5 eq.) + **4.49** (1 eq.), **Lane 5**: enolase + TCEP (10 eq.) + **4.49** (1 eq.), **Lane 6**: enolase + TCEP (1 eq.) + **3.3** (100 eq.) + **4.49** (1 eq.), **Lane 7**: enolase + TCEP (5 eq.) + **3.3** (100 eq.) + **4.49** (1 eq.), **Lane 8**: enolase + TCEP (10 eq.) + **3.3** (100 eq.) + **4.49** (1 eq.). The SDS-PAGE gel was stained with Coomassie solution and analysed utilising Image Studio Lite software.

The presence of TCEP with 4-VP-PEG2kDa derivative **4.49** in the reactions resulted in extremely low yields of PEGylated protein (**Figure 22**, **Lanes 3**-**5**). Much lower yields (0-4 %, **Table 4.3**) were obtained when comparing to similar experiments utilising maleimide-PEG2kDa to PEGylate yeast enolase (11-42 %, **Chapter 3, Table 3.2** and included in Table **4.3**) in the presence of TCEP. The 4-VP-PEG2kDa derivative **4.49** appears to be less reactive than maleimide-PEG2kDa with regards to thiol alkylation and reacts with the excess TCEP present in the reaction, resulting in low PEGylation yields.

The addition of the alkyl azide **3.3** (**Figure 4.22**, **Lanes 6**-**8**) was successful in oxidising TCEP, which resulted in higher yields (79-86 %) of PEGylated yeast enolase (**Table 4.3**) when utilising the 4-VP-PEG2kDa derivative **4.49**. The yields are similar to the yields (76-85 %, **Chapter 3**, **Table 3.2** and included in Table **4.3**) achieved in similar experiments utilising maleimide-PEG2kDa. The addition of alkyl azide **3.3** is an effective strategy to oxidise TCEP and produce PEGylated protein in a high yield, without necessity for intermediate purification protocols.

The addition of the alkyl azide **3.3** to oxidise the alternative reducing agent THPP to facilitate high bioconjugation yields between yeast enolase and 4-VP-PEG2kDa derivative **4.49** was next investigated. Yeast enolase was first denatured in argon purged Tris buffer (0.5 M, pH = 7.2) containing 5 mM EDTA and 8 M urea. Varying amounts of THPP (1-10 eq.) were then added to aliquots of protein and incubated for 45 minutes at 25 °C. The 4-VP-PEG2kDa derivative **4.49** (1 eq.) was subsequently added and the reactions were incubated at 37 °C for 18 hours (**Figure 4.23**, **lanes 3**-**5**). In parallel experiments the alkyl azide **3.3** (100 eq.) was added to aliquots of enolase containing varying amounts of THPP (1-10 eq.). The samples were incubated for 1 hour at 37 °C prior to addition of 4-VP-PEG2kDa derivative **4.49** (1 eq.) followed by incubation at 37 °C for 18 hours (**Figure 4.23**, **lanes 6**-**8**).

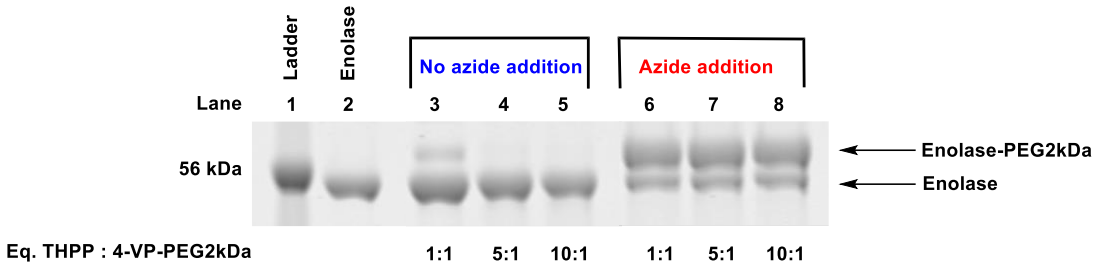

Figure 4.23: SDS-PAGE analysis of reactions between **4.49** (1 eq.) and yeast enolase in the presence of varying THPP amounts (1-10 eq.) and in the presence or absence of the alkyl azide **3.3** (100 eq.). **Lane 1**: ladder, **Lane 2**: enolase, **Lane 3**: enolase + THPP (1 eq.) + **4.49** (1 eq.), **Lane 4**: enolase + THPP (5 eq.) + **4.49** (1 eq.), **Lane 5**: enolase + THPP (10 eq.) + **4.49** (1 eq.), **Lane 6**: enolase + THPP (1 eq.) + **3.3** (100 eq.) + **4.49** (1 eq.), **Lane 7**: enolase + THPP (5 eq.) + **3.3** (100 eq.) + **4.49** (1 eq.), **Lane 8**: enolase + THPP (10 eq.) + **3.3** (100 eq.) + **4.49** (1 eq.). The SDS-PAGE gel was stained with Coomassie solution and analysed utilising Image Studio Lite software.

The presence of THPP with 4-VP-PEG derivative **4.49** in the reactions resulted in extremely low yields of PEGylated protein (**Figure 21**, **Lanes 3**-**5**). Lower yields (0-11 %, **Table 4.3**) were obtained when comparing similar experiments utilising maleimide-PEG2kDa to PEGylate yeast enolase (3-37 %) in the presence of THPP (**Chapter 3**, **Table 3.2** and included in Table **4.3**). The maleimide derivatives are more reactive than 4-VP derivatives with regards to thiol alkylation and are, therefore, less affected by the presence of excess reducing agent in solution.

The addition of the alkyl azide **3.3** (**Figure 4.23**, **Lanes 6**-**8**) was successful in oxidising excess THPP, which resulted in higher yields (63-65 %) of PEGylated yeast enolase (**Table 4.3**) when utilising 4-VP-PEG2kDa derivative **4.49**. The yields are similar to the yields of 68-76 % (**Chapter 3**, **Table 3.2** and included in **Table 4.3**) achieved in similar experiments utilising maleimide-PEG2kDa, illustrating that 4-VP derivatives can produce conjugation yields similar to well established chemistry such as maleimide.

The addition of the alkyl azide **3.3** (**Figure 4.23**, **Lanes 6**-**8**) was successful in oxidising THPP, which resulted high yields of PEGylated yeast enolase, without necessity for intermediate purification protocols.

		Eq. Reducing Agent : 4-VP-PEG2kDa (4.49)			Eq. Reducing Agent : Maleimide-PEG2kDa		
		1:1	5:1	10:1	1:1	5:1	10:1
Reducing Agent	Alkyl Azide (3.3)	Yield of PEGylated Yeast Enolase (%)			Yield of PEGylated Yeast Enolase (%)		
TCEP	-	3.5	0	0	42.3	16.6	10.5
TCEP	+	78.6	82.4	86.3	76.4	82.4	84.7
THPP	-	11.0	0	0	37.0	6.7	3.1
THPP	+	62.8	62.1	64.7	68.0	73.4	75.8

Table 4.3: Comparison of PEGylated yeast enolase yields achieved by 4-VP-PEG2kDa derivative **4.49** and maleimide-PEG2kDa, with and without the use of the alkyl azide **3.3** to oxidise reducing agents TCEP (**2.6**) or THPP (**2.7**).

4.10) Time Dependant PEGylation of Yeast Enolase by Maleimide-PEG2kDa versus 4-VP-PEG2kDa Derivatives 4.48 and 4.49

The yields of PEGylated yeast enolase achieved when using a commercial maleimide-PEG2kDa reagent versus 4-VP-PEG2kDa derivatives **4.48** and **4.49** over a 24 hour incubation period were investigated. The experiments were performed to determine the time required to achieve maximum conjugate yields when utilising 4-VP thiol alkylating reagents in comparison to the use of maleimide reagents. The thiol-containing protein yeast enolase was reduced utilising TCEP, followed by the use of the alkyl azide **3.3** to oxidise excess reducing agent prior to the addition of the PEGylation reagents.

Yeast enolase was denatured in argon purged Tris buffer (0.5 M, pH = 7.2) containing 5 mM EDTA and 8 M urea at 85 °C for 15 minutes. The solution was allowed to cool to room temperature before aliquoting solutions of yeast enolase (100 μL) for the experiments. TCEP (5 eq.) was added to aliquots of protein in solution and incubated for 45 minutes at 25 °C. The alkyl azide **3.3** (100 eq.) was added and the solutions were incubated for 1 hour at 37 °C. Maleimide-PEG2kDa or 4-VP-PEG2kDa derivatives **4.48** or **4.49** (1 eq.) were subsequently added to the reactions and incubated at 37 °C for a total of 24 hours. Aliquots were taken from each of the reactions at time points, 1 hour, 4 hours and 24 hours and analysed by

SDS-PAGE (**Figure 4.24**) and yields quantified utilising Image Studio Lite version 4.0 software (**Table 4.4**).

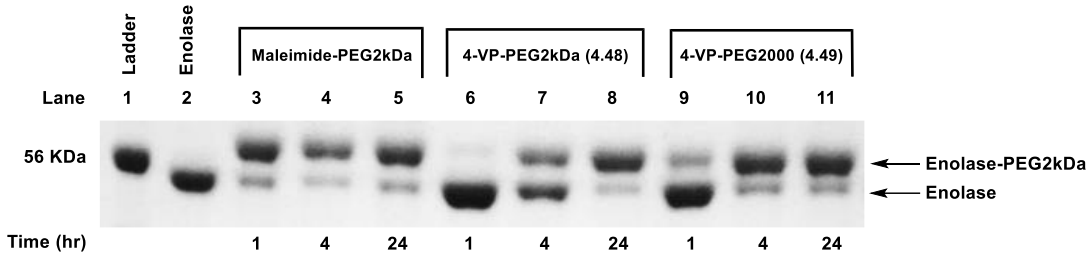

Figure 4.24: SDS-PAGE of time dependant PEGylation of yeast enolase by maleimide-PEG2kDa, 4-VP-PEG2kDa **4.48** and 4-VP-PEG2kDa **4.49**. **Lane 1**: ladder, **Lane 2**: enolase, **Lane 3**: enolase + TCEP (5 eq.) + **3.3** (100 eq.) + maleimide-PEG2kDa (1 eq.), t = 1 hr., **Lane 4**: enolase + TCEP (5 eq.) + **3.3** (100 eq.) + maleimide-PEG2kDa (1 eq.), t = 4 hrs., **Lane 5**: enolase + TCEP (5 eq.) + **3.3** (100 eq.) + maleimide-PEG2kDa (1 eq.), t = 24 hrs., **Lane 6**: enolase + TCEP (5 eq.) + **3.3** (100 eq.) + **4.48** (1 eq.), t = 1 hr., **Lane 7**: enolase + TCEP (5 eq.) + **3.3** (100 eq.) + **4.48** (1 eq.), t = 4 hrs., **Lane 8**: enolase + TCEP (5 eq.) + **3.3**, (100 eq.) + **4.48** (1 eq.), t = 24 hrs., **Lane 9**: enolase + TCEP (5 eq.) + **3.3** (100 eq.) + **4.49** (1 eq.), t = 1 hr., **Lane 10**: enolase + TCEP (5 eq.) + **3.3** (100 eq.) + **4.49** (1 eq.), t = 4 hrs. **Lane 11**: enolase + TCEP (5 eq.) + **3.3** (100 eq.) + **4.49** (1 eq.), t = 24 hrs. The SDS-PAGE gel was stained with Coomassie solution and analysed utilising Image Studio Lite software.

The PEGylation of yeast enolase by maleimide-PEG2kDa was rapid, with a yield of 78 % achieved within the first hour of incubation (**Table 4.4**). A small increase in yield of 84 % was achieved by the fourth hour of the reaction (**Table 4.4**). High yields of PEGylated protein can, therefore, be achieved in 1-4 hours when utilising maleimide-functionalised PEG. In comparison, the 4-VP-PEG derivatives were less reactive than the maleimide-PEG derivative, with the 4-VP-PEG2kDA derivative **4.48** proving to be the least reactive of the three PEG derivatives utilised. A low conjugate yield of 4 % was observed in the first hour of incubation, which improved to 45 % by the fourth hour of the reaction (**Table 4.4**). An excellent yield of 88 % was, however, achieved after 24 hours of incubation (**Table 4.4**). The 4-VP-PEG2kDa derivative **4.49** proved to be more reactive than 4-VP-PEG2kDa derivative **4.48**. A PEGylated protein yield of 21 % (**Table 4.4**) was observed after 1 hour of incubation, which increased significantly to 80 % (**Table 4.4**) after 4 hours of incubation. The yield marginally increased to 81 % after 24 hours of incubation (**Table 4.4**). High

yields of PEGylated protein can, therefore, be achieved within 4 hours when utilising 4-VP-PEG2kDa derivative **4.49**. The 4-VP-PEG2kDa derivative **4.49** is more reactive than 4-VP-PEG2kDa derivative **4.48** likely due to the higher pKa value of the nitrogen atom of the pyridine ring (**Table 4.1**). These experiments have illustrated that 4-VP-PEG derivatives can be utilised to produce PEGylated proteins in high yields, which are comparable to yields obtained with maleimide-PEG. Furthermore, the 4-VP-PEG2kDa derivative **4.49** can produce comparable alkylation yields to maleimide-PEG2kDa after 4 hours.

	Reaction time (hours)		
	1	4	24
PEG derivative	**Yield of PEGylated yeast enolase (%)**		
maleimide-PEG2kDa	77.8	84.4	81.1
4-VP-PEG2kDa (**4.48**)	4.0	44.6	87.9
4-VP-PEG2kDa (**4.49**)	21.3	79.6	81.3

Table 4.4: Yields of PEGylated yeast enolase achieved by maleimide-PEG2kDa, 4-VP-PEG2kDa derivative **4.48** and 4-VP-PEG2kDa derivative **4.49** after 1, 4 and 24 hours of incubation.

4.11) Conclusion

A variety of 4-VP linkers for bioconjugation *via* thiol alkylation were successfully synthesised. Methyl substitution at C-6 of the pyridine ring and extending the alkyl chain of the linker attached at C-2 of the pyridine ring was successful in raising the pKa of the pyridine ring to pKa ~ 6. The increased pKa resulted in more favourable thiol alkylation rates at both pH = 7 and pH = 8, generally a pH that is a compromise between the pKa of the nitrogen of the pyridine ring of the 4-VP derivatives and the pKa of the thiol acceptor. The 4-VP derivatives also demonstrated specificity for thiol alkylation over amine alkylation at both pH = 7 and pH = 8. A selection of 4-VP derivatives were functionalised with carbohydrate and PEG ligands and utilised for thiol alkylation of peptides and proteins. Water soluble trialkylphosphines such as TCEP and THPP were demonstrated to react with 4-VP and, therefore, require either removal or complete consumption prior to addition of 4-VP derivatised ligands to a conjugation reaction. A protocol developed in **Chapter 3** utilising a water soluble alkyl azide to oxidise TCEP or THPP *in situ* was effective in ensuring high PEGylated protein yields when 4-VP derivatised PEG's were incubated with thiol-containing proteins. A 4-VP-PEG derivative was also successful in producing PEGylated protein in a similar yield when compared to a maleimide-PEG derivative.

Chapter 5: Development of a Novel Method for Thiol Alkylation of S-Nitrosated (SNO) Proteins

5.0) Aim of Investigation

The thiol functional group of cysteine is mostly recognised as a key residue for structural or catalytic functions in proteins. The thiol functional group of cysteine is, however, also involved in the additional function of signal transduction in biological systems. The covalent attachment of nitric oxide (NO), a biological secondary messenger, to the sulfur atom of cysteine, generates a S-nitroso (SNO) peptide or protein. This nitrosation of thiols is a transient post translational modification, which is implicated in a variety of biological processes, such as cellular trafficking, muscle contractility and apoptosis [153]. The specific modification of a cysteine thiol to a SNO functional group may offer a site for the specific attachment of ligands to proteins for the production of bioconjugates. This method of attachment of ligands to cysteine containing proteins may provide an alternative method for the production of homogenous bioconjugates. A simple method of ligand conjugation to a SNO bond was therefore sought.

5.1) Background

Nitric oxide (NO) was first discovered by Jason Priestly in 1772, referring to it as nitrous air [154]. It is a reactive, colourless gas that exists as a neutral radical. During the 1980's NO was recognised as a powerful biomessenger, with diverse physiological functions [155]. The increased research into the biology of NO-dependant signalling won it the prize as molecule of the year in 1992. In 1998 the research into nitric oxide's involvement in the cardiovascular and nervous system won R.F. Furchgott, L. J. Ignaro and F. Murad the Nobel prize in Physiology and Medicine [156]. It is now recognised as a fundamental molecule in the processes of vascular dilation, neuronal signalling and immunology [157, 158].

The primary source of biological NO is the oxidation of the guanidino nitrogen of L-arginine to L-citrulline and nitric oxide by the enzyme nitric oxide synthase (NOS) [154]. There are 3 major isoforms of NOS: neuronal NOS (nNOS), inducible NOS (iNOS) and endothelial NOS (eNOS). The expression of these enzymes is not as limited as their names might imply and can be found in many different cell types [159].

Nitric oxide is a highly diffusible molecule and can elicit effects a distance from its initial production. NO is able to rapidly diffuse through cellular membranes, an advantageous property of a biological messenger. It is, however, a radical, and is a fairly reactive and short lived species, especially in an aqueous environment, with a half-life of 0.5-1 s in blood [160]. The reactivity of NO can be a beneficial quality as a short-lived messenger, since high, uncontrolled concentrations can cause cellular damage such as DNA deamination [154]. Cellular mechanisms have evolved for the necessary production of the ubiquitously required biomessenger and also the trafficking of this reactive molecule as a stable entity, such as S-nitrosation of peptides and proteins.

The classical NO signalling pathway involves the ability of NO to act as an allosteric modulator of guanylyl cyclase (sGC) activity. The sGC enzyme is a heterodimeric protein that catalyses the formation of the biomessenger cyclic guanosine monophosphate (cGMP) from guanosine triphosphate (GTP). The molecule cGMP is a cyclic nucleotide that binds to phosphodiesterases (PDE), ion-gated channels and cGMP-dependant kinases (cGK) regulating functions such as smooth muscle relaxation and neurotransmission [159]. The allosteric binding of NO to sGC leads to a 100-400 fold increase in activity [161].

The non-classical NO signalling pathway is through NO-induced post translational modification of proteins. The nitrosation of a cysteine thiol (RSNO) is a method for the storage or stable delivery of the reactive NO moiety to biological targets. It can also influence the activity of the nitrosated biomolecule similar to post translational modifications such as phosphorylation [162]. A variety of RSNO's have been

identified from low molecular weight S-nitrosocysteine (CysNO) and S-nitrosoglutathione (GSNO) to high molecular weight S-nitrosoalbumin (SNO-alb), with reported endogenous levels ranging from 28 nM to 7 μM [160].

NO does not react directly with thiols or thiolates under biological conditions but requires either oxidation of the thiol to the thiyl radical or the prior oxidation of NO to generate NO^+ donors. NO can react with oxygen (O_2) or superoxide ($O_2^{\bullet-}$) to produce reactive nitrogen species such as dinitrogen trioxide (N_2O_3), which is a NO^+ donor for the nitrosation of cysteine residues [163, 164]. RSNO's can also be formed through transition metal catalysed pathways. NO has a high affinity for heme centres, a common moiety of biological proteins such as haemoglobin (**Figure 5.1**). The metal atoms of the heme group can catalyse nitrosothiol formation *via* transient oxidation of NO to NO^+ [165]. Translocation of the NO^+ group from one sulfur atom to another in a transnitrosation reaction is another method of RSNO formation and is implicated as an important post-translation modification mechanism involved in cellular signalling [162]. The post-translational modification of cysteine by nitric oxide may alter the activity of the protein and lead to downstream effects on the biological signalling processes. This transient modification of proteins, therefore, needs to be highly specific to affect the necessary biological outcome. There are a number of factors that ensures nitrosation only occurs at specific cysteine residues of a protein.

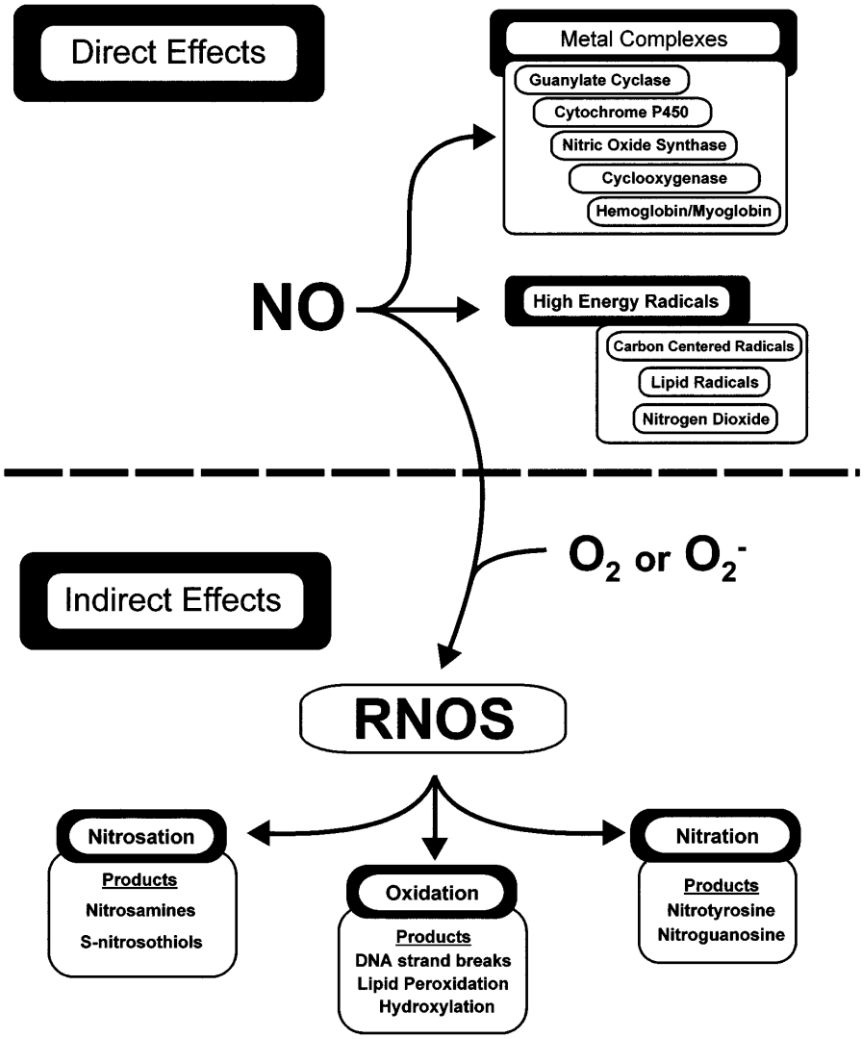

Figure 5.1: The diverse physiological effects of nitric oxide. Taken from [166].

Proteomic analysis of SNO-proteins has suggested that the specificity of nitrosation may be governed by the recurrence of an acid-base motif within 8 Å of the target cysteine thiol for nitrosation. The acidic aspartic acid (Asp) and glutamic acid (Glu) residues and basic arginine (Arg), histidine (His) and lysine (Lys) residues are suggested to aid the nitrosation of cysteine. Arginine (Arg), histidine (His) or lysine (Lys) residues are suggested to aid in the deprotonation of the cysteine thiol to generate a nucleophilic thiolate to facilitate transnitrosation (**Figure 5.2**) [167]. The coordination of metal ions to specific cysteine thiols is also thought to decrease the thiol pKa and facilitate transnitrosation reactions. Allostery is thought to play an important part in causing structural changes in the protein that influences the availability and reactivity of the cysteine thiol for nitrosation [167].

Compartmentalisation of cysteine residues in hydrophobic regions of a protein is also thought to favour a nitrosation reaction. The hydrophobic regions provide a suitable environment to concentrate the lipophilic nitric oxide and molecular oxygen to form N_2O_3, which is a NO^+-donor for SNO formation [167].

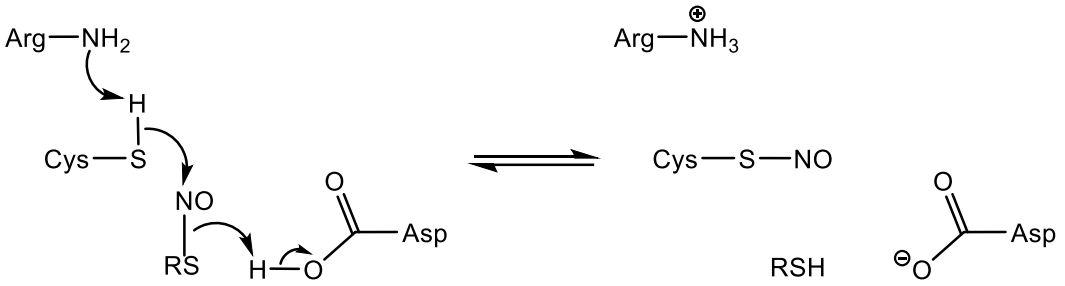

Figure 5.2: Acid-base catalysis for protein transnitrosation. Deprotonation of a cysteine thiol by arginine (Arg) promotes its nucleophilicity for a transnitrosation reaction with a RSNO, which is further facilitated by proton donation to the RSNO donor by aspartic acid (Asp). R = alkyl. Adapted from [167].

5.2) Direct SNO-Protein Detection

The generally low abundance of SNO-proteins requires sensitive detection methods that are also specific for SNO-proteins. The SNO bond is fairly labile, which can make identification difficult when laborious protocols are utilised. The SNO bond is also susceptible to decomposition by light and the presence of transition metals. A number of techniques have been developed for the identification of SNO proteins and the characterisation of the NO modified site.

5.2.1) Detection of SNO-Proteins by X-Ray Crystallography

X-ray crystallography is a powerful tool for the analysis of nitrosated proteins. X-ray crystallography has the potential to identify the site of nitrosation as well as the structural changes that the modification induces. There are, however, a few drawbacks to this technique. The protein needs to have been previously identified as a nitrosated species, isolated from the sample matrix and be susceptible to crystallisation conditions. The SNO bond also needs to be stable during the

crystallisation process. A number of SNO-proteins have now been successfully crystallised, including S-nitrosated hemeproteins and thioredoxin [168, 169].

5.2.2) Detection of SNO-Proteins by Mass Spectrometry

Mass spectrometry provides the potential to analyse either intact or protease digested SNO proteins. A mass shift of 29 atomic mass units in nitrosated samples relative to non-nitrosated samples can suggest the presence of nitric oxide. Modern mass spectrometric methods allow sequencing of peptide fragments which can prove useful in determining the nitrosation sites. SNO proteins are not, however, compatible with all ionisation methods, proving unstable to matrix assisted laser desorption ionisation mass spectrometry (MALDI-MS) [170]. The protease digestion protocols may also prove deleterious to the labile SNO linkage, although this may depend on individual sample characteristics.

5.2.3) Detection of SNO-Proteins by SNO-Specific Antibodies

Immunoglobulins recognising the SNO motif were first recognised in MS patients and soon developed into research tools such as ELISA and immunohistochemistry-based analysis of SNO proteins [171, 172]. There are some limitations to this technique. The SNO linkage must be stable during the course of the assay, SNO antibodies may only be raised at solvent accessible SNO sites and antibodies may show low specificity for SNO-cysteine versus cysteine, which may lead to false positive detection [173].

5.3) Indirect SNO-Protein Detection

5.3.1) Biotin Switch Technique (BST)

The BST method was first described by Jaffrey *et al* as a method for identifying the SNO sites in proteins [174]. Many variations of the method have since been developed such as SNO-resin assisted capture (SNO-RAC) and SNO-site identification (SNO-SID), which are summarised in **Figure 5.3**. The BST method and

its variations generally rely on 4 steps, including (**1**) free thiol capping, (**2**) reduction of the SNO site to a thiol functional group, (**3**) biotin labelling of the resultant free thiol and (**4**) detection of the biotin labelled thiol [175]. SNO-SID is a modification of the BST method, where biotinylated protein samples are trypsinised. The biotinylated peptides are captured on avidin or streptavidin beads, eluted and analysed by mass spectrometry [173].

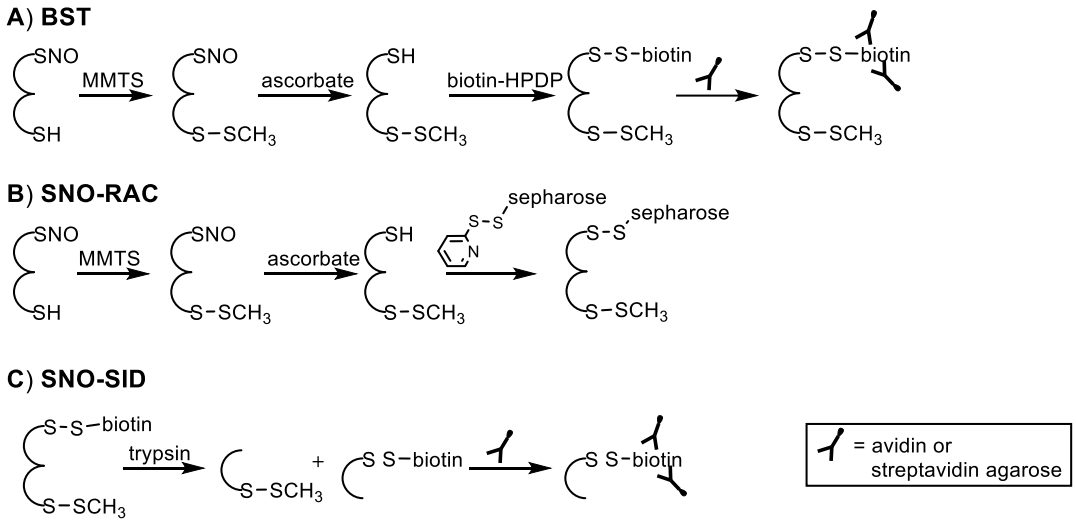

Figure 5.3: Biotin-based protocols for the enrichment of SNO-peptides and proteins. Adapted from [173].

The BST technique of SNO identification is very versatile and has been applied to purified protein, cultured cells and plasma [176, 177] but there are some pitfalls associated with each of the 4 steps of the BST protocol, which are summarised below.

5.3.1.1) Thiol Capping Utilised in the BST Protocol

The first step for the BST method and its variations involves capping of the free thiols present in the protein. Thiol capping is performed to prevent the identification of false positives since S-nitrosation is generally a cysteine-specific modification. The free thiols are generally capped with methyl methanethiosulfate (MMTS) to generate mixed disulfides. A disulfide is a relatively labile bond and may not survive the subsequent chemical steps. The capping reagent can be replaced by

N-ethyl maleimide (NEM) or iodoacetamide (IAM) to generate more stable thio-ether bonds. A disadvantage of the capping step is the lability of the SNO linkage. If the SNO bond is hydrolysed, it could lead to the capping of the target cysteine residue, leading to a failure of identifying the SNO site. Residual capping reagent is removed before the next step in the protocol, usually by protein precipitation or spin column filtration.

5.3.1.2) Reduction of the SNO Linkage in the BST Protocol

The second step in the BST protocol requires the selective reduction of any SNO bonds in the protein to the thiol functional group for the subsequent labelling of the cysteine thiol using a biotin-functionalised molecule. The initial protocol relied on ascorbate for reduction of the SNO linkage but this has raised some potential pitfalls. The ascorbate dependant reduction of SNO exhibits slow kinetics [178]. Trace metals such as Cu(I) are attributed to the SNO reduction, with ascorbate serving to reduce Cu(II) back to Cu(I). The addition of Cu(I) to the ascorbate solution has been shown to improve the reduction of the SNO bond and improve yields of subsequent biotinylated samples [179]. Ascorbate has also been shown to reduce disulfides [180]. This may lead to the identification of false positives when the MMTS capping reagent is utilised in the first step of the BST protocol [181].

5.3.1.3) Labelling of the Thiol Following SNO Reduction in the BST Protocol

Immediately after SNO reduction, the free thiol is labelled with a biotin-functionalised tag. The original tag utilised was biotin-(N-[6-(Biotinamido)hexyl]-3'-(2'-pyridyldithio)propionamide, Bt-HPDP, **5.1**), resulting in a mixed disulfide linkage between the protein and biotin molecule. The lability of a disulfide bond may lead to loss of biotinylated product during the subsequent purification steps. The presence of ascorbate in the solution from the previous step may reduce the protein-biotin disulfide bond, which could also cause a decrease of biotinylated product. Biotin functionalised with thiol-alkylating functional groups such as maleimide or iodoacetamide offer a solution to the above mentioned problems.

Maleimide and iodoacetamide, however, can also react with amines present on the protein such as lysine and histidine to produce artefacts into the experiment.

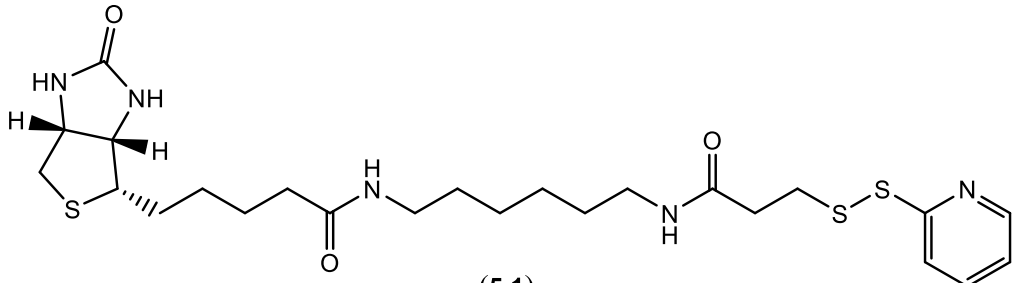

(**5.1**)

5.3.1.4) Detection of Biotinylated Thiols in the BST Protocol

Isolation of the biotinylated proteins is achieved by affinity purification using avidin or streptavidin beads. A variety of methods are utilised to characterise the isolated products including Western blot analysis and mass spectrometry [182].

The variety of potential pitfalls associated with the BST protocol has prompted the development of alternative strategies for the functionalisation and isolation of SNO-proteins.

5.3.2) Phosphine-Based Detection of S-Nitrosothiols

Xian and colleagues have developed a method for the detection of RSNO's using phosphine ester derivatives. The first generation of phosphine ester derivatives were capable of specifically reacting with a SNO functional groups to generate stable sulfenamide derivatives (**Figure 5.4**, **No. 5.3**) [183]. The concept was further developed and modified for the detection and isolation of SNO-proteins by affinity capture methods. Biotin-conjugate phosphine thioester derivatives were synthesised and reacted with a SNO-protein. A SNO-protein reacts with a phosphine thioester derivative **5.4** to initially generate an azaylide intermediate **5.5**. An intramolecular acyl transfer results in protein sulfenamide **5.6** and biotin-thiolate **5.7** intermediates, which further react to generate a phosphine oxide by-product **5.8** and a protein-biotin disulfide derivative **5.9** [184].

Although the reductive ligation method offers a simple alternative to the BST protocol for the direct detection of S-nitroso proteins, there are still a few pitfalls associated with the protocol. The reductive ligation method does not include a thiol-blocking step which may result in competition between thiolate-proteins in the sample matrix and the biotin-thiolate in the reaction mechanism for disulfide formation and could lower yields of protein-biotin production. The protein-biotin disulfide bond is prone to scission which may lower also lower yields. The protein-biotin disulfide may also undergo disulfide exchange with other protein thiols present in the sample matrix, leading to identification of false positives.

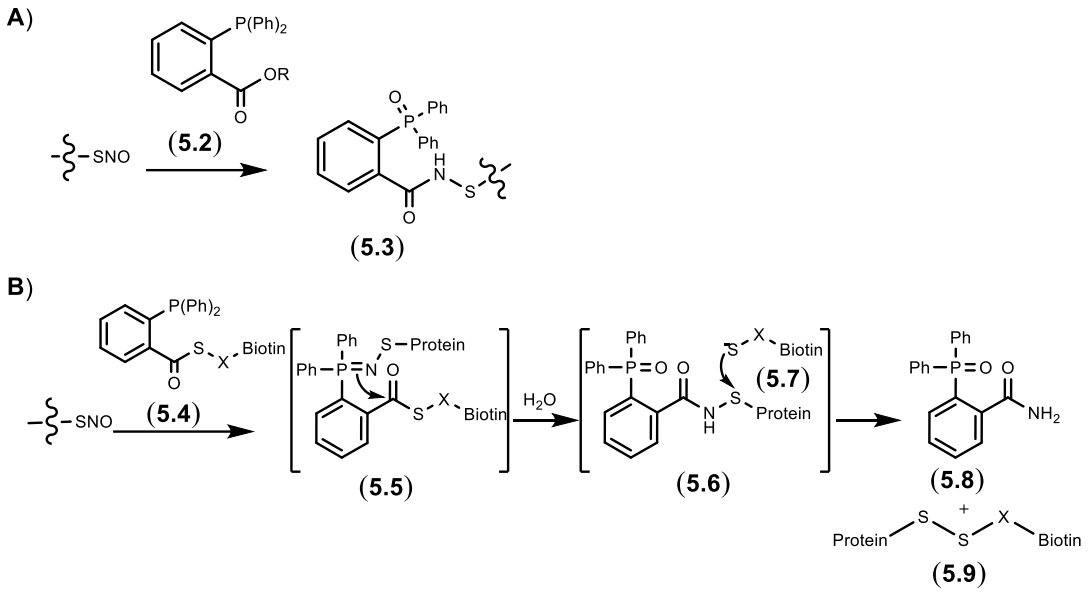

Figure 5.4: Reductive ligation protocols for S-nitrosothiol-protein detection. **A**) A S-nitrosothiol is reacted with a phosphine ester derivative **5.2** to yield a sulfenamide derivative **5.3**. **B**). A SNO-protein reacts with a phosphine thioester derivative **5.4** to generate a phosphine oxide products **5.8** and a protein-biotin disulfide derivative **5.9**.

5.4) A Novel Direct Method for SNO-Protein Functionalisation and Detection

The potential pitfalls highlighted in the BST and phosphine reductive ligation methods highlighted above prompted an investigation into developing an alternative method for SNO functionalisation and detection. A more simple, direct

and robust method of SNO functionalisation was sought whereby the SNO bond could be specifically targeted over cysteine thiols. A reaction specific for the SNO bond could potentially negate the thiol capping and SNO reduction steps in the BST method and also avoid yield loss and false positives arising from the use of mixed disulfide chemistry.

5.4.1) Characterisation the Cavero Reaction between a Sterically Hindered SNO Derivative and an Alkene

Cavero *et al* have reported a free radical addition of a tritylthionitrite (**5.10**) to alkenes in organic solvents to form α-alkylthio or α-arylthio oximes, however, no product characterisation was reported for the published reactions (**Figure 5.5**) [185].

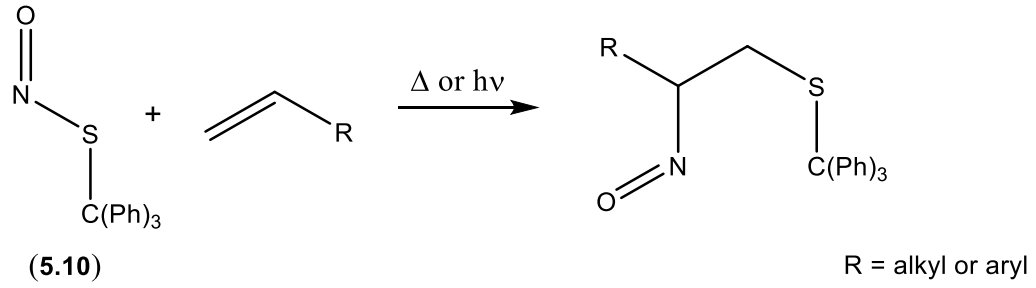

Figure 5.5: General scheme reported by Cavero *et al.* describing the reaction between tritylthionitrite (**5.10**) and an alkene to give either α-alkylthio or α-arylthio oxime products. Adapted from [185].

Here the Cavero method was repeated utilising 4-VP (**4.33**) and tritylthionitrite (**5.10**) in isopropyl alcohol (IPA) and toluene to characterise the reported oxime product to determine the potential of 4-VP to directly functionalise *S*-nitrosated ligands (**Figure 5.6**). Purification of the reaction resulted in the successful isolation of (*E,Z*)-N-[1-(pyridine-4-yl)-2-[(triphenylmethyl)sufanyl]ethylidene]hydroxylamine (**5.11**). The isolation and characterisation of **5.11** verified the reaction reported by Cavero and provided evidence for the potential to use such chemistry to detect SNO-proteins.

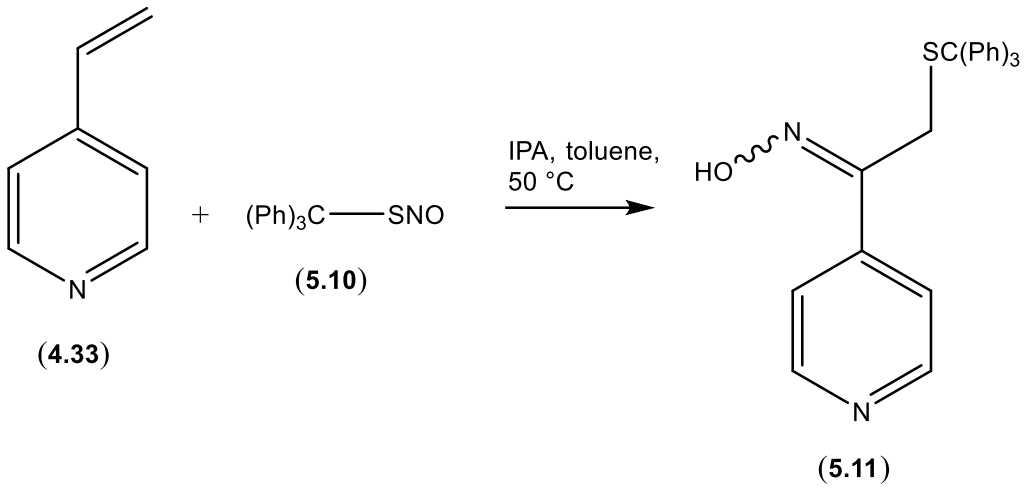

Figure 5.6: Reaction of 4-VP (**4.33**) with tritylthionitrite (**5.10**) to generate the oxime derivative **5.11**.

However, as discussed previously (**Chapter 4**), 4-VP is also utilised as a Michael acceptor for thiol alkylation of peptides and proteins. The Michael addition of 4-VP with thiols will be problematic when considering its use for specific SNO functionalisation. The use of 4-VP to functionalise a SNO bond would require a pre-capping step of any free thiols that may be present in the protein, similar to that performed in the BST protocol. The Michael addition between 4-VP and a thiol was confirmed by the isolation of 4-[2-(tritylsulfanyl)ethyl]pyridine (**5.13**) after the reaction of 4-VP (**4.33**) with triphenylmethanethiol (**5.12**), in IPA and toluene (**Figure 5.7**).

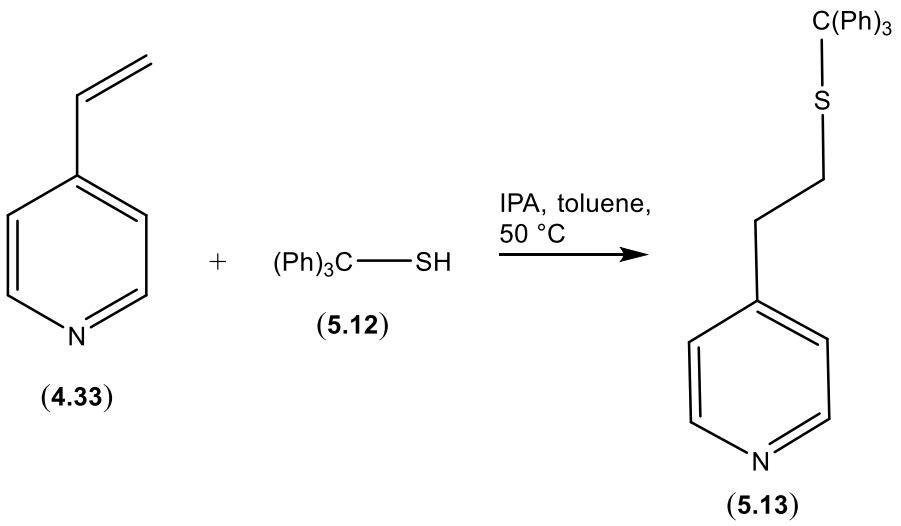

(**4.33**) (**5.12**) (**5.13**)

Figure 5.7: Reaction of 4-VP (**4.33**) with triphenylmethanethiol (**5.12**) to yield the Michael addition product **5.13**.

5.4.2) Characterisation of the Reaction of an Amino Acid-SNO with 4-VP

Despite the potential pitfall (Michael addition) of utilising 4-VP in a SNO functionalisation protocol, the reaction of 4-VP with the SNO-amino acid, methyl *N*-acetyl-*S*-nitroso-L-cysteinate (**5.14**) was investigated (**Figure 5.8**). This reaction was performed to investigate the reaction of 4-VP with a more biologically relevant SNO-ligand (SNO-amino acid) compared to the SNO-derivative **5.10**. The reaction of **4.33** with **5.14** was also performed to compare the potential yield of the oxime derivative **5.15** to that of the Michael addition product **5.16** and to identify any other possible by-products. Purification of the reaction between **4.33** and **5.14** yielded a number of different products. The oxime product methyl *N*-acetyl-*S*-[(2*E*,*Z*)-2-hydroxyimino-2-(pyridin-4-yl)ethyl]-L-cysteinate (**5.15**) was successfully isolated in a 43 % yield. The second major side product isolated was dimethyl N,N'-diacetyl-L-cystinate (**5.17**) in a 52 % yield as well as minor amounts of 4,4'-but-1-ene-2,4-diyldipyridine (**5.18**) in 3 % yield. The Michael addition product methyl N-acetyl-S-[2-(pyridin-4-yl)ethyl]-L-cysteinate (**5.16**) was detected by mass spectrometric analysis of the crude material but could not be isolated (**Figure 5.8**).

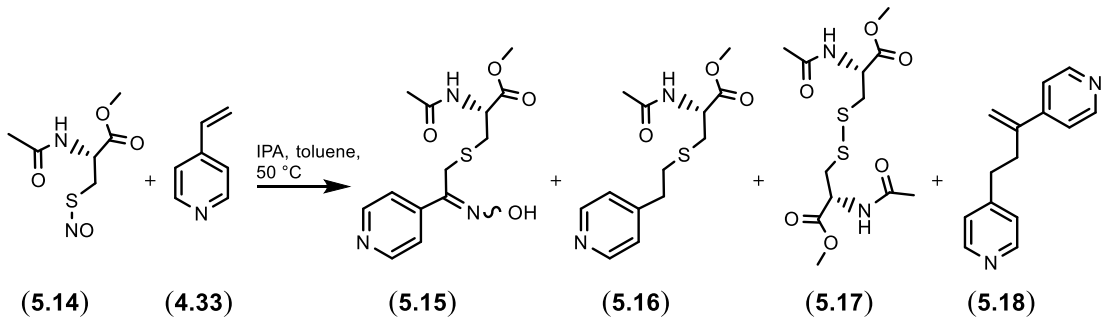

Figure 5.8: Reaction of 4-VP (**4.33**) with the SNO-amino acid derivative **5.14**.

Although 4-VP (**4.33**) was capable of functionalising **5.14** in a moderate yield to generate the desired oxime **5.15**, a number of unwanted side reactions had occurred. The most important side reaction identified was the Michael addition of 4-VP (**4.33**) to form **5.16**. The identification of **5.16** confirmed the pitfall of potentially utilising 4-VP for specific SNO-protein functionalisation, without a prior thiol capping step. A protocol was, therefore sought, whereby a pre-capping step would not be required, by utilising chemistry that could differentiate between a SNO and a thiol functional group. As such, the allyl functional group was investigated as an alternative method to specifically functionalise SNO-proteins.

5.5) Investigation of the Potential Reaction of an Allyl Functional Group with a SNO Linkage

5.5.1) Reaction of the Allyl Functional Group in an Organic Solvent with a Hindered SNO Derivative

A method was sought that could simplify the protocol for potentially functionalising and isolating SNO-proteins. The allyl functional group was investigated as an alternative to 4-VP for the covalent addition to a SNO bond. The allyl functional group may potentially react with the SNO bond through a radical mechanism, but not act as a Michael acceptor with thiol functional groups as previously seen in the reaction of 4-VP with a free thiol. A specific reaction between an allyl functional

group and a SNO bond may offer the potential to use an allyl derivative to directly functionalise SNO-proteins in the presence of free thiols.

N-allylacetamide (**5.20**) was synthesised from allylamine (**5.19**) and subsequently reacted with tritylthionitrite (**5.10**) utilising the conditions described by Cavero [185]. Mass spectrometric analysis of the reaction successfully identified *N*-[(2*E*,*Z*)-2-(hydroxyimino)-3-(tritylsulfanyl)propyl]acetamide (**5.21**), however, isolation of this product by silica gel chromatography was not possible, indicating a poor yielding reaction (**Figure 5.9**). This result indicated that the reaction of an allyl functionalised ligand with and SNO-protein may not useful as a technique for production of bioconjugates but may be more suitable as an analytical tool for the detection of SNO-proteins. The investigation was directed towards developing an allyl functionalised ligand for the detection of SNO-proteins by affinity capture techniques and mass spectrometry.

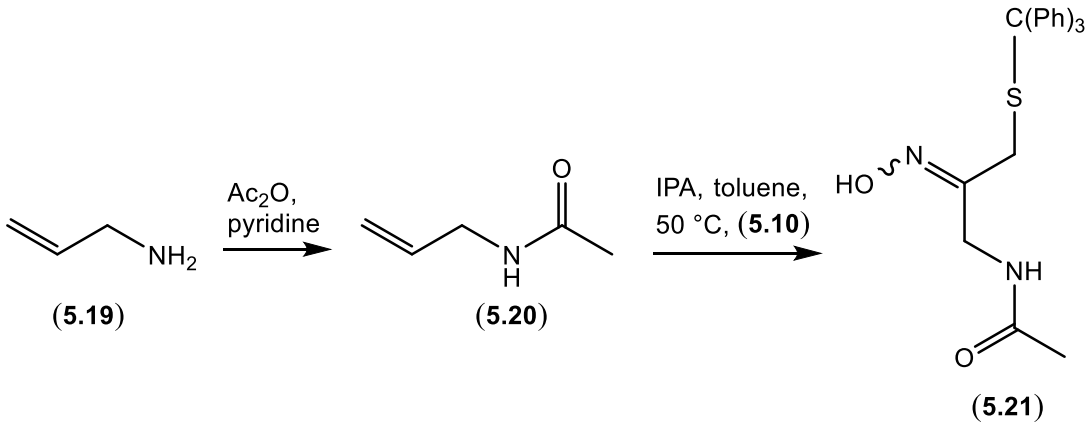

Figure 5.9: Synthesis of N-allylacetamide (**5.20**) followed by reaction with tritylthionitrite (**5.10**) to generate **5.21**, which was confirmed by mass spectrometry.

5.5.2) Reaction of D-Allyl Biotin with a SNO-Peptide in an Aqueous/Organic Solvent Mixture

The moderate success of the reaction between N-allylacetamide (**5.20**) and tritylthionitrite (**5.10**) to generate the oxime product **5.21** prompted the synthesis of a D-allyl biotin (**5.23**) from D-biotin (**5.22**, **Figure 5.10**) for detection of SNO proteins by affinity capture techniques. Compound **5.23** has the potential to react with SNO-peptides and proteins *via* the allyl functional group and enable sample enrichment for detection by Western blotting.

D-Allyl biotin (**5.23**) was reacted with the SNO-peptide S-nitrosoglutathione (**5.24**) in a buffer/DMSO solvent combination to facilitate dissolution of the reagents and also mimic conditions that may be employed in reactions of **5.23** with SNO-proteins. Incubation of **5.23** with **5.24** at 50 °C was successful in generating the oxime derivative **5.25** (**Figure 5.10**). The oxime **5.25** could not be isolated by chromatography, but encouragingly was detected by mass spectrometry. The advantage of a simple method to directly detect SNO linkages without laborious sample preparation required in the BST method may outweigh the disadvantage of low yields and could find use in some applications. This may be applicable to developing a sensitive detection assay where product yields may not be a major issue. The allyl-biotin derivative **5.23** should ensure sample enrichment by affinity chromatography to provide sufficient signal for detection by techniques such as SDS-PAGE, Western blotting or mass spectrometry.

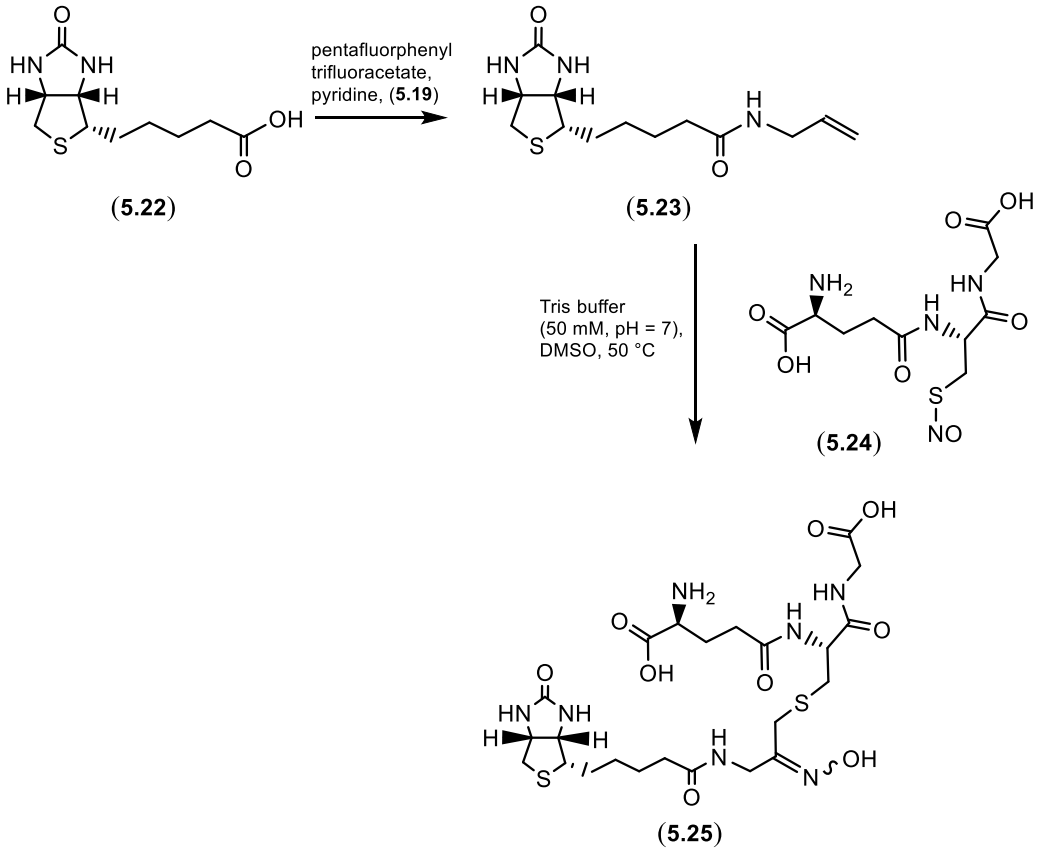

Figure 5.10: Synthesis of D-allyl biotin (**5.23**) from D-biotin (**5.22**) followed by reaction of **5.23** with S-nitrosoglutathione (**5.24**) to yield the biotin derivative **5.25**, which was confirmed by mass spectrometry.

5.5.3) Reaction of Allyl-Biotin Compounds with a SNO Protein

The moderate success of D-allyl biotin (**5.23**) to functionalise the SNO peptide S-nitrosoglutathione (**5.24**) prompted an investigation into utilising **5.23** to functionalise a S-nitrosated protein. The D-Biotin-allyl derivatives **5.26** and **5.27** were also synthesised to potentially functionalise a SNO-protein (**Figure 5.11**). The allyl-biotin derivatives **5.26** and **5.27** possess longer alkyl chains than derivative **5.23** to investigate the impact of steric bulk that may be present around the S-nitrosated cysteine in the protein, which may prevent access of the allyl functional group to the reaction site. The saturated D-biotin derivative **5.28** was also synthesised as a negative control for the protein functionalisation experiments (**Figure 5.11**).

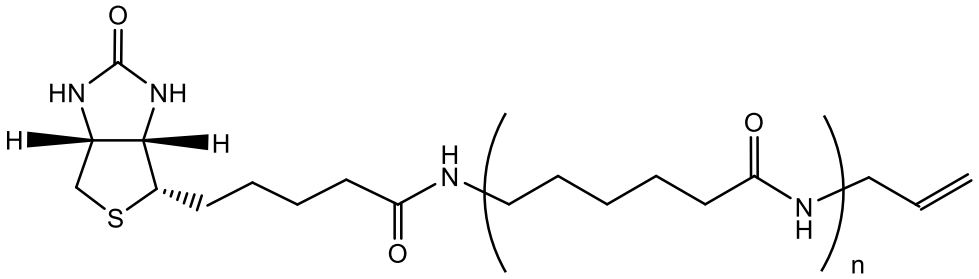

(**5.26**) n = 1
(**5.27**) n = 2

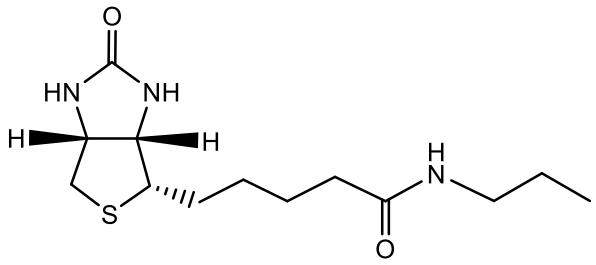

(**5.28**)

Figure 5.11: Structures of D-allyl-biotin derivatives **5.26** & **5.27** for the functionalisation of SNO-proteins and the negative control biotin derivative **5.28** for Western blot experiments.

The commercially available protein bovine serum albumin (BSA) was considered to be an appropriate model protein for S-nitrosation experiments as it contains 12 disulfide bridges as well as one free surface cysteine residue (Cys58). It has previously been shown that human serum albumin acts as a carrier of NO *in vivo* so the bovine equivalent was postulated as a cheap and suitable model protein [186]. Samples of BSA (30 µg/mL, Tris buffer, pH = 7) were nitrosated using the NO releasing reagent diethylamine (DEA) NONOate and subsequently treated with 450 µM of either allylamide derivatives **5.23**, **5.26** or **5.27** or the propylamide control **5.28** for 15 minutes at 60 °C. In parallel experiments, control samples of native (non-nitrosated) BSA were also treated under identical conditions. Protein samples were then resolved using SDS-PAGE and the presence of biotin was detected by Western blot analysis using a Horseradish peroxidase (HRP)-NeutrAvidin conjugate which possesses a high affinity for biotinylated derivatives (**Figure 5.12**).

The incorporation of biotin onto nitrosated (DEA-NONOate treated) BSA was clearly observed through Western blotting (**Figure 5.12**, **lanes 1**, **3** & **5**), however, no biotin could be detected in the control samples of BSA which had not been nitrosated (**Figure 5.12**, **lanes 2**, **4** & **6**). No incorporation of biotin was observed on either the nitrosated (**Figure 5.12**, **lane 7**) or non-nitrosated (**Figure 5.12**, **lane 8**) samples of BSA when utilising the negative control **5.28**, demonstrating that the allyl functional group is essential for conjugation to occur.

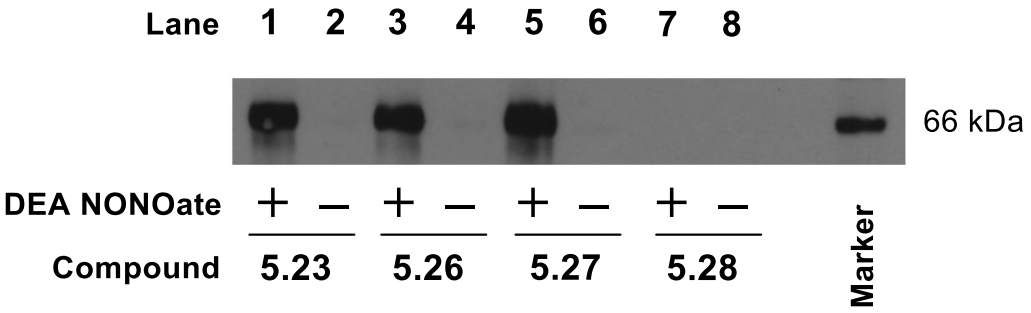

Figure 5.12: Labelling of BSA (30 µg/mL) with biotinylated compounds **5.23**, **5.26**, **5.27** (450 µM) for 15 minutes at 60°C in the presence (+) or absence (-) of pre-treatment with the NO donor DEA NONOate (1 mM, 20 min), then visualised by Western Blot analysis [187].

5.5.4) MS Analysis of Biotinylated BSA to Confirm Site of Nitrosation

A peptide mapping experiment was performed to confirm that the observed functionalisation of *S*-nitrosated BSA was through the reaction of the allylamide with a *S*-nitrosothiol group [188]. Compound **5.27** (450 µM) was treated with *S*-nitrosated BSA (2 mg/mL, pH 7) for 1 hour at 37°C. The protein was subsequently subjected to pepsin digestion (4 hours, pH = 2) and the biotinylated peptides were isolated using CaptAvidin™ resin. The purified protein digest was then analysed by in-line ESI-LC/MS, which identified the presence of a single species with exact masses of 998.2881 Da ($M+H^+$) and 1020.2826 ($M+Na^+$). The masses of the species detected correspond to an adduct of compound **5.27** covalently bound to the thiol containing peptide fragment QQCP (**5.29**), where the observed cysteine residue in this peptide corresponds to the surface cysteine of BSA, Cys58 (**Figure 5.13**). The observed mass of this species indicates that the biotinylated adduct exists in the

ketone form, rather than the oxime, likely owing to the strongly acidic conditions employed during LC and MS analysis.

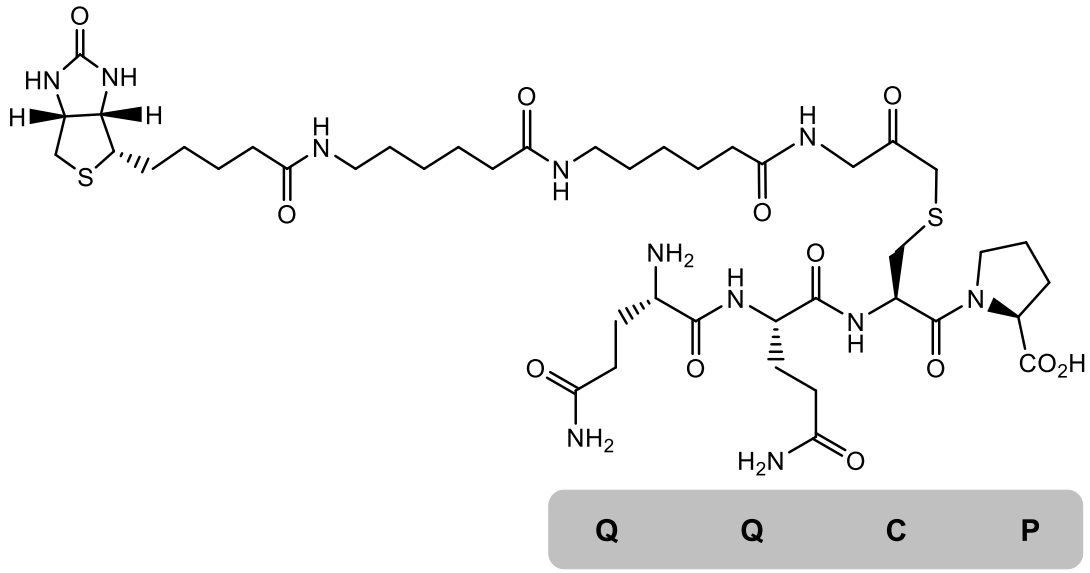

(**5.29**)

Figure 5.13: Structure of the peptide QQCP labelled using compound **5.27**.

5.6) Conclusion

Biotinylated allylamides have been demonstrated to act as agents for the functionalsation and detection of *S*-nitrosothiols through a single chemical step under aqueous conditions. The biotinylated allylamide compounds proved to be effective for the visualisation of a *S*-nitrosated protein (BSA) using Western blot analysis, which was further characterised by proteolytic analysis of biotinylated BSA. An LC isolated peptide fragment identified the surface cysteine, Cys58, as the site of nitrosation. The biotinylated allylamides described were capable of functionalising a *S*-nitrosated protein (BSA), suggesting that these compounds may prove to be important tools in the future for the investigation of protein *S*-nitrosation in biological systems.

Chapter 6: Experimental

Chemical reagents were purchased from Sigma-Aldrich unless specifically stated. Anhydrous solvents were purchased from Sigma-Aldrich. All other solvents were purchased from Fisher Scientific. Thin layer chromatography (TLC) was carried out on Merck aluminium backed TLC plates silica gel 60 F254 (0.25 mm thickness), viewed using UV light of wavelength 254 nm or stained with potassium permanganate solution. Silica gel chromatography was performed on silica gel 60 Å (200-400 mesh) from Sigma-Aldrich. Reverse phase chromatography was performed using a VersaFlash hand held column (23 x 110 mm) from Supelco. Melting points were obtained using a Thermo Fisher IA9000 digital melting point apparatus. ^{1}H, ^{13}C and ^{31}P and ^{19}F NMR spectra were recorded using Bruker Advance III (400 and 500 MHz) spectrometers. Deuterated solvents were purchased from Cambridge Isotope Laboratories. The NMR chemical shifts δ are recorded in parts per million (ppm) with reference to tetramethylsilane for ^{1}H and ^{13}C and phosphoric acid for ^{31}P NMR spectroscopy. High resolution mass spectrometry was performed using a BrukerMicrOTOF electrospray ionisation mass spectrometer. Infrared spectra were recorder on a PerkinElmer Spectrum 65 FT-IR spectrometer. HPLC was performed on a Dionex Ultimate 3000 instrument equipped with a variable wavelength detector. SDS-PAGE was performed utilising an Invitrogen xCell SureLock™ cell and a Biorad PowePac HV. SDS gels were scanned utilising a Licor Odyssey CLx imager and data was quantified utilising Image Studio Lite version 4.0.

Synthesis of *N-ethyl-3-(tris(carboxyethyl)phosphorylidene)pyrrolidine-2,5-dione* (**2.9**).

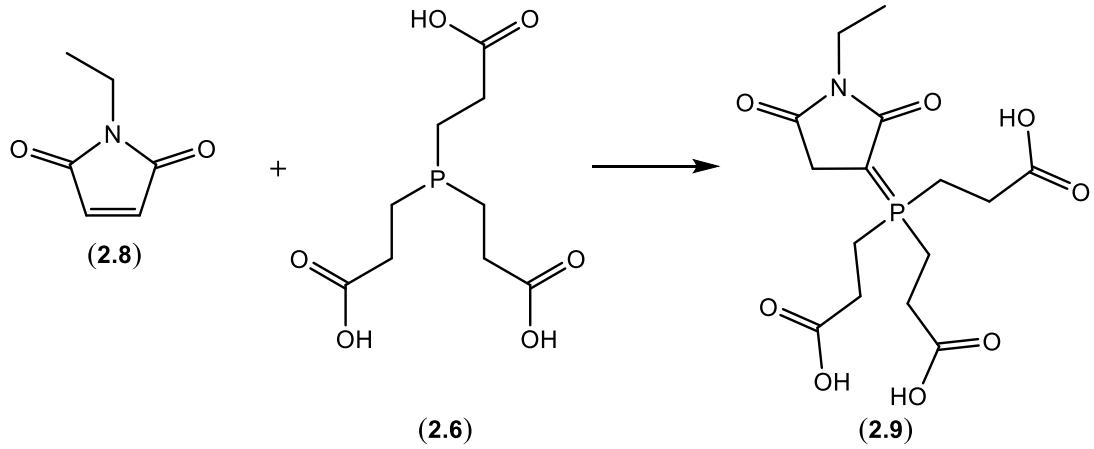

N-Ethyl maleimide (**2.8**, 10.0 mg, 0.080 mmol) and TCEP (**2.6**, 0.9 eq., 20.6 mg, 0.0719 mmol) were dissolved in a mixture of THF (1 mL) and argon purged aqueous sodium phosphate (0.1 M, pH = 7.0, 9 mL) and stirred under argon at room temperature for 1 hour. The solution was then concentrated *in vacuo* to 3 mL and the residual liquid then loaded onto a C-18 column for purification (100 % $H_2O \rightarrow$ 20 % MeCN/H_2O) to yield **2.9** as a white sticky solid (19.7 mg, 73 %). ^{1}H NMR, D_2O, 400 MHz: δ 3.49 (q, 2H, NC$\underline{H_2}$, *J* = 7.2 Hz), 3.26-3.09 (m, 2H, CC$\underline{H_2}$CO), 2.84-2.73 (m, 12H, 3 x C$\underline{H_2}$C$\underline{H_2}$CO), 1.05 (t, 3H, C$\underline{H_3}$, *J* = 7.2 Hz). ^{13}C NMR, D_2O, 125 MHz: δ 175.97 (d, $CH_2\underline{C}$ON, *J* = 8.8 Hz), 174.16 (d, 3C, 3 x $CH_2\underline{C}O_2H$, *J* = 11.9 Hz), 172.95 (C$\underline{C}$O, *J* = 3.0 Hz), 35.05 (N$\underline{C}H_2$), 33.51 (m, $CH_2\underline{C}$CO), 29.39 (C$\underline{C}H_2$CO), 25.82 (d, 3C, 3 x $CH_2\underline{C}H_2CO_2H$, *J* = 3.5 Hz), 14.34 (d, 3C, P$\underline{C}H_2$, *J* = 49.9 Hz), 11.54 ($\underline{C}H_3$). ^{31}P NMR, D_2O, 162 MHz: δ 39.2. HRMS: Expected for $C_{15}H_{21}N_1O_8P_1$ (M-H^+) = *m/z* 374.1005. Found: *m/z* 374.1029. Infrared (KBr): 3442, 1700 cm^{-1}. HPLC: column: Phenomenex Luna-C18 (250 x 4.60 mm), gradient elution: (0.7 mL/min), 100 % water containing 0.1 % TFA $\rightarrow$ 100 % MeCN over 16 minutes, retention time, 12.81 mins., purity: 93 %. Detection at 225 nm.

Synthesis of *N*^{6}*-[3-(2,5-dioxo-2,5-dihydro-1H-pyrrol-1-yl)propanoyl]-L-lysine* (**2.11**).

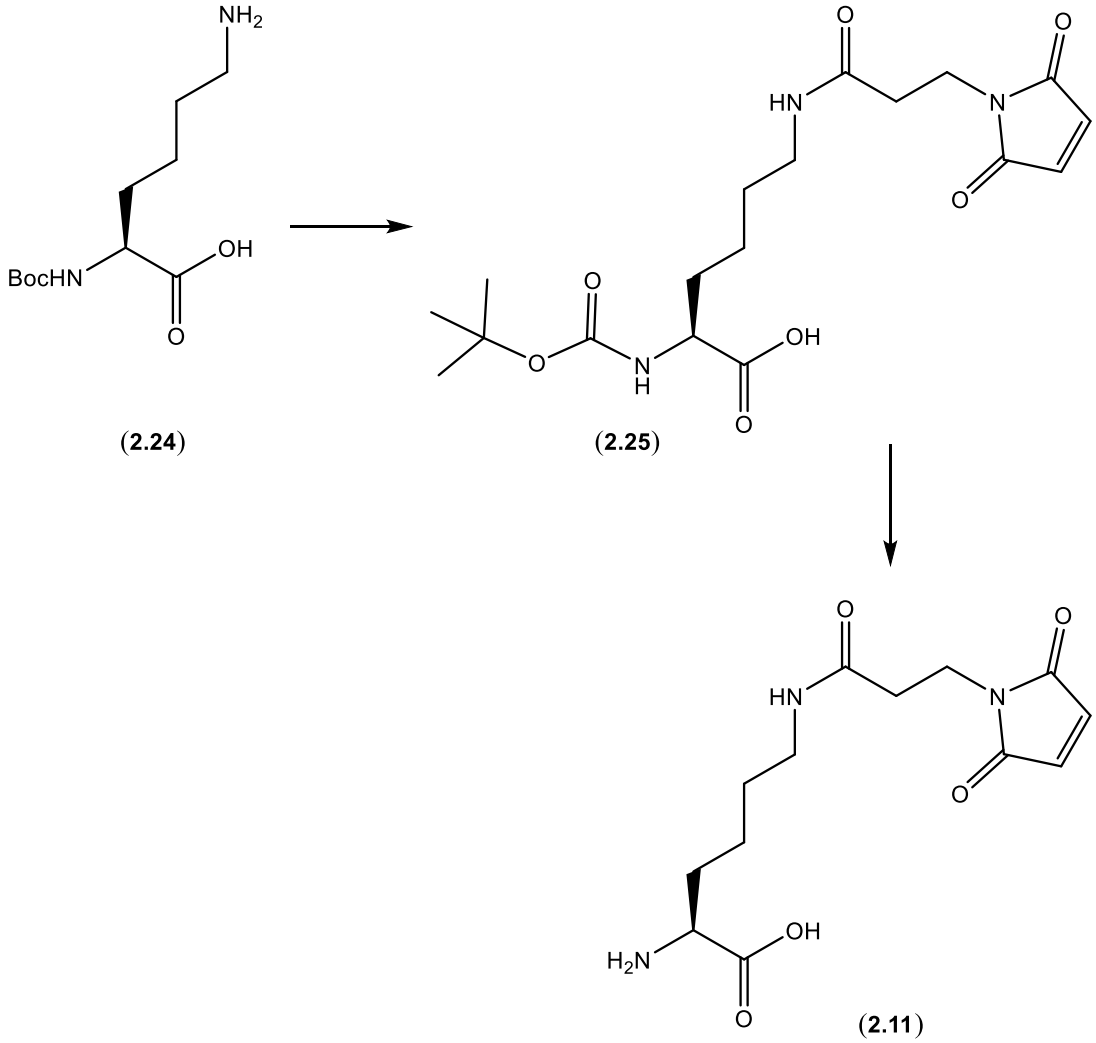

N^{2}-(tert-Butoxycarbonyl)-L-lysine (**2.24**, 190.4 mg, 0.771 mmol) was dissolved in anhydrous DMF (5 mL). Triethylamine (1 eq., 108 µL, 0.771 mmol) and 3-maleimidopropionic acid N-hydroxysuccinimide ester (1.2 eq., 246.9 mg, 0.928 mmol) were added and the reaction was stirred at room temperature while under nitrogen gas for 18 hours. The solution was concentrated and purified by silica gel chromatography (5 % MeOH/DCM $\rightarrow$ 20 % MeOH/DCM) to yield N^{2}-(tert-butoxycarbonyl)-N^{6}-[3-(2,5-dioxo-2,5-dihydro-1H-pyrrol-1-yl)propanoyl]-L-lysine (**2.25**) as a white sticky solid (261.1 mg, 85 %). ^{1}H NMR, CD_3OD, 400 MHz: δ 6.83

(s, 2H, COC<u>H</u>C<u>H</u>CO), 3.98 (m, 1H, NHC<u>H</u>CO_2H), 3.77 (t, 2H, NC<u>H_2</u>, *J* = 7.0 Hz), 3.12 (m, 2H, NHC<u>H_2</u>CH_2), 2.45 (t, 2H, COC<u>H_2</u>CH_2, *J* = 7.0 Hz), 1.84-1.60 (m, 2H, CHC<u>H_2</u>CH_2), 1.55-1.37 (m, 13H, $CHCH_2C$<u>H_2</u>C<u>H_2</u>CH_2, 3 x C<u>H_3</u>). ^{13}C NMR, CD_3OD, 100 MHz: δ 179.14 (CH<u>C</u>O_2H), 172.86 (NH<u>C</u>OCH_2), 172.13 (2 x <u>C</u>OCH), 158.03 (NH<u>C</u>O_2C), 135.50 (2 x CO<u>C</u>H), 80.28 (O<u>C</u>CH_3), 56.08 (NH<u>C</u>HCO_2H), 40.22 (NH<u>C</u>H_2CH_2), 35.81 (NHCO<u>C</u>H_2CH_2), 35.48 (N<u>C</u>H_2CH_2), 33.08 (CH<u>C</u>H_2CH_2), 29.91 ($NHCH_2$<u>C</u>H_2CH_2), 28.78 (C<u>C</u>H_3), 24.26 ($CHCH_2$<u>C</u>H_2CH_2). HRMS: Expected for $C_{18}H_{26}N_3O_7$ ($M\text{-}H^+$) = *m/z* 396.1776. Found: *m/z* 396.1809. Infrared (KBr): 3370, 1713, 1649 cm^{-1}. HPLC: column: Waters Symmetry Shield-RP8 (100 x 4.60 mm), gradient elution: (1.0 mL/min) 90 % water/MeCN containing 0.1 % TFA $\rightarrow$ 90 % MeCN/H_2O over 13 minutes, retention time, 6.15 mins., purity: 97%. Detection at 225 nm.

The Boc-protected derivative **2.25** (80.0 mg, 0.201 mmol) was suspended in THF (1 mL) and cooled to 0 °C. TFA (4 mL) was slowly added to the solution which was left to warm to room temperature and then stirred for a further 5 hours. The solution was concentrated and the residue was redissolved in 2 mL of water. The solution was neutralised with K_2CO_3 and subsequently purified by C-18 chromatography (100 % H_2O $\rightarrow$ 20 % MeOH/H_2O) to yield **2.11** as a transparent solid (42.5 mg, 71 %). ^1H NMR, D_2O, 400 MHz: δ 3.79 (t, 2H, NC<u>H_2</u>CH_2, *J* = 7.0 Hz), 3.72 (t, 1H, NHC<u>H</u>CO_2H, *J* = 5.9 Hz), 3.12 (t, 2H, NHC<u>H_2</u>CH_2, *J* = 6.9 Hz), 2.48 (t, 2H, COC<u>H_2</u>CH_2, *J* = 6.4 Hz), 1.85 (m, 2H, CHC<u>H_2</u>CH_2), 1.45 (m, 2H, $NHCH_2$C<u>H_2</u>CH_2), 1.33 (m, 2H, $CHCH_2$C<u>H_2</u>). ^{13}C NMR, D_2O, 100 MHz: δ 174.67 (CH<u>C</u>O_2H), 173.37 (NH<u>C</u>OCH_2), 172.57 (2 x N<u>C</u>OCH), 134.45 (2 x NCO<u>C</u>H), 54.62 (NH<u>C</u>HCO_2H), 38.96 (NH<u>C</u>H_2CH_2), 34.76 (CO<u>C</u>H_2CH_2), 34.53 (N<u>C</u>H_2CH_2), 30.02 (CH<u>C</u>H_2CH_2), 27.88 ($NHCH_2$<u>C</u>H_2CH_2), 21.76 ($CHCH_2$<u>C</u>H_2CH_2). HRMS: Expected for $C_{13}H_{18}N_3O_5$ ($M\text{-}H^+$) = *m/z* 296.1252. Found: *m/z* 296.1229. Infrared (KBr): 3325, 1714, 1630 cm^{-1}. HPLC: column: Phenomenex Luna-NH_2 (250 x 4.60 mm), gradient elution: (1.0 mL/min) 10 % MeCN in water containing 0.1 % TFA $\rightarrow$ 100 % MeCN over 20 minutes, retention time, 2.63 mins., purity: 100 %. Detection at 225 nm.

Synthesis of *N⁶-(3-{2,5-dioxo-3-[tris(2-carboxyethyl)-λ⁵-phosphanylidene]pyrrolidin-1-yl}propanoyl)-L-lysine* (**2.12**).

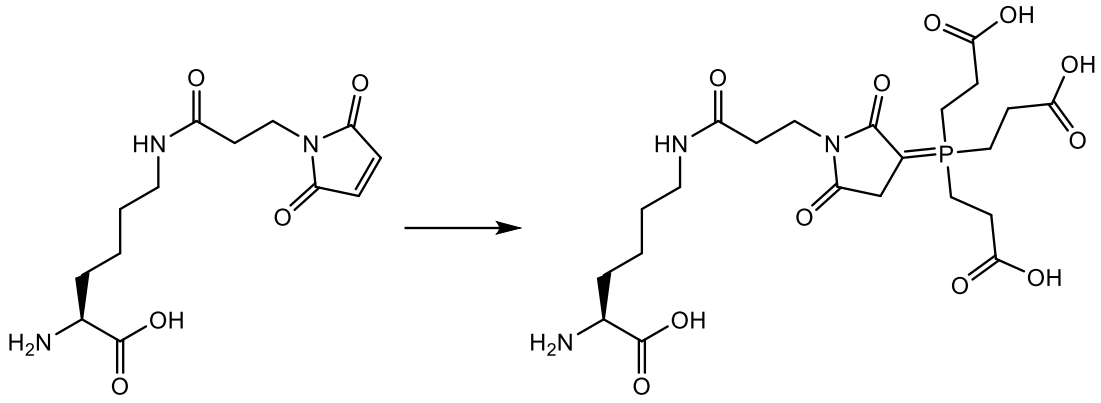

(**2.11**) (**2.12**)

Compound **2.11** (15.4 mg, 0.0518 mmol) and TCEP (**2.6**, 0.9 eq., 13.4 mg, 0.0466 mmol) was dissolved in 2 mL of argon purged aqueous sodium phosphate (0.1 M, pH = 7). The reaction was stirred, under argon, and at room temperature for 1 hour. The reaction was the subsequently purified by C-18 chromatography (100 % water). The product was lyophilised to give **2.12** as an amorphous white solid (18.0 mg, 70 %). ^{1}H NMR, D_2O, 400 MHz: δ 3.80 (t, 2H, NC*H₂*CH_2, *J* = 6.6 Hz), 3.76 (t, 1H, NH_2C*H*CO_2H, *J* = 6.3 Hz), 3.34-3.21 (m, 2H, CC*H₂*CO), 3.14 (t, 2H, NHC*H₂*CH_2, *J* = 6.9 Hz), 2.79-2.74 (m, 12H, 3 x C*H₂*C*H₂*CO), 2.51 (t, 2H, NHCOC*H₂*, *J* = 6.6 Hz), 1.90-1.83 (m, 2H, CHC*H₂*CH_2), 1.55-1.47 (m, 2H, $NHCH_2$C*H₂*CH_2), 1.45-1.33 (m, 2H, $CHCH_2$C*H₂*CH_2). ^{13}C NMR, D_2O, 100 MHz: δ 175.6 (d, NCOCH_2, *J* = 8.7 Hz), 175.5 (d, 3 x CH_2CO_2H, *J* = 11.8 Hz), 174.5 (CHCO_2H), 172.8 ($NHCOCH_2$), 172.7 (d, NCOC, *J* = 3.4 Hz), 54.4 (NH_2CHCO_2H), 39.0 (NHCH_2CH_2), 36.4 (NCH CH_2), 34.0 (m, COCCH_2), 33.2 (CO*C*H_2CH_2), 29.9 (CH*C*H_2CH_2), 29.5 (CO*C*H_2C), 27.8 ($NHCH_2$CH_2CH_2), 26.9 (d, 3 x CH_2CH_2CO_2H, *J* = 3.8 Hz), 21.7 ($CHCH_2$CH_2CH_2), 15.0 (d, PCH_2CH_2, *J* = 49.5 Hz). ^{31}P NMR, D_2O, 162 MHz: δ 38.9. HRMS: Expected for $C_{22}H_{33}N_3O_{11}P_1$ ($M\text{-}H^+$) = *m/z* 546.1858. Found: *m/z* 546.1864. Infrared (KBr): 3456, 1708, 1642 cm^{-1}. HPLC: column: Phenomenex Luna-C18 (250 x 4.60 mm), gradient elution: (0.7 mL/min)

100 % water containing 0.1 % TFA → 100 % MeCN over 16 minutes, retention time, 11.68 mins, purity, 87%). Detection at 225 nm.

Synthesis of *3,3',3''-[(1-ethyl-2,5-dioxopyrrolidin-3-ylidene, 4-deutero)-λ^5-phosphanetriyl]tripropanoic acid* (**2.14**).

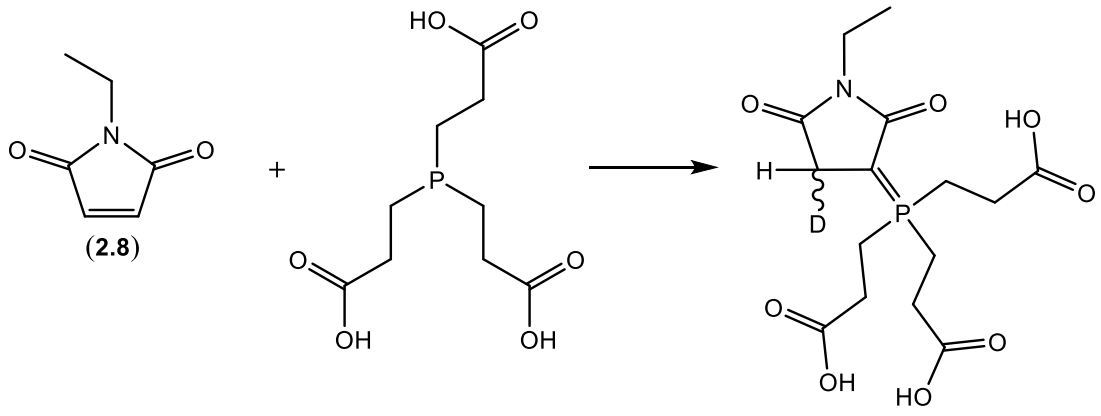

(**2.8**) (**2.6**) (**2.14**)

N-Ethyl maleimide (**2.8**, 10.0 mg, 0.0800 mmol) and TCEP (**2.6**, 0.9 eq., 20.6 mg, 0.0719 mmol) was dissolved in THF (1 mL) and argon purged deuterated aqueous sodium phosphate (0.1 M, pH = 7.0, 9 mL) and stirred under argon at room temperature for 1 hour. The reaction was concentrated *in vacuo* to 3 mL and then loaded onto a C-18 column for purification (100 % H_2O → 20 % MeCN/H_2O) to yield **2.14** as a pale yellow sticky solid (21.4 mg, 79 %). ^{1}H NMR, D_2O, 400 MHz: δ 3.54 (q, 2H, N*C*H_2CH$_3$, *J* = 7.3 Hz), 3.26-3.14 (m, 1H, CC*H*DCO), 2.89-2.77 (m, 12H, 3 x C*H$_2$*C*H$_2$*CO$_2$H), 1.10 (t, 3H, CH$_2$C*H$_3$*, *J* = 7.3 Hz). ^{13}C NMR, D_2O, 125 MHz: δ 176.0 (d, N*C*OCHD, *J* = 8.8 Hz), 174.2 (d, CH$_2$*C*O$_2$H, *J* = 11.8 Hz), 173.0 (d, N*C*OC, *J* = 3.5 Hz), 35.0 (N*C*H$_2$CH$_3$), 33.6 (m, CO*C*CHD), 29.2 (m, CO*C*HDC), 25.8 (d, 3 x CH$_2$*C*H$_2$CO$_2$H, *J* = 4.0 Hz), 14.4 (d, 3 x *C*H$_2$CH$_2$CO$_2$H, *J* = 49.8 Hz), 11.5 (CH$_2$*C*H$_3$). ^{31}P NMR, D_2O, 162 MHz: δ 39.2. HRMS: Expected for $C_{15}H_{22}D_1N_1O_8P_1$ (M+H$^+$) = *m/z* 377.1219. Found: *m/z* 377.1222. Infrared (KBr): 3439, 1705 cm^{-1}. HPLC: column: Phenomenex Luna-C18 (250 x 4.60 mm), gradient elution (0.7 mL/min), water containing 0.1 % TFA →

100 % MeCN over 16 minutes, retention time, 12.73 mins, purity, 91 %. Detection at 225 nm.

Synthesis of N-ethyl succinimide (**2.15**).

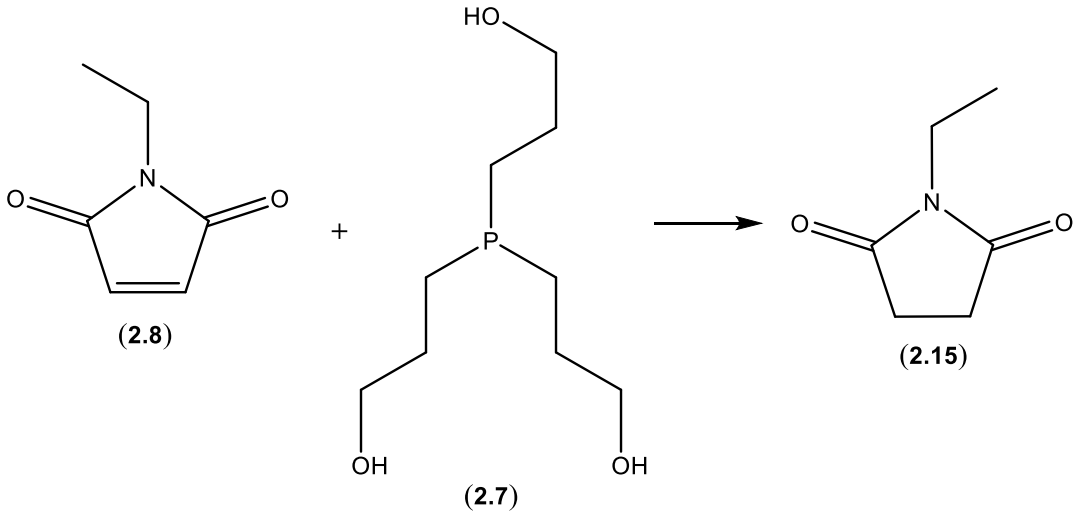

(**2.8**) (**2.7**) (**2.15**)

A solution of THPP (**2.7**, 0.9 eq., 29.9 mg, 0.144 mmol) was prepared in THF (1 mL) and argon purged aqueous sodium phosphate (0.1 M, pH = 7.0, 9 ml). N-Ethyl maleimide (**2.8**, 20.0 mg, 0.160 mmol) was added slowly to the rapidly stirring solution of THPP. The reaction was left to stir for 30 minutes at room temperature. A further 0.1 eq. of THPP was added and left to stir for an additional 30 minutes. The reaction was diluted with 25 mL of diethyl ether and extracted with water (30 mL). The aqueous layer was extracted with diethyl ether (2 x 30 mL). The organic extraction layers were combined and dried using $MgSO_4$. The mixture was filtered and the organic solution was concentrated (550 mbar, 25 °C). The crude was purified by silica gel chromatography ($CH_2Cl_2 \rightarrow$ 2 % acetone/CH_2Cl_2) to yield **2.15** as a clear oil (12.4 mg, 61 %). Spectral data was consistent with that reported in the literature [189]. ^{1}H NMR, $CDCl_3$, 400 MHz: δ 3.46 (q, 2H, NC$\underline{H_2}$CH$_3$, *J* = 7.2 Hz), 2.61 (s, 4H, 2 x COC$\underline{H}$), 1.07 (t, 3H, CH$_2$C$\underline{H_3}$, *J* = 7.2 Hz). ^{13}C NMR, $CDCl_3$, 100 MHz: δ 177.0 (2 x N$\underline{C}$OCH), 33.5 (N$\underline{C}$H$_2$CH$_3$), 28.0 (2 x CO$\underline{C}$H), 12.8 (CH$_2$$\underline{C}H_3$). HRMS: Expected for $C_6H_9N_1Na_1O_2$ (M+Na$^+$) = *m/z* 150.0525. Found: *m/z* 150.0531.

Synthesis of *N*^{6}*-[3-(2,5-dioxopyrrolidin-1-yl)propanoyl]-L-lysine* (**2.16**).

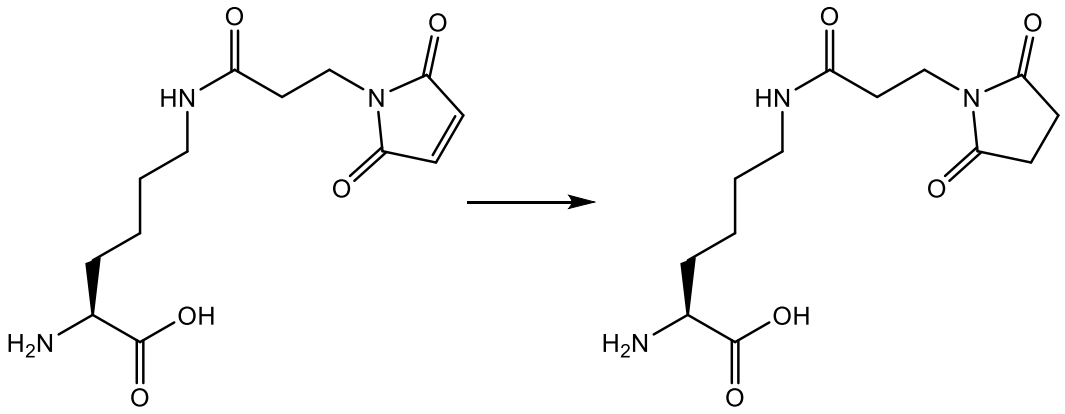

(**2.11**) (**2.16**)

Compound **2.11** (10.0 mg, 0.0336 mmol) and THPP (**2.7**, 0.9 eq., 6.30 mg, 0.0303 mmol) was dissolved in 1 mL of argon purged aqueous sodium phosphate (0.1 M, pH = 7). The reaction was stirred, under argon, and at room temperature for 1 hour. The reaction was the subsequently purified by C-18 chromatography (100 % water → 20 % MeCN/water). The product was lyophilised to give **2.16** as a white amorphous solid (5.35 mg, 59 %). ^{1}H NMR, D_2O, 400 MHz: δ 3.77-3.69 (m, 3H, NC$\underline{H_2}$CH$_2$ & NH$_2$C$\underline{H}$CO$_2$H), 3.14 (t, 2H, NHC$\underline{H_2}$CH$_2$, *J* = 6.8 Hz), 2.77 (s, 4H, COC$\underline{H_2}$C$\underline{H_2}$CO), 2.46 (t, 2H, NHCOC$\underline{H_2}$CH$_2$, *J* = 6.8 Hz), 1.91-1.83 (m, 2H, CHC$\underline{H_2}$CH$_2$), 1.55-1.43 (m, 2H, NHCH$_2$C$\underline{H_2}$CH$_2$), 1.41-1.33 (m, 2H, CHCH$_2$C$\underline{H_2}$CH$_2$). ^{13}C NMR, D_2O, 100 MHz: δ 181.11 (2 x N$\underline{C}$OCH), 174.72 (CH$\underline{C}$O$_2$H), 173.22 (NH$\underline{C}$OCH$_2$), 54.65 (NH$_2\underline{C}$HCO$_2$H), 38.99 (NH$\underline{C}$H$_2$CH$_2$), 35.47 (N$\underline{C}$H$_2$CH$_2$CO), 33.79 (CO$\underline{C}$H$_2$CH$_2$), 30.02 (CH$\underline{C}$H$_2$CH$_2$), 27.98 (2 x CO$\underline{C}$H), 27.84 (NHCH$_2\underline{C}$H$_2$CH$_2$), 21.73 (CHCH$_2\underline{C}$H$_2$CH$_2$). Expected for $C_{13}H_{20}N_3O_5$ (M-H$^+$) = *m/z* 298.1408. Found: *m/z* 298.1412. Infrared (KBr): 3447, 1696 cm^{-1}. HPLC: column: Phenomenex Luna-NH$_2$ (250 x 4.60 mm), gradient elution: (1.0 mL/min) 10 % MeCN in water containing 0.1 % TFA → 100 % MeCN over 20 minutes, retention time, 2.77 mins., purity, 97%). Detection at 225 nm.

Synthesis of *1-ethyl-3-dideutero-(4R,S)-deutero-pyrrolidine-2,5-dione* (**2.17**).

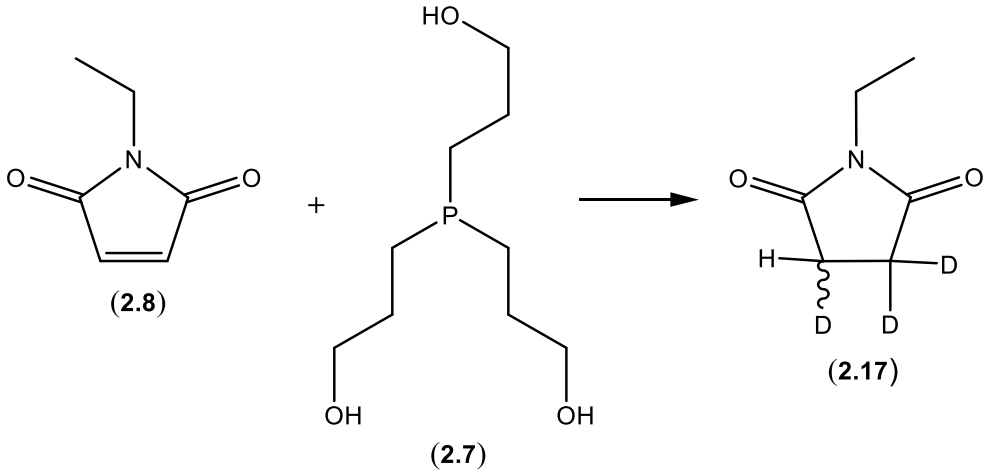

(**2.8**) (**2.7**) (**2.17**)

A solution of THPP (**2.7**, 0.9 eq., 29.9 mg, 0.144 mmol) was prepared in THF (1 mL) and purged deuterated aqueous sodium phosphate (0.1 M, pH = 7.0, 9 ml). N-Ethyl maleimide (**2.8**, 20.0 mg, 0.160 mmol) was added slowly to the rapidly stirring solution of THPP. The reaction was left to stir for 30 minutes at room temperature. A further 0.1 eq. of THPP was added and left to stir for an additional 30 minutes. The reaction was diluted with 25 mL of diethyl ether and extracted with water (30 mL). The aqueous layer was extracted with diethyl ether (2 x 30 mL). The organic extraction layers were combined and dried using $MgSO_4$. The mixture was filtered and the organic solution was concentrated (550 mbar, 25 °C). The crude was purified by silica gel chromatography ($CH_2Cl_2 \rightarrow$ 2 % acetone/CH_2Cl_2) to yield **2.17** as a clear oil (10.8 mg, yield: 52 %). ^{1}H NMR, $CDCl_3$, 400 MHz: δ 3.50 (q, 2H, NC*H*$_2$CH$_3$, *J* = 7.2 Hz), 2.62 (br. s, 1H, COC*H*DCD$_2$), 1.10 (t, 3H, CH$_2$C*H*$_3$, *J* = 7.2 Hz). ^{13}C NMR, $CDCl_3$, 100 MHz: δ 177.1 (2 x N*C*O), 33.5 (N*C*H$_2$CH$_3$), 27.7 (m, CO*C*HD*C*D$_2$CO), 12.9 (CH$_2$*C*H$_3$). ESI-HRMS: Expected for $C_6H_6D_3N_1O_2$ (M+Na$^+$) = *m/z* 153.0714. Found: *m/z* 153.0704. Infrared (thin film): 1695 cm^{-1}. HPLC: column: Phenomenex Luna-NH_2 (250 x 4.60 mm), gradient elution: (1.0 mL/min) 10 % MeCN in water containing 0.1 % TFA $\rightarrow$ 100 % MeCN over 20 minutes, retention time, 2.90 mins, purity 99 %. Detection at 225 nm.

Synthesis *of 3,3'-{5-oxo-2-[2-(phenylsulfonyl)ethyl]-1,2 λ^5-oxaphospholane-2,2-diyl}dipropanoic acid* (**2.20**).

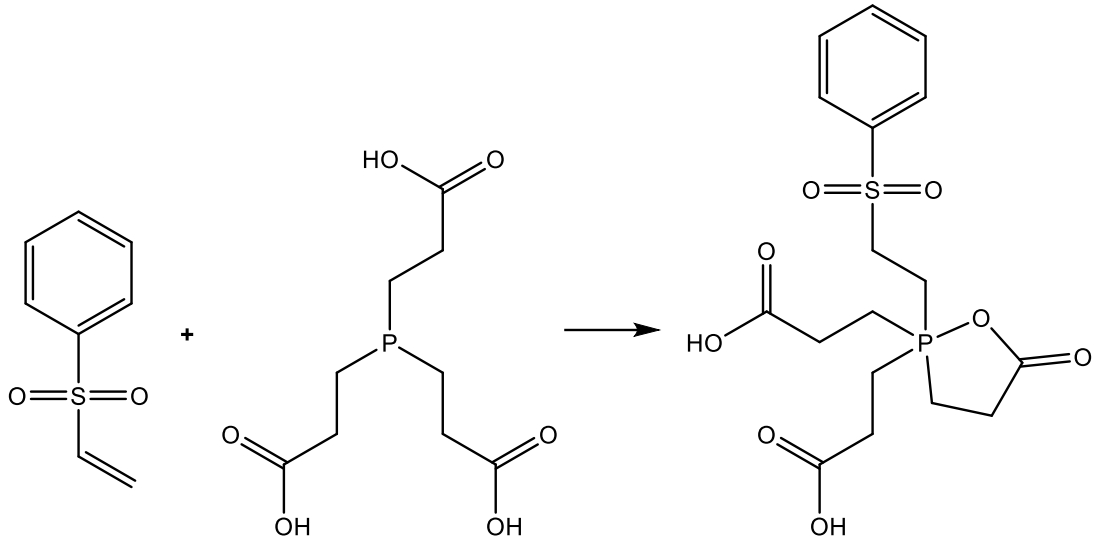

(**2.18**) (**2.6**) (**2.20**)

Phenyl vinyl sulfone (**2.18**, 10.0 mg, 0.0594 mmol) and TCEP (**2.6**, 0.9 eq., 15.3 mg, 0.0535 mmol) was dissolved in THF (2 mL) and argon purged aqueous sodium phosphate (0.1 M, pH = 7.0, 8 ml) and stirred under argon at room temperature for 1 hour. The reaction was concentrated *in vacuo* to 3 mL and then loaded onto a C-18 column for purification (100 % $H_2O \rightarrow$ 40 % MeCN/H_2O) to yield **2.20** as a white solid (18.8 mg, 84 %). δ ^{1}H NMR, D_2O, 400 MHz: 7.95-7.67 (m, 5H, Ar-*H*), 3.72 (m, 2H, SC*H*$_2$CH$_2$), 2.74-2.66 (m, 2H, SCH$_2$C*H*$_2$), 2.63-2.54 (m, 12H, 3 x C*H*$_2$C*H*$_2$CO). ^{13}C NMR, D_2O, 100 MHz: δ 175.3 (d, 3 x CH$_2$ *C*O$_2$H, *J* = 12.7 Hz), 135.45 (*ipso* -*C* & *para* Ar-*C*), 130.0 & 128.09 (4C, *ortho* & *meta* Ar-*C*), 47.2 (S*C*H$_2$CH$_2$), 26.5 (d, 3 x CH$_2$*C*H$_2$CO$_2$, *J* = 3.8 Hz), 14.6 (d, 3 x *C*H$_2$CH$_2$CO$_2$, *J* = 50.1 Hz), 13.5 (d, P*C*H$_2$CH$_2$, *J* = 49.3 Hz). ^{31}P NMR, D_2O, 162 MHz: δ 37.7. HRMS: Expected for $C_{17}H_{22}O_8P_1S_1$ (M-H$^+$) = *m/z* 417.0778. Found: *m/z* 417.0797. Melting point: 115 °C. Infrared (KBr): 3427, 2925, 1721, 1419, 1153 cm^{-1}. HPLC: column: Phenomenex Luna-C18 (250 x 4.60 mm), gradient elution: (0.7 mL/min) 10 % MeCN in water containing 0.1 % TFA $\rightarrow$ 100 % MeCN over 20 minutes, retention time, 12.43 mins., purity, 97 %. Detection at 280 nm.

Reaction of THPP with vinyl sulfone: a thiol-alkylating functional group.

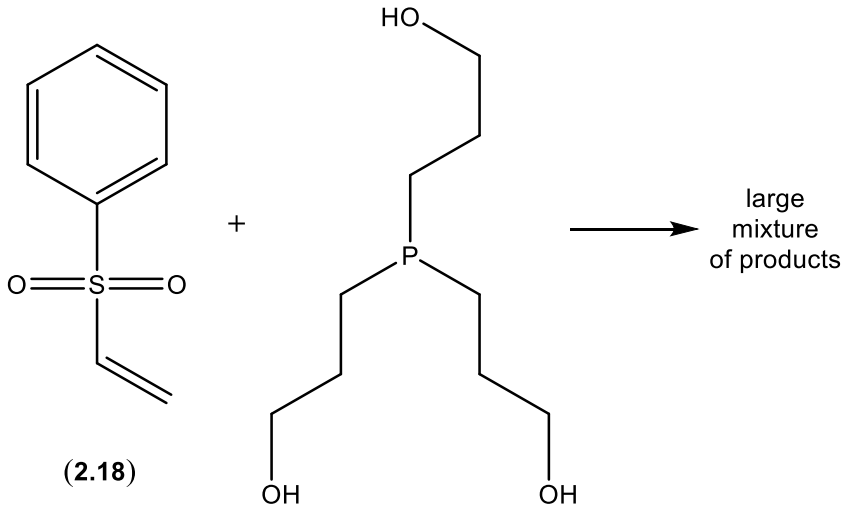

(**2.18**) (**2.7**)

Phenyl vinyl sulfone (**2.18**, 10.0 mg, 0.0594 mmol) and THPP (**2.7**, 0.9 eq., 11.1 mg, 0.0535 mmol) was dissolved in THF (2 mL) and argon purged aqueous sodium phosphate (0.1 M, pH = 7.0, 8 mL) and stirred under argon at room temperature for 1 hour. The reaction was concentrated *in vacuo* to 3 mL and then loaded onto a C-18 column for purification (100 % $H_2O \rightarrow$ 80 % MeCN/H_2O). No product could be isolated for characterisation.

Reaction of the TCEP-maleimide adduct **2.9** with thiols.

At pH = 4. N-Ethyl maleimide (**2.8**, 3.9 mg, 0.032 mmol) was dissolved in argon purged deuterated aqueous citric acid/sodium phosphate (0.5 mL, 0.1 M, pH = 4). TCEP (**2.6**, 1 eq., 9.05 mg, 0.032 mmol) was added and the reaction was incubated at room temperature for 1 hour. The TCEP-maleimide adduct **2.9** was evident by ^{31}P NMR (δ 38.9). Reduced glutathione (**2.21**, 1.5 eq., 14.6 mg, 0.047 mmol) was added and the reaction was left at room temperature overnight. The reaction was monitored by ^{31}P NMR. The δ 38.90 ppm signal for **2.9** was still evident, with no appearance of new peaks in the spectrum.

At pH = 7. N-Ethyl maleimide (**2.8**, 8.0 mg, 0.064 mmol) was dissolved in argon purged aqueous sodium phosphate (1.0 mL, 0.1 M, pH = 7.0). TCEP (**2.6**, 1 eq., 18.3 mg, 0.064 mmol) was added and the reaction was incubated at room temperature for 1 hour. Reduced glutathione (**2.21**, 1.2 eq., 23.6 mg, 0.077 mmol) was added and the reaction was stirred at room temperature overnight. The reaction was monitored by HRMS. No glutathione-maleimide product was evident. The TCEP-maleimide adduct **2.9** (*m/z* 374.1040 ($M-H^+$)) was still visible as well as unreacted glutathione (*m/z* 306.0787 ($M-H^+$)).

At pH = 8. N-Ethyl maleimide (**2.8**, 4.0 mg, 0.032 mmol) was dissolved in argon purged, deuterated aqueous sodium phosphate (0.5 mL, 0.1 M, pH = 8.0). TCEP (**2.6**, 1 eq., 9.2 mg, 0.032 mmol) was added and the reaction was incubated at room temperature for 1 hour. Reduced glutathione (**2.21**, 1.5 eq., 14.7 mg, 0.048 mmol) was added and the reaction was left at room temperature overnight. The reaction was monitored by ^{31}P NMR. No change of the δ 38.90 ppm signal for **2.9** was evident.

The effect of not removing TCEP or THPP prior to maleimide PEGylation of a model protein.

Yeast enolase (1 mg/mL, Sigma Aldrich) was denatured in argon purged buffer (0.5 M Tris, pH = 7.2, 5 mM EDTA) containing 8 M urea at 85 °C for 15 minutes. The solution was allowed to cool to room temperature before aliquoting out 100 μL samples for the experiments. Varying concentrations of TCEP or THPP (1-10 mM) were added to aliquots of protein solution (11 μM) and incubated for 45 minutes at 25 °C. Maleimide-PEG2kDa (1 mM) was subsequently added and the reaction was incubated at 37 °C for 18 hours. Samples (15 μL) were taken from each of the reactions and added to Laemmli sample buffer (15 μL). Aliquots (9 μL) of these solutions were loaded into a precast gradient gel (4-12 % Bis-Tris, Invitrogen) along with a protein ladder (EZ-Run, Fisher Scientific) and resolved by SDS Page electrophoresis [MOPS running buffer (Invitrogen), 180 V, 60 mins]. The precast

gels were stained by Coomassie solution and destained using a water/ethanol/acetic acid (16:3:1) solution.

Synthesis of N-(5-isocyanatopentyl)maleimide (**2.23**).

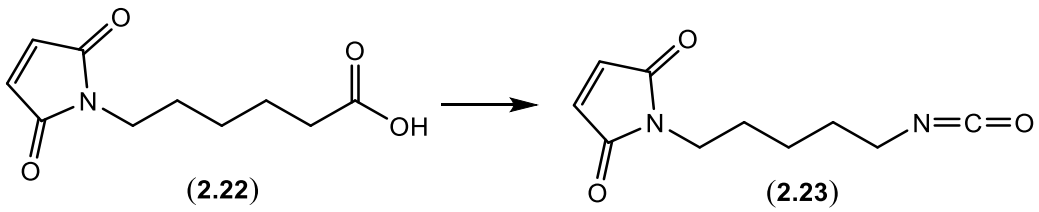

6-Maleimidohexanoic acid (**2.22**, 0.25 g, 1.18 mmol) was dissolved in anhydrous THF (4 mL) containing triethylamine (0.3 mL). Diphenylphosphoryl azide (0.38 mL, 1.76 mmol) was added and the reaction was stirred at room temperature for 2 hours. Anhydrous toluene (100 mL) was subsequently added and the solution was concentrated to a volume of 5 mL. The solution was heated at 70 °C for 2 hours and then allowed to cool back to room temperature. The solution was loaded directly onto a silica gel column for purification: 100 % petroleum ether $\rightarrow$ 30 % EtOAc/petroleum ether to yield **2.23** as a transparent oil (125.7 mg, 51 %). Spectral data was consistent with that reported in the literature [190]. ^{1}H NMR $CDCl_3$, 400 MHz: δ 6.69 (s, 2H, COC*H*C*H*CO), 3.52 (t, 2H, NC*H*$_2$CH$_2$, *J* = 7.2 Hz), 3.29 (t, 2H, CH$_2$C*H*$_2$NCO, *J* = 6.7 Hz), 1.66-1.58 (m, 4H, NCH$_2$C*H*$_2$ & CH$_2$C*H*$_2$CH$_2$NCO), 1.42-1.37 (m, 2H, C*H*$_2$CH$_2$CH$_2$NCO). ^{13}C NMR $CDCl_3$, 100 MHz: δ 170.78 (2 x *C*OCH), 134.05 (2 x CO*C*H), 121.89 (CH$_2$N*C*O), 42.69 (*C*H$_2$NCO), 37.44 (N*C*H$_2$CH$_2$), 30.57 & 27.82 (CHCONCH$_2$*C*H$_2$ & OCNCH$_2$*C*H$_2$CH$_2$), 23.62 (OCNCH$_2$CH$_2$*C*H$_2$). ESI-MS: Expected for $C_{10}H_{12}N_2Na_1O_3$ (M+Na$^+$) = *m/z* 231.0740. Found *m/z* 231.0739. Infrared (thin film): 2277, 1706 cm^{-1}.

Synthesis of Pn6B-maleimide (**2.24**).

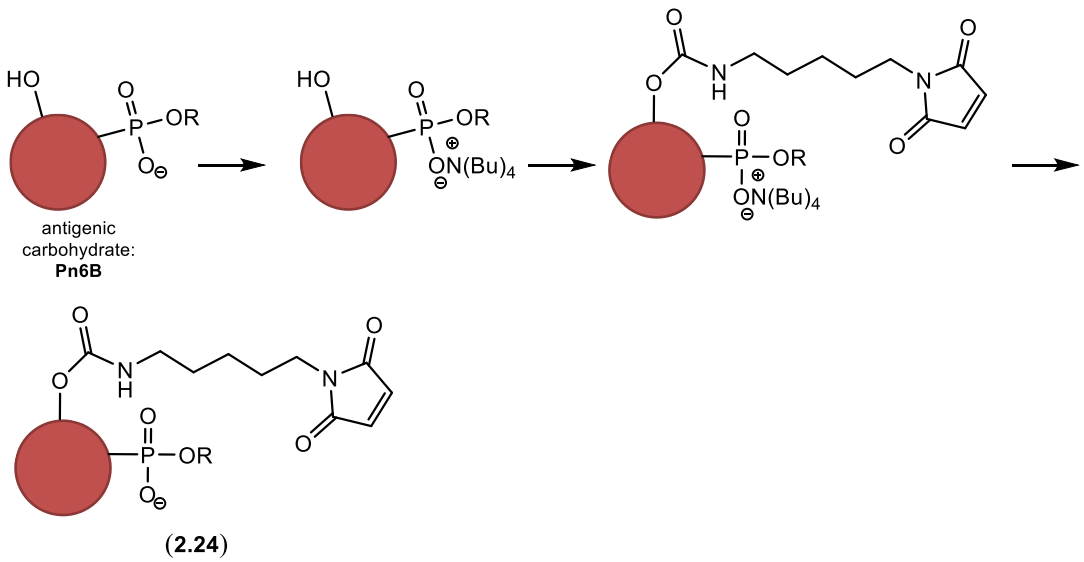

Pn6B (10 mg, LGC Standards) was added to 2 mL of water and stirred at room temperature until the carbohydrate until dissolved. The viscous solution was then loaded onto an ion exchange column (Dowex 50W x 4, 200 mesh, tetrabutylammonium form) and incubated for 30 minutes before allowing elution. The fractions containing carbohydrate were pooled and subsequently freeze dried to yield a white solid. The solid was added to 4 mL of anhydrous DMSO and stirred at 30 °C under N_2 overnight to dissolve the carbohydrate. An anhydrous DMSO solution (0.5 mL) of **2.23** (3 mg) was added to the carbohydrate solution and allowed to stir for 2 hours at room temperature. The solution was transferred to a dialysis bag (12-14 KDa cut-off) and dialysed against 5 litres of 0.1 M aqueous sodium phosphate (pH = 7), followed by 5 litres of 0.01 M aqueous sodium phosphate (pH = 7), and finally 5 litres of water. The solution within the dialysis bag was frozen and lyophilised to yield 6 mg of white solid (**2.24**). A portion of product (0.5 mg) was analysed by NMR spectroscopy to determine the maleimide/carbohydrate ratio.

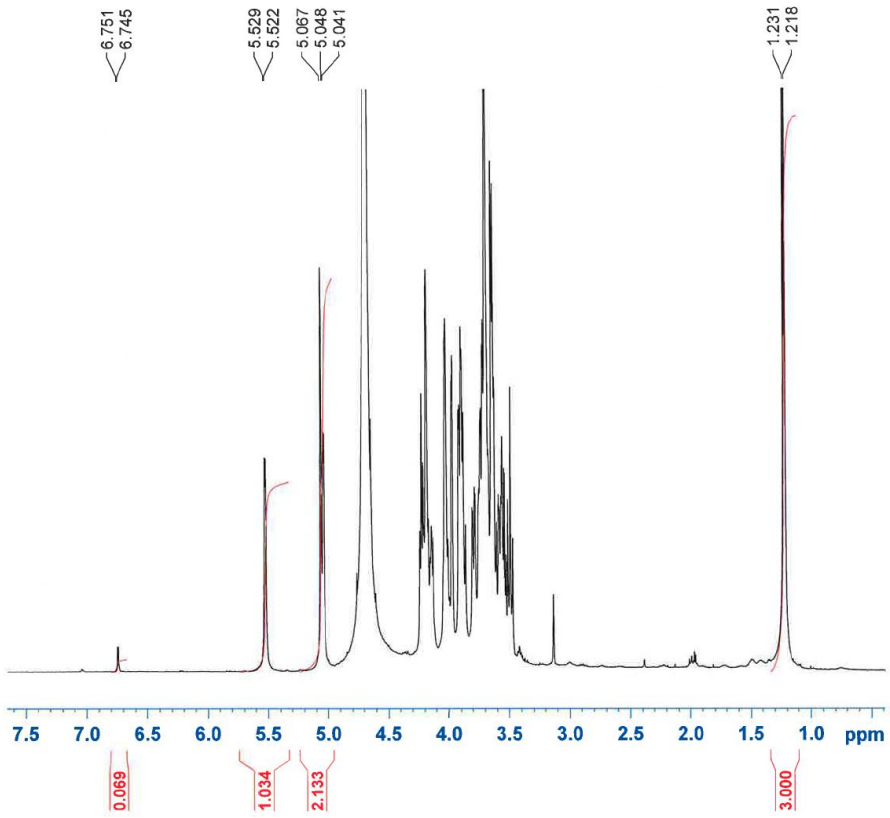

^{1}H NMR spectrum of Pn6B-maleimide (**2.24**).

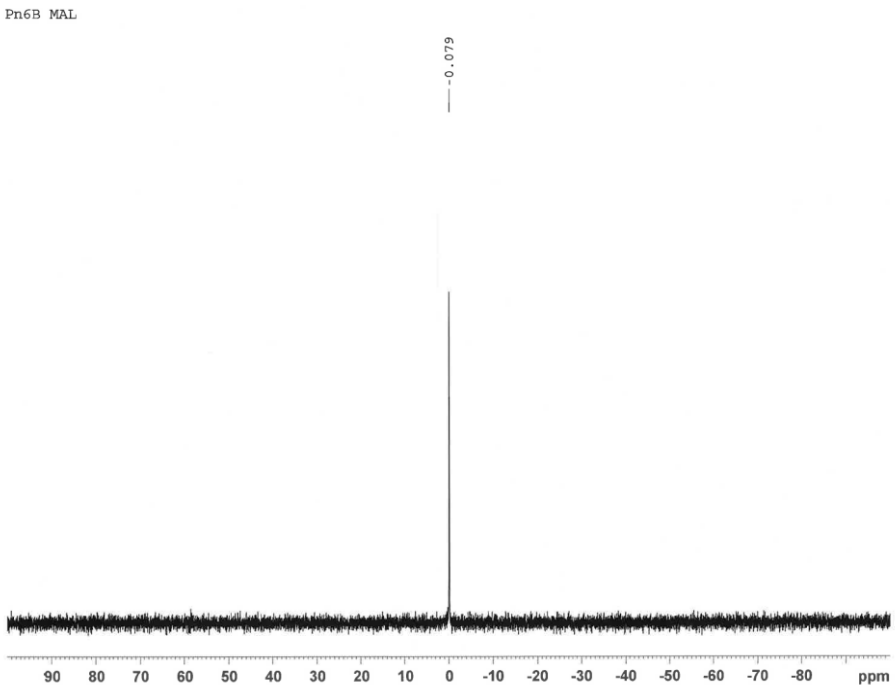

^{31}P NMR spectrum of Pn6B-maleimide.

Synthesis of Pn6B-maleimide-TCEP adduct.

Control: Maleimide functionalised Pn6B (1.0 mg) was dissolved in D_2O (0.45 mL) and analysed by ^{31}P NMR spectroscopy. ^{31}P NMR, D_2O, 162 MHz: δ -0.08.

Experiment: Maleimide functionalised Pn6B (1.0 mg) was dissolved in water (1 mL) containing TCEP (2.0 mg). The reaction was incubated at room temperature for 1 hour then purified using a PD-10 desalting column. The fractions containing carbohydrate were pooled and lyophilised. The lyophilised powder was redissolved in D_2O and analysed by ^{31}P NMR spectroscopy. ^{31}P NMR, D_2O, 162 MHz: δ -0.08 & 38.4.

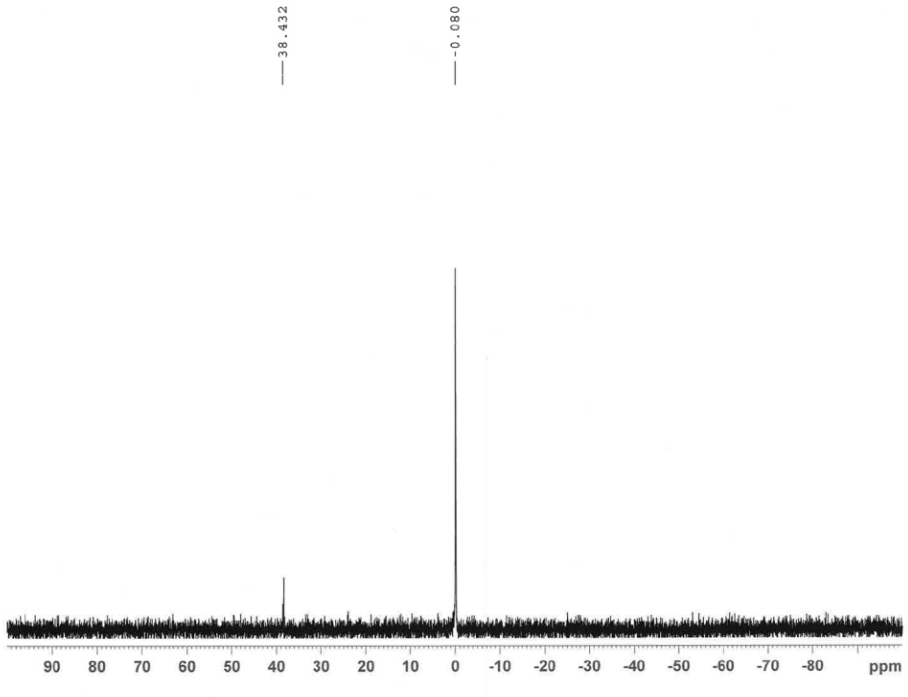

^{31}P NMR spectrum of Pn6B-maleimide-TCEP adduct.

Synthesis of 1,14-diazido-3,6,9,12-tetraoxatetradecane (**3.3**).

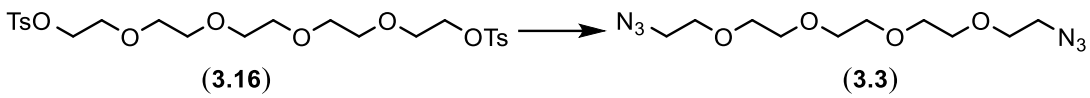

(**3.16**) (**3.3**)

Penta(ethylene glycol)di-*p*-toluenesulfonate (**3.16**, 2.0 g, 3.66 mmol) was dissolved in anhydrous DMF (15 mL). Sodium azide (4 eq., 0.95 g, 14.6 mmol) was added and the reaction was stirred at 80 °C, under argon for 6 hours. The reaction was allowed to cool to room temperature and then filtered. The organic solution was concentrated and then resuspended in ethyl acetate (200 mL). The solution was washed with saturated $NaHCO_3$ solution (100 mL) and then saturated brine solution (50 mL). The organic layer was dried over $MgSO_4$, filtered and concentrated to yield the crude material. This was purified by silica gel chromatography: 10 % EtOAc/Pet. ether $\rightarrow$ 60 % EtOAc/Pet. Ether) to give **3.3** as a colourless oil (0.89 g, 84 %). Experimental data was consistent with that reported in the literature [191]. ^{1}H NMR, $CDCl_3$, 400 MHz: δ 3.67-3.64 (m, 16H, 4 x C$\underline{H_2}$OC$\underline{H_2}$), 3.37 (t, 4H, 2 x $N_3C\underline{H_2}$, *J* = 5.0 Hz). ^{13}C NMR, $CDCl_3$, 100 MHz: δ 70.61, 70.59, 70.53, 69.94 ($N_3CH_2\underline{C}H_2$), 50.59 ($N_3\underline{C}H_2CH_2$). ESI-HRMS: Expected for $C_{10}H_{21}N_6O_4$ ($M+H^+$) = *m/z* 289.1619. Found: *m/z* 289.1618.

Synthesis of *ethyl S-[(3R,S)-1-ethyl-2,5-dioxopyrrolidin-3-yl]-L-cysteinate* (**3.7a**) after TCEP reduction. No addition of alkyl azide **3.3**.

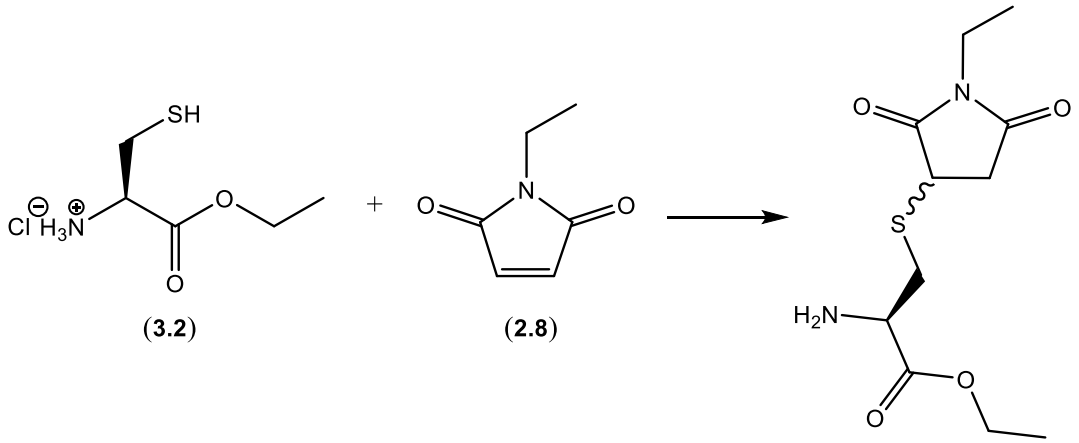

L-Cysteine ethyl ester hydrochloride salt (**3.2**, 10.0 mg, 0.0539 mmol) was dissolved in deoxygenated aqueous sodium phosphate (1 M, pH = 7.0, 1 mL) and stirred under argon at room temperature. TCEP (3 eq., 46.3 mg, 0.162 mmol) was added to the stirring solution and left to stir for 30 minutes. N-Ethyl maleimide (**2.8**, 1.2 eq., 8.1 mg, 0.0646 mmol) was subsequently added and the reaction was stirred for 30 minutes. The reaction was analysed by HRMS.

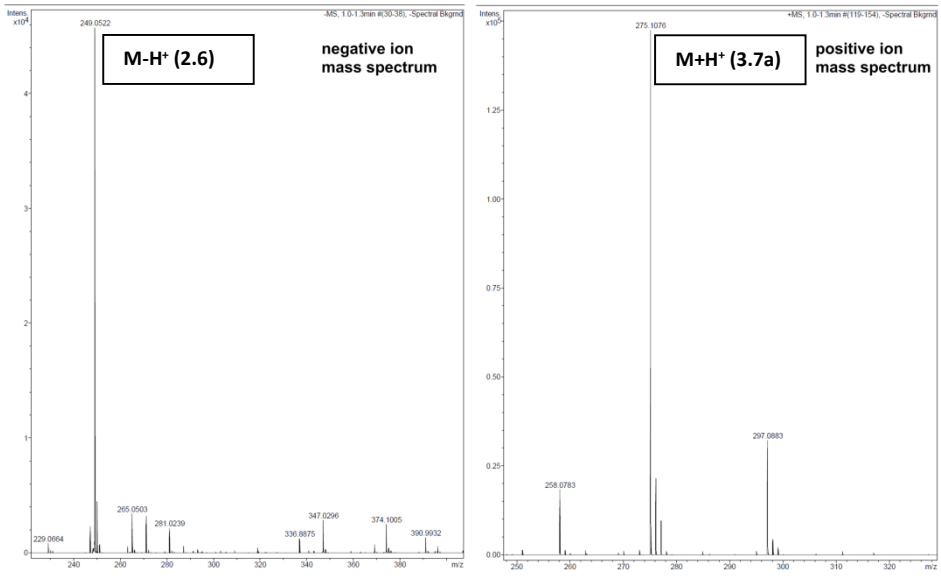

Mass spectra of synthesis of ethyl S-[(3R,S)-1-ethyl-2,5-dioxopyrrolidin-3-yl]-L-cysteinate (**3.7a**).

Synthesis of *ethyl S-[(3R,S)-1-ethyl-2,5-dioxopyrrolidin-3-yl]-L-cysteinate* (**3.7a**) after TCEP reduction. Addition of alkyl azide **3.3**.

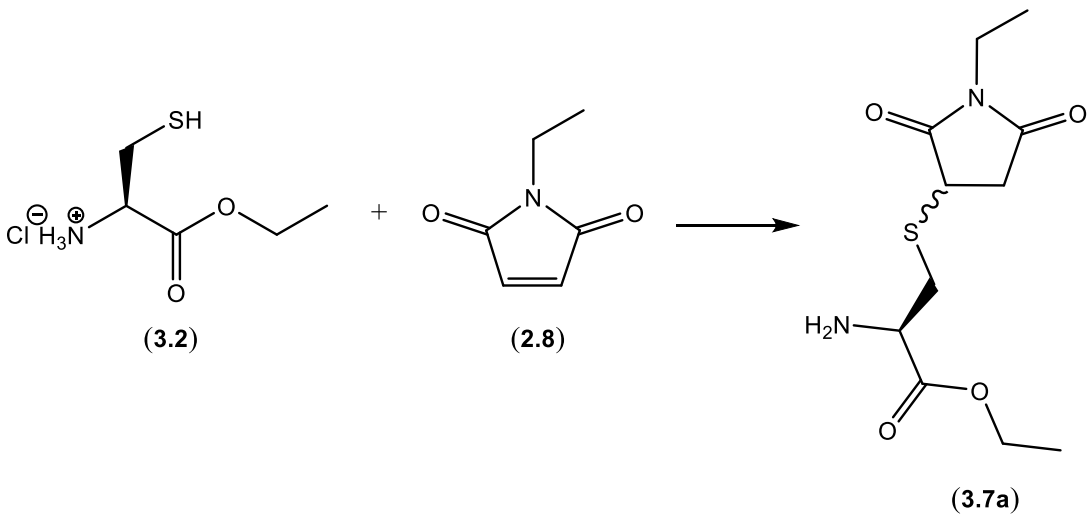

L-Cysteine ethyl ester hydrochloride salt (**3.2**, 10.0 mg, 0.0539 mmol) was dissolved in deoxygenated aqueous sodium phosphate (1 M, pH = 7.0, 1 mL) and stirred under argon at room temperature. TCEP (3 eq., 46.3 mg, 0.162 mmol) was added to the stirring solution and left to stir for 30 minutes. The alkyl azide **3.3** (3 eq., 46.6

mg, 0.162 mmol) was added and the reaction was stirred rapidly for 30 minutes. N-Ethyl maleimide (**2.8**, 1.2 eq., 8.09 mg, 0.0646 mmol) was subsequently added and the reaction was stirred for 30 minutes. The reaction was analysed by HRMS.

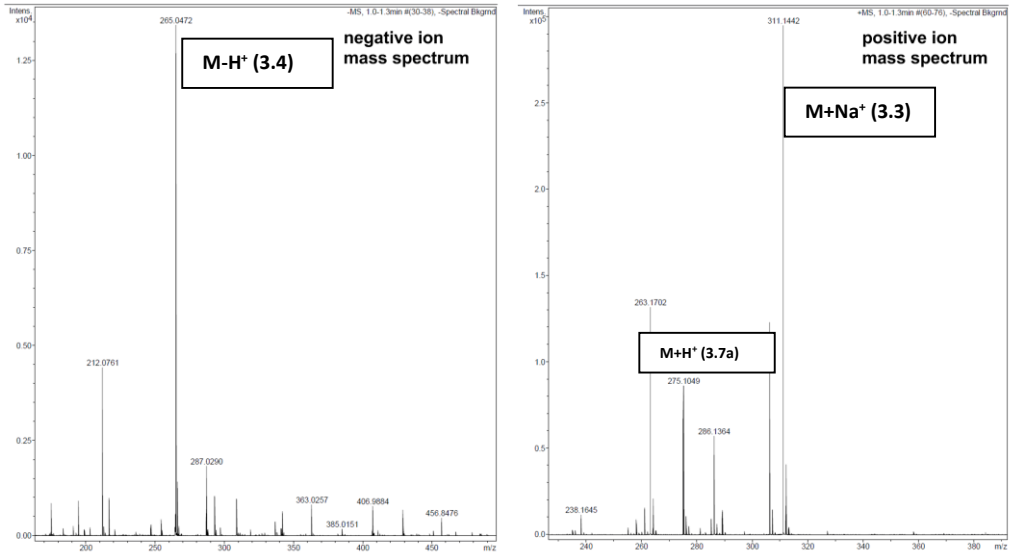

Mass spectra of synthesis of ethyl S-[(3R,S)-1-ethyl-2,5-dioxopyrrolidin-3-yl]-L-cysteinate (**3.7a**).

Synthesis of *ethyl S-[(3R,S)-1-ethyl-2,5-dioxopyrrolidin-3-yl]-L-cysteinate* (**3.7a**) after THPP reduction. No addition of alkyl azide **3.3**.

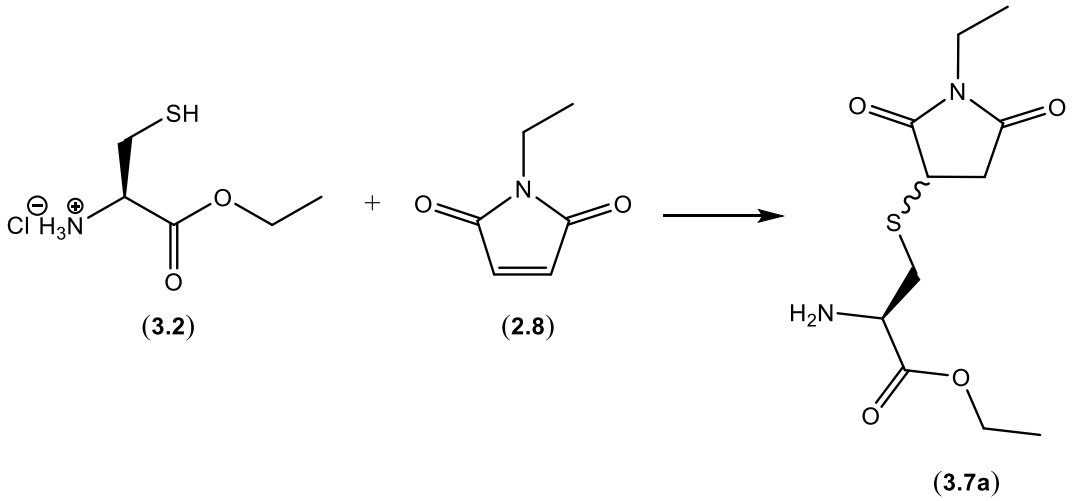

(**3.2**) (**2.8**) (**3.7a**)

L-Cysteine ethyl ester hydrochloride salt (10.0 mg, 0.0539 mmol) was dissolved in deoxygenated aqueous sodium phosphate (1 M, pH = 7.0, 1 mL) and stirred under argon at room temperature. THPP (3 eq., 33.7 mg, 0.162 mmol) was added to the stirring solution and left to stir for 30 minutes. N-Ethyl maleimide (**2.8**, 1.2 eq., 8.09 mg, 0.0646 mmol) was subsequently added and the reaction was stirred for 30 minutes. The reaction was analysed by HRMS.

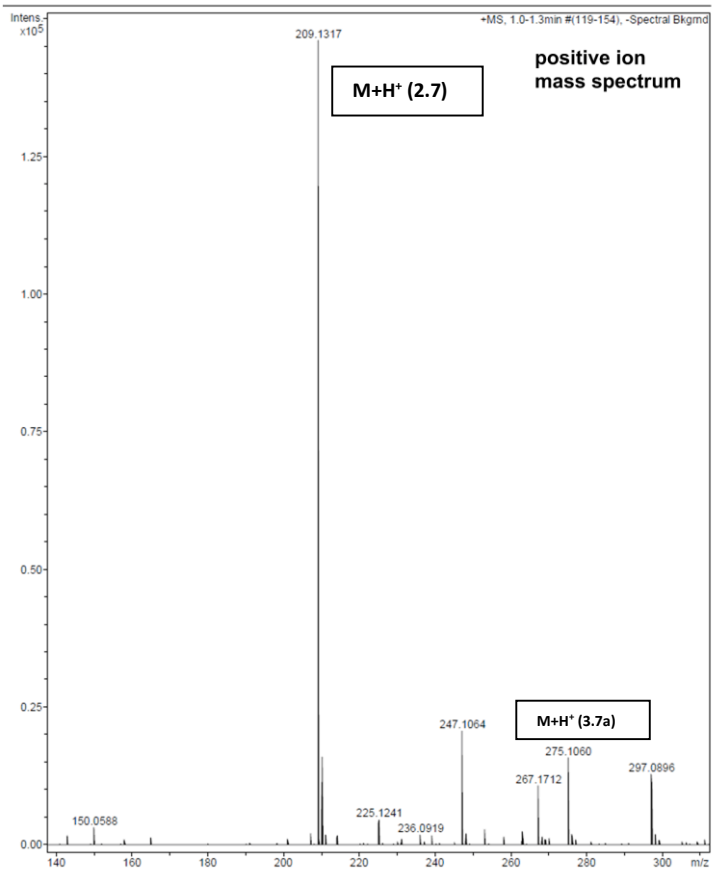

Mass spectrum of synthesis of ethyl S-[(3R,S)-1-ethyl-2,5-dioxopyrrolidin-3-yl]-L-cysteinate (**3.7a**).

Synthesis of *ethyl S-[(3R,S)-1-ethyl-2,5-dioxopyrrolidin-3-yl]-L-cysteinate* (**3.7a**) after THPP reduction. Addition of alkyl azide **3.3**.

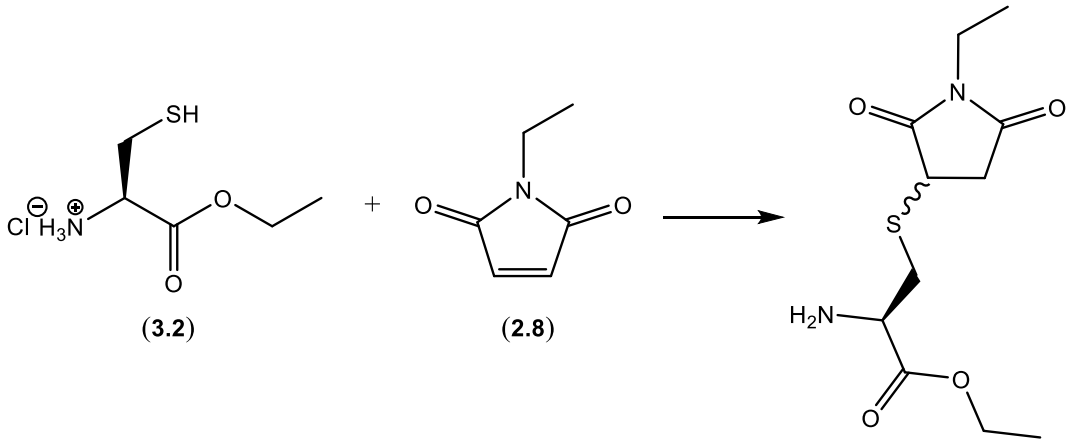

L-Cysteine ethyl ester hydrochloride salt (10.0 mg, 0.0539 mmol) was dissolved in deoxygenated aqueous sodium phosphate (1 M, pH = 7.0, 1 mL) and stirred under argon at room temperature. THPP (3 eq., 33.6 mg, 0.162 mmol) was added to the stirring solution and left to stir for 30 minutes. The alkyl azide **3.3** (3 eq., 46.6 mg, 0.162 mmol) was added and the reaction was stirred rapidly for 30 minutes. N-Ethyl maleimide (**2.8**, 1.2 eq., 8.1 mg, 0.0646 mmol) was subsequently added and the reaction was stirred for 30 minutes. The reaction was analysed by HRMS.

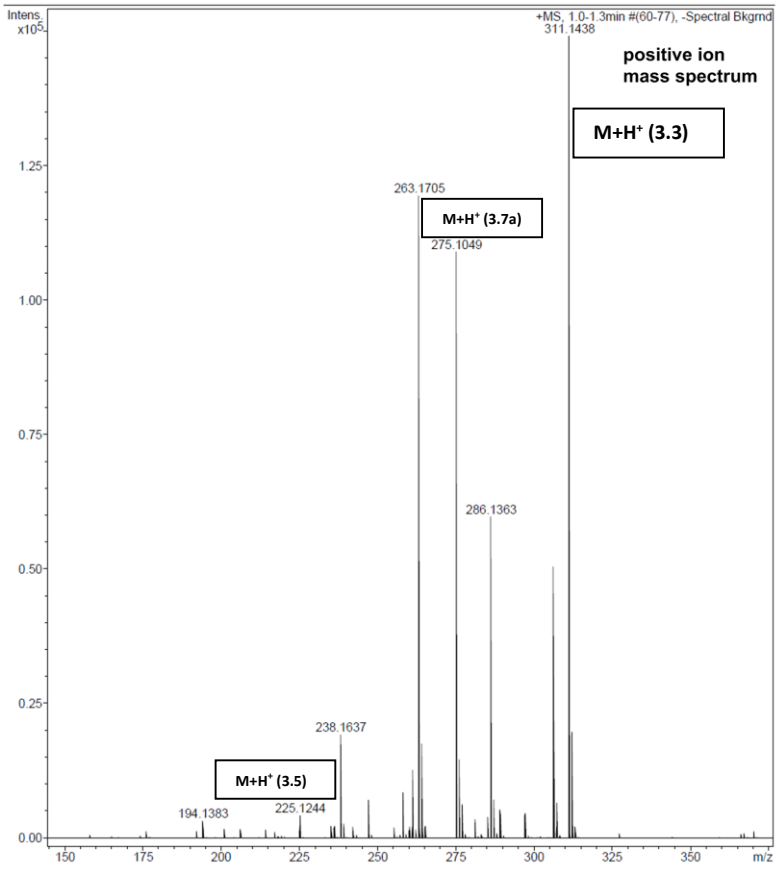

Mass spectrum of synthesis of ethyl S-[(3R,S)-1-ethyl-2,5-dioxopyrrolidin-3-yl]-L-cysteinate (**3.7a**).

Synthesis of *N-acetyl-S-[(3R,S)-1-ethyl-2,5-dioxopyrrolidin-3-yl]-L-cysteinate* (**3.7b**) after TCEP reduction. No addition of alkyl azide **3.3**.

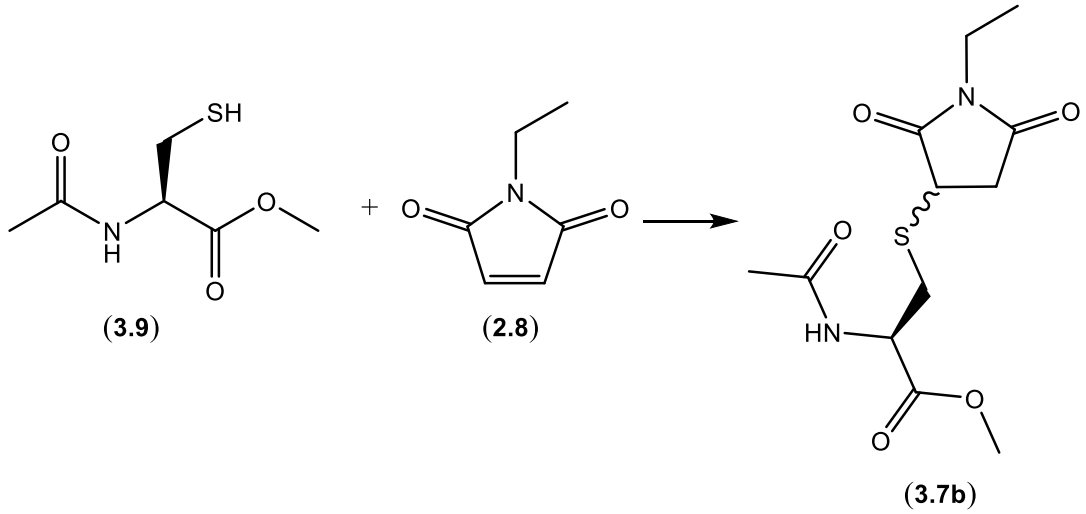

N-Acetyl-L-cysteine methyl ester (20.0 mg, 0.113 mmol) was dissolved in deoxygenated THF (2 mL) and Tris buffer (500 mM, pH = 7.2, 8 mL) and stirred under argon at room temperature. TCEP (5 eq., 161.8 mg, 0.564 mmol) was added to the stirring solution and left to stir for 30 minutes. N-Ethyl maleimide (**2.8**, 1.1 eq., 15.5 mg, 0.124 mmol) was subsequently added and the reaction was stirred for 1 hour. The reaction was extracted with diethyl ether (2 x 30 mL). The organic layer was dried ($MgSO_4$), filtered and concentrated. The residue was purified by silica gel chromatography: 10 % EtOAc/petroleum ether $\rightarrow$ 70 % EtOAc/petroleum ether to yield (**3.7b**) as a white solid (9.8 mg, 27 %). ^{1}H NMR, $CDCl_3$, 400 MHz: Diastereomeric mixture: δ 7.03 (br. d, 1H, N*H*, *J* = 7.8 Hz), 6.57 (br. d, 1H, N*H*, *J* = 7.7 Hz), 4.89 (m, 2H, 2 x NHC*H*CO_2), 3.88 (dd, 1H, COC*H*CH_2CO, *J* = 3.9 & 9.1 Hz), 3.75-3.72 (m, 7H, COC*H*CH_2CO, 2 x OC*H*$_3$), 3.57-3.42 (m, 6H, 2 x NC*H*$_2CH_3$, 2 x CHC*H*HS), 3.16-3.06 (m, 4H, 2 x CHCH*H*S, 2 x COC*H*HCHCO), 2.49-2.37 (m, 2H, 2 x COCH*H*CHCO), 2.04 (s, 3H, NHCOC*H*$_3$), 2.03 (s, 3H, NHCOC*H*$_3$), 1.16-1.12 (m, 6H, 2 x CH_2C*H*$_3$). ^{13}C NMR, $CDCl_3$, 100 MHz: δ 176.7, 176.5, 174.1, 173.9, 171.1, 170.9, 170.1, 170.0, 52.8, 52.7, 52.2, 51.2, 40.1, 38.6, 36.3, 35.6, 34.8, 34.1, 34.0, 33.9, 23.0, 22.9. ESI-HRMS: Expected for $C_{12}H_{18}N_2O_5S_1$ ($M+Na^+$) = *m/z* 325.0829. Found: *m/z* 325.0847. Infrared (KBr): 1745, 1698 cm^{-1}.

Synthesis of *N-acetyl-S-[(3R,S)-1-ethyl-2,5-dioxopyrrolidin-3-yl]-L-cysteinate* (**3.7b**) after TCEP reduction. Addition of alkyl azide **3.3**.

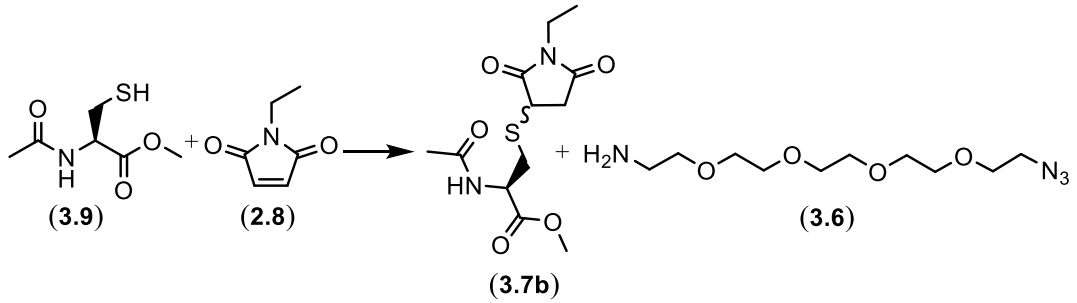

N-Acetyl-L-cysteine methyl ester (20.0 mg, 0.113 mmol) was dissolved in deoxygenated THF (2 mL) and Tris buffer (500 mM, pH = 7.2, 8 mL) and stirred under argon at room temperature. TCEP (5 eq., 162.7 mg, 0.565 mmol) was added to the stirring solution and left to stir for 30 minutes. The alkyl azide **3.3** (10 eq., 327 mg, 1.14 mmol) was added and the reaction was stirred rapidly for 1 hour at room temperature. N-Ethyl maleimide (**2.8**, 1.1 eq., 15.5 mg, 0.124 mmol) was subsequently added and the reaction was stirred for 1 hour at room temperature. The reaction was extracted with diethyl ether (2 x 30 mL). The organic layer was dried ($MgSO_4$), filtered and concentrated to dryness. The residue was purified by silica gel chromatography (10 % EtOAc/petroleum ether $\rightarrow$ 70 % EtOAc/petroleum ether) to yield **3.7b** as a white solid (25.4 mg, 74 %). The aqueous layer was purified by C-18 chromatography (100 % H_2O $\rightarrow$ 30 % MeOH/H_2O) to yield **3.6** as a transparent oil (116.9 mg, 79 %). Experimental data was consistent with that reported in the literature [192]. ^{1}H NMR, CD_3OD, 400 MHz: δ 3.76 (t, 2H, $NH_2CH_2C\underline{H_2}$, J = 5.1 Hz), 3.70 (m, 14H, 7 x $C\underline{H_2}$), 3.44 (t, 2H, $N_3C\underline{H_2}$, J = 4.8 Hz), 3.16 (t, 2H, $NH_2C\underline{H_2}$, J = 5.1 Hz). ^{13}C NMR, CD_3OD, 100 MHz: δ 71.45, 71.41, 71.36, 71.35, 71.10, 70.97, 67.97 ($NH_2CH_2\underline{C}H_2$), 51.77 ($N_3\underline{C}H_2$), 40.68 ($NH_2\underline{C}H_2$). ESI-HRMS: Expected for $C_{10}H_{23}N_4O_4$ ($M+H^+$) = *m/z* 263.1714. Found: *m/z* 263.1748.

Synthesis of *N-acetyl-S-[(3R,S)-1-ethyl-2,5-dioxopyrrolidin-3-yl]-L-cysteinate* (**3.7b**) after THPP reduction. No addition of alkyl azide **3.3**.

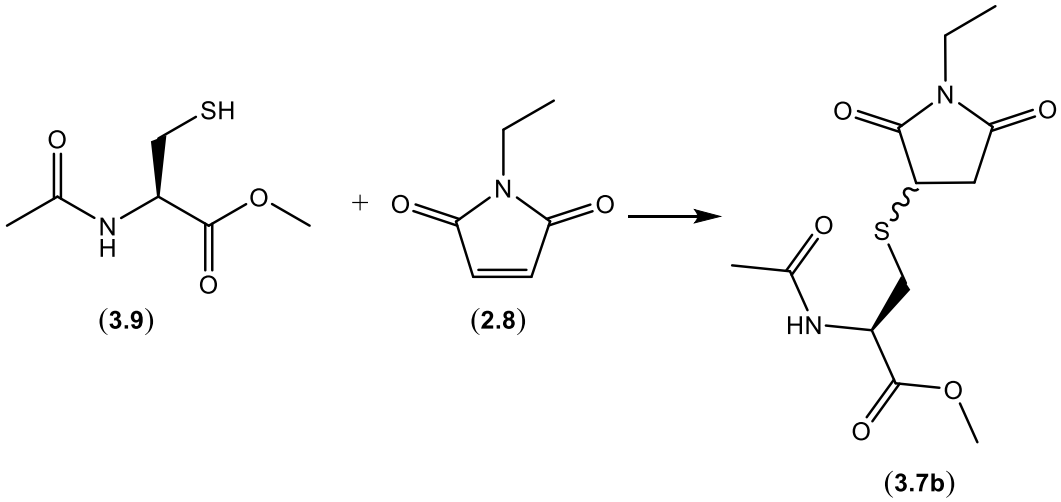

N-Acetyl-L-cysteine methyl ester (20.0 mg, 0.113 mmol) was dissolved in deoxygenated THF (2 mL) and Tris buffer (500 mM, pH = 7.2, 8 mL) and stirred under argon at room temperature. THPP (5 eq., 118.2 mg, 0.568 mmol) was added to the stirring solution and left to stir for 30 minutes. N-Ethyl maleimide (**2.8**, 1.1 eq., 15.5 mg, 0.124 mmol) was subsequently added and the reaction was stirred for 1 hour. The reaction was extracted with diethyl ether (2 x 30 mL). The organic layer was dried ($MgSO_4$), filtered and concentrated to dryness. The crude material was purified by silica gel chromatography: 10 % EtOAc/petroleum ether $\rightarrow$ 70 % EtOAc/petroleum ether to **3.7b** as a white solid (7.21 mg, 21 %).

Synthesis of *N-acetyl-S-[(3R,S)-1-ethyl-2,5-dioxopyrrolidin-3-yl]-L-cysteinate* (**3.7b**) after THPP reduction. Addition of alkyl azide **3.3**.

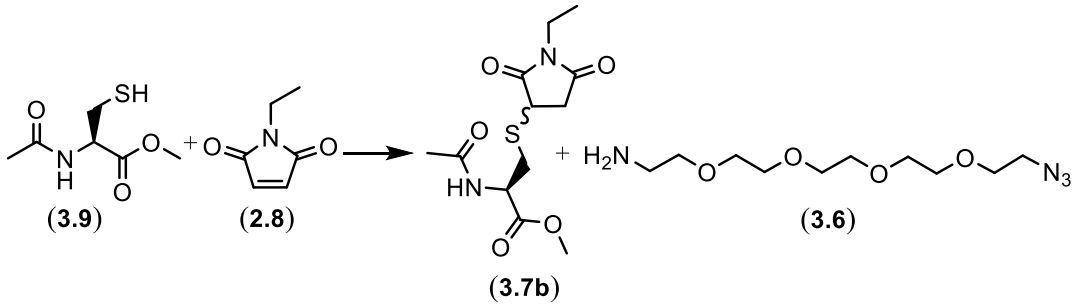

N-Acetyl-L-cysteine methyl ester (20.0 mg, 0.113 mmol) was dissolved in deoxygenated THF (2 mL) and Tris buffer (500 mM, pH = 7.2, 8 mL) and stirred under argon at room temperature. THPP (5 eq., 118.2 mg, 0.568 mmol) was added to the stirring solution and left to stir for 30 minutes. The alkyl azide **3.3** (10 eq., 327.2 mg, 1.14 mmol) was added and the reaction was stirred rapidly for 1 hour at room temperature. N-Ethyl maleimide (**2.8**, 1.1 eq., 15.5 mg, 0.124 mmol) was subsequently added and the reaction was stirred for 1 hour at room temperature. The reaction was extracted with diethyl ether (2 x 30 mL). The organic layer was dried ($MgSO_4$), filtered and concentrated to dryness. The residue was purified by silica gel chromatography (10 % EtOAc/petroleum ether $\rightarrow$ 70 % EtOAc/petroleum ether) to yield **3.10** as a white solid (23.8 mg, 69 %). The aqueous layer was purified by C-18 chromatography (100 % H_2O $\rightarrow$ 30 % MeOH/H_2O) to yield **3.6** as a transparent oil (105.7 mg, 71 %).

Investigating the potential reaction of maleimide with alkyl azide **3.3**.

N-Ethyl maleimide (**2.8**, 5.0 mg, 0.0400 mmol) and the alkyl azide **3.3** (11.5 mg, 0.400 mmol) were dissolved in deuterium oxide (450 μL). The solution was immediately analysed by NMR spectroscopy. No reaction between the reagents was detected. The solution was left at room temperature for 16 hours then analysed by NMR spectroscopy. New peaks were detected in the NMR spectrum to infer a reaction between the two reagents.

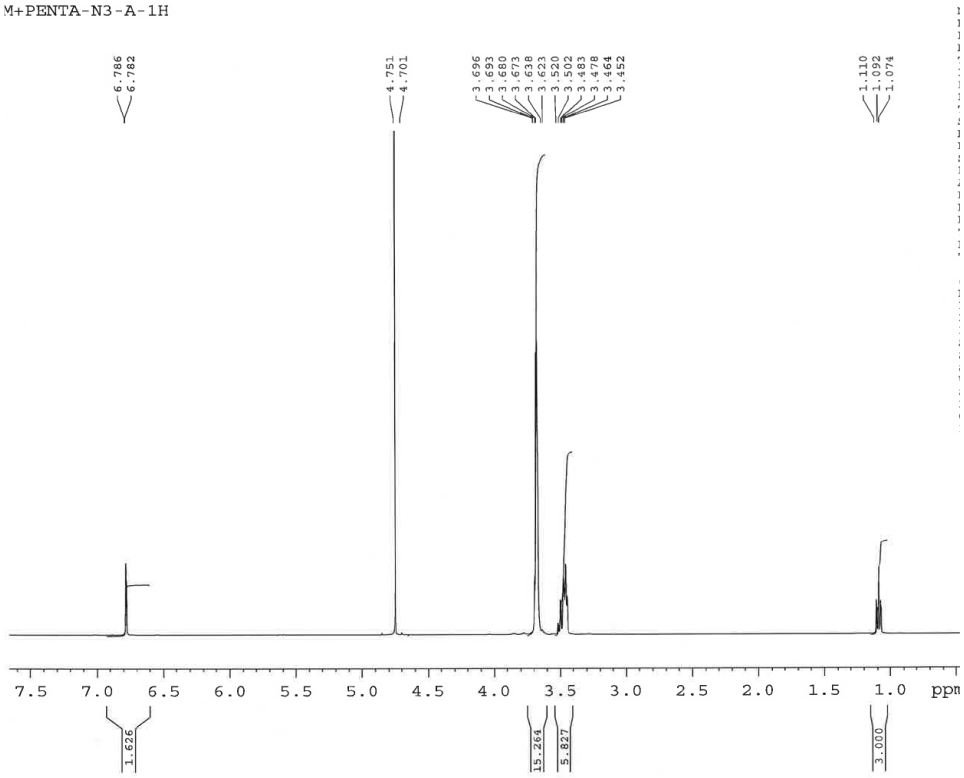

^{1}H NMR spectrum N-ethyl maleimide (**2.8**) and alkyl azide **3.3.**

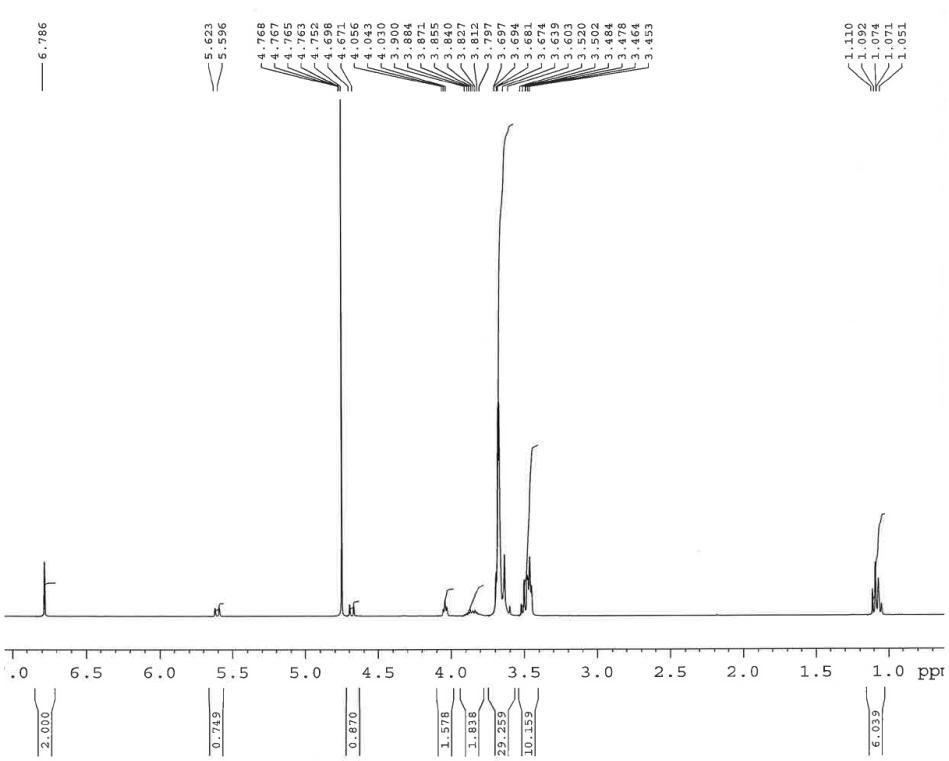

^{1}H NMR spectrum N-ethyl maleimide (**2.8**) and alkyl azide **3.3** after 16 hours.

Synthesis of *1-(14-azido-3,6,9,12-tetraoxatetradec-1-yl)-5-ethyl-3a,6a-dihydropyrrolo[3,4-d][1,2,3]triazole-4,6(1H,5H)-dione* (**3.8**) and *1,1'-(3,6,9,12-tetraoxatetradecane-1,14-diyl)bis(5-ethyl-3a,6a-dihydropyrrolo[3,4-d][1,2,3]triazole-4,6(1H,5H)-dione)* (**3.9**).

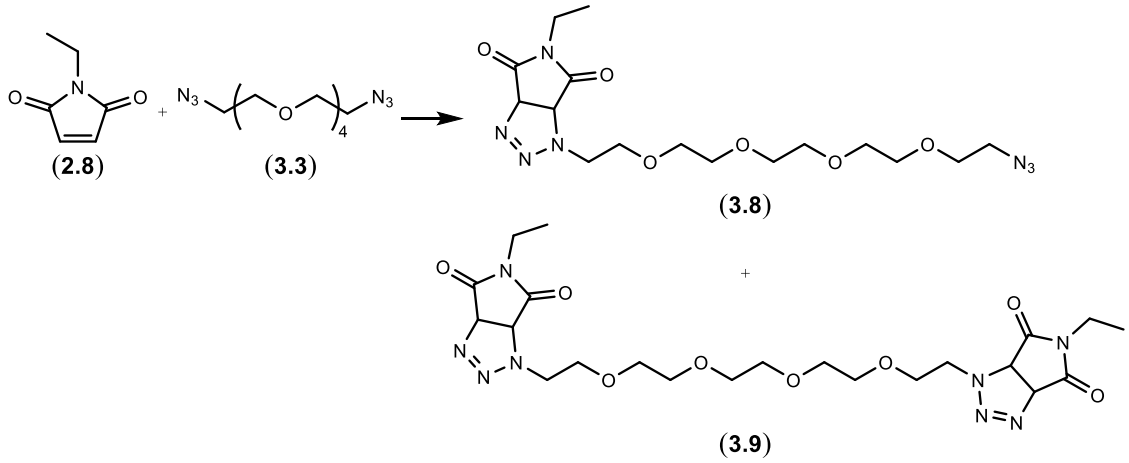

1,14-diazido-3,6,9,12-tetraoxatetradecane (**3.3**, 50.0 mg, 0.173 mmol) and N-ethyl maleimide (**2.8**, 1.5 eq., 32.6 mg, 0.260 mmol) were stirred in aqueous sodium phosphate (0.1 M, pH = 7.0, 2 mL) at room temperature for 2.5 days. The reaction was diluted with water (20 mL) and extracted with ethyl acetate (2 x 50 mL). The organic layer was dried over $MgSO_4$, filtered and concentrated. The crude was purified by silica gel chromatography: 10 % EtOAc/petroleum ether $\rightarrow$ 60 % EtOAc/petroleum ether to yield **3.8** as a transparent oil (30.1 mg, 42 %) and **3.9** as a transparent oil (23.4 mg, 25 %). Compound **3.8**: ^{1}H NMR, $CDCl_3$, 400 MHz: δ 5.49 (d, 1H, NCOC*H*NCH$_2$, *J* = 11.0 Hz), 4.62 (d, 1H, NCOC*H*N$_2$, *J* = 11.0 Hz), 4.15-4.09 (dt, 1H, NC*H*HCH$_2$O, *J* = 4.5 & 15.1 Hz), 4.00-3.93 (ddd, 1H, NCH*H*CH$_2$O, *J* = 3.9, 7.9 & 14.8 Hz), 3.86-3.81 (m, 1H, NCH$_2$C*H*HO), 3.78-3.72 (m, 1H, NCH$_2$CH*H*O), 3.65-3.55 (m, 14H), 3.50 (q, 2H, NC*H*$_2$CH$_3$, *J* = 7.2 Hz), 3.36 (t, 2H, CH$_2$C*H*$_2$N$_3$, *J* = 5.2 Hz), 1.11 (t, 3H, CH$_2$C*H*$_3$, *J* = 7.2 Hz). ^{13}C NMR, $CDCl_3$, 100 MHz: δ 172.2 (N*C*OCHN$_2$), 170.6 (N*C*OCHNCH$_2$), 81.2 (NCO*C*HNCH$_2$), 70.58, 70.54, 70.41, 70.38, 70.32, 70.12, 69.87, 69.1 (NCH$_2$C*H*$_2$O), 58.5 (NCO*C*HN$_2$), 50.5 (CH$_2$*C*H$_2$N$_3$), 48.1 (N*C*H$_2$CH$_2$O), 34.1 (N*C*H$_2$CH$_3$), 12.7 (CH$_2$*C*H3). ESI-HRMS: Expected for $C_{16}H_{27}N_7Na_1O_6$ (M+Na$^+$) = *m/z*

436.1915. Found: *m/z* 436.1946. Infrared (thin film): 2107, 1714 cm^{-1}. HPLC: column: Waters Symmetry Shield RP_8 (100 x 4.60 mm), gradient: (0.5 mL/min) 5 % MeCN in water → 100 % MeCN over 20 minutes, retention time, 13.50 mins., purity, 98.3 %). Detection at 254 nm. Compound **3.9**: ^{1}H NMR, $CDCl_3$, 400 MHz: δ 5.55 (d, 1H, COC*H*NCH_2, *J* = 11.0 Hz), 5.54 (d, 1H, COC*H*NCH_2, *J* = 11.0 Hz), 4.67 (d, 1H, COC*H*N_2,*J* = 11.0 Hz) & 4.66 (d, 1H, COC*H*N_2, *J* = 11.0 Hz), 4.19-4.12 (m, 2H, 2 x NC*H*HCH_2O), 4.02-3.94 (m, 2H, 2 x NCH*H*CH_2O), 3.89-3.83 (m, 2H, 2 x NCH_2C*H*HO), 3.80-3.74 (m, 2H, 2 x NCH_2CH*H*O), 3.68-3.56 (m, 12H), 3.53 (q, 4H, 2 x NC*H*$_2$$CH_3$, *J* = 7.2 Hz), 1.14 (t, 6H, 2 x CH_2C*H*$_3$, *J* = 7.2 Hz). ^{13}C NMR, $CDCl_3$, 100 MHz: δ 172.41 & 172.39 (2 x N*C*OCHN_2), 170.79 & 170.73 (2 x N*C*O$CHNCH_2$), 81.34 & 81.33 (2 x CO*C*$HNCH_2$), 70.49, 70.36, 70.08, 69.21 & 69.06 (2 x NCH_2*C*H_2O), 58.62 & 58.59 (2 x NCO*C*HN_2), 48.14 & 48.12 (2 x N*C*H_2CH_2O), 34.24 (2 x N*C*H_2CH_3), 12.76 (2 x CH_2*C*H_3). ESI-HRMS: Expected for $C_{22}H_{34}N_8Na_1O_8$ ($M+Na^+$) = *m/z* 561.2392. Found: *m/z* 561.2365. Infrared (thin film): 1714 cm^{-1}. HPLC: column: Waters Symmetry Shield RP_8 (100 x 4.60 mm), gradient: (0.5 mL/min) 5 % MeCN in water → 100 % MeCN over 20 minutes (retention time, 13.53 mins., purity, 99.4 %. Detection at 254 nm.

Reaction of N-ethyl maleimide with glutathione in a deuterated buffer to generate **3.10.**

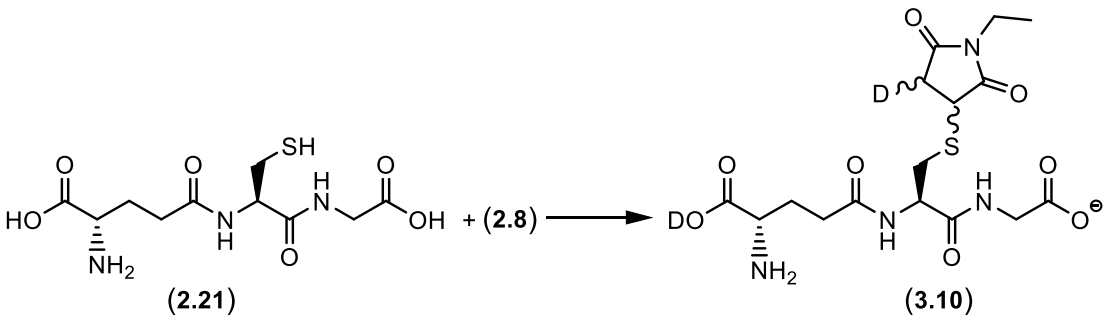

N-Ethyl maleimide (**2.8**, 1 mM) was dissolved in deuterated phosphate buffer (0.5 M, pH = 7.2) and analysed by ^{1}H NMR spectroscopy to identify the singlet at δ ~7 ppm representing the alkene protons of the maleimide ring. Reduced glutathione (**2.21**, 1 mM), was added to the solution and immediately analysed by ^{1}H NMR

spectroscopy. The ^{1}H NMR spectrum showed complete disappearance of the singlet representing the maleimide alkene protons, confirmation of a rapid reaction between N-ethyl maleimide (**2.8**) and glutathione (**2.21**). The thiol alkylated peptide **3.10** was also confirmed by HRMS (*m/z* 433.1381 ($M-H^{+}$)).

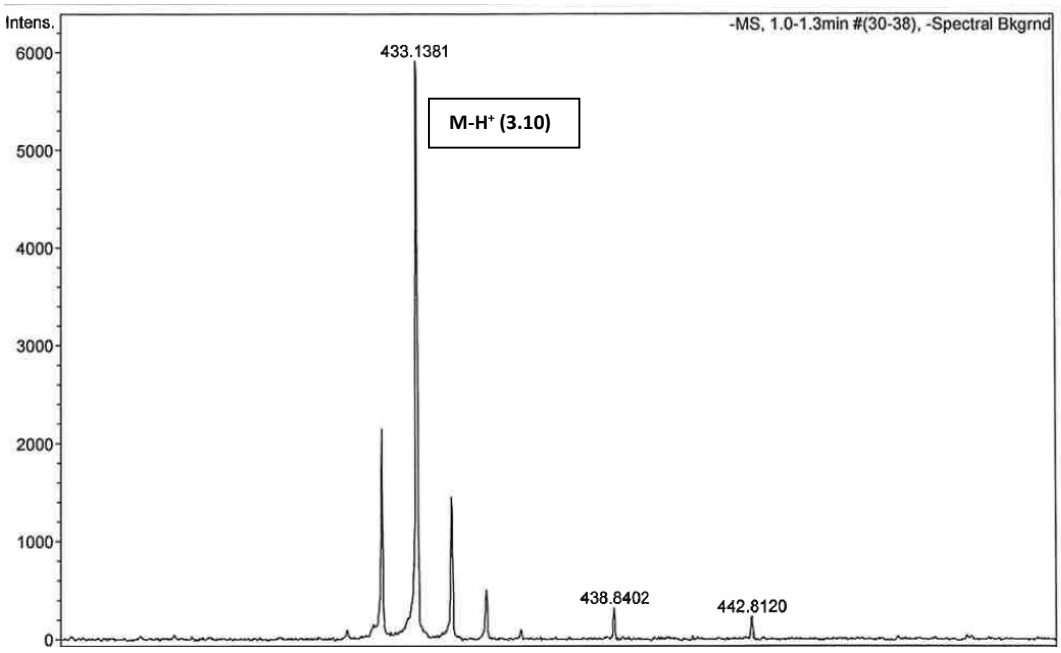

Mass spectrum of reaction of glutathione (**2.21**) with N-ethyl maleimide (**2.8**) in a deuterated buffer to yield **3.10**.

Reaction of glutathione (**2.21**) with N-ethyl maleimide (**2.8**) in the presence of alkyl azide **3.3** to generate **3.10**.

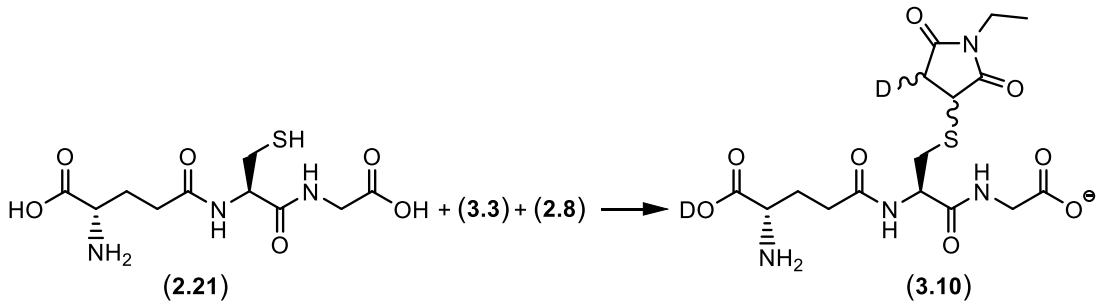

Reduced glutathione (**2.21**, 1 mM) was dissolved in deuterated aqueous phosphate (0.5 M, pH = 7.2, 1 mL), containing alkyl azide (**3.3,** 50 mM). N-Ethyl maleimide (**2.8**, 1 mM) was subsequently added and the reaction was immediately analysed by ^{1}H NMR spectroscopy. The ^{1}H NMR spectrum showed complete disappearance of the singlet representing the maleimide alkene protons. There was no evidence in the NMR spectrum of a pair of doublets at ~ δ 4.68 and ~ 5.61 ppm with coupling constants of 11 Hz, which would be a positive indication of triazoline formation. This evidence was verified by HRMS analysis. The positive identification of **3.10** (*m/z* 433.1375 ($M\text{-}H^{+}$)) and the absence of any peaks in the HRMS spectrum representing triazoline derivatives supported the evidence provided by the NMR data.

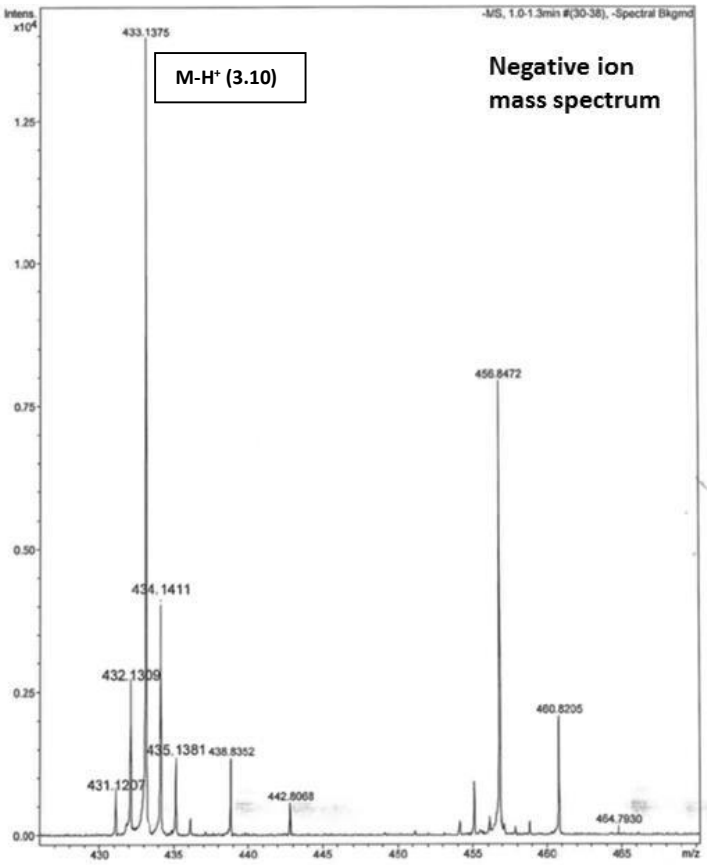

Mass spectrum of reaction containing glutathione (**2.21**), alkyl azide **3.3** and N-ethyl maleimide (**2.8**).

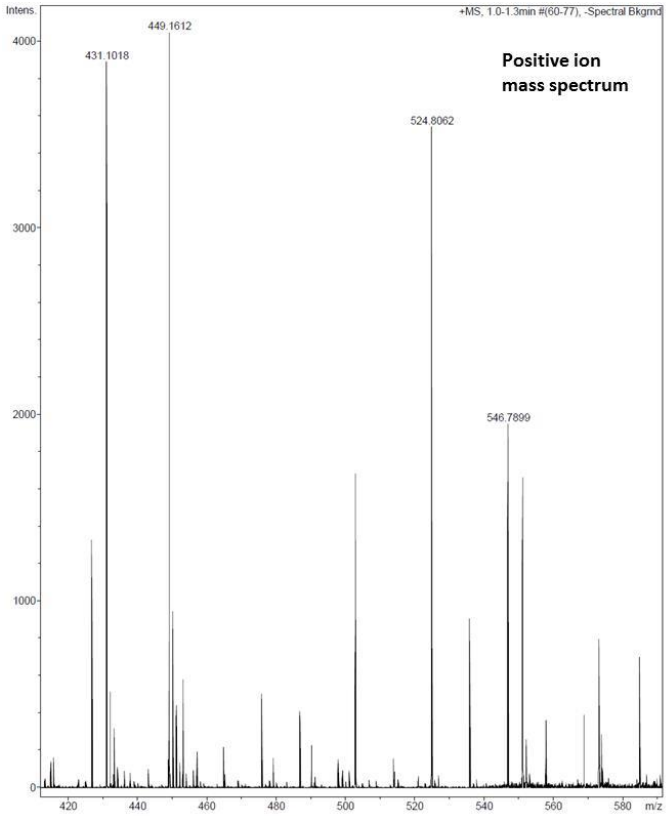

Mass spectrum of reaction containing glutathione (**2.21**), alkyl azide **3.3** and N-ethyl maleimide (**2.8**).

NMR experiment to determine the rate of triazoline formation with maleimide derivatives.

Either N-ethyl maleimide (**2.8**, 1 mM) or maleimide-PEG2kDa (1 mM) was dissolved in deuterated phosphate buffer (0.5 M, pH = 7.2, 1 mL) containing alkyl azide **3.3** (100 mM). The reaction was monitored by ^{1}H NMR spectroscopy at room temperature. The reaction was monitored through the consumption of maleimide (diminishing singlet representing the alkene protons) and the appearance of triazoline product (increasing doublets representing the bridgehead protons).

Synthesis of *1-(14-azido-3,6,9,12-tetraoxatetradecan-1-yl)-4-(benzenesulfonyl)-4,5-dihydro-1H-1,2,3-triazole* (**3.11**).

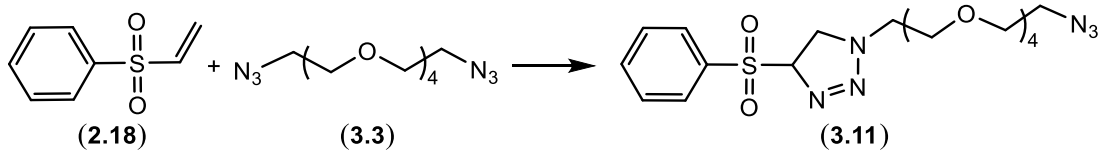

(**2.18**) (**3.3**) (**3.11**)

The alkyl azide **3.3** (0.11 g, 0.38 mmol) was dissolved in THF/H_2O (2:8, 10 mL). Phenyl vinyl sulfone (**2.18**, 2 eq., 0.128 g, 0.763 mmol) was added and the reaction was stirred at room temperature for 4 days. The reaction was concentrated and purified silica gel chromatography: 10 % EtOAc/petroleum ether $\rightarrow$ 60 % EtOAc/petroleum ether to yield **3.11** as a transparent oil (0.10 g, 59 %). ^{1}H NMR, $CDCl_3$, 400 MHz: δ 7.98-7.55 (m, 5H, Ar-*H*), 5.59 (dd, 1H, SC*H*CH_2, *J* = 7.6 & 13.0 Hz), 4.06 (dd, 1H, SCHC*H*H, *J* = 7.6 & 13.0 Hz), 3.80 (t, 2H, $CH_2C\underline{H_2}N_3$, *J* = 5.0 Hz), 3.71-3.62 (m, 17H, SCHCH*H* & 8 x C*H*$_2$), 3.37 (t, 2H, $CH_2NC\underline{H_2}$, *J* = 5.2 Hz). ^{13}C NMR, $CDCl_3$, 100 MHz: δ 136.21 (*ipso*-Ar-*C*), 134.36 (*para*-Ar-*C*), 129.60 (2 x *ortho*-Ar-*C*), 129.04 (2 x *meta*-Ar-*C*), 93.58 (S*C*HCH_2), 70.64, 70.58, 70.54, 70.47, 69.95, 69.65, 50.62 ($CH_2N\underline{C}H_2$), 49.61 ($OCH_2\underline{C}HHN_3$), 46.22 ($SCH\underline{C}H_2N$). ESI-HRMS: Expected for $C_{18}H_{29}N_6O_6S_1$ ($M+H^+$) = *m/z* 457.1864. Found: *m/z* 457.1907. Infrared (thin film): 2872, 2111, 1447 cm^{-1}. HPLC: column: Waters Symmetry Shield RP_8 (100 x 4.60 mm), gradient: (0.5 mL/min) 5 % MeCN in water $\rightarrow$ 100 % MeCN over 20 minutes, retention time, 14.59 mins., purity, 98.5 %). Detection at 280 nm.

Reaction of phenyl vinyl sulfone (**2.18**) with glutathione (**2.21**) in the presence of alkyl azide **3.3** to generate **3.12**.

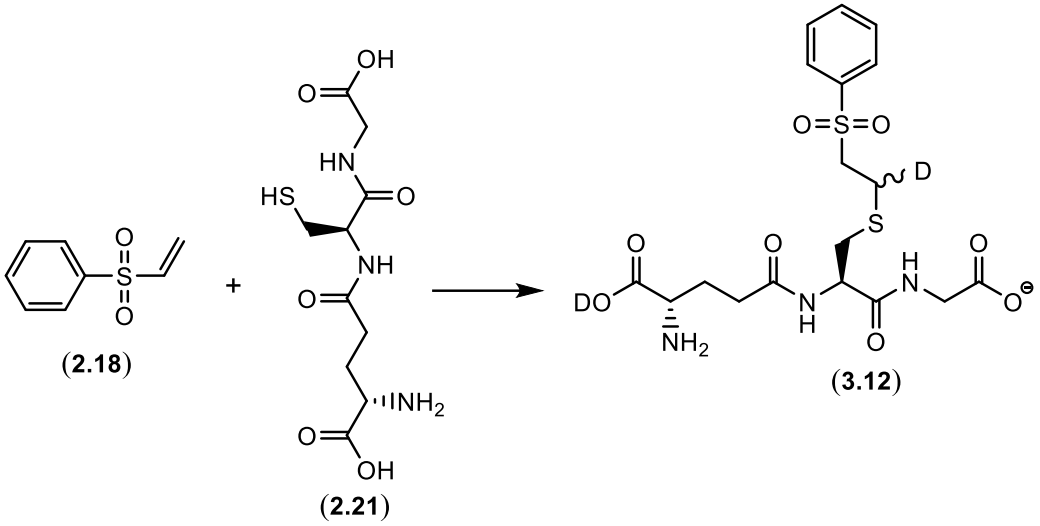

Reduced glutathione (**2.21**, 1 mM) was dissolved with alkyl azide **3.3** (50 mM) in deuterated aqueous phosphate (0.5 M, pH = 7.2, 1 mL), followed by the addition of phenyl vinyl sulfone (**2.18**, 1 mM). The reaction was monitored by ^{1}H NMR spectroscopy and HRMS. The ^{1}H NMR spectra showed disappearance of the peaks representing the vinyl protons, indicating an addition reaction, which was confirmed as **3.12** by HRMS (*m/z* 476.1143 (M-H^{+})). There was no evidence of triazoline formation in the NMR spectra or HRMS data.

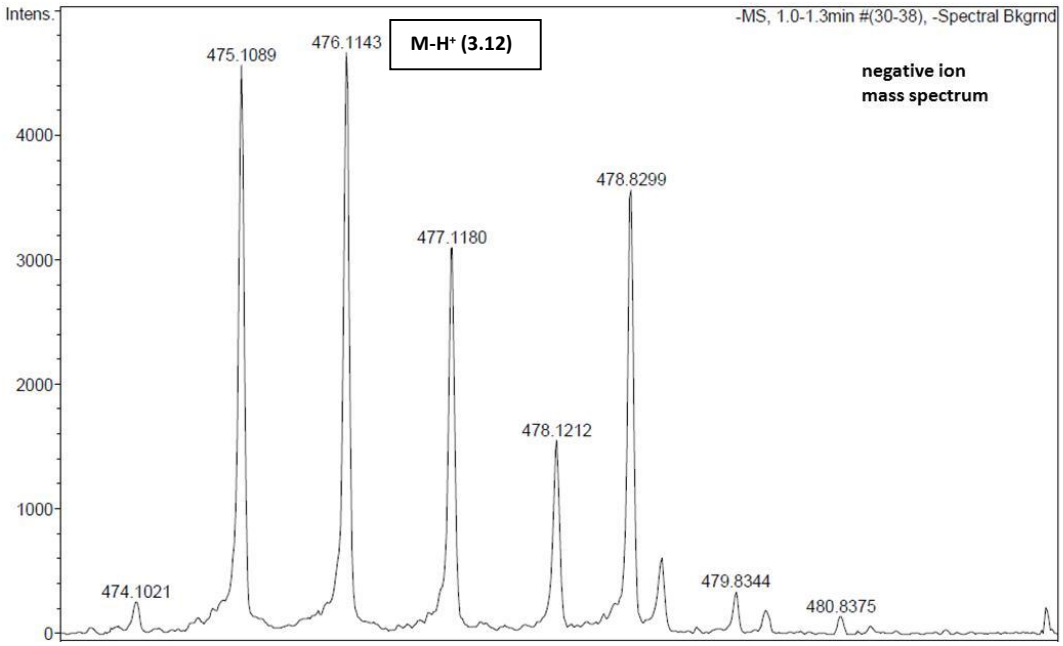

Mass spectrum of reaction containing glutathione (**2.21**), alkyl azide **3.3** and phenyl vinyl sulfone (**2.18**).

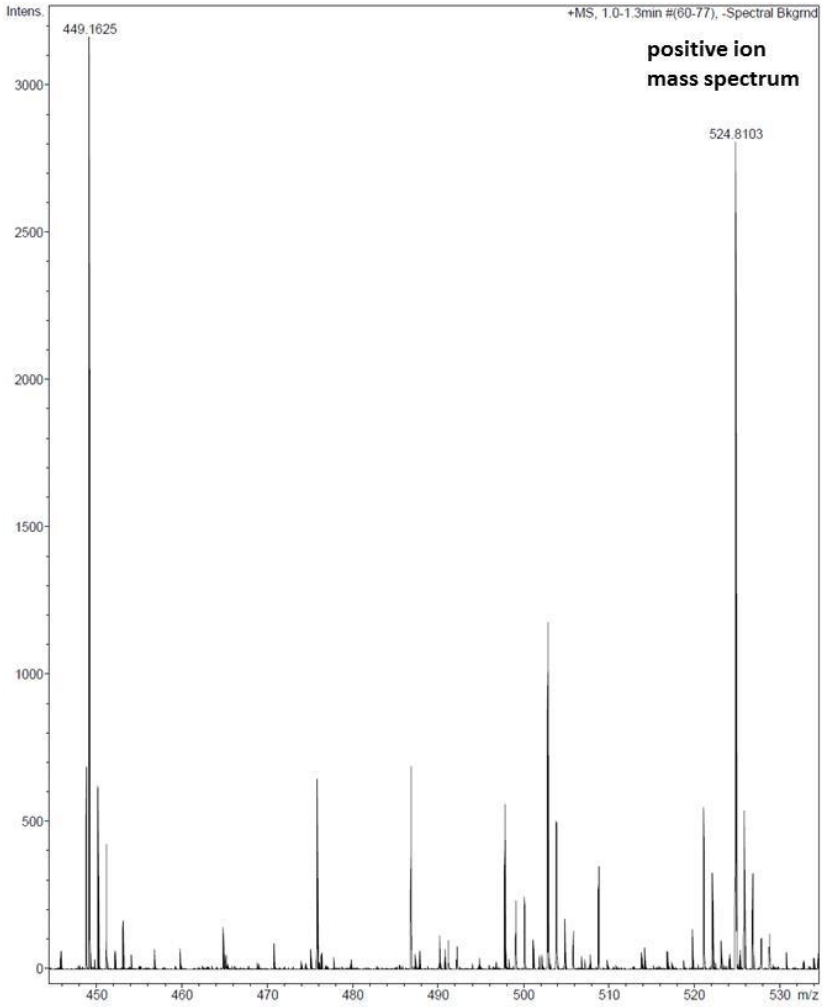

Mass spectrum of reaction containing glutathione (**2.21**), alkyl azide **3.3** and phenyl vinyl sulfone (**2.18**).

TCEP and THPP oxidation by the alkyl azide **3.3** in bioconjugation reactions.

TCEP (**2.6**, 10 mM) or THPP (**2.7**, 10 mM) were incubated with **3.3** (100 mM) in Tris buffer (0.5 M, pH = 7.2, 1 mL) at 37 °C. After 30 minutes aliquots of the reactions were diluted in water (~ 0.1 mg/mL) and analysed by HRMS.

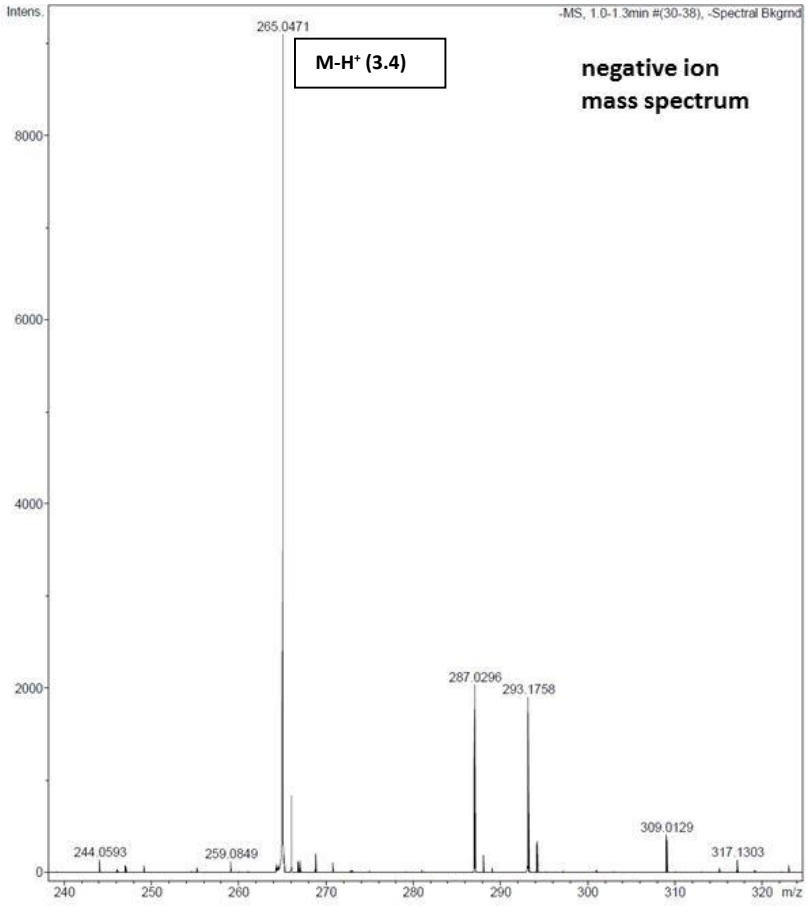

Mass spectrum of TCEP (**2.6**) incubated with the alkyl azide **3.3**.

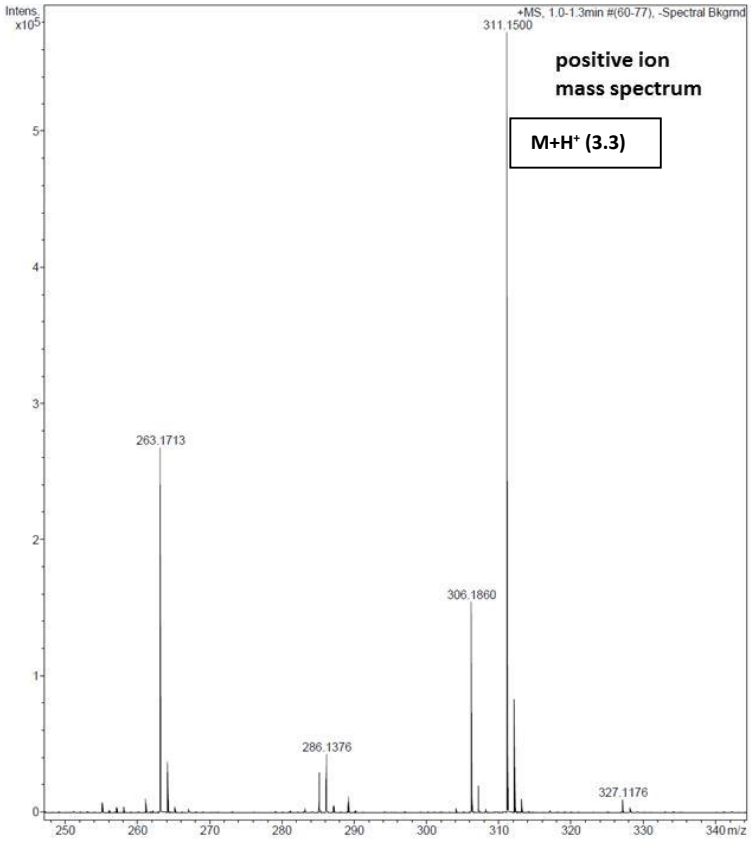

Mass spectrum of TCEP (**2.6**) incubated with the alkyl azide **3.3**.

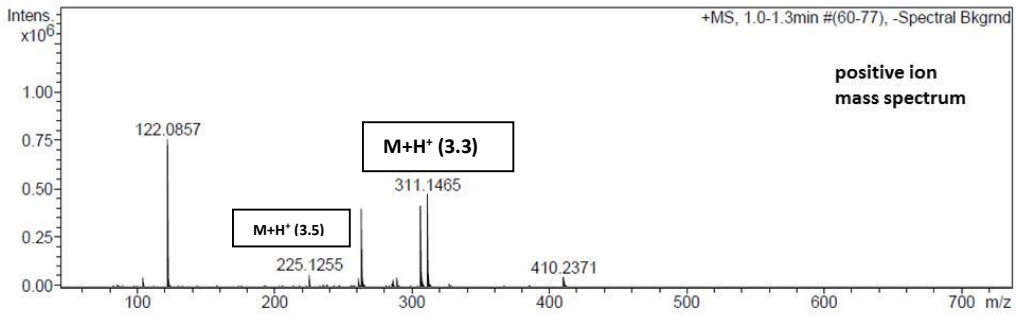

Mass spectrum of THPP (**2.7**) incubated with the alkyl azide **3.3**.

Use of alkyl azide **3.3** to oxidise excess TCEP or THPP to ensure high protein-maleimide-fluorescein conjugate yields.

1) Yeast enolase (1 mg/mL) was denatured in argon purged buffer (0.5 M Tris, pH = 7.2, 5 mM EDTA) containing 8 M urea at 85 °C for 15 minutes. The solution was allowed to cool to room temperature before aliquoting out 100 μL samples for the

experiments. Varying concentrations of TCEP or THPP (1-10 mM) were added to aliquots of protein solution (11 μM) and incubated for 45 minutes at 25 °C. Maleimide fluorescein (1 mM) was subsequently added to the reactions with no addition of **3.3** and incubated at 37 °C for 18 hours. Samples that had addition of **3.3** (100 mM) required pre-incubation for 1 hour at 37 °C. Maleimide- fluorescein (1 mM) was subsequently added to the reactions and incubated at 37 °C for 18 hours. Samples (15 μL) were taken from each of the reactions and added to Laemmli sample buffer (15 μL). Aliquots (9 μL) of these solutions were loaded into a precast gradient gel (4-12 % Bis-Tris, Invitrogen) along with a protein ladder (EZ-Run, Fisher Scientific) and resolved by SDS Page electrophoresis [MOPS running buffer (Invitrogen), 180 V, 60 mins]. The precast gels were stained by Coomassie solution and destained using a water/ethanol/acetic acid (16:3:1) solution.

2) Sbi was diluted to 1 mg/mL in buffer (0.5 M Tris, pH = 7.2, 5 mM EDTA), followed by aliquoting 100 μL samples for the experiments. Varying concentrations of TCEP or THPP (1-10 mM) were added to aliquots of protein solution (33 μM) and incubated for 45 minutes at 25 °C. Maleimide-fluorescein (1 mM) was subsequently added to the reactions with no addition of **3.3** and incubated at 37 °C for 18 hours. Samples that had addition of **3.3** (100 mM) required pre-incubation for 1 hour at 37 °C. Maleimide fluorescein (1 mM) was subsequently added to the reactions and incubated at 37 °C for 18 hours. Samples (15 μL) were taken from each of the reactions and added to Laemmli sample buffer (15 μL). Aliquots (9 μL) of these solutions were loaded into a precast gradient gel (4-12 % Bis-Tris, Invitrogen) along with a protein ladder (EZ-Run, Fisher Scientific) and resolved by SDS Page electrophoresis [MOPS running buffer (Invitrogen), 180 V, 60 mins]. The precast gels were stained by Coomassie solution and destained using a water/ethanol/acetic acid (16:3:1) solution.

Addition of the alkyl azide **3.3** to oxidise TCEP/THPP to ensure high yeast protein-PEG2kDa conjugate yields.

1) Yeast enolase (1 mg/mL) was denatured in argon purged buffer (0.5 M Tris, pH = 7.2, 5 mM EDTA) containing 8 M urea at 85 °C for 15 minutes. The solution was allowed to cool to room temperature before aliquoting out 100 μL samples for the experiments. Varying concentrations of TCEP or THPP (1-10 mM) were added to aliquots of protein solution (11 μM) and incubated for 45 minutes at 25 °C. Maleimide-PEG2kDa (1 mM) was subsequently added to the reactions with no addition of **3.3** and incubated at 37 °C for 18 hours. Samples that had addition of **3.3** (100 mM) required pre-incubation for 1 hour at 37 °C. Maleimide- PEG2kDa (1 mM) was subsequently added to the reactions and incubated at 37 °C for 18 hours. Samples (15 μL) were taken from each of the reactions and added to Laemmli sample buffer (15 μL). Aliquots (9 μL) of these solutions were loaded into a precast gradient gel (4-12 % Bis-Tris, Invitrogen) along with a protein ladder (EZ-Run, Fisher Scientific) and resolved by SDS Page electrophoresis [MOPS running buffer (Invitrogen), 180 V, 60 mins]. The precast gels were stained by Coomassie solution and destained using a water/ethanol/acetic acid (16:3:1) solution.

2) Sbi (1 mg/mL) in Tris buffer (0.5 M, pH = 7.2, 5 mM EDTA), was aliquoted into 100 μL samples for the experiments. Varying concentrations of TCEP or THPP (1-10 mM) were added to aliquots of protein solution (33 μM) and incubated for 45 minutes at 25 °C. Maleimide-PEG2kDa (1 mM) was subsequently added to the reactions with no addition of **3.3** and incubated at 37 °C for 18 hours. Samples that had addition of **3.3** (100 mM) required pre-incubation for 1 hour at 37 °C. Maleimide-PEG2kDa (1 mM) was subsequently added to the reactions and incubated at 37 °C for 18 hours. Samples (15 μL) were taken from each of the reactions and added to Laemmli sample buffer (15 μL). Aliquots (9 μL) of these solutions were loaded into a precast gradient gel (4-12 % Bis-Tris, Invitrogen) along with a protein ladder (EZ-Run, Fisher Scientific) and resolved by SDS Page electrophoresis [MOPS running buffer

(Invitrogen), 180 V, 60 mins]. The precast gels were stained by Coomassie solution and destained using a water/ethanol/acetic acid (16:3:1) solution.

Synthesis of 4-bromo-2-methylpyridine 1-oxide (**4.6**).

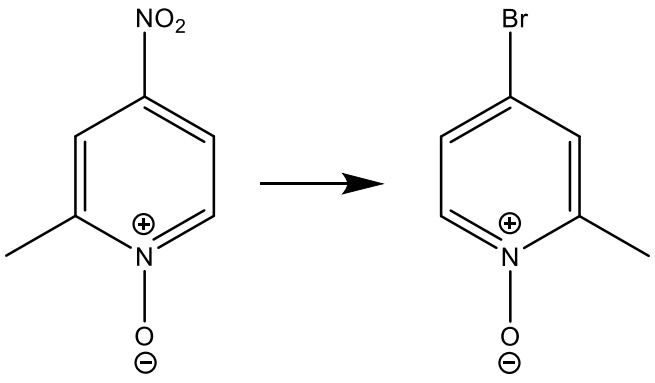

(**4.5**) (**4.6**)

2-Methyl-4-nitropyridine 1-oxide (**4.5**, 0.30 g, 1.95 mmol) was dissolved in 2 mL of acetic acid and heated to 55 °C. Acetyl bromide (20 eq., v = 2.9 mL, 39 mmol) was added and the reaction was refluxed at 120 °C for 3 hours. The reaction was allowed to cool and then poured onto ice cold saturated $NaHCO_3$ solution (100 mL) and stirred for 5 minutes. This solution was extracted with ethyl acetate (2 x 100 mL). The organic layer was dried over $MgSO_4$, filtered and concentrated. The residue was purified by silica gel chromatography: 10 % EtOAc/petroleum ether → 10 % MeOH/EtOAc to yield **4.6** as a yellow oil (216 mg, 59 %). Spectral data was consistent with that reported in the literature [145]. ^{1}H NMR, $CDCl_3$, 400 MHz: δ 8.08 (d, 1H, H-6, *J* = 6.9 Hz), 7.39 (d, 1H, H-3, *J* = 2.7 Hz), 7.25 (dd, 1H, H-5, *J* = 2.7 & 6.9 Hz), 2.47 (s, 3H, C*H*$_3$). ^{13}C NMR, $CDCl_3$, 100 MHz: δ 150.4 (C-2), 140.1 (C-6), 129.4 (C-3), 126.8 (C-5), 118.5 (C-4), 17.7 (*C*H$_3$). ESI-MS: Expected for $C_6H_7Br_1N_1O_1$ ($M+H^+$) = *m/z* 187.9706. Found: *m/z* 187.9717.

Synthesis of (4-bromopyridin-2-yl)methanol (**4.7**).

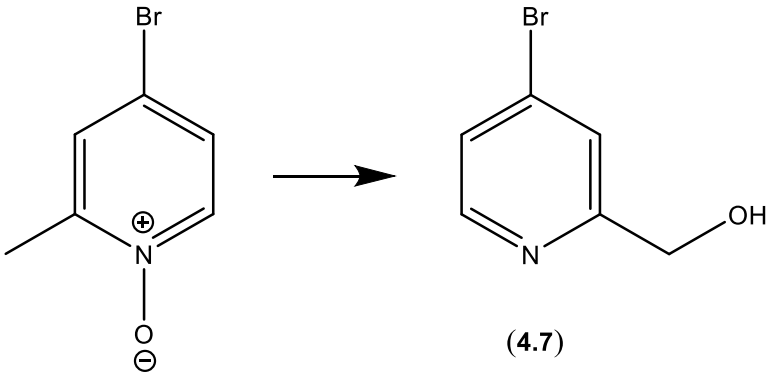

(**4.6**) (**4.7**)

4-Bromo-2-methylpyridine 1-oxide (**4.6**, 0.20 g, 1.06 mmol) was dissolved in anhydrous dichloromethane (10 mL) and cooled to 0 °C. Trifluoroacetic anhydride (5 eq., 5.3 mmol, v = 0.74 mL) was slowly added. The reaction was allowed to warm to room temperature then refluxed for 3 hours. The reaction was allowed to cool then concentrated. The crude was resuspended in 10 mL of dichloromethane and 2 M NaOH was added until pH = 12. The reaction was rapidly stirred for 2.5 hours then extracted with water. The organic layer was dried over $MgSO_4$, filtered and concentrated. The residue was purified by silica gel chromatography: 10 % EtOAc/petroleum ether $\rightarrow$ 100 % EtOAc to yield 154 mg **4.7** as a yellow oil (154 mg, 77 %). Spectral data was consistent with that reported in the literature [145] ^{1}H NMR, $CDCl_3$, 400 MHz: δ 8.35 (d, 1H, H-6, *J* = 5.3 Hz), 7.50 (d, 1H, H-3, *J* = 1.0 Hz), 7.38 (dd, 1H, H-5, *J* = 1.0 & 5.3 Hz), 4.74 (s, 2H, CC*H*$_2$OH), 3.68 (br. s, 1H, O*H*). ^{13}C NMR, $CDCl_3$, 100 MHz: δ 161.0 (C-2), 149.3 (C-6), 133.5 (C-4), 125.7 (C-3), 123.9 (C-5), 63.9 (C*C*H$_2$OH). ESI-MS: Expected for $C_6H_7Br_1N_1O_1$ (M+H$^+$) = *m/z* 187.9706. Found: *m/z* 187.9721.

Synthesis of (4-bromopyridin-2-yl)methyl acetate (**4.8**).

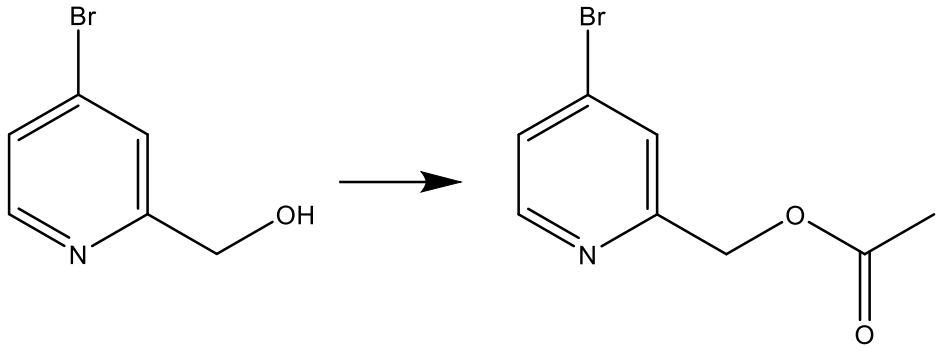

(**4.7**) (**4.8**)

(4-Bromopyridin-2-yl)methanol (**4.7**, 120 mg, 0.64 mmol) was dissolved in anhydrous pyridine (5 mL). Acetic anhydride (2 eq., 1.28 mmol, v = 0.12 mL) was added and the reaction was stirred at room temperature for 5 hours, while under N_2. The reaction was cooled to 0 °C and methanol (0.5 mL) was slowly added. The reaction was subsequently concentrated and co-evaporated with toluene (2 x 20 mL). The crude was purified by silica gel chromatography: 10 % EtOAc/petroleum ether $\rightarrow$ 50 % EtOAc to yield **4.8** as a slightly yellow oil (135 mg, 92 %). Compound is reported in the literature and is commercially available [193, 194]. ^{1}H NMR, $CDCl_3$, 400 MHz: δ 8.39 (s, 1H, H-6, *J* = 5.3 Hz), 7.52 (s, 1H, H-3), 7.40 (dd, 1H, H-5, *J* = 1.6 & 5.3 Hz), 5.19 (s, 2H, CC*H*$_2$O), 2.17 (s, 3H, OCOC*H*$_3$). ^{13}C NMR, $CDCl_3$, 100 MHz: δ 170.4 (O*C*OCH$_3$), 157.4 (C-2), 150.1 (C-6), 133.5 (C-4), 126.1 (C-3), 124.9 (C-5), 66.0 (C*C*H$_2$O), 20.8 (OCO*C*H$_3$). ESI-MS: Expected for $C_8H_9Br_1N_1O_2$ ($M+H^+$) = *m/z* 229.9811. Found: *m/z* 229.9802.

Synthesis of *(4-ethenylpyridin-2-yl)methyl acetate* (**4.1**).

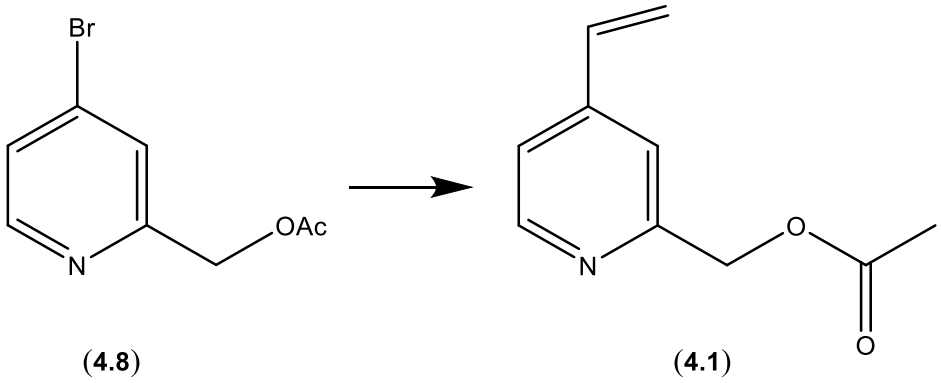

(**4.8**) (**4.1**)

(4-Bromopyridin-2-yl)methyl acetate (**4.8**, 80.0 mg, 0.35 mmol) was dissolved in 5 mL of deoxygenated toluene. Tetrakis(triphenylphosphine)palladium(0) (10 mol %, 40.2 mg, 0.035 mmol) and tributyl(vinyl)tin (2 eq., 0.20 mL, 0.70 mmol) was added. The reaction was refluxed under inert atmosphere for 1.5 hours then allowed to cool. The reaction was loaded directly onto a silica gel column containing 10 % (w/w) KF. The reaction was purified by silica gel chromatography: 5 % EtOAc/petroleum ether → 40 % EtOAc/petroleum ether to yield **4.1** as a yellow oil (50.5 mg, 82%). δ ^{1}H NMR, $CDCl_3$, 400 MHz: 8.53 (d, 1H, H-6, *J* = 5.1 Hz), 7.31 (s 1H, H-3), 7.21 (dd, 1H, H-5, *J* = 1.4 & 5.1 Hz), 6.68 (dd, 1H, CC*H*CH_2, *J* = 10.8 & 17.6 Hz), 6.00 (d, 1H, CCHC*H*H, *J* = 17.6 Hz), 5.50 (d, 1H, CCHCH*H*, *J* = 10.8 Hz), 5.21 (s, 2H, CC*H*$_2$O), 2.16 (s, 3H, OCOC*H*$_3$). ^{13}C NMR, $CDCl_3$, 100 MHz: δ 170.6 (O*C*OCH_3), 156.1 (C-2), 149.7 (C-6), 145.7 (C-4), 134.6 (C*C*HCH_2), 119.9 (CH*C*H_2), 119.0 (C-3 & C-5), 66.8 (C*C*H_2O), 20.8 (OCO*C*H_3). ESI-MS: Expected for $C_{10}H_{12}N_1O_2$ ($M+H^+$) = *m/z* 178.0863. Found: *m/z* 178.0861. Infrared (NaCl disc): 1744, 1608, 1238 cm^{-1}. HPLC: column: Waters Symmetry Shield RP_8 (100 x 4.60 mm), gradient: (0.5 mL/min) 5 % MeCN in water → 100 % MeCN over 20 minutes, retention time, 13.03 mins., purity, 89 %). Detection at 280 nm.

Synthesis of 4-bromo-2,6-dimethylpyridine 1-oxide (**4.10**).

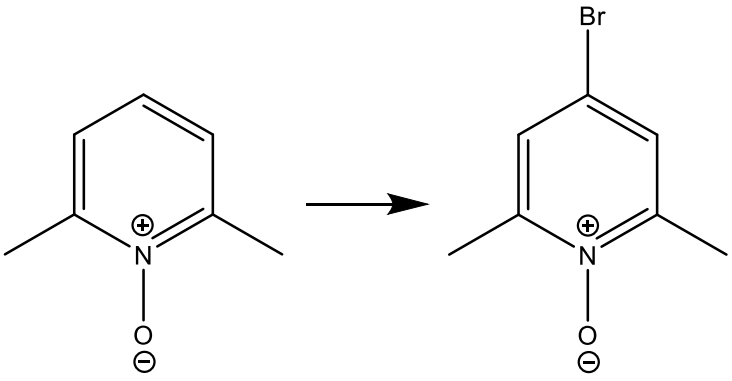

(**4.9**) (**4.10**)

2,6-Dimethylpyridine 1-oxide (**4.9**, 200 mg, 1.19 mmol) was dissolved in 2 mL of glacial acetic acid and cooled to 0 °C. Acetyl bromide (20 eq., 1.76 mL) was added and the reaction was refluxed for 3 hours. The reaction was allowed to cool and poured onto ice water. The reaction was neutralised with K_2CO_3 and extracted with dichloromethane (3 x 100 mL). The organic layer was dried over $MgSO_4$, filtered and concentrated. The residue was purified by silica gel chromatography: 10 % EtOAc/petroleum ether $\rightarrow$ 10 % MeOH/EtOAc to yield **4.10** as a light yellow solid (173 mg, 72 %). Commercially available [195]. ^{1}H NMR, $CDCl_3$, 400 MHz: δ 7.28 (s, 2H, H-3 & H-5), 2.48 (s, 6H,2 x CC*H*$_3$). ^{13}C NMR, $CDCl_3$, 100 MHz: δ 150.1 (C-2 & C-6), 126.9 (C-3 & C-5), 117.4 (C-4), 18.2 (2 x C*C*H$_3$). ESI-MS: Expected for $C_7H_8Br_1N_1Na_1O_1$ (M+Na$^+$) = *m/z* 223.9681. Found: *m/z* 223.9683.

Synthesis of (4-bromo-6-methylpyridin-2-yl)methanol (**4.11**).

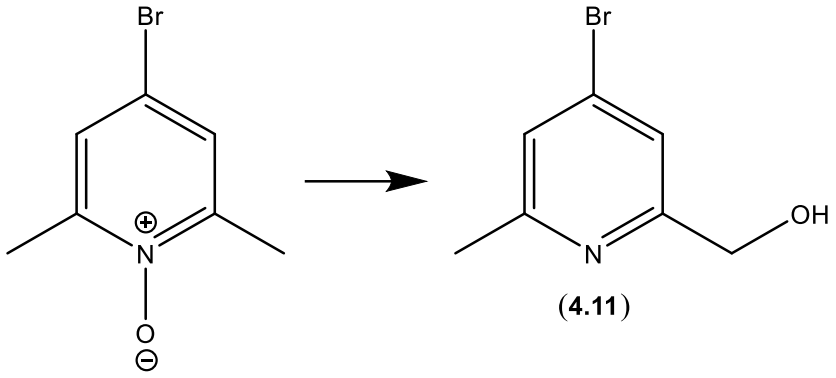

(**4.10**) (**4.11**)

4-Bromo-2,6-dimethylpyridine 1-oxide (**4.10**, 158 mg, 0.78 mmol) was dissolved in anhydrous dichloromethane and cooled to 0 °C. Trifluoroacetic anhydride (5 eq., 3.9 mmol, 0.55 mL) was slowly added. The reaction was allowed to warm to room temperature then refluxed for 3 hours. The reaction was allowed to cool then concentrated. The crude was resuspended in 10 mL of dichloromethane and 2 M NaOH was added until pH = 12. The reaction was rapidly stirred for 2.5 hours then extracted with water. The organic layer was dried over $MgSO_4$, filtered and concentrated. The residue was purified by silica gel chromatography: 10 % EtOAc/petroleum ether $\rightarrow$ 100 % EtOAc to yield **4.11** as a pale yellow solid (130 mg, 64 %). Commercially available [196] and spectral data consistent with that reported in the literature [197]. ^{1}H NMR, $CDCl_3$, 400 MHz: δ 7.27 (s, 1H, H-3), 7.22, (s, 1H, H-5), 4.74 (s, 2H, CC*H*$_2$OH), 2.49 (s, 3H, CC*H*$_3$). ^{13}C NMR, $CDCl_3$, 100 MHz: δ 160.2 (C-6), 158.8 (C-2), 133.6 (C-4), 125.0 (C-5), 120.8 (C-3), 63.8 (C*C*H$_2$OH), 23.8 (C*C*H$_3$). ESI-MS: Expected for $C_7H_8Br_1N_1Na_1O_1$ = *m/z* 223.9681. Found: *m/z* 223.9691. Melting point: 92 °C. Infrared (thin film): 3218, 1574, 1089 cm^{-1}. HPLC: column: Waters Symmetry Shield RP$_8$ (100 x 4.60 mm), gradient: (0.5 mL/min) 5 % MeCN in water $\rightarrow$ 100 % MeCN over 20 minutes, retention time, 12.02 mins., purity, 90.6 %. Detection at 280 nm.

Synthesis of *(4-bromo-6-methylpyridin-2-yl)methyl 4-methylbenzenesulfonate* (**4.12**).

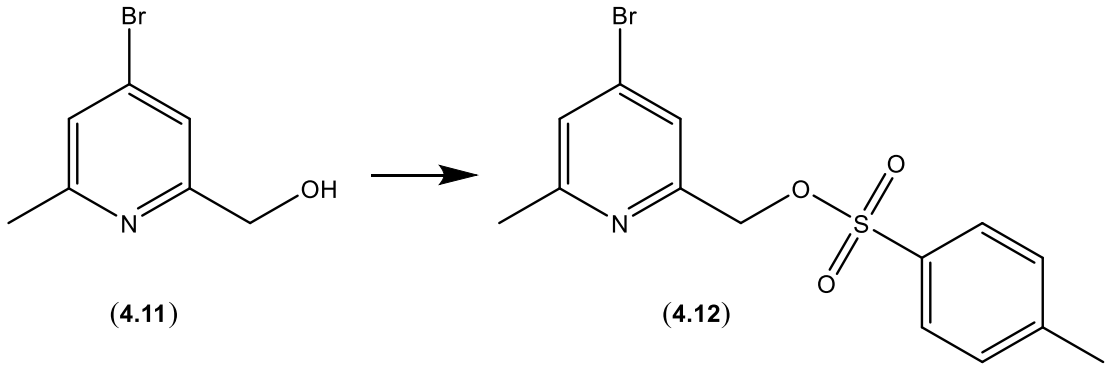

(**4.11**) (**4.12**)

(4-Bromopyridin-2-yl)methanol (**4.11**, 100 mg, 0.53 mmol) was dissolved in dry THF (10 mL) and cooled to 0 °C. Tosyl chloride (2 eq., 202.8 mg, 1.06 mmol) and 1 M NaOH (0.7 mL) was added and the reaction was rapidly stirred for 2 hours while being allowed to warm to room temperature. The reaction was concentrated, resuspended in 100 mL of dichloromethane and extracted with water and brine. The dichloromethane was dried over $MgSO_4$, filtered and concentrated. The residue was purified by silica gel chromatography: 10 % → 50 % EtOAc/petroleum ether to yield **4.12** as a white solid (171 mg, yield: 94 %). ^{1}H NMR, 400 MHz ($CDCl_3$): δ 7.79 (d, 2H, 2 x Ar-*H*, *J* = 8.3 Hz), 7.33 (m, 3H, 3 x Ar-*H*), 7.23 (s, 1H, 1 x Ar-*H*), 5.05 (s, 2H, CC*H*$_2$O), 2.43 (s, 3H, NCC*H*$_3$), 2.42 (s, 3H, CC*H*$_3$). ^{13}C NMR, 100 MHz ($CDCl_3$): δ 159.5 (pyridine-C-6), 154.4 (pyridine-C-2), 145.1 (tosyl-C-1), 133.7 (pyridine-C-4), 132.7 (pyridine-C-2), 129.9 (tosyl-C-3 & C-5), 128.0 (tosyl-C-2 & C-6), 125.9 (pyridine-C-5), 121.9 (pyridine-C-3), 70.9 (NC*C*H$_2$O), 23.9 (NC*C*H$_3$), 21.6 (tosyl C*C*H$_3$). ESI-MS: Expected for $C_{14}H_{14}Br_1N_1Na_1O_3S_1$ ($M+Na^+$) = *m/z* 377.9770 and 379.9750. Found: *m/z* 377.9779 and 379.9762. Melting point: 58 °C. Infrared (KBr): 3092, 1574, 1187 cm^{-1}. HPLC: column: Waters Symmetry Shield RP_8 (100 x 4.60 mm), gradient: (0.5 mL/min) 5 % MeCN in water → 100 % MeCN over 20 minutes, retention time, 17.65 mins., purity, 96.6 %. Detection at 280 nm.

Synthesis of *methyl 2-(((4-bromo-6-methylpyridin-2-yl)methyl)thio)acetate* (**4.13**).

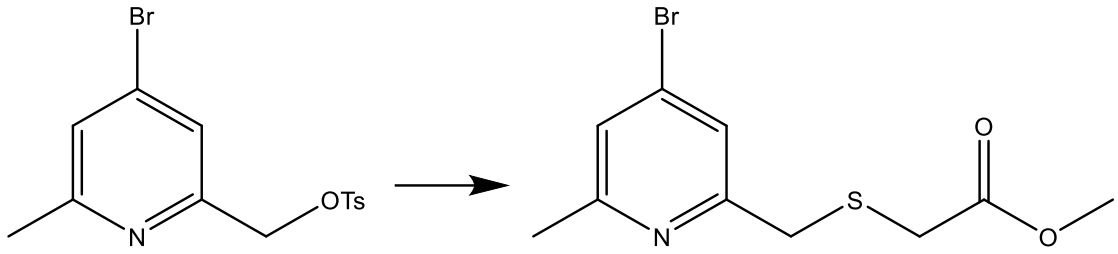

(**4.12**) (**4.13**)

(4-Bromo-6-methylpyridin-2-yl)methyl 4-methylbenzenesulfonate (**4.12**, 170 mg, 0.50 mmol) was dissolved in dry DMF (10 mL). Caesium carbonate (2 eq., 325.7 mg, 1.00 mmol) and methyl thioglycolate (5 eq., 2.50 mmol, 0.23 mL) were added and the reaction was stirred rapidly under nitrogen at room temperature for 3 hours. The reaction was concentrated, resuspended in dichloromethane and extracted with water and brine. The dichloromethane was dried over $MgSO_4$, filtered and concentrated. The residue was purified by silica gel chromatography: 10 % $\rightarrow$ 50 % EtOAc/petroleum ether to yield **4.13** as a yellow oil (99.4 mg, 72 %). ^{1}H NMR, 400 MHz ($CDCl_3$): δ 7.34 (d, 1H, H-5, *J* = 1.2 Hz), 7.21 (d, 1H, H-3, *J* = 1.2 Hz), 3.88 (s, 2H, NC$\underline{C}H_2$S), 3.70 (s, 3H, OC$\underline{H_3}$), 3.24 (s, 2H, SC$\underline{H_2}$CO), 2.50 (s, 3H, NCC$\underline{H_3}$). ^{13}C NMR, 100 MHz ($CDCl_3$): δ 170.4 ($CH_2\underline{C}O_2$), 159.6 (C-6), 158.4 (C-2), 133.3 (C-4), 124.9 (C-5), 123.3 (C-3), 52.3 (O$\underline{C}H_3$), 37.8 (S$\underline{C}H_2$CO), 32.8 (NC$\underline{C}H_2$), 24.2 (NC$\underline{C}H_3$). ESI-MS: Expected for $C_{10}H_{12}Br_1N_1Na_1O_2S_1$ ($M+Na^+$) = *m/z* 311.9664. Found: *m/z* 311.9674. Infrared (NaCl disc): 1740, 1573, 1283 cm^{-1}. HPLC: column: Waters Symmetry Shield RP_8 (100 x 4.60 mm), gradient: (0.5 mL/min) 5 % MeCN in water $\rightarrow$ 100 % MeCN over 20 minutes, retention time, 15.20 mins., purity, 89 %. Detection at 280 nm.

Synthesis of *methyl {[(4-ethenyl-6-methylpyridin-2-yl)methyl]sulfanyl}acetate* (**4.2**).

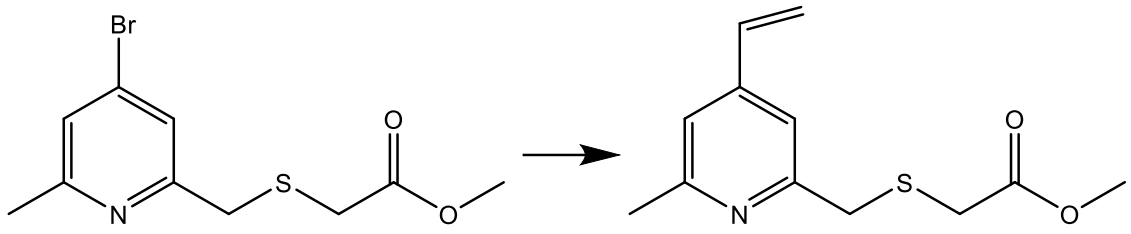

(**4.13**) (**4.2**)

Methyl 2-(((4-bromo-6-methylpyridin-2-yl)methyl)thio)acetate (**4.13**, 85 mg, 0.29 mmol) was dissolved in 10 mL of deoxygenated toluene. Tetrakis(triphenylphosphine)palladium(0) (10 mol %, 33.9 mg, 0.029 mmol) and tributyl(vinyl)tin (2 eq., 0.17 mL, 0.58 mmol) was added. The reaction was refluxed under inert atmosphere for 1 hour then allowed to cool. The reaction was loaded directly onto a silica gel column containing 10 % (w/w) KF. The reaction was purified by silica gel chromatography: 5 % EtOAc/petroleum ether → 40 % EtOAc/petroleum ether to yield **4.2** as a yellow oil (59.8 mg, 86 %). ^{1}H NMR, $CDCl_3$, 400 MHz: δ 7.14 (s, 1H, H-3), 7.00 (s, 1H, H-5), 6.61 (dd, 1H, CC*H*CH_2, *J* = 10.9 & 17.6 Hz), 5.94 (d, 1H, CCHC*H*H, *J* = 17.6 Hz), 5.44 (d, 1H, CCHCH*H*, *J* = 10.9 Hz), 3.90 (s, 2H, NCC*H*$_2$), 3.70 (s, 3H, OC*H*$_3$), 3.24 (s, 2H, SC*H*$_2$CO), 2.52 (s, 3H, NCC*H*$_3$). ^{13}C NMR, $CDCl_3$, 100 MHz: δ 170.6 (*C*O_2CH_3), 158.7 (C-6), 157.2 (C-2), 145.7 (C-4), 134.8 (C*C*HCH_2), 118.9 (C-5), 118.4 (CCH*C*H_2), 117.3 (C-3), 52.3 (O*C*H_3), 38.3 (NC*C*H_2), 32.9 (S*C*H_2CO), 24.3 (NC*C*H_3). ESI-MS: Expected for $C_{12}H_{16}N_1O_2S_1$ ($M+H^+$) = *m/z* 238.0896. Found: *m/z* 238.0914. Infrared (NaCl disc): 1737, 1601, 1283 cm^{-1}. HPLC: column: Waters Symmetry Shield RP_8 (100 x 4.60 mm), gradient: (0.5 mL/min) 5 % MeCN in water → 100 % MeCN over 20 minutes, retention time, 14.68 mins., purity, 98.48 %. Detection at 280 nm.

Synthesis of *methyl 3-(6-methylpyridin-2-yl)propanoate* (**4.16**).

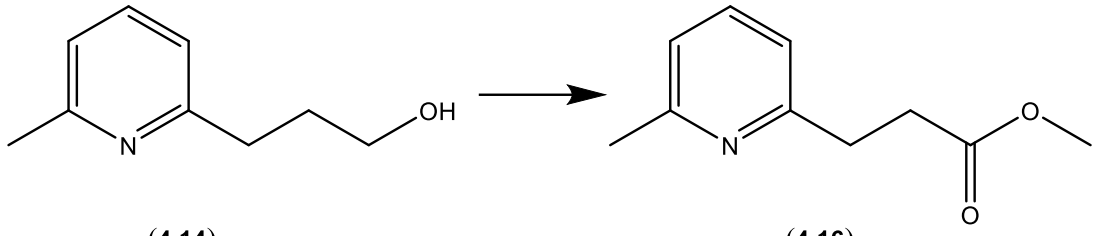

(**4.14**) (**4.16**)

3-(6-Methylpyridin-2-yl)propan-1-ol (**4.14**, 200 mg, 1.32 mmol, Ukrorgsyntez Ltd.) was suspended in 1 mL of CH_3CN. The solution was slowly added to a rapidly stirring solution of $RuCl_3$ (25 mg) and $NaIO_4$ (2.5 eq., 707.3 mg, 3.30 mmol) in a solution of CCl_4 (3 mL), CH_3CN (3 mL) and H_2O (4 mL). The reaction was sonicated for 2 minutes then left to rapidly stir for 2 hours. The reaction was diluted with CCl_4 and MeCN (1:1, 50 mL) and water (50 mL), filtered through celite and the solid washed with CH_3CN. The aqueous and organic layers were separated. The organic wash was filtered through celite and concentrated. The aqueous layer was concentrated to 10 mL then filtered through celite. The solution was then concentrated to dryness. This crude was added to the crude from the organic layer. The combined residue was dried on a high vacuum pump then resuspended in anhydrous MeOH (50 mL). Four drops of concentrated H_2SO_4 were carefully added and the reaction was refluxed overnight. The reaction was allowed to cool then neutralised by addition of solid K_2CO_3. The mixture was filtered and concentrated. The residue was purified by silica gel chromatography: 10 % EtOAc/petroleum ether $\rightarrow$ 50 % EtOAc/petroleum ether to yield **4.16** as a yellow oil (130 mg, 55 %). ^{1}H NMR, $CDCl_3$, 400 MHz: δ 7.43 (t, 1H, H-4, *J* = 7.6 Hz), 6.95 (m, dd 2H, H-3 & H-5, *J* = 1.5 & 7.6 Hz), 3.65 (s, 3H, OC*H*$_3$), 3.05 (t, 2H, NCC*H*$_2$, *J* = 7.6 Hz), 2.76 (t, 2H, CH_2C*H*$_2$CO, *J* = 6.5 Hz), 2.49 (s, 3H, NCC*H*$_3$). ^{13}C NMR, $CDCl_3$, 100 MHz: δ 173.5 ($\underline{C}O_2CH_3$), 159.3 (C-2), 157.8 (C-6), 136.6 (C-4), 120.8 (C-5), 119.7 (C-3), 51.5 (O$\underline{C}H_3$), 33.6 (NC$\underline{C}H_2$), 33.0 ($CH_2\underline{C}H_2CO$), 24.4 (NC$\underline{C}H_3$). ESI-MS: Expected for $C_{10}H_{13}N_1Na_1O_2$ ($M+Na^+$) = *m/z* 202.0838. Found: *m/z* 202.0851. Infrared (NaCl disc): 1744, 1460, 1163 cm^{-1}. HPLC: column: Waters Symmetry Shield RP_8 (100 x 4.60 mm), gradient: (0.5 mL/min) 5 % MeCN in water

→ 100 % MeCN over 20 minutes, retention time, 12.98 mins., purity, 93.4 %. Detection at 280 nm.

Synthesis of *2-(3-methoxy-3-oxopropyl)-6-methylpyridine 1-oxide* (**4.17**).

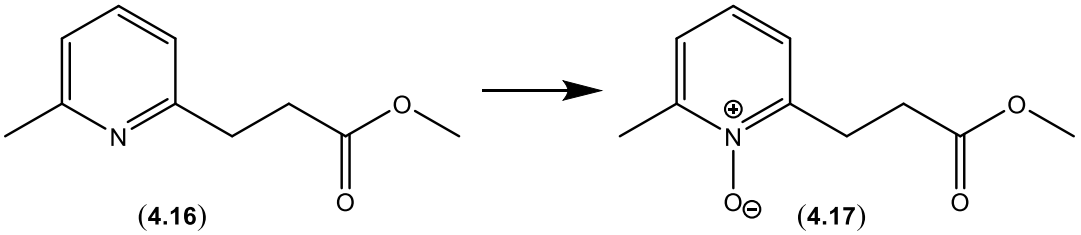

Methyl 3-(6-methylpyridin-2-yl)propanoate (**4.16**, 260 mg, 1.45 mmol) was dissolved in 10 mL of anhydrous dichloromethane. *m*-CPBA (1.5 eq., 375.5 mg, 2.90 mmol) was slowly added and reaction was stirred at room temperature for 4 hours. The reaction was neutralised with saturated Na_2SO_3. The solution was diluted with dichloromethane (100 mL), washed with water (50 mL) then 0.5 M NaOH solution (30 mL). The organic layer was dried over $MgSO_4$, filtered and concentrated. The residue was purified by silica gel chromatography: 1 → 10 % MeOH/DCM to yield **4.17** as a white solid (190 mg, 67 %). ^{1}H NMR, $CDCl_3$, 400 MHz: δ 7.12-7.00 (m, 3H, H-3, H-4 & H-5), 3.57 (s, 3H, OC*H*$_3$), 3.14 (t, 2H, NCC*H*$_2$, *J* = 7.1 Hz), 2.78 (t, 2H, CH_2C*H*$_2$CO, *J* = 7.1 Hz), 2.44 (s, 3H, NCC*H*$_3$). ^{13}C NMR, $CDCl_3$, 100 MHz: δ 173.0 (*C*O_2CH_3), 150.1 (C-2), 149.0 (C-6), 124.4 & 123.5 (C-3, C-4 & C-5), 51.5 (O*C*H_3), 30.0 (CH_2*C*H_2CO), 26.7 (NC*C*H_2), 18.0 (NC*C*H_3). ESI-MS: Expected for $C_{10}H_{14}N_1O_3$ ($M+H^+$) = *m/z* 196.0968. Found: *m/z* 196.1007. Melting point: 70 °C. Infrared (KBr): 1733, 1252, 1215 cm^{-1}. HPLC: column: Waters Symmetry Shield RP_8 (100 x 4.60 mm), gradient: (0.5 mL/min) 5 % MeCN in water → 100 % MeCN over 20 minutes, retention time, 9.11 mins., purity, 98.80 %. Detection at 280 nm.

Synthesis of *4-bromo-2-(3-methoxy-3-oxopropyl)-6-methylpyridine 1-oxide* (**4.18**).

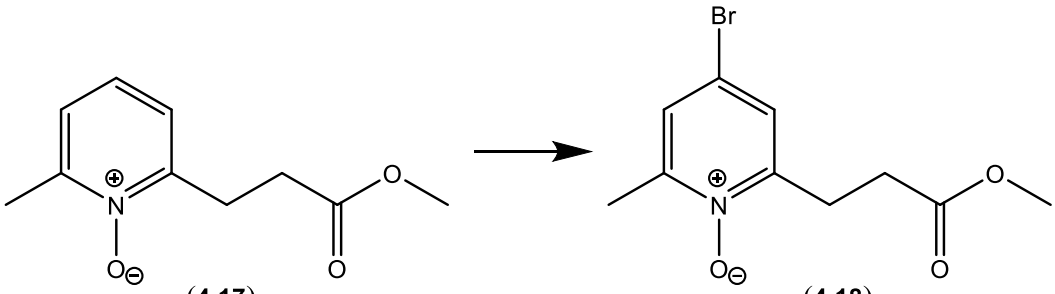

(**4.17**) (**4.18**)

2-(3-Methoxy-3-oxopropyl)-6-methylpyridine 1-oxide (**4.17**, 200 mg, 1.02 mmol) was dissolved in 1 mL of acetic acid. Br_2 (0.5 mL) was added and the reaction was refluxed for 12 hours. The reaction was allowed to cool. The reaction was neutralised with 4 M NaOH solution. The solution was then extracted three times with EtOAc. The organic layer was dried over $MgSO_4$, filtered and concentrated. The crude was purified by silica gel chromatography: 20 % EtOAc/petroleum ether $\rightarrow$ 10 % MeOH/EtOAc to yield **4.18** as a slightly yellow solid (146 mg, 52 %). ^{1}H NMR, $CDCl_3$, 400 MHz: δ 7.33 (d, 1H, H-3, *J* = 2.6 Hz), 7.31 (d, 1H, H-5, *J* = 2.6 Hz), 3.67 (s, 3H, OC*H*$_3$), 3.17 (t, 2H, NCC*H*$_2$, *J* = 7.0 Hz), 2.83 (t, 2H, CH_2C*H*$_2$CO, *J* = 7.0 Hz), 2.48 (s, 3H, NCC*H*$_3$). ^{13}C NMR, $CDCl_3$, 100 MHz: δ 172.8 (*C*O_2CH_3), 151.3 (C-2), 150.2 (C-6), 127.3 (C-3), 127.0 (C-5), 117.5 (C-4), 51.7 (O*C*H_3), 29.8 (CH_2*C*H_2CO), 26.8 (NC*C*H_2), 18.0 (NC*C*H_3). Melting point: 79 °C. Infrared (KBr): 1733, 1215 cm^{-1}. ESI-MS: Expected for $C_{10}H_{13}Br_1N_1O_3$ ($M+H^+$) = *m/z* 274.0074 & 276.0053. Found = *m/z* 274.0073 & 276.0082. HPLC: column: Waters Symmetry Shield RP_8 (100 x 4.60 mm), gradient: (0.5 mL/min) 5 % MeCN in water $\rightarrow$ 100 % MeCN over 20 minutes, retention time, 11.98 mins., purity, 99.9 %). Detection at 280 nm.

Synthesis of *methyl 3-(4-bromo-6-methylpyridin-2-yl)propanoate* (**4.19**).

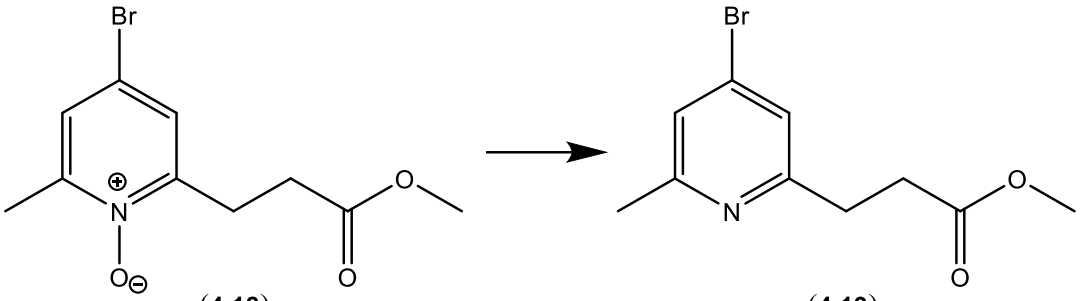

(**4.18**) (**4.19**)

4-Bromo-2-(3-methoxy-3-oxopropyl)-6-methylpyridine 1-oxide (**4.18**, 122 mg, 0.45 mmol) was dissolved in 5 mL of deoxygenated toluene and cooled to 0 °C while under N_2. PBr_3 (1.2 eq., 50 μL, 0.53 mmol) was slowly added. The reaction was allowed to warm to room temperature and stirred for 1 hour. The reaction was cooled to 0 °C and neutralised by addition of saturated $NaHCO_3$ solution. The solution was suspended in excess EtOAc and washed with saturated $NaHCO_3$ solution. The organic layer was dried over $MgSO_4$, filtered and concentrated. The crude was purified by silica gel chromatography: 10 % EtOAc/petroleum ether → 40 % EtOAc/petroleum ether to yield **4.19** as a transparent oil (100 mg, 87 %). ^{1}H NMR, $CDCl_3$, 400 MHz: δ 7.18 (s, 2H, H-3 & 5), 3.69 (s, 3H, OC*H*$_3$), 3.05 (t, 2H, NCC*H*$_2$, *J* = 7.4 Hz), 2.78 (t, 2H, CH_2C*H*$_2$CO, *J* = 7.4 Hz), 2.49 (s, 3H, NCC*H*$_3$). ^{13}C NMR, $CDCl_3$, 100 MHz: δ 173.2 (*C*O_2CH_3), 160.8 (C-2), 159.3 (C-6), 133.1 (C-4), 124.1 (C-5), 123.2 (C-3), 51.6 (O*C*H_3), 33.1 (NC*C*H_2), 32.7 (CH_2*C*H_2CO), 24.2 (NC*C*H_3). ESI-MS: Expected for $C_{10}H_{13}Br_1N_1O_2$ ($M+H^+$) = *m/z* 258.0124. Found: *m/z* 258.0131. Infrared (thin film): 1738, 1573, 1169 cm^{-1}. HPLC: column: Waters Symmetry Shield RP_8 (100 x 4.60 mm), gradient: (0.5 mL/min) 5 % MeCN in water → 100 % MeCN over 20 minutes, retention time, 12.23 mins., purity, 84.4 %).Detection at 280 nm.

Synthesis of *methyl 3-(4-ethenyl-6-methylpyridin-2-yl)propanoate* (**4.3**).

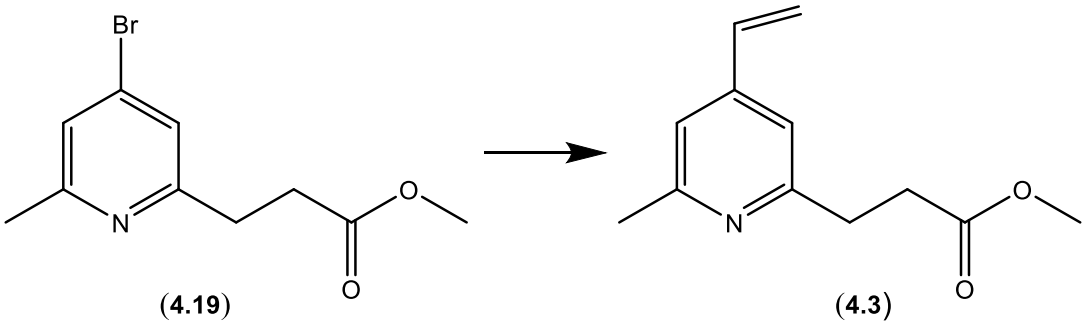

(**4.19**) (**4.3**)

Methyl 3-(4-bromo-6-methylpyridin-2-yl)propanoate (**4.19**, 100 mg, 0.39 mmol) was dissolved in 10 mL of deoxygenated toluene. Tetrakis(triphenylphosphine)palladium(0) (10 mol %, 44.8 mg, 0.039 mmol) and tributyl(vinyl)tin (2 eq., 0.23 mL, 0.78 mmol) was added. The reaction was refluxed under inert atmosphere for one hour then allowed to cool. The reaction was loaded directly onto a silica gel column containing 10 % (w/w) KF. The reaction was purified by silica gel chromatography: 5 % EtOAc/petroleum ether → 40 % EtOAc/petroleum ether to yield **4.3** as a transparent oil (68 mg, 86 %). ^{1}H NMR, $CDCl_3$, 400 MHz: δ 6.99 (s, 2H, H-3 & 5), 6.62 (dd, 1H, CC*H*CH_2, *J* = 10.8 & 17.6 Hz), 5.94 (dd, 1H, CCHC*H*H, *J* = 0.7 & 17.6 Hz), 5.44 (dd, 1H, CCHCH*H*, *J* = 0.7 & 10.8 Hz), 3.69 (s, 3H, OC*H*$_3$), 3.09 (t, 2H, NCC*H*$_2$, *J* = 7.5 Hz), 2.80 (t, 2H, CH_2C*H*$_2$CO, *J* = 17.7 Hz), 2.53 (s, 3H, NCC*H*$_3$). ^{13}C NMR, $CDCl_3$, 100 MHz: δ 173.5 (*C*O_2CH_3), 159.8 (C-2), 158.3 (C-6), 145.4 (C-4), 135.1 (C*C*HCH_2), 118.0 (CCH*C*H_2), 117.9 & 117.0 (C-3 & 5), 51.5 (O*C*H_3), 33.6 (NC*C*H_2), 33.0 (CH_2*C*H_2CO), 24.4 (NC*C*H_3). ESI-MS: Expected for $C_{12}H_{16}N_1O_2$ ($M+H^+$) = *m/z* 206.1176. Found: *m/z* 206.1183. Infrared (thin film): 1745, 1606, 1201 cm^{-1}. HPLC: column: Waters Symmetry Shield RP_8 (100 x 4.60 mm), gradient: (0.5 mL/min) 5 % MeCN in water → 100 % MeCN over 20 minutes, retention time, 14.89 mins., purity, 92.9 %. Detection at 280 nm.

Synthesis of *3-(6-methylpyridin-2-yl)propyl acetate* (**4.20**).

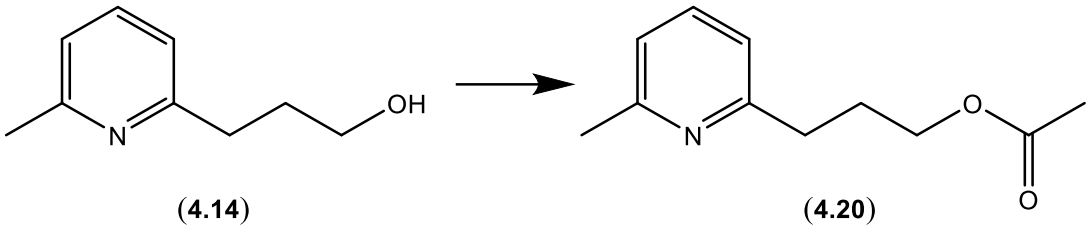

(**4.14**) (**4.20**)

3-(6-Methylpyridin-2-yl)propan-1-ol (**4.14**, 0.25 g, 1.65 mmol) was dissolved in anhydrous pyridine (10 mL). Acetic anhydride (2 eq., 3.31 mmol, 0.31 mL) was added and the reaction was stirred at room temperature for 6 hours, while under N_2. The reaction was cooled to 0 °C and methanol (1 mL) was slowly added. The reaction was subsequently concentrated and co-evaporated with toluene (2 x 20 mL). The crude was purified by silica gel chromatography: 10 % EtOAc/petroleum ether → 50 % EtOAc to yield **4.20** as a transparent oil (0.31 mg, 95 %). ^{1}H NMR, $CDCl_3$, 400 MHz: δ 7.46 (t, 1H, H-4, *J* = 7.6 Hz), 6.94 (m, 2H, H-3 & 5), 4.10 (t, 2H, $CH_2C\underline{H_2}O$, *J* = 6.6 Hz), 2.81 (t, 2H, $NCC\underline{H_2}$, *J* = 7.6 Hz), 2.51 (s, 3H, $NCC\underline{H_3}$), 2.05 (m, 5H, $CH_2C\underline{H_2}CH_2$ & $COC\underline{H_3}$). ^{13}C NMR, $CDCl_3$, 100 MHz: δ 171.16 ($O\underline{C}OCH_3$), 160.28 (C-2), 157.93 (C-6), 136.58 (C-4), 120.68 & 119.56 (C-3 & 5), 63.99 ($CH_2\underline{C}H_2O$), 34.74 ($NC\underline{C}H_2$), 28.74 ($CH_2\underline{C}H_2CH_2$), 24.52 ($NC\underline{C}H_3$), 20.97 ($OCO\underline{C}H_3$). ESI-MS: Expected for $C_{11}H_{15}N_1Na_1O_2$ ($M+Na^+$) = *m/z* 216.0995. Found: *m/z* 216.0994. Infrared (thin film): 1744, 1243 cm^{-1}. HPLC: column: Waters Symmetry Shield RP_8 (100 x 4.60 mm), gradient: (0.5 mL/min) 5 % MeCN in water → 100 % MeCN over 20 minutes, retention time, 13.91 mins., purity, 96.76 %. Detection at 280 nm.

Synthesis of *2-(3-acetoxypropyl)-6-methylpyridine 1-oxide* (**4.21**).

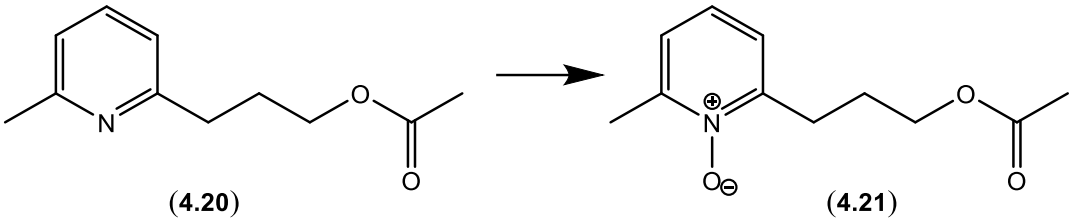

(**4.20**) (**4.21**)

3-(6-Methylpyridin-2-yl)propyl acetate (**4.20**, 369 mg, 1.47 mmol) was dissolved in 10 mL of dry dichloromethane. *m*-CPBA (1.5 eq., 380.6 mg, 2.21 mmol) was slowly added and reaction was stirred at room temperature for 4 hours. The reaction was neutralised with saturated Na_2SO_3. The solution was diluted with dichloromethane (100 mL), washed with water (50 mL), then 0.5 M NaOH solution (30 mL). The organic layer was dried over $MgSO_4$, filtered and concentrated. The residue was purified by silica gel chromatography: 1 $\rightarrow$ 10 % MeOH/DCM to yield **4.21** as a white solid (314 mg, 79 %). ^{1}H NMR, CD_3OD, 400 MHz: δ 7.50-7.45 (m, 3H, H-3, 4 & 5), 4.22 (t, 2H, $CH_2C\underline{H_2}O$, *J* = 6.3 Hz), 3.10 (dd, 2H, $NCC\underline{H_2}CH_2$, *J* = 6.2 & 7.7 Hz), 2.61 (s, 3H, $NCC\underline{H_3}$), 2.20-2.12 (m, 2H, $CH_2C\underline{H_2}CH_2$), 2.09 (s, 3H, $OCOC\underline{H_3}$). ^{13}C NMR, CD_3OD, 100 MHz: δ 170.9 ($O\underline{C}OCH_3$), 151.0 (C-2), 149.1 (C-6), 124.4 (C-4), 124.1 (C-5), 123.0 (C-3), 63.7 ($CH_2\underline{C}H_2O$), 27.9 ($NC\underline{C}H_2$), 25.0 ($CH_2\underline{C}H_2CH_2$), 20.8 ($OCO\underline{C}H_3$), 18.1 ($NC\underline{C}H_3$). ESI-MS: Expected for $C_{11}H_{16}N_1O_3$ ($M+H^+$) = *m/z* 210.1125. Found: *m/z* 210.1142. Melting point: 42 °C. Infrared (KBr): 1742, 1243 cm^{-1}. HPLC: column: Waters Symmetry Shield RP_8 (100 x 4.60 mm), gradient: (0.5 mL/min) 5 % MeCN in water $\rightarrow$ 100 % MeCN over 20 minutes, retention time, 10.24 mins., purity, 95.8 %. Detection at 280 nm.

Synthesis of *2-(3-acetoxypropyl)-4-bromo-6-methylpyridine 1-oxide* (**4.22**).

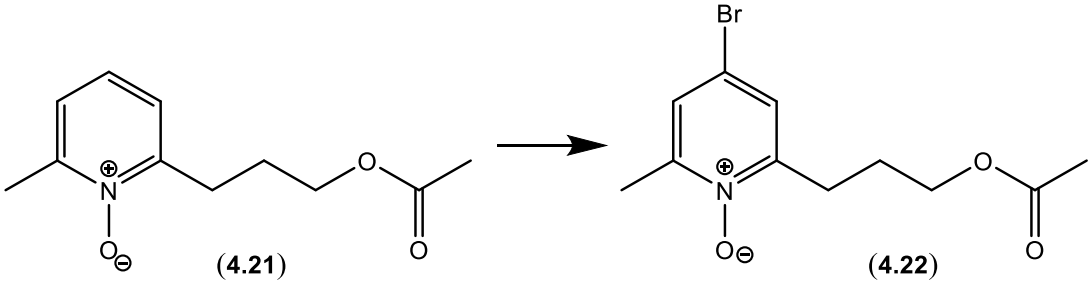

(**4.21**) (**4.22**)

2-(3-Acetoxypropyl)-6-methylpyridine 1-oxide (**4.21**, 436 mg, 2.08 mmol) was dissolved in 2 mL of acetic acid. Br_2 (0.5 mL) was added and the reaction was refluxed for 12 hours. The reaction was allowed to cool. The reaction was neutralised with cold saturated $NaHCO_3$ solution. The solution was then extracted three times with EtOAc. The organic layer was dried over $MgSO_4$, filtered and concentrated. The crude was purified by silica gel chromatography: 20 % EtOAc/petroleum ether → 10 % MeOH/EtOAc to yield **4.22** as a white solid (317.6 mg, 56 %). ^{1}H NMR, CD_3OD, 400 MHz: δ 7.72 (d, 1H, Ar-*H*, *J* = 2.8 Hz), 7.69 (d, 1H, Ar-*H*, *J* = 2.8 Hz), 4.21 (t, 2H, CH_2CH_2O, *J* = 6.2 Hz), 3.06 (t, 2H, $NCCH_2$, *J* = 7.4 Hz), 2.57 s, 3H, $NCCH_3$), 2.15 (m, 2H, $CH_2CH_2CH_2$), 2.10 (s, 3H, $COCH_3$). ^{13}C NMR, CD_3OD, 100 MHz: δ 172.8 ($OCOCH_3$), 154.4 (C-2), 152.3 (C-6), 122.4 (C-4), 64.9 (CH_2CH_2O), 29.0 ($NCCH_2$), 26.4 ($CH_2CH_2CH_2$), 20.8 ($OCOCH_3$), 18.1 ($NCCH_3$). ESI-MS: Expected for $C_{11}H_{14}Br_1N_1O_3$ ($M+Na^+$) = *m/z* 310.0055 & 312.0029. Found: *m/z* 310.0084 & 312.0065. Melting point: 52 °C. Infrared (KBr): 3069, 1728, 1037 cm^{-1}. HPLC: column: Waters Symmetry Shield RP_8 (100 x 4.60 mm), gradient: (0.5 mL/min) 5 % MeCN in water → 100 % MeCN over 20 minutes, retention time, 12.53 mins., purity, 99.8 %. Detection at 280 nm.

Synthesis of *3-(4-bromo-6-methylpyridin-2-yl)propyl acetate* (**4.23**).

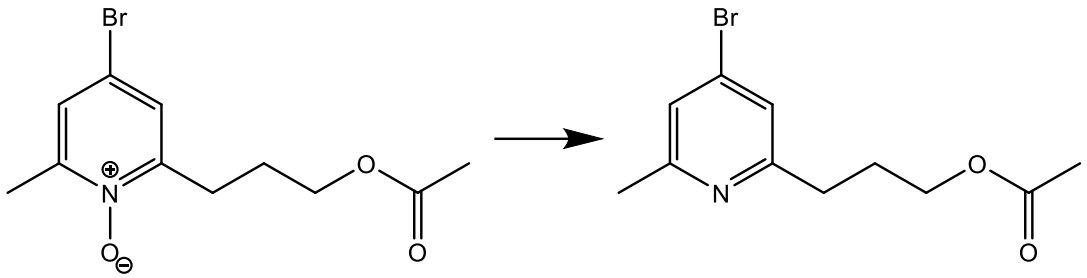

(**4.22**) (**4.23**)

2-(3-Acetoxypropyl)-4-bromo-6-methylpyridine 1-oxide (**4.22**, 200 mg, 0.69 mmol) was dissolved in 5 mL of deoxygenated toluene and cooled to 0 °C while under N_2. PBr_3 (1.2 eq., 79 μL, 0.83 mmol) was slowly added. The reaction was allowed to warm to room temperature and stirred for 1 hour. The reaction was cooled to 0 °C and neutralised by addition of saturated $NaHCO_3$ solution. The solution was suspended in excess EtOAc and washed with saturated $NaHCO_3$ solution. The organic layer was dried over $MgSO_4$, filtered and concentrated. The residue was purified by silica gel chromatography: 10 % EtOAc/petroleum ether → 50 % EtOAc/petroleum ether to yield **4.23** as a light yellow oil (160.6 mg, 85 %). ^{1}H NMR, $CDCl_3$, 400 MHz: δ 7.16 (d, 1H, Ar-*H*, *J* = 1.3 Hz), 7.13 (d, 1H, Ar-*H*, *J* = 1.3 Hz), 4.10 (t, 2H, CH_2CH_2O, *J* = 6.5 Hz), 2.78 (t, 2H, $NCCH_2$, *J* = 7.6 Hz), 2.48 (s, 3H, $NCCH_3$), 2.07-2.00 (m, 5H, $CH_2CH_2CH_2$ & $COCH_3$). ^{13}C NMR, $CDCl_3$, 100 MHz: δ 171.1 ($OCOCH_3$), 161.7 (C-2), 159.3 (C-6), 133.1 (C-4), 123.9 (C-5), 122.9 (C-3), 63.7 (CH_2CH_2O), 34.4 ($NCCH_2$), 28.4 ($CH_2CH_2CH_2$), 24.2 ($NCCH_3$), 20.9 ($OCOCH_3$). ESI-MS: Expected for $C_{11}H_{14}Br_1N_1Na_1O_2$ ($M+Na^+$) = *m/z* 294.0100. Found: *m/z* 294.0108. Infrared (thin film): 1742, 1567, 1042 cm^{-1}. HPLC: column: Waters Symmetry Shield RP_8 (100 x 4.60 mm), gradient: (0.5 mL/min) 5 % MeCN in water → 100 % MeCN over 20 minutes, retention time, 15.49 mins., purity, 93.4 %. Detection at 280 nm.

Synthesis of *3-(4-bromo-6-methylpyridin-2-yl)propan-1-ol* (**4.24**).

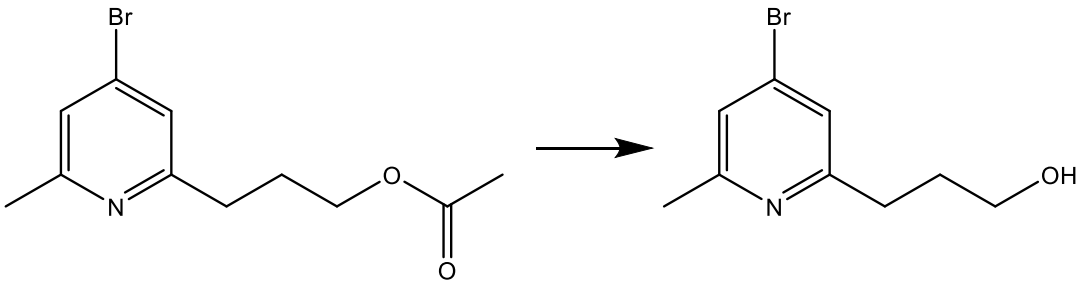

(**4.23**) (**4.24**)

3-(4-Bromo-6-methylpyridin-2-yl)propyl acetate (**4.23**, 382 mg, 1.4 mmol) was dissolved in 10 mL of anhydrous methanol. A 0.5 M solution of sodium methoxide (1.5 eq., 4 mL) was slowly added and the reaction was stirred under N_2 for 1 hour, monitoring by TLC. The reaction was neutralised with 1 M HCl solution and concentrated. The residue was purified by silica gel chromatography: 1 $\rightarrow$ 10 % MeOH/DCM to yield **4.24** as a white solid (304 mg, 94 %). ^{1}H NMR, CD_3OD, 400 MHz: δ 7.40 (s, 2H, H 3 & H-5), 3.65 (t, 2H, $CH_2C\underline{H_2}OH$, *J* = 6.4 Hz), 2.86 (t, 2H, $NCC\underline{H_2}$, *J* = 7.7 Hz), 2.55 (s, 3H, $NCC\underline{H_3}$), 1.96 (ddd, 2H, $CH_2C\underline{H_2}CH_2$, *J* = 6.5, 7.0 & 15.2 Hz). δ ^{13}C NMR, CD_3OD, 100 MHz: 164.1 (C-2), 160.6 (C-6), 135.1 (C-4), 125.4 (C-5), 124.7 (C-3), 62.2 ($CH_2\underline{C}H_2OH$), 35.1 9 ($CH_2\underline{C}H_2CH_2$), 33.7 ($NC\underline{C}H_2$), 23.7 ($NC\underline{C}H_3$). ESI-MS: Expected for $C_9H_{13}Br_1N_1O_1$ ($M+H^+$) = *m/z* 230.0175. Found: *m/z* 230.0166. Melting point: 39 °C. Infrared (KBr): 3302, 1570 cm^{-1}. HPLC: column: Waters Symmetry Shield RP_8 (100 x 4.60 mm), gradient: (0.5 mL/min) 5 % MeCN in water $\rightarrow$ 100 % MeCN over 20 minutes, retention time, 12.99 mins., purity, 97.7 %. Detection at 280 nm.

Synthesis of *ethyl 3-(3-(4-bromo-6-methylpyridin-2-yl)propoxy)propanoate* (**4.25**).

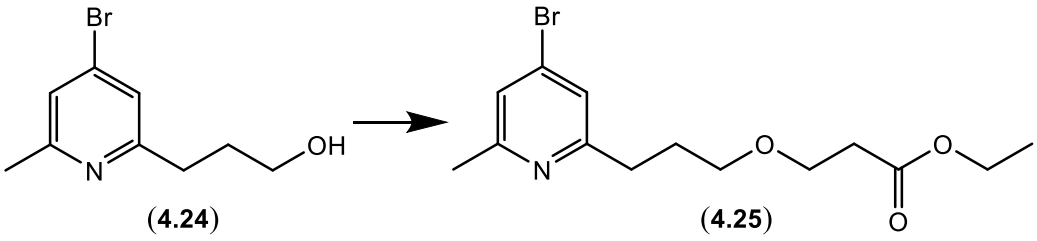

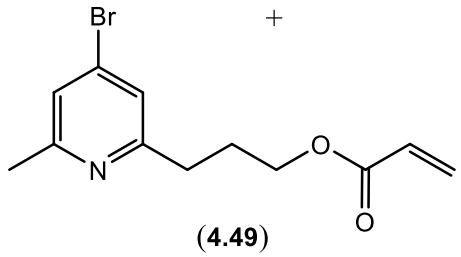

3-(4-Bromo-6-methylpyridin-2-yl)propan-1-ol (**4.24**, 293 mg, 1.27 mmol) was added to 20 µL of Triton B (40 % in methanol) and subsequently co-evaporated with toluene (2 x 20 mL). The mixture was then dried under vacuum for 1 hour. The round bottom flask was then cooled to 0 °C and cold ethyl acrylate (0.5 mL) was slowly added. The reaction was allowed to warm to room temperature and left to stir for 4 days. The reaction was loaded directly onto a silica gel column and purified: 100 % DCM → 10 % MeOH/DCM, which yielded **4.25** as transparent oil (143 mg, 34 %). ^{1}H NMR, $CDCl_3$, 400 MHz: δ 7.13 (s, 2H, H-3 & H-5), 4.15 (q, 2H, OC*H*$_2$$CH_3$, *J* = 7.2 & 14.3 Hz), 3.68 (t, 2H, OC*H*$_2$$CH_2$, *J* = 6.4 Hz), 3.46 (t, 2H, CH_2C*H*$_2$O, *J* = 6.4 Hz), 2.76 (t, 2H, NCC*H*$_2$, *J* = 7.5 Hz), 2.54 (t, 2H, CH_2C*H*$_2$CO, *J* = 6.4 Hz), 2.47 (s, 3H, NCC*H*$_3$), 1.94 (m, 2H, CH_2C*H*$_2$$CH_2$), 1.25 (t, 3H, OCH_2C*H*$_3$, *J* = 7.2 Hz). ^{13}C NMR, $CDCl_3$, 100 MHz: δ 171.5 (*C*O_2CH_2), 162.5 (C-2), 159.2 (C-6), 133.0 (C-4), 123.6 (C-5), 122.9 (C-3), 70.0 (CH_2*C*H_2O), 66.1 (CO_2*C*H_2), 60.4 (O*C*H_2CH_2), 35.1 (NC*C*H_2), 34.4 (*C*H_2CO_2), 29.4 (CH_2*C*H_2CH_2), 24.2 (NC*C*H_3), 14.2 (OCH_2*C*H_3). ESI-MS: Expected for $C_{14}H_{20}Br_1N_1Na_1O_3$ ($M+Na^+$) = *m/z* 352.0519. Found: *m/z* 352.0539. Infrared (thin film): 1742, 1569, 1187 cm^{-1}. HPLC: column: Waters Symmetry Shield RP_8 (100 x

4.60 mm), gradient: (0.5 mL/min) 5 % MeCN in water → 100 % MeCN over 20 minutes, retention time, 16.37 mins., purity, 93.4 %. Detection at 280 nm.

The compound **4.49** was also isolated as a transparent oil (65.1 mg, 18 %): ^{1}H NMR, $CDCl_3$, 400 MHz: δ 7.17 (s, 1H, H-5), 7.15 (s, 1H, H-3), 6.39 (dd, 1H, COCHC*H*H, *J* = 1.3 & 17.3 Hz), 6.11 (dd, 1H, COC*H*CH_2, *J* = 10.4 & 17.3 Hz), 5.82 (dd, 1H, COCHCH*H*, *J* = 1.3 & 10.4 Hz), 4.21 (t, 2H, $CH_2C\underline{H_2}O$, *J* = 6.4 Hz), 2.82 (t, 2H, NCC*H*$_2$, *J* = 7.4 Hz), 2.50 (s, 3H, NCC*H*$_3$), 2.10 (m, 2H, $CH_2C\underline{H_2}CH_2$). ^{13}C NMR, $CDCl_3$, 100 MHz: δ 166.2 (O*C*OCH), 161.7 (C-2), 159.4 (C-6), 133.2 (C-4), 130.7 (COCH*C*H_2), 128.4 (CO*C*HCH_2), 124.0 (C-5), 123.0 (C-3), 63.9 ($CH_2\underline{C}H_2O$), 34.5 (NC*C*H_2), 28.5 ($CH_2\underline{C}H_2CH_2$), 24.2 (NC*C*H_3). Infrared (thin film): 1726, 1567, 1194 cm^{-1}. HPLC: column: Waters Symmetry Shield RP_8 (100 x 4.60 mm), gradient: (0.5 mL/min) 5 % MeCN in water → 100 % MeCN over 20 minutes, retention time, 16.35 mins., purity, 97.6 %. Detection at 280 nm.

Synthesis of *ethyl 3-[3-(4-ethenyl-6-methylpyridin-2-yl)propoxy]propanoate* (**4.4**).

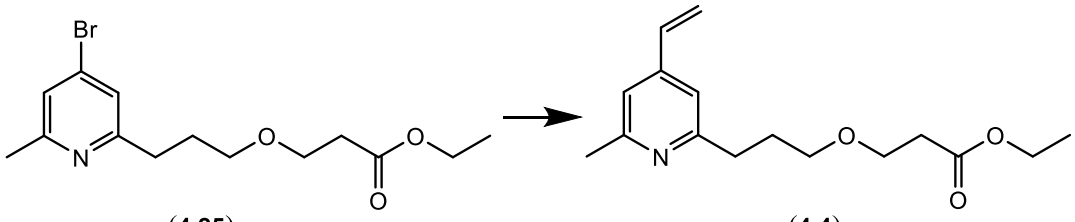

(**4.25**) (**4.4**)

Ethyl 3-(3-(4-bromo-6-methylpyridin-2-yl)propoxy)propanoate (**4.25**, 250 mg, 0.76 mmol) was dissolved in 10 mL of deoxygenated toluene. Tetrakis(triphenylphosphine)palladium(0) (10 mol %, 87.5 mg, 0.076 mmol) and tributyl(vinyl)tin (2 eq., 0.44 mL, 1.52 mmol) was added. The reaction was refluxed under inert atmosphere (N_2) for 1.5 hours then allowed to cool. The reaction was loaded directly onto a silica gel column containing 10 % (w/w) KF. The reaction was purified by silica gel chromatography: 5 % EtOAc/petroleum ether → 50 % EtOAc/petroleum ether to yield **4.4** as a transparent oil (157 mg, 75 %). ^{1}H NMR,

$CDCl_3$, 400 MHz: δ 6.95 (s, 2H, H-3 & H-5), 6.60 (dd, 1H, CC*H*CH_2, *J* = 10.9 & 17.6 Hz), 5.92 (dd, 1H, CCHC*H*H, *J* = 0.7 & 17.6 Hz), 5.42 (dd, 1H, CCHCH*H*, *J* = 0.7 & 10.9 Hz), 4.16 (q, 2H, OC*H*$_2$$CH_3$, *J* = 7.2 Hz), 3.70 (t, 2H, OC*H*$_2$$CH_2CO$, *J* = 6.4 Hz), 3.48 (t, 2H, CH_2C*H*$_2$O, *J* = 6.4 Hz), 2.79 (dd, 2H, NCC*H*$_2$, *J* = 7.6 & 9.2 Hz), 2.56 (t, 2H, OCH_2C*H*$_2$CO, *J* = 6.4 Hz), 2.51 (s, 3H, NCC*H*$_3$), 2.00 (m, 2H, CH_2C*H*$_2$$CH_2$O), 1.26 (t, 3H, OCH_2C*H*$_3$, *J* = 7.2 Hz). ^{13}C NMR, $CDCl_3$, 100 MHz: δ 171.7 (*C*O_2CH_2), 161.4 (C-2), 158.1 (C-6), 145.4 (C-4), 135.2 (C*C*HCH_2), 117.9 (CCH*C*H_2), 117.8, 117.0 (C-3 & 5), 70.3 (CH_2*C*H_2O), 66.1 (O*C*H_2CH_2CO), 60.4 (O*C*H_2CH_3), 35.2 (CH_2*C*H_2CO), 34.7 (NC*C*H_2), 29.8 (CH_2*C*H_2CH_2), 24.3 (NC*C*H_3), 14.2 (OCH_2*C*H_3). ESI-MS: Expected for $C_{16}H_{24}N_1O_3$ ($M+H^+$) = *m/z* 278.1751. Found: *m/z* 278.1827. Infrared (thin film): 1737, 1192 cm^{-1}. HPLC: column: Waters Symmetry Shield RP_8 (100 x 4.60 mm), gradient: (0.5 mL/min) 5 % MeCN in water $\rightarrow$ 100 % MeCN over 20 minutes, retention time, 16.83 mins., purity, 87 %. Detection at 280 nm.

Experimental determination of the pKa of the pyridine ring for compounds **4.1-4.4**.

The 4-VP derivatives **4.1**-**4.4** (4-10 mg) were dissolved in DMSO (100 µL) and deionised water (900 µL). The solution was sonicated for 30 s then adjusted to pH < 3 by addition of dilute HCl solution (5 mM) at 25 °C. The pH was accurately recorded. The solution was subsequently titrated against a dilute NaOH solution (5 mM). The pH of the solution was recorded with the incremental addition of the basic solution. This data was subsequently plotted as pH vs volume of base added. The end point of the titration (pH >10) was accurately recorded for the start of the reverse titration. The solution was titrated against a dilute HCl solution (5 mM). The pH of the solution was recorded along with the incremental addition of the acidic solution. This data was subsequently plotted as pH vs volume of acid added. The pKa of the 4-VP analogues were determined by the intersection point between the two co-plotted titration curves.

Synthesis of *γ-L-glutamyl-S-(2-{2-[(acetyloxy)methyl]pyridin-4-yl}ethyl)-L-cysteinylglycine* (**4.26**).

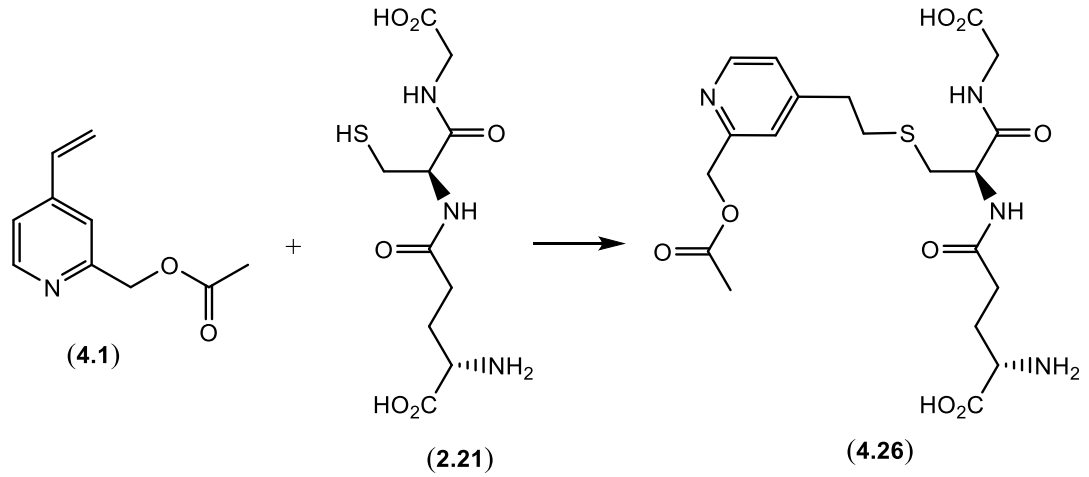

(4-Ethenylpyridin-2-yl)methyl acetate (**4.1**, 10.0 mg, 0.0564 mmol) was dissolved in a solution of THF (1 mL) and aqueous sodium phosphate (0.1 M, pH = 7, 5 mL). Glutathione (**2.21**, 0.9 eq., 15.6 mg, 0.0508 mmol) was added and the reaction was rapidly stirred at room temperature for 3 hours. The reaction was subsequently purified by C-18 chromatography (100 % $H_2O \rightarrow$ 40 % MeCN/H_2O) which yielded the product **4.26** as a sticky solid (19.9 mg, 81 %). ^{1}H NMR, D_2O, 400 MHz: δ 8.36 (d, 1H, H-6, *J* = 5.2 Hz), 7.37 (s, 1H, H-3), 7.29 (dd, 1H, H-5, *J* = 1.3 & 5.2 Hz), 5.14 (s, 2H, NCC*H*$_2$), 4.47 (dd, 1H, NHC*H*CO, *J* = 5.1 & 8.9 Hz), 3.68 (m, 3H, NHC*H*$_2$$CO_2H$ & CH_2C*H*NH_2), 3.00-2.74 (m, 6H, CC*H*$_2$$CH_2S$, CCH_2C*H*$_2$S, SC*H*$_2$CH), 2.43 (t, 2H, COC*H*$_2$$CH_2$, *J* = 8.0 Hz), 2.11 (s, 3H, OCOC*H*$_3$), 2.05 (m, 2H, CH_2C*H*$_2$CH, *J* = 6.9 Hz). ^{13}C NMR, D_2O, 100 MHz: δ 176.1, 174.8, 173.9, 173.8, 171.9 (5 x CO), 154.1 (C-2), 152.7 (C-4), 148.0 (C-6), 124.3 (C-5), 123.2 (C-3), 66.2 (C*C*H_2O), 54.1 (CH_2*C*HCO_2H), 53.0 (NH*C*HCO), 43.3 (NH*C*H_2CO_2H), 34.1, 32.8, 31.43, 31.39, 26.2 (CH_2*C*H_2CHCO_2H), 20.3 (OCO*C*H_3). ESI-MS: Expected for $C_{20}H_{27}N_4O_8S_1$ ($M\text{-}H^+$). = *m/z* 483.1555. Found: *m/z* 483.1566. Infrared (KBr): 3340, 1744, 1591 cm^{-1}.

Synthesis of *γ-L-glutamyl-S-[2-(2-{[(2-methoxy-2-oxoethyl)sulfanyl]methyl}-6-methylpyridin-4-yl)ethyl]-L-cysteinylglycine* (**4.27**).

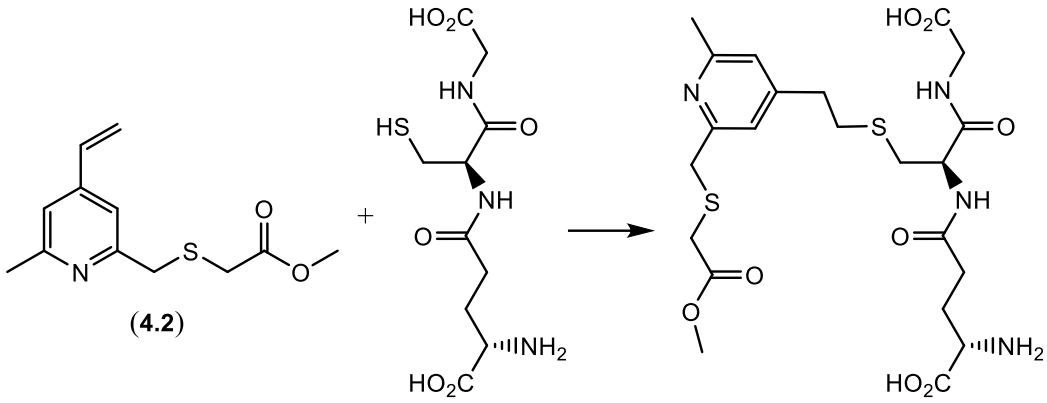

(**4.2**) (**2.21**) (**4.27**)

Methyl {[(4-ethenyl-6-methylpyridin-2-yl)methyl]sulfanyl}acetate (**4.2**, 10.0 mg, 0.0421 mmol) was dissolved in a solution of THF (1 mL) and aqueous sodium phosphate (0.1 M, pH = 7, 5 mL). Glutathione (**2.21**, 0.9 eq., 11.7 mg, 0.0379 mmol) was added and the reaction was rapidly stirred at room temperature for 3 hours. The reaction was subsequently purified by C-18 chromatography (100 % $H_2O \rightarrow$ 40 % MeCN/H_2O) which yielded the product **4.27** as a pale yellow sticky solid (17.8 mg, 86 %). ^{1}H NMR, 500 MHz (D_2O): δ 7.01 (s, 1H, H-3), 7.00 (s, 1H, H-5), 4.45 (dd, 1H, NHC*H*CO, *J* = 5.0 & 8.7 Hz), 3.73 (s, 2H, NCC*H*$_2$S), 3.70-3.61 (m, 3H, CH_2CHNH_2 & NHC*H*$_2$$CO_2H$), 3.47 (s, 3H, CO_2CH_3), 3.23 (s, 2H, SC*H*$_2$CO), 2.96 (dd, 1H, SC*H*HCHNH, *J* = 4.9 & 14.2 Hz), 2.80-2.72 (m, 5H, CC*H*$_2$$CH_2S$, $CH_2CH_2SCH_2$ & SCH*H*CHNH), 2.49 (t, 2H, COC*H*$_2$$CH_2$, *J* = 7.5 Hz), 2.45 (s, 3H, NCC*H*$_3$), 2.11 (m, 2H, $CH_2CH_2CHNH_2$). ^{13}C NMR, 125 MHz (D_2O): δ 176.1, 174.9, 174.3, 173.2 & 171.8 (5 x CO), 158.3 (C-2), 156.1 (C-6), 151.7 (C-4), 122.9 (C-5), 121.5 (C-3), 54.1 (CH_2CHNH_2), 53.0 (NH*C*HCO), 52.9 (CO_2CH_3), 33.9, 32.9, 31.5, 31.4, 26.4 ($CH_2CH_2CHNH_2$), 22.6 (NC*C*H_3). ESI-MS: Expected for $C_{22}H_{31}N_4O_8S_2$ (M-H$^+$). = *m/z* 543.1589. Found: *m/z* 543.1628. Infrared (KBr): 3321, 1734, 1607 cm^{-1}. HPLC: column: Phenomenex Luna-C18 (250 x 4.60

mm), gradient: (0.7 mL/min) 5 % MeCN/H_2O → 90 % MeCN/H_2O over 20 minutes, retention time, 12.65 mins., purity, 96.8 %. Detection at 280 nm.

Synthesis of *γ-L-glutamyl-S-{2-[2-(3-methoxy-3-oxopropyl)-6-methylpyridin-4-yl]ethyl}-L-cysteinylglycine* (**4.28**).

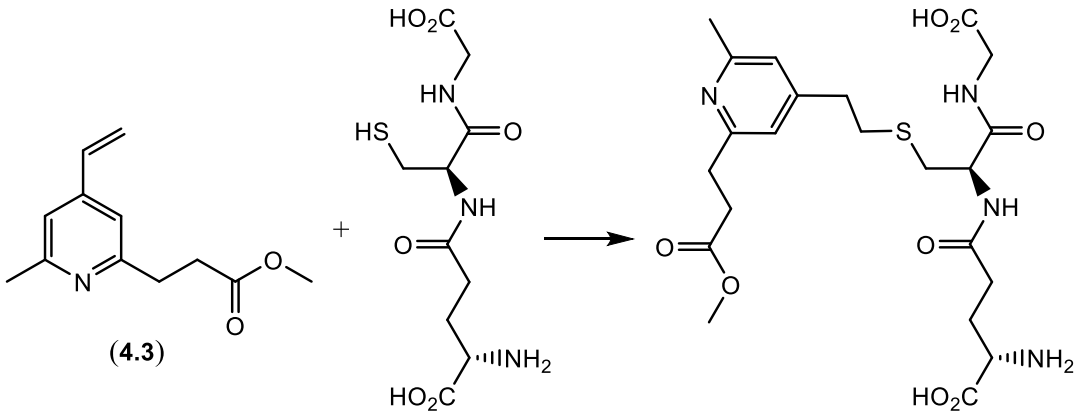

Methyl 3-(4-ethenyl-6-methylpyridin-2-yl)propanoate (**4.3**, 10.0 mg, 0.0487 mmol) was dissolved in a solution of THF (1 mL) and aqueous sodium phosphate (0.1 M, pH = 7, 5 mL). Glutathione (**2.21**, 0.9 eq., 13.5 mg, 0.0438 mmol) was added and the reaction was rapidly stirred at room temperature for 3 hours. The reaction was subsequently purified by C-18 chromatography (100 % H_2O → 40 % MeCN/H_2O) which yielded the product **4.28** as a transparent sticky solid (20 mg, 89 %). ^{1}H NMR, 400 MHz (D_2O): δ 7.60 (s, 2H, H-3 & H-5), 4.62 (dd, 1H, NHC*H*CO, *J* = 5.1 & 8.5 Hz), 3.82 (m, 3H, $CH_2C\underline{H}NH_2$ & NHC$\underline{H_2}CO_2H$), 3.73 (s, 3H, $CO_2C\underline{H_3}$), 3.30 (t, 2H, NCC$\underline{H_2}CH_2$, *J* = 7.2 Hz), 3.19-3.09 (m, 3H, CC$\underline{H_2}CH_2S$ & SC*H*HCHNH), 3.04-2.90 (m, 5H, $CH_2C\underline{H_2}CO_2CH_3$, $CH_2C\underline{H_2}SCH_2$ & SCH*H*CHNH), 2.73 (s, 3H, NCC$\underline{H_3}$), 2.58 (t, 2H, COC$\underline{H_2}CH_2CHNH_2$, *J* = 7.3 Hz), 2.20 (m, 2H, $CH_2C\underline{H_2}CHNH_2$). ^{13}C NMR, 100 MHz ($D_2O$): δ 176.1, 174.9, 174.5, 173.9, 171.8 (5 x CO), 160.6 (C-4), 154.3 (C-2), 153.4 (C-6), 125.4 (C-5), 123.8 (C-3), 54.2 ($CH_2\underline{C}HNH_2$), 53.1 (NH*C*HCO), 52.5 ($CO_2\underline{C}H_3$), 43.4 (NH$\underline{C}H_2CO_2H$), 34.7 (C$\underline{C}H_2CH_2S$), 32.9 (S$\underline{C}H_2CHNH$), 32.4 ($CH_2\underline{C}H_2CO_2CH_3$), 31.5 (CO$\underline{C}H_2CH_2CHNH_2$), 30.9 ($CH_2\underline{C}H_2SCH_2$), 28.0 (C$\underline{C}H_2CH_2CO$), 26.3 ($CH_2\underline{C}H_2CHNH_2$), 19.0 (NC$\underline{C}H_3$). ESI-MS: Expected for $C_{22}H_{31}N_4O_8S_1$ (M-H$^+$) = *m/z* 511.1868 Found:

m/z 511.1882. Infrared (KBr): 3299, 1732, 1610, 1419 cm^{-1}. HPLC: column: Phenomenex Luna-C18 (250 x 4.60 mm), gradient: (0.7 mL/min) 5 % MeCN/H_2O → 90 % MeCN/H_2O over 20 minutes, retention time, 12.53 mins., purity, 99.0 %. Detection at 280 nm.

Synthesis of *γ-L-glutamyl-S-(2-{2-[3-(3-ethoxy-3-oxopropoxy)propyl]-6-methylpyridin-4-yl}ethyl)-L-cysteinylglycine* (**4.29**).

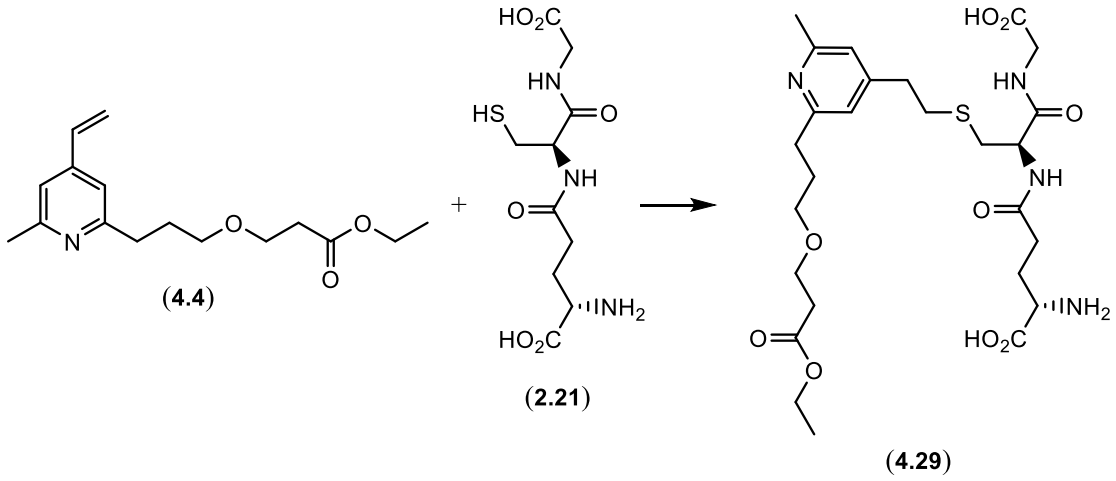

Ethyl 3-[3-(4-ethenyl-6-methylpyridin-2-yl)propoxy]propanoate (**4.4**, 10.0 mg, 0.0361 mmol) was dissolved in a solution of THF (1 mL) and aqueous sodium phosphate (0.1 M, pH = 7, 5 mL). Glutathione (**2.21**, 0.9 eq., 10.0 mg, 0.0324 mmol) was added and the reaction was rapidly stirred at room temperature for 3 hours. The reaction was subsequently purified by C-18 chromatography (100 % H_2O → 40 % MeCN/H_2O) which yielded the product **4.29** as a transparent sticky solid (16.2 mg, 85 %). ^{1}H NMR, 400 MHz (D_2O): δ 7.42 (s, 2H, H-3 & H-5), 4.54 (dd, 1H, NHC*H*CO, *J* = 5.1 & 8.6 Hz), 4.14 (q, 2H, $CO_2C\underline{H_2}CH_3$, *J* = 7.1 Hz), 3.74-3.65 (m, 5H, $OC\underline{H_2}CH_2CO_2$, $CH_2C\underline{H}NH_2$ & $NHC\underline{H_2}CO_2H$), 3.53 (t, 2H, $CH_2C\underline{H_2}OCH_2$, *J* = 6.1 Hz), 3.07-3.01 (m, 3H, $CC\underline{H_2}CH_2S$ & $SC\underline{H}HCHNH$), 2.97-2.81 (m, 5H, $NCC\underline{H_2}CH_2$, $CH_2C\underline{H_2}SCH_2$ & $SCH\underline{H}CHNH$), 2.61 (s, 3H, $NCC\underline{H_3}$), 2.56 (t, 2H, $CH_2C\underline{H_2}CO_2$, *J* = 5.9 Hz), 2.49 (t, 2H, $SC\underline{H_2}CHNH$, *J* = 7.4 Hz), 2.12 (m, 2H, $CH_2C\underline{H_2}CHNH_2$), 1.99 (m, 2H, $CCH_2C\underline{H_2}CH_2$), 1.22 (t, 3H, $OCH_2C\underline{H_3}$, *J* = 4.2 Hz). ^{13}C NMR, 100 MHz (D_2O): δ 176.1, 174.9, 174.4, 173.9, 171.8

(5 x CO), 159.0 (C-4), 156.6 (C-2), 153.9 (C-6), 124.5 (C-5), 123.5 (C-3), 69.4 ($CH_2\underline{C}H_2OCH_2$), 65.8 ($O\underline{C}H_2CH_2CO$), 61.9 ($CO_2\underline{C}H_2CH_3$), 54.1 ($CH_2C\underline{H}NH_2$), 53.1 ($NH\underline{C}HCO$), 43.4 ($NH\underline{C}H_2CO_2H$), 34.7 ($CH_2\underline{C}H_2CO_2$), 34.6 ($C\underline{C}H_2CH_2S$), 32.9 ($S\underline{C}H_2CHNH$), 31.6 ($CO\underline{C}H_2CH_2CH$), 31.0 ($CH_2\underline{C}H_2SCH_2$), 30.5 ($NC\underline{C}H_2CH_2$), 28.2 ($CH_2\underline{C}H_2CH_2O$), 26.3 ($COCH_2\underline{C}H_2CH$), 19.5 ($NC\underline{C}H_3$), 13.4 ($OCH_2\underline{C}H_3$). ESI-MS: Expected for $C_{26}H_{39}N_4O_9S_1$ ($M\text{-}H^+$) = *m/z* 583.2443 Found: *m/z* 583.2474. Infrared (KBr): 3314, 1736, 1606 cm^{-1}. HPLC: column: Phenomenex Luna-C18 (250 x 4.60 mm), gradient: (0.7 mL/min) 5 % MeCN/H_2O $\rightarrow$ 90 % MeCN/H_2O over 20 minutes, retention time, 13.30 mins., purity, 99.8 %. Detection at 280 nm.

General procedure for experimentally determining the rate of thiol alkylation as a function of pH for 4-VP derivatives **4.1-4.4**.

An aliquot of 10 % (v/v) of DMSO-$_{d6}$ was added to deuterated aqueous sodium phosphate (100 mM, pH = 6, 7 or 8) containing reduced glutathione (final concentration of 30 mM) within an NMR tube. The solution was sonicated for 10 s. A volume of DMSO-$_{d6}$ was added to a vial containing the 4-VP analogue (4-10 mg). This solution was transferred to the buffered solution in the NMR tube so that a final concentration of 4-VP was 20 mM and the glutathione concentration was 30 mM. The solution was vortexed for 5 seconds then transferred to the NMR instrument for spectroscopic analysis. The progress of the reaction was continually monitored over a 90 minute period at 25 °C. The relative integral changes were plotted as a function of time which allowed the determination of a rate constant for the reaction. This was reinterpreted as a half-life under the experimental conditions.

Synthesis of *N-acetyl-S-[2-(2-{[(2-methoxy-2-oxoethyl)sulfanyl]methyl}-6-methylpyridin-4-yl)ethyl]-L-cysteinate* (**4.31**).

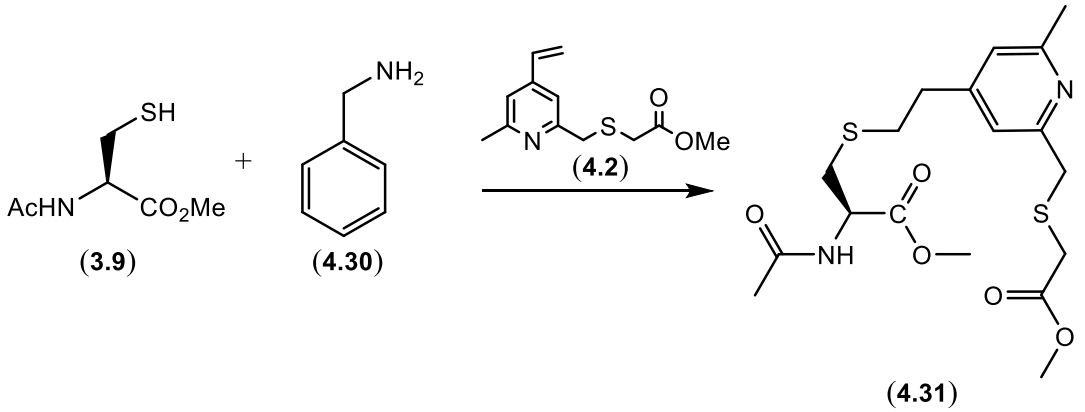

N-acetyl-L-cysteine (9 mg, 0.0508 mmol, **3.9**) and benzyl amine (**4.30**, 1 eq., 5.5 μL, 0.0508 mmol) was dissolved in argon purged 10 % THF in aqueous sodium phosphate (0.9 mL, 0.1 M, pH = 7 or pH = 8). A solution of **4.2** (1 eq., 12.1 mg, 0.0508 mmol) in THF (0.1 mL) was added and the reaction was rapidly stirred at room temperature for 3 hours. The reaction was initially investigated by mass spectrometry, followed by silica gel chromatography purification (10 % EtOAc/petroleum ether → 5 % MeOH/EtOAc) to yield **4.31** as a transparent sticky oil (16.0 mg, 76 %) at pH = 7 and (16.6 mg, 79 %) at pH = 8. ^{1}H NMR, 400 MHz ($CDCl_3$): δ 7.00 (s, 1H, H-3), 6.86 (s, 1H, H-5), 6.33 (br. d, 1H, NH, *J* = 7.2 Hz), 4.82 (m, 1H, NHC*H*CH_2S), 3.87 (s, 2H, NCC*H*$_2$S), 3.75 (s, 3H, OC*H*$_3$), 3.71 (s, 3H, OC*H*$_3$), 3.23 (s, 2H, SC*H*$_2$$CO_2$), 3.00 (dd, 2H, NHCHC*H*$_2$S, *J* = 5.0 & 13.8 Hz), 2.79 (m, 4H, CC*H*$_2$$CH_2$S & CCH_2C*H*$_2$S), 2.50 (s, 3H, NCC*H*$_3$), 2.04 (s, 3H, NHCOC*H*$_3$). ^{13}C NMR, 100 MHz ($CDCl_3$): δ 171.2, 170.7, 169.8 (3 x CO), 158.5 (C-6), 156.9 (C-2), 149.6 (C-4), 121.9 (C-5), 120.3 (C-3), 52.7 (O*C*H_3), 52.4 (O*C*H_3), 51.9 (NH*C*HCH_2S), 38.2 (NC*C*H_2S), 35.0, 34.3 (NHCH*C*H_2S), 32.8 (2C), 24.3 (NC*C*H_3), 23.1 (NHCO*C*H_3). ESI-MS: Expected for $C_{18}H_{26}N_2Na_1O_5S_2$ ($M+Na^+$) = *m/z* 437.1175. Found: *m/z* 437.1246. Infrared (thin film): 1737, 1664, 1292 cm^{-1}. HPLC: column: Waters Symmetry Shield RP_8 (100 x 4.60 mm), gradient: (0.5 mL/min) 5 % MeCN in water → 100 % MeCN over 20 minutes, retention time, 13.25 mins., purity, 99.4 %. Detection at 280 nm.

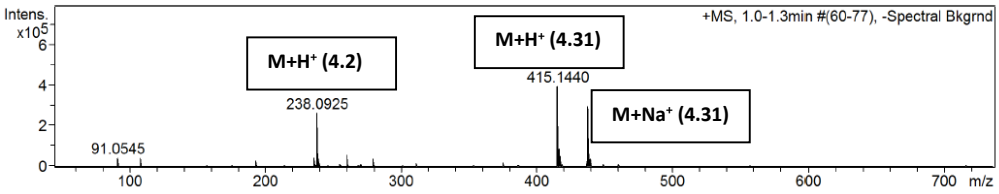

#	m/z	I	I %	Area	S/N
1	91.0545	43718	11.1	732	16097.7
2	108.0833	42405	10.8	899	9072.6
3	236.0785	44524	11.3	1138	891.6
4	238.0925	261554	66.6	8831	4995.1
5	260.0710	56200	14.3	2589	934.3
6	415.1440	392801	100.0	17494	4415.0
7	416.1401	89000	22.7	6674	967.1
8	417.1360	51444	13.1	4048	541.0
9	437.1262	293250	74.7	15131	1959.7
10	438.1221	65876	16.8	5233	449.5

Mass spectrum of reaction containing **3.9**, **4.30**, and **4.2** at pH = 7.

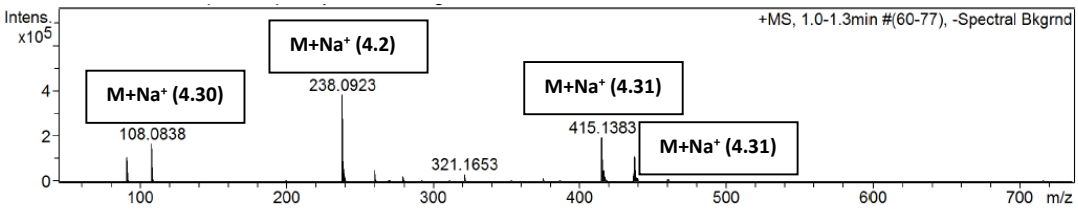

#	m/z	I	I %	Area	S/N
1	91.0545	105582	27.7	1724	50690.5
2	108.0838	166541	43.8	3209	46221.7
3	238.0923	380588	100.0	11813	14821.5
4	239.0938	54014	14.2	2177	2040.9
5	260.0717	48380	12.7	2133	1513.0
6	321.1653	32950	8.7	1667	3435.1
7	415.1383	196365	51.6	12237	5753.3
8	416.1401	49263	12.9	3615	1396.3
9	417.1361	25558	6.7	2023	701.7
10	437.1192	112817	29.6	8589	1985.6

Mass spectrum of reaction containing **3.9**, **4.30**, and **4.2** at pH = 8.

Synthesis of *N-acetyl-S-{2-[2-(3-methoxy-3-oxopropyl)-6-methylpyridin-4-yl]ethyl}-L-cysteinate* (**4.32**).

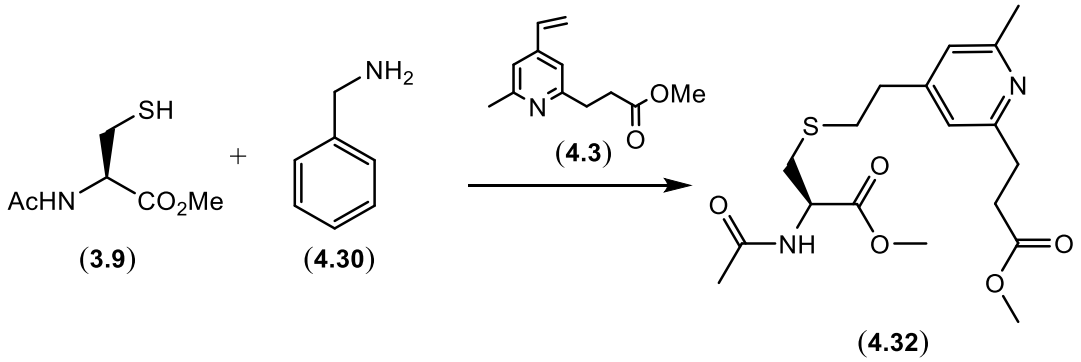

N-acetyl-L-cysteine (**3.9**, 7 mg, 0.0395 mmol,) and benzyl amine (**4.30**, 1 eq., 5.5 μL, 0.0395 mmol) was dissolved in argon purged 10 % THF in aqueous sodium phosphate (0.9 mL, 0.1 M, pH = 7 or pH = 8). A solution of **4.3** (1 eq., 8.1 mg, 0.0395 mmol) in THF (0.1 mL) was added and the reaction was rapidly stirred at room temperature for 3 hours. The reaction was initially investigated by mass spectrometry, followed by silica gel chromatography purification (10 % EtOAc/petroleum ether → 5 % MeOH/EtOAc) to yield **4.32** as a transparent sticky oil (11.3 mg, 75 %) at pH = 7 and (12.2 mg, 81 %) at pH = 8. ^{1}H NMR, 400 MHz ($CDCl_3$): δ 6.82 (s, 2H, H-3 & H-5), 6.27 (br. d, 1H, NH, *J* = 6.8 Hz), 4.83 (m, 1H, NHC*H*CO_2), 3.77 (s, 3H, OC*H*$_3$), 3.67 (s, 3H, OC*H*$_3$), 3.07-2.96 (m, 4H, NCC*H*$_2$$CH_2$ & NHCHC*H*$_2$S), 2.77 (m, 6H, CH_2C*H*$_2$$CO_2$, CC*H*$_2$$CH_2$S & CCH_2C*H*$_2$S), 2.49 (s, 3H, NCC*H*$_3$), 2.05 (s, 3H, NHCOC*H*$_3$). ^{13}C NMR, 100 MHz ($CDCl_3$): δ 173.6, 171.3 & 169.8 (3 x CO), 159.3 (C-2), 158.1 (C-6), 149.3 (C-4), 121.0 (C-5), 120.0 (C-3), 52.7 (O*C*H_3), 51.9 (NH*C*HCO_2), 51.6 (O*C*H_3), 35.2, 34.4, 33.6, 32.9, 24.3 (NC*C*H_3), 23.1 (NHCO*C*H_3). ESI-MS: Expected for $C_{18}H_{26}N_2Na_1O_5S_1$ ($M+Na^+$) = *m/z* 405.1455. Found: *m/z* 405.1489. Infrared (thin film): 1734, 1659, 1436 cm^{-1}. HPLC: column: Waters Symmetry Shield RP_8 (100 x 4.60 mm), gradient: (0.5 mL/min) 5 % MeCN in water → 100 % MeCN over 20 minutes, retention time, 13.62 mins., purity, 91.2 %. Detection at 280 nm.

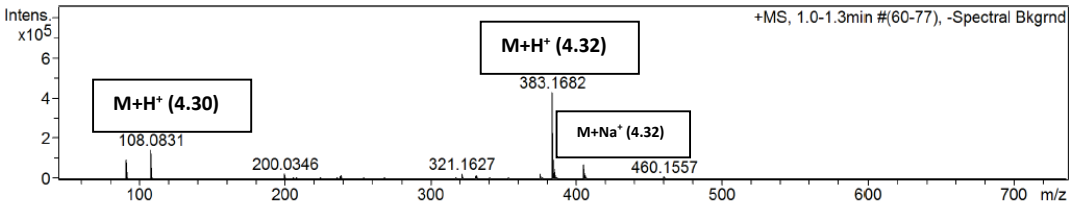

#	m/z	I	I %	Area	S/N
1	91.0540	93255	21.9	1431	34191.8
2	108.0831	142910	33.5	2879	30497.8
3	200.0346	25920	6.1	1011	4430.5
4	321.1627	25254	5.9	1428	2236.3
5	331.1782	17933	4.2	1140	1257.3
6	375.0645	26276	6.2	2046	385.8
7	383.1682	426336	100.0	19665	5254.1
8	384.1646	95427	22.4	6548	1153.3
9	385.1620	35573	8.3	2570	421.7
10	405.1443	70710	16.6	5423	1135.6

Mass spectrum of reaction containing **3.9**, **4.30**, and **4.3** at pH = 7.

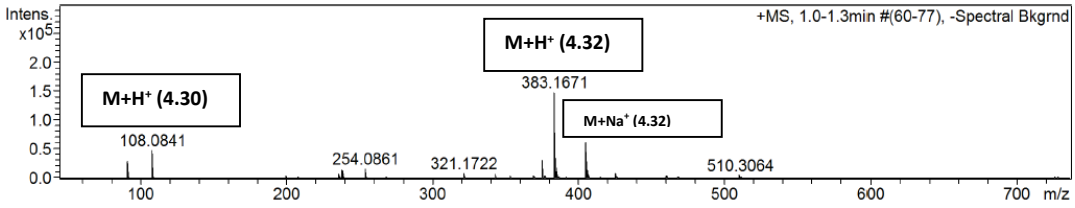

#	m/z	I	I %	Area	S/N
1	91.0539	29588	20.0	386	43692.1
2	108.0841	48340	32.6	894	42432.8
3	238.1421	13511	9.1	625	2108.6
4	254.0861	16368	11.0	202	1979.3
5	375.0663	30740	20.7	2279	661.0
6	383.1671	148303	100.0	9644	2682.7
7	384.1672	34494	23.3	2803	612.0
8	385.1599	12036	8.1	901	209.5
9	405.1456	62150	41.9	4929	1333.6
10	406.1474	14401	9.7	1221	316.3

Mass spectrum of reaction containing **3.9**, **4.30**, and **4.3** at pH = 8.

Synthesis of *3,3'-{5-oxo-2-[2-(pyridin-4-yl)ethyl]-1,2l^5-oxaphospholane-2,2-diyl} dipropanoic acid* (**4.34**).

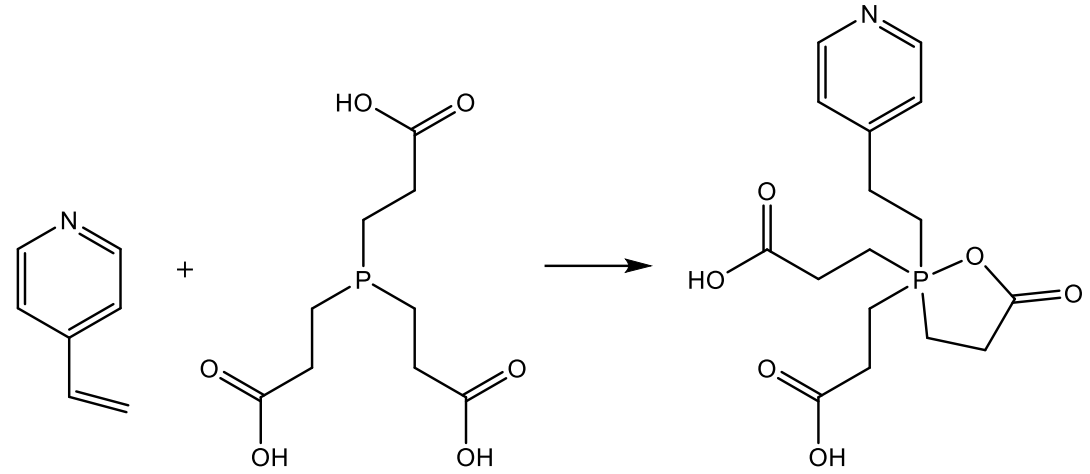

(**4.33**) (**2.6**) (**4.34**)

4-Vinyl pyridine (**4.33,** 20 mg, 0.190 mmol) and TCEP (**2.6**, 0.9 eq., 49.1 mg, 0.171 mmol) was dissolved in THF (2 mL) and argon purged aqueous sodium phosphate (0.1 M, pH = 7.0, 8 mL) and stirred under argon at room temperature for 3 hours. The reaction was concentrated *in vacuo* to 3 mL and then loaded onto a C-18 column for purification (100 % H_2O $\rightarrow$ 40 % MeCN/H_2O) to yield **4.34** as a transparent solid (38.9 mg, 64 %). ^{1}H NMR, D_2O, 400 MHz: δ 8.57 (d, 2H, H-2 & H-6, *J* = 6.8 Hz), 7.85 (d, 2H, H-3 & H-5, *J* = 6.8 Hz), 3.19 (m, 2H, CHCC$\underline{H_2}$CH$_2$P), 2.65 (m, 2H, CHCCH$_2$C$\underline{H_2}$P), 2.51 (m, 12H, 3 x C$\underline{H_2}$C$\underline{H_2}$CO$_2$). ^{13}C NMR, D_2O, 125 MHz: δ 176.8 (d, 3 x CH$_2$CH$_2$$\underline{C}O_2$, *J* = 12.5 Hz), 160.2 (d, C-4, *J* = 16.2 Hz), 141.4 (C-2 & C-6), 126.8 (C-3 & C-5), 27.6 (d, 3 x CH$_2$$\underline{C}H_2CO_2$, *J* = 4.2 Hz), 26.9 (d, CHC$\underline{C}$H$_2$CH$_2$, *J* = 2.0 Hz), 18.3 (d, P$\underline{C}$H$_2$CH$_2$CCH, *J* = 48.3 Hz), 15.1 (d, 3 x $\underline{C}$H$_2$CH$_2$CO$_2$, *J* = 49.6 Hz). ^{31}P NMR, D_2O, 202 MHz: 36.6. HRMS: $C_{16}H_{21}N_1O_6P_1$ (M-H$^+$) = *m/z* 354.1106. Found: *m/z* 354.1123. Infrared (thin film): 3407, 1716 cm^{-1}. HPLC: column: Phenomenex Luna-C18 (250 x 4.60 mm), gradient: (0.7 mL/min) 5 % MeCN/H_2O $\rightarrow$ 90 % MeCN/H_2O over 20 minutes, retention time, 11.32 mins., purity, 96.4 %. Detection at 280 nm.

Synthesis of *3,3'-{2-[2-(pyridin-4-yl)ethyl]-1,2l^5-oxaphospholane-2,2-diyl}dipropan-1-ol* (**4.35**).

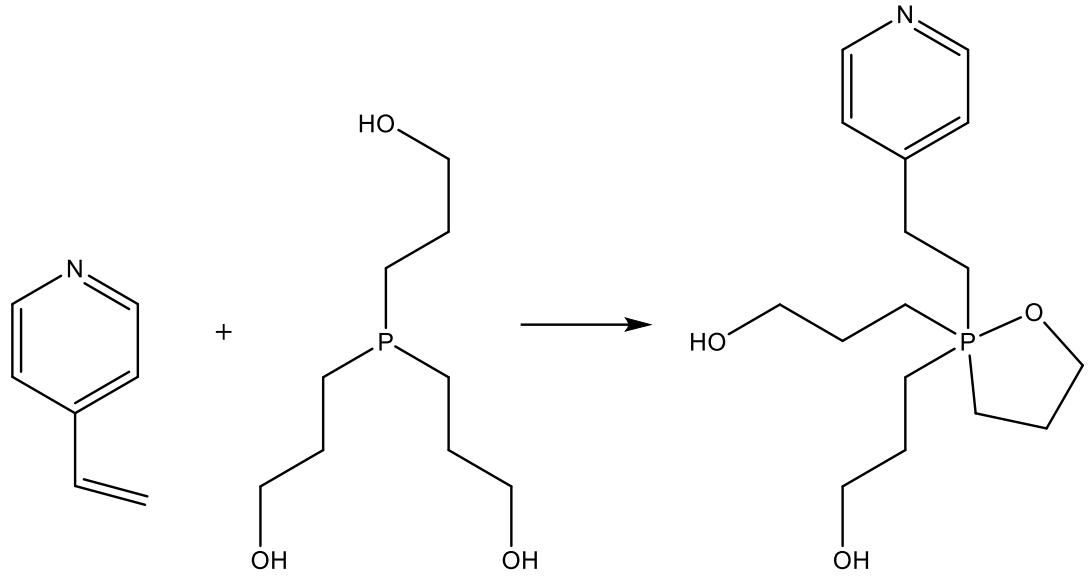

(**4.33**) (**2.7**) (**4.35**)

4-Vinyl pyridine (**4.33**, 15 mg, 0.143 mmol) and THPP (**2.7**, 0.9 eq., 26.7 mg, 0.128 mmol) was dissolved in THF (2 mL) and argon purged aqueous sodium phosphate (0.1 M, pH = 7.0, 8 mL) and stirred under argon at room temperature for 3 hours. The reaction was concentrated *in vacuo* to 3 mL and then loaded onto a C-18 column for purification (100 % H_2O $\rightarrow$ 40 % MeCN/H_2O) to yield **4.35** as a transparent solid (24.6 mg, 61 %). ^{1}H NMR, D_2O, 400 MHz: δ 8.48 (s, 2H, H-2 & H-6), 7.41 (d, 2H, H-3 & H-5, *J* = 5.9 Hz), 3.68 (t, 6H, 3 x $CH_2C\underline{H_2}O$, *J* = 6.0 Hz), 3.06 (m, 2H, $CHCC\underline{H_2}CH_2$), 2.72 (m, 2H, $PC\underline{H_2}CH_2C$), 2.37 (m, 6H, 3 x $C\underline{H_2}CH_2CH_2O$), 1.75 (m, 6H, 3 x $CH_2C\underline{H_2}CH_2O$). ^{13}C NMR, D_2O, 100 MHz: δ 149.6 & 149.5 (d, C-4, *J* = 13.7 Hz), 149.0 (C-2 & C-6), 123.9 (C-3 & C-5), 60.9 (d, 3 x $CH_2\underline{C}H_2O$, *J* = 16.8 Hz), 25.9 ($CHC\underline{C}H_2CH_2$), 23.4 (d, 3 x $CH_2\underline{C}H_2CH_2O$, *J* = 4.2 Hz), 18.4 (d, $P\underline{C}H_2CH_2C$, *J* = 47.9 Hz), 15.0 (d, 3 x $\underline{C}H_2CH_2CH_2O$, *J* = 49.7 Hz). ^{31}P NMR, D_2O, 162 MHz: 36.1. HRMS: $C_{16}H_{29}N_1O_3P_1$ ($M+H^+$) = *m/z* 314.1880. Found: *m/z* 314.1888. Infrared (thin film): 3361, 1613, 1424 cm^{-1}. HPLC: column: Waters Symmetry Shield RP_8 (100 x 4.60 mm), gradient: (0.5 mL/min) 5 % MeCN in water $\rightarrow$ 100 % MeCN over 20 minutes, retention time, 12.00 mins., purity, 95.2 %. Detection at 280 nm.

Investigating a possible reaction of 4-VP with alkyl azide **3.3**.

4-VP (**4.33**, 36 mg) was dissolved in THF (1.5 mL) and aqueous sodium phosphate (0.25 M, pH = 7, 1.5 mL) containing the alkyl azide **3.3** (1 eq., 100 mg). The reaction was rapidly stirred at room temperature and monitored by TLC and HRMS. After 2 days no evidence of triazoline formation was evident by either TLC or HRMS. The investigation proved that the addition of alkyl azide **3.3** for excess phosphine oxidation can be used in a reaction containing thiol alkylating reagents based on 4-vinyl pyridine.

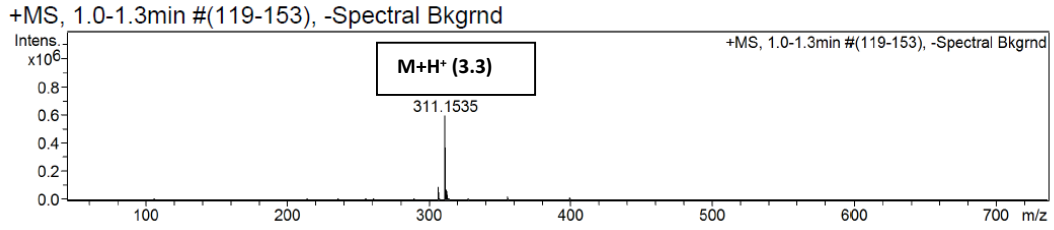

Mass spectrum of reaction of **4.33** with **3.3** after 3 hours.

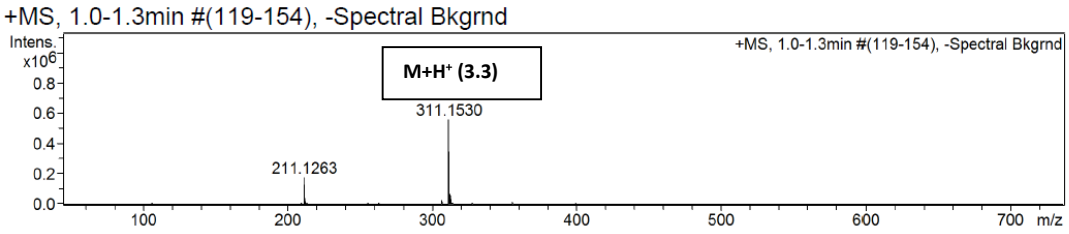

Mass spectrum of reaction of **4.33** with **3.3** after 2 days.

Synthesis of *3-(4-ethenyl-6-methylpyridin-2-yl)propyl acetate* (**4.38**).

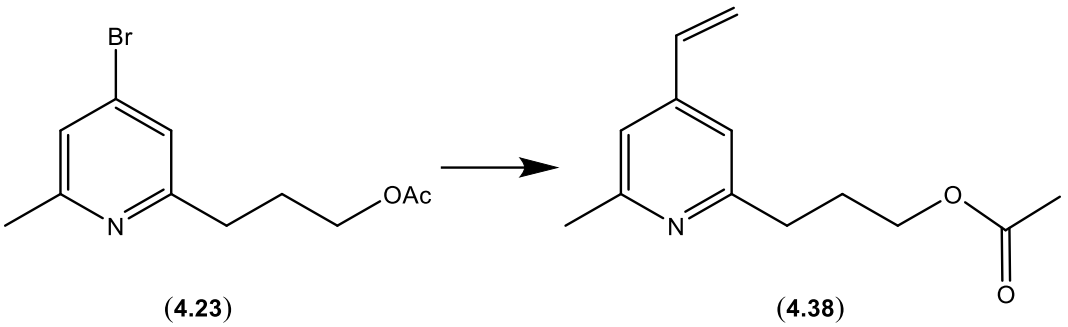

(**4.23**) (**4.38**)

3-(4-Bromo-6-methylpyridin-2-yl)propyl acetate (**4.23**, 0.30 g, 1.10 mmol) was dissolved in 10 mL of deoxygenated toluene. Tetrakis(triphenylphosphine)palladium(0) (10 mol %, 127.4 mg, 0.110 mmol) and tributyl(vinyl)tin (2 eq., 0.64 mL, 2.20 mmol) were added. The reaction was refluxed under inert atmosphere (N_2) for 2 hours then allowed to cool. The reaction was loaded directly onto a silica gel column containing 10 % (w/w) KF. The reaction was purified by silica gel chromatography: 5 % EtOAc/petroleum ether $\rightarrow$ 50 % EtOAc/petroleum ether to yield **4.38** as a transparent oil (203.1 mg, 84 %). ^{1}H NMR, $CDCl_3$, 500 MHz: δ 6.97 (s, 1H, H-3), 2.95 (s, 1H, H-5), 6.60 (dd, 1H, CC*H*CH_2, *J* = 10.9 & 17.6 Hz), 5.93 (d, 1H, CCHC*H*H, *J* = 17.6 Hz), 5.43 (d, 1H, CCHCH*H*, *J* = 10.9 Hz), 4.12 (t, 2H, CH_2C*H*$_2$O, *J* = 6.5 Hz), 2.83 (t, 2H, NCC*H*$_2CH_2$, *J* = 7.5 Hz), 2.52 (s, 3H, NCC*H*$_3$), 2.07 (m, 2H, CH_2C*H*$_2CH_2$O), 2.04 (s, 3H, OCOC*H*$_3$). ^{13}C NMR, $CDCl_3$, 125 MHz: δ 171.17 (O*C*OCH$_3$), 160.62 (C-2), 158.21 (C-6), 145.68 (C-4), 135.04 (C*C*HCH_2), 118.27 (CCH*C*H_2), 118.07 (C-3), 116.99 (C-5), 64.02 (CH_2*C*H_2O), 34.59 (NC*C*H_2CH_2), 28.77 (CH_2*C*H_2CH_2), 24.32 (NC*C*H$_3$), 20.98 (OCO*C*H$_3$). ESI-MS: Expected for $C_{13}H_{17}N_1Na_1O_2$ ($M+Na^+$) = *m/z* 242.1151. Found: *m/z* 242.1151. Infrared (NaCl disc): 1742, 1243 cm^{-1}. HPLC: column: Waters Symmetry Shield RP_8 (100 x 4.60 mm), gradient: (0.5 mL/min) 5 % MeCN in water $\rightarrow$ 100 % MeCN over 20 minutes, retention time, 15.53 mins., purity, 97.56 %. Detection at 280 nm.

Synthesis of *3-(4-ethenyl-6-methylpyridin-2-yl)propan-1-ol* (**4.39**).

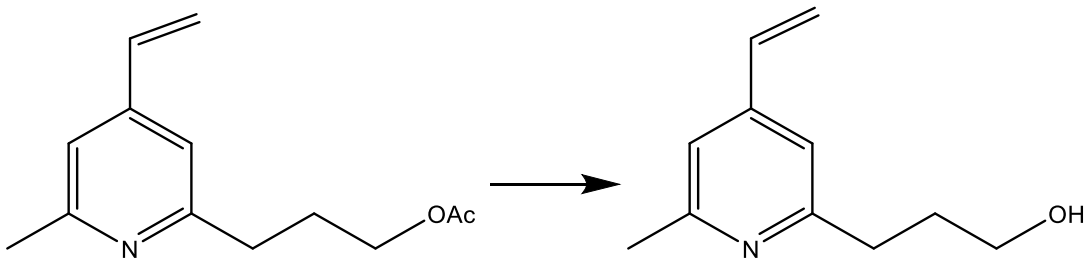

(**4.38**) (**4.39**)

3-(4-Ethenyl-6-methylpyridin-2-yl)propyl acetate (**4.38**, 0.20 g, 0.912 mmol) was dissolved in 10 mL of anhydrous methanol. Sodium methoxide (1.5 eq., 0.5 M, 2.7 mL) was slowly added and the reaction was stirred under N_2 for 1.5 hours, monitoring by TLC. The reaction was neutralised with 1 M HCl solution and concentrated. The residue was purified by silica gel chromatography: 1 $\rightarrow$ 10 % MeOH/DCM to yield **4.39** as a transparent oil (130.9 mg, 81 %). ^{1}H NMR, CD_3OD, 400 MHz: δ 7.13 (s, 2H, H-3 & H-5), 6.68 (dd, 1H, CC*H*CH_2, *J* = 10.9 & 17.6 Hz), 6.05 (d, 1H, CCHC*H*H, *J* = 17.6 Hz), 5.48 (d, 1H, CCHCH*H*, *J* = 10.9 Hz), 3.59 (t, 2H, $CH_2C\underline{H_2}OH$, *J* = 6.4 Hz), 2.80 (t, 2H, $NCC\underline{H_2}CH_2$, *J* = 8.3 Hz), 2.48 (s, 3H, $NCC\underline{H_3}$), 1.90 (m, 2H, $CH_2C\underline{H_2}CH_2$). ^{13}C NMR, CD_3OD, 100 MHz: δ 162.75 (C-2), 159.21 (C-6), 148.05 (C-4), 136.11 ($C\underline{C}HCH_2$), 119.47 ($CCH\underline{C}H_2$), 119.42 & 118.68 (C-3 & C-5), 62.32 ($CH_2\underline{C}H_2OH$), 35.10 ($NC\underline{C}H_2CH_2$), 34.09 ($CH_2\underline{C}H_2CH_2$), 23.71 ($NC\underline{C}H_3$). ESI-MS: Expected for $C_{11}H_{15}N_1Na_1O_1$ ($M+Na^+$) = *m/z* 200.1046. Found: *m/z* 200.1053. Infrared (thin film): 3358, 1607, 1560 cm^{-1}. HPLC: column: Waters Symmetry Shield RP_8 (100 x 4.60 mm), gradient: (0.5 mL/min) 5 % MeCN in water $\rightarrow$ 100 % MeCN over 20 minutes, retention time, 14.16 mins., purity, 97.58 %. Detection at 280 nm.

Synthesis of 2,3,4,6-tetra-*O*-acetyl-*β*-D-galactopyranosyl-(1→4)-2,3,4,6-tetra-*O*-acetyl-α-D-glucopyranose (**4.41**).

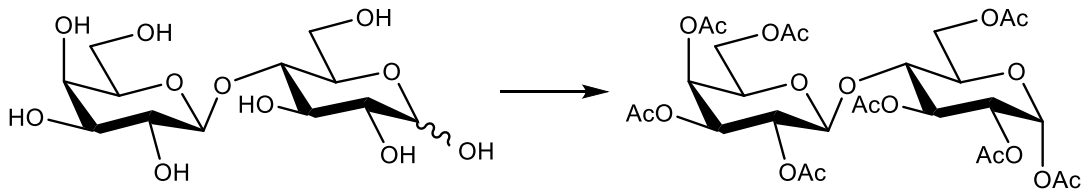

(**4.40**) (**4.41**)

D-Lactose (**4.40**, 5.0 g, 14.6 mmol) was dissolved in anhydrous pyridine (40 mL). Acetic anhydride (12 eq., 175.3 mmol, 16.6 mL) was added to the stirring solution. The reaction was stirred over night at room temperature under N_2 gas. The reaction was cooled to 0 °C in an ice bath, followed by the slow addition of methanol (25 mL). The reaction was left to stir for 5 minutes and then concentrated. The crude was co-evaporated with toluene (5 x 100 mL) then purified by silica gel chromatography: 10 % EtOAc/petroleum ether → 70 % EtOAc/petroleum ether to yield **4.41** as a sticky white solid (10.8 g, 92 %). Spectral data consistent with literature [198]. ^{1}H NMR, $CDCl_3$, 400 MHz: δ 6.22 (d, 1H, *J* = 3.7 Hz), 5.43 (t, 1H, *J* = 9.3 Hz), 5.33 (m, 1H), 5.09 (dd, 1 H, *J* = 7.9 & 10.4 Hz), 4.99-4.92 (m, 2H), 4.47-4.40 (m, 2 H), 4.15-4.02 (m, 4H), 4.00-3.96 (m, 1H), 3.88-3.81 (m, 2H), 2.15 (s, 3H), 2.13 (s, 3H), 2.10 (s, 3H), 2.04 (s, 3H), 2.03 (s, 3H), 2.02 (s, 3H), 1.98 (s, 3H), 1.94 (s, 3H). ^{13}C NMR, $CDCl_3$, 100 MHz: δ 170.3, 170.2, 170.1, 170.0, 169.9, 169.5, 169.1, 168.9, 101.1, 88.9, 75.7, 70.9, 70.6, 69.5, 69.3, 69.0, 66.5, 65.8, 61.4, 60.7, 20.9, 20.8, 20.7, 20.6, 20.5, 20.4. Expected for $C_{28}H_{38}Na_1O_{19}$ ($M+Na^+$) = *m/z* 701.1900. Found: *m/z* 701.2050.

Synthesis of 2,3,4,6-tetra-*O*-acetyl-*β*-D-galactopyranosyl-(1→4)-2,3,6-tri-*O*-acetyl-α-D-glucopyranose (**4.42**).

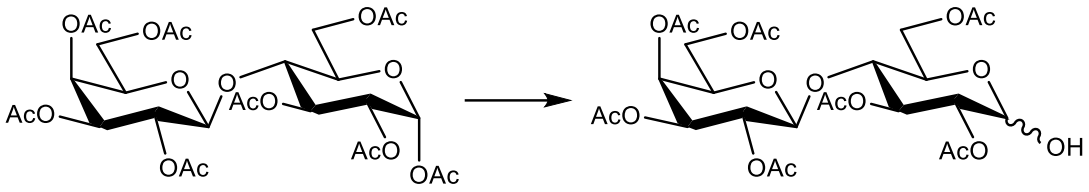

(**4.41**) (**4.42**)

2,3,4,6-Tetra-*O*-acetyl-*β*-D-galactopyranosyl-(1→4)-2,3,4,6-tetra-*O*-acetyl-α-D-glucopyranose (**4.41**, 0.50 g, 0.737 mmol) was dissolved in anhydrous methanol and dichloromethane (1:1, 15 mL). Hydrazine acetate (1.2 eq., 81.4 mg, 0.884 mmol) was added and the reaction was rapidly stirred for 6 hours at room temperature while under N_2 gas. The reaction was concentrated then purified by silica gel chromatography: 10 % EtOAc/petroleum ether → 80 % EtOAc/petroleum ether to yield **4.42** as a sticky solid (324 mg, 69 %). Spectral data was consistent with that reported in the literature [198]. ^{1}H NMR ($CDCl_3$, 400 MHz) and ^{13}C NMR ($CDCl_3$, 100 MHz) data shows a α/β mixture. Expected for $C_{26}H_{36}Na_1O_{18}$ ($M+Na^+$) = *m/z* 659.1794. Found: *m/z* 659.1934. Infrared (KBr): 3485, 1751 cm^{-1}.

Synthesis of 2,3,4,6-tetra-*O*-acetyl-α-lactopyranosyl trichloroacetimidate (**4.43**).

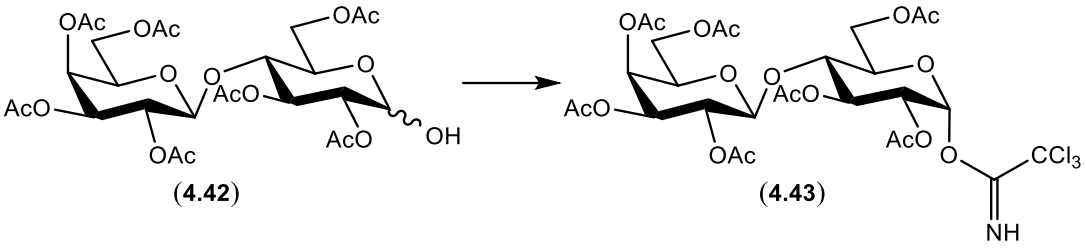

2,3,4,6-Tetra-*O*-acetyl-*β*-D-galactopyranosyl-(1→4)-2,3,6-tri-*O*-acetyl-α-D-glucopyranose (**4.42**, 0.85 g, 1.34 mmol) was dissolved in anhydrous dichloromethane (10 mL) and cooled to 0 °C, while under N_2 gas. Trichloroacetonitrile (5 eq., 6.68 mmol, 0.67 mL) was added to the stirring solution, followed by the addition of DBU (0.1 eq., 0.134 mmol, 20.0 μL). The reaction was allowed to warm to room temperature and left to stir for 2 hours. The reaction was concentrated and purified by silica gel chromatography: 10 % EtOAc/petroleum ether → 50 % EtOAc/petroleum ether to yield **4.43** as a sticky solid (0.83 g, 80 %). Spectral data consistent with that reported in the literature [199]. ^{1}H NMR, $CDCl_3$, 400 MHz: δ 8.65 (s, 1H), 6.45 (d, 1H, *J* = 3.8 Hz), 5.54 (t, 1H, *J* = 9.8 Hz), 5.33 (dd, 1H, *J* = 0.8 & 3.4 Hz), 5.11 (dd, 1H, *J* = 7.9 & 10.4 Hz), 5.04 (dd, 1H, *J* = 3.8 & 10.2 Hz), 4.93 (dd, 1H, *J* = 3.4 & 10.4 Hz), 4.51-4.44 (m, 2H), 4.16-4.04 (m, 4H), 3.89-3.82 (m, 2H), 2.13 (s, 3H), 2.09 (s, 3H), 2.04 (s, 6H), 2.02 (s, 3H), 1.98 (s, 3H), 1.95 (s, 3H). ^{13}C NMR, $CDCl_3$, 100 MHz: δ 170.3, 170.2, 170.1, 170.03, 170.02, 169.3, 169.0, 160.9, 101.2, 92.8, 90.6, 75.8, 71.0, 70.8, 70.6, 69.9, 69.5, 69.0, 66.5, 61.4, 60.7, 60.3, 21.0, 20.8, 20.77, 20.71, 20.6, 20.5, 20.4. ESI-MS: Expected for $C_{28}H_{36}Cl_3N_1Na_1O_{18}$ ($M+Na^+$) = *m/z* 802.0891 & 804.0861. Found: *m/z* 802.1009 & 804.0997.

Synthesis of *3-(4-ethenyl-6-methylpyridin-2-yl)propyl-β-D-lactose hepta acetate* (**4.44**).

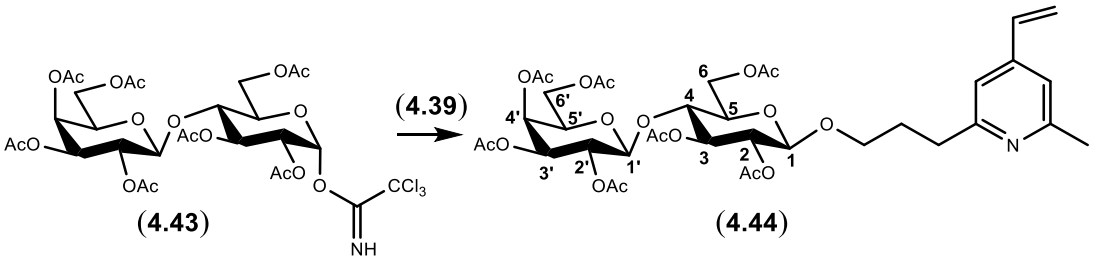

2,3,4,6-Tetra-*O*-acetyl-α-lactopyranosyl trichloroacetimidate (**4.43**, 0.10 g, 0.128 mmol) and 4-VP derivative **4.39** (2 eq., 45.4 mg, 0.256 mmol) were dissolved in anhydrous dichloromethane (3 mL) containing crushed 4 Å molecular sieves (0.1 g). The reagents were stirred at room temperature, under N_2 for 1 hour. The mixture was subsequently cooled to -25 °C. Trimethylsilyl triflate (2.2 eq., 51 µL, 0.282 mmol) was added slowly. The mixture was stirred at -25°C for 1 hour, then allowed to warm to room temperature and left to stir for a further 1 hour. The mixture was then cooled to 0 °C and the reaction neutralised by the addition of triethylamine (2.2 eq., 39.3 µL, 0.282 mmol). The mixture was left to warm to room temperature and then filtered through celite. The filtrate was concentrated and residue was purified by silica gel chromatography: 10 % EtOAc/petroleum ether → 100% EtOAc to yield **4.44** as a white foam (68.3 mg, 67 %). ^{1}H NMR, $CDCl_3$, 400 MHz: δ 6.96 (s, 1H, CC*H*CCH_3), 6.92 (s, 1H, CC*H*CCH_2), 6.60 (dd, 1H, CC*H*CH_2, *J* = 10.8 & 17.6 Hz), 5.93 (dd, 1H, CCHC*H*H, *J* = 0.6 & 17.6 Hz), 5.43 (dd, 1H, CCHCH*H*, *J* = 0.6 & 10.8 Hz), 5.34 (dd, 1H, H-4', *J* = 1.0 & 2.5 Hz), 5.20 (t, 1H, H-3, *J* = 9.3 Hz), 5.11 (dd, 1H, H-2', *J* = 7.9 &10.4 Hz), 4.97 - 4.90 (m, 2H, H-2 & 3'), 4.49 - 4.45 (m, 3H, H-1, 1' & 6_a), 4.16-4.06 (m, 3H, H-6_b, $6'_a$ & $6'_b$), 3.91 – 3.85 (m, 2H, H-5' & OC*H*HCH_2CH_2), 3.79 (t, 1H, H-4, *J* = 9.6 Hz), 3.62 – 3.57 (m, 1H, H-5), 3.55-3.49 (m, 1H, OCH*H*CH_2CH_2), 2.78–2.73 (m, 2H, NCC*H*$_2$$CH_2$), 2.51 (s, 3H, NCC*H*$_3$), 2.15-1.96 (m, 23H, OCH_2C*H*$_2$$CH_2$ & 7 x OCOC*H*$_3$). ^{13}C NMR, $CDCl_3$, 100 MHz: δ 170.32, 170.23, 170.08, 169.98, 169.74, 169.59, 169.03, 161.01 (N*C*CH_3), 158.24 (N*C*CH_2), 145.43 (CH*C*$CHCH_2$), 135.14 (C*C*HCH_2), 118.00 (CCH*C*H_2), 117.85 (C*C*$HCCH_3$), 116.94 (C*C*$HCCH_2$), 101.04 & 100.60

(C-1 & 1'), 76.35 (C-4), 72.91 (C-3), 72.64 (C-5), 71.83, 71.01, 70.73, 69.40, 69.18, 66.68, 62.13, 60.85, 34.37, 29.66, 24.35, 20.77, 20.68, 20.56, 20.44. ESI-HRMS: $C_{37}H_{49}N_1Na_1O_{18}$ ($M+Na^+$) = *m/z* 818.2842. Found: *m/z* 818.2833. Infrared (thin film): 1751, 1224, 1056 cm^{-1}. HPLC: column: Waters Symmetry Shield RP_8 (100 x 4.60 mm), gradient: (0.5 mL/min) 5 % MeCN in water → 100 % MeCN over 20 minutes, retention time, 17.57 mins., purity, 96.31 %. Detection at 280 nm.

Synthesis of *3-(4-ethenyl-6-methylpyridin-2-yl)propyl-β-D-lactose* (**4.45**).

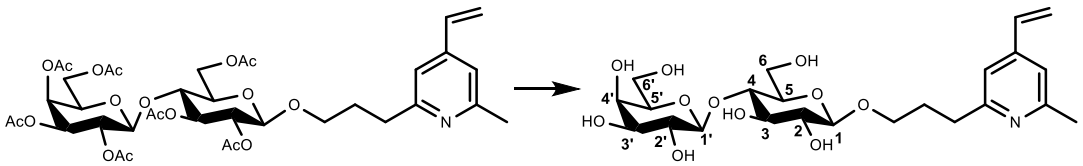

(**4.44**) (**4.45**)

3-(4-Ethenyl-6-methylpyridin-2-yl)propyl-β-D-lactose hepta acetate (**4.44**, 60.0 mg, 0.0754 mmol) was dissolved in anhydrous methanol (5 mL) and stirred at room temperature while under N_2 gas. A 0.5 M solution of sodium methoxide in MeOH (1.5 mL, 0.754 mmol) was added dropwise with stirring over five minutes. The solution was left to stir for 2 hours. The reaction was then neutralised by the slow addition of HCl solution (0.1 M). The solution was concentrated and the residue redissolved in water (2 mL) loaded onto a C-18 column for purification (100 % H_2O → 80 % MeOH/H_2O) to yield **4.45** as a white amorphous solid (29.1 mg, 77 %). ^1H NMR, D_2O, 400 MHz: δ 7.15 (s, 1H, Ar-*H*), 7.14 (s, 1H, Ar-*H*), 6.67 (dd, 1H, CC*H*CH_2, *J* = 11.0 & 17.7 Hz), 6.04 (d, 1H, CCHC*H*H, *J* = 17.7 Hz), 5.52 (d, 1H, CCHCH*H*, *J* = 11.0 Hz), 4.44 (d, 2H, H-1 & 1', *J* = 7.5 Hz), 3.96-3.89 (m, 3H), 3.82-3.51 (m, 10H), 3.33 (m, 1H), 2.79 (t, 2H, H-16, *J* = 7.3 Hz), 2.43 (s, 3H, NCC*H*$_3$), 1.97 (m, 2H, OC*H*$_2$$CH_2$). ^{13}C NMR, D_2O, 100 MHz: δ 160.67, 157.98, 146.76, 134.49, 119.34, 118.52, 117.62, 102.92, 102.01, 78.39, 75.34, 74.73, 74.38, 72.82, 72.50, 70.93, 69.40, 68.52, 61.00, 60.06, 33.08, 29.25, 22.52. ESI-HRMS: $C_{23}H_{35}N_1Na_1O_{11}$ ($M+Na^+$) = *m/z* 524.2102. Found: *m/z* 524.2176. Infrared (KBr): 3415, 1076 cm^{-1}. HPLC: column: Waters Symmetry Shield RP_8 (100 x 4.60 mm), gradient: (0.5 mL/min) 5 % MeCN in water

→ 100 % MeCN over 20 minutes, retention time, 12.72 mins., purity, 98.57 %. Detection at 280 nm.

Synthesis of *γ-L-glutamyl-S-(2-{2-[3-(β-D-lactosyl-oxopropyl)]-6-methylpyridin-4-yl}ethyl)-L-cysteinylglycine* (**4.46**).

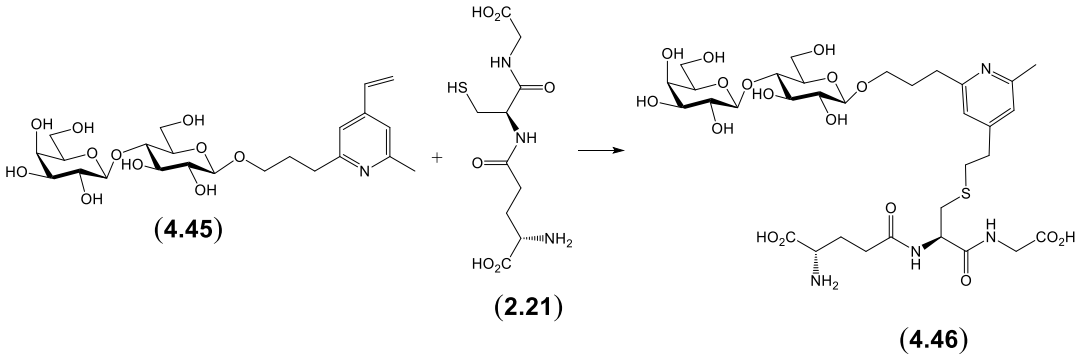

A solution of **4.45** (10 mg, 0.0199 mmol) and glutathione (**2.21**, 0.9 eq., 5.5 mg, 0.0179 mmol) in THF (1 mL) and aqueous sodium phosphate (0.1 M, pH = 7, 3 mL) were stirred for 4 hours at room temperature. The solution was loaded directly onto a C-18 column and purified (100 % water → 30 % MeOH/water) to yield **4.46** as a clear glassy solid (9.4 mg, 65 %). ^{1}H NMR, CD_3OD, 500 MHz: δ 1.98 (q, 2H), 2.15 (q, 2H), 2.48 (s, 3H), 2.55 (m, 2H), 2.78–2.87 (m, 6H), 3.09 (dd, 1H), 3.28 (dd, 1H), 3.30-3.32 (m, 13H), 3.40 (m, 1H), 3.49-3.93 (m, 16H), 4.29 (d, 1H), 4.38 (d, 1H), 4.58 (dd, 1H), 7.01, (s, 1H), 7.08 (s, 1H). ^{13}C NMR, CD_3OD, 100 MHz: δ 23.57, 27.99, 31.22, 33.11, 33.33, 34.50, 34.70, 44.55, 54.52, 55.68, 61.40, 61.91, 62.30, 62.53, 69.66, 70.34, 72.57, 74.82, 74.85, 76.39, 76.47, 77.09, 80.64, 104.35, 105.13, 122.31, 122.71, 152.83, 158.70, 162.08, 172.26, 174.06, 175.45, 175.96. ESI-MS: Expected for $C_{33}H_{51}N_4O_{17}S_1$ (M-H$^+$) = *m/z* 807.2975. Found: *m/z* 807.3025. Infrared (KBr): 3444, 1644, 1402 cm^{-1}. HPLC: column: Phenomenex Luna-C18 (250 x 4.60 mm), gradient: (0.7 mL/min) 5 % MeCN/H_2O → 90 % MeCN/H_2O over 20 minutes, retention time, 11.66 mins., purity, 99.5 %. Detection at 280 nm.

HPLC of Sbi peptide thiol alkylation by **4.45**.

The reaction of the $Sbi_{3,4\text{-}Cys}$ 20 amino acid peptide (**4.47**, 0.37 mM) with **4.45** (1.1 mM) was performed in aqueous sodium phosphate (0.1 M, pH = 7). Aliquots of the reaction (10 µl) were analysed by HPLC. The native peptide sequence eluted at 12.8 minutes, while the glycosylated peptide eluted at 12.2 minutes under the elution conditions developed on the HPLC instrument: Phenomenex C-18 Luna column, detector 220 nm, elution: 10 $\rightarrow$ 50% MeCN/H_2O (with 0.1 % TFA). A plot of the glycosylation reaction was performed through analysis of the integrals associated with the diminishing reactant peak and increasing product peak over the time course. The product eluting at 12.2 minutes was subsequently collected and analysed by mass spectrometry. The product was identified in the MS with a mass of *m/z* 2773.43 which was expected for the glycosylated product. Expected for $C_{123}H_{202}N_{29}O_{41}S_1$ $(M+H^+)$ = *m/z* 2773.43.

Synthesis of *2-{[(4-ethenyl-6-methylpyridin-2-yl)methyl]sulfanyl}-N-[(polyethyleneglycol-2kDa)]acetamide* (**4.48**).

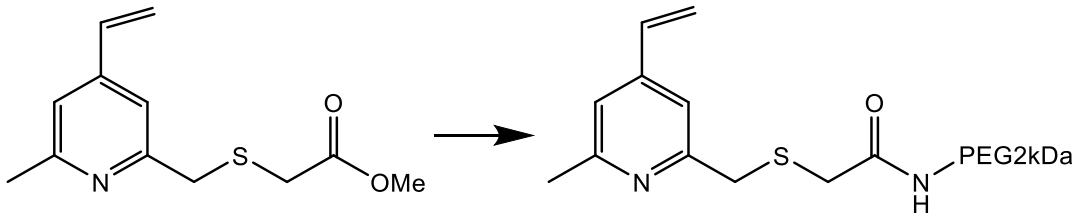

(**4.2**) (**4.48**)

Methyl {[(4-ethenyl-6-methylpyridin-2-yl)methyl]sulfanyl}acetate (**4.2**, 100 mg, 0.421 mmol) was dissolved in THF (5 mL) with NaOH (1 M, 1.5 eq., v = 0.63 mL, 0.632 mmol). The reaction was rapidly stirred at room temperature for 6 hours. The reaction was neutralised with 1 M HCl solution, concentrated and used directly in the following reaction. The residue was dissolved in anhydrous DMF (10 mL), along with NH_2-PEG2kDa (0.5 g, 0.25 mmol, JenKem USA) and triethylamine (0.1 mL), while under N_2. The solution was cooled to 0 °C. HATU (144.5 mg, 0.38 mmol) was slowly added and the reaction was allowed to warm to room temperature and left to stir overnight. The reaction was concentrated and purified by silica gel chromatography (100 % CH_2Cl_2 → 15 % MeOH/CH_2Cl_2) to yield **4.48** as a white amorphous solid (0.34 g, 61 %). ^{1}H NMR, $CDCl_3$, 400 MHz: δ 7.89 (br. s, N*H*), 7.10 (s, 1H, Ar-*H*), 7.03 (s, 1H, Ar-*H*), 6.61 (dd, 1H, CC*H*CH_2, *J* = 10.8 & 17.6 Hz), 5.95 (d, 1H, CCHC*H*H, *J* = 17.6 Hz), 5.46 (d, 1H, CCHCH*H*, *J* = 10.8 Hz), 3.80 (s, 2H, NCCH_2S), 3.58 (s, 188H, OCH_2CH_2O), 3.36 (s, 3H, OCH_3), 3.12 (s, 2H, SCH_2CONH), 2.52 (s, 3H, NCCH_3). HPLC: column: Waters Symmetry Shield RP_8 (100 x 4.60 mm), gradient: (0.5 mL/min) 5 % MeCN in water → 100 % MeCN over 20 minutes, retention time, 15.0 mins., purity, 95.2 %. Detection at 280 nm.

Synthesis of *3-(4-ethenyl-6-methylpyridin-2-yl)-N-[(polyethyleneglycol-2kDa)]propanamide* (**4.49**).

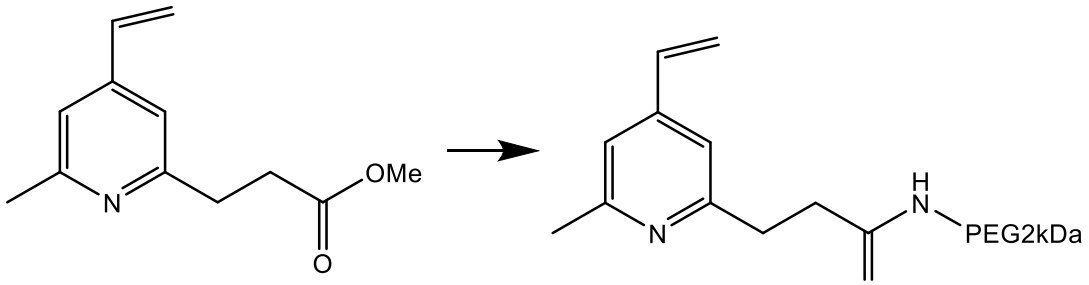

(**4.3**) (**4.49**)

Methyl 3-(4-ethenyl-6-methylpyridin-2-yl)propanoate (**4.3**, 100 mg, 0.487 mmol) was dissolved in THF (5 mL) with NaOH (1 M, 1.5 eq., v = 0.73 mL, 0.731 mmol). The reaction was rapidly stirred at room temperature for 6 hours. The reaction was neutralised with 1 M HCl solution, concentrated and used directly in the following reaction. The residue was dissolved in anhydrous DMF (10 mL), along with NH_2-PEG2kDa (0.5 g, 0.25 mmol, JenKem USA) and triethylamine (0.1 mL), while under N_2. The solution was cooled to 0 °C. HATU (144.5 mg, 0.38 mmol) was slowly added and the reaction was allowed to warm to room temperature and left to stir overnight. The reaction was concentrated and purified by silica gel chromatography (100 % CH_2Cl_2 → 15 % MeOH/CH_2Cl_2) to yield **4.49** as a white amorphous solid (0.31 g, 57 %). ^{1}H NMR, $CDCl_3$, 400 MHz: δ 7.19 (s, 1H, Ar-*H*), 7.15 (s, 1H, Ar-*H*), 7.00 (br. s, N*H*), 6.65 (dd, 1H, CC*H*CH_2, *J* = 10.9 & 17.7 Hz), 6.06 (d, 1H, CCHC*H*H, *J* = 17.7 Hz), 5.57 (d, 1H, CCHCH*H*, *J* = 10.9 Hz), 3.65 (s, 170H, OC*H*$_2$C*H*$_2$O), 3.41 (s, 3H, OC*H*$_3$), 3.12 (t, 2H, NCC*H*$_2$, *J* = 6.9 Hz), 2.71 (t, 2H, CCH_2C*H*$_2$CO, *J* = 6.9 Hz), 2.59 (s, 3H, NCC*H*$_3$). HPLC: column: Waters Symmetry Shield RP_8 (100 x 4.60 mm), gradient: (0.5 mL/min) 5 % MeCN in water → 100 % MeCN over 20 minutes, retention time, 15.55 mins., purity, 96.4 %. Detection at 280 nm.

4-VP derivatised PEG's as reagents for protein PEGylation.

Yeast enolase (1 mg/mL) was denatured in argon purged buffer (0.5 M Tris, pH = 7.2, 5 mM EDTA) containing 8 M urea at 85 °C for 15 minutes. The solution was allowed to cool to room temperature before aliquoting out 100 μL samples for the experiments. Varying concentrations of TCEP or THPP (1-10 mM) were added to aliquots of protein solution (11 μM) and incubated for 45 minutes at 25 °C. 4-VP-PEG2kDa derivatives **4.48** or **4.49** (1 mM) were subsequently added to the reactions with no addition of alkyl azide **3.3** and incubated at 37 °C for 18 hours. Samples that had addition of **3.3** (100 mM) required pre-incubation for 1 hour at 37 °C. 4-VP-PEG2kDa derivatives **4.48** or **4.49** (1 mM) were subsequently added to the reactions and incubated at 37 °C for 18 hours. Samples (15 μL) were taken from each of the reactions and added to Laemmli sample buffer (15 μL). Aliquots (9 μL) of these solutions were loaded into a precast gradient gel (4-12 % Bis-Tris, Invitrogen) along with a protein ladder (EZ-Run, Fisher Scientific) and resolved by SDS Page electrophoresis [MOPS running buffer (Invitrogen), 180 V, 60 mins]. The precast gels were stained by Coomassie solution and destained using a water/ethanol/acetic acid (16:3:1) solution.

Time dependant PEGylation of yeast enolase by maleimide-PEG2kDa versus 4-VP-PEG2kDa derivatives **4.48** and **4.49**.

Yeast enolase (1 mg/mL) was denatured in argon purged buffer (0.5 M Tris, pH = 7.2, 5 mM EDTA) containing 8 M urea at 85 °C for 15 minutes. The solution was allowed to cool to room temperature before aliquoting out 100 μL samples for the experiments. TCEP (5 mM) was added to aliquots of protein solution (11 μM) and incubated for 45 minutes at 25 °C. The alkyl azide **3.3** (100 mM) was added and the solutions were incubated for 1 hour at 37 °C. Maleimide-PEG2kDa or 4-VP-PEG2kDa derivatives **4.48** or **4.49** (1 mM) were subsequently added to the reactions and incubated at 37 °C for a total of 24 hours. Samples (15 μL) were taken from each of the reactions at time points, 1 hour, 4 hours and 24 hours and added to Laemmli

sample buffer (15 μL). Aliquots (9 μL) of these solutions were loaded into a precast gradient gel (4-12 % Bis-Tris, Invitrogen) along with a protein ladder (EZ-Run, Fisher Scientific) and resolved by SDS Page electrophoresis [MOPS running buffer (Invitrogen), 180 V, 60 mins]. The precast gels were stained by Coomassie solution and destained using a water/ethanol/acetic acid (16:3:1) solution.

Synthesis of (*E,Z*)-N-[1-(pyridine-4-yl)-2-[(triphenylmethyl)sufanyl]ethylidene]hydroxylamine (**5.11**).

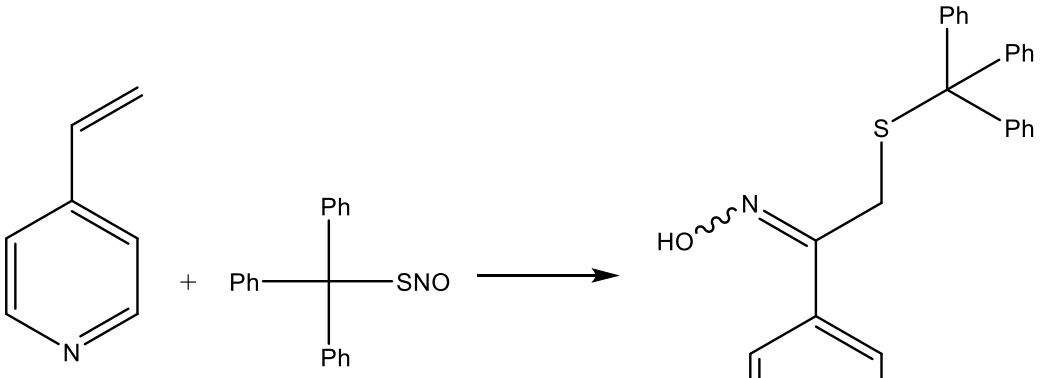

(**4.33**) (**5.10**) (**5.11**)

4-Vinyl pyridine (**4.33**, 200 mg, 1.90 mmol) was dissolved in 2-propanol (2 mL) and toluene (1 mL). Trityl thionitrite (**5.10**, 5 eq., 116 mg, 0.380 mmol) was added to the stirring solution and the reaction was heated from room temperature to 50 °C. This temperature was maintained for 4 hours. The reaction was concentrated and the residue was purified by silica gel chromatography (10 % EtOAc/petroleum ether → 100 % EtOAc) to yield **5.11** as a white solid (115 mg, 74 %). ^{1}H NMR, acetone-d_6, 400 MHz: δ 11.41 (s, 1H, NO*H*), 8.49 (dd, 2H, H-2 & H-6, *J* = 1.6 & 4.5 Hz), 7.53-7.26 (m, 17H, H-3, H-5 & 3 x Ar-*H*), 3.43 (s, 2H, SC*H*$_2$CNOH). ^{13}C NMR, acetone-d_6, 125 MHz: δ 152.5 (C*C*NOH), 151.6 (C-2 & C-6), 146.0 (3 x *ipso* Ar-*C*), 143.9 (C-4), 131.2 (6 x *ortho* Ar-*C*), 129.7 (6 x *meta* Ar-*C*), 128.6 (3 x *para* Ar-*C*), 121.6 (C-3 & C-5), 68.9 (S*C*(Ph)$_3$), 26.7 (S*C*H$_2$CNOH). Infrared (KBr): 3060, 1598, 948 cm^{-1}. ESI-MS: Expected for $C_{26}H_{23}N_2O_1S_1$ (M+H$^+$) = *m/z* 411.1526. Found: *m/z* 411.1545. HPLC:

column: Phenomenex Luna-C18 (250 x 4.60 mm), gradient (0.7 mL/min) 100 % water → 9:1 (acetonitrile:water) over 20 minutes, retention time, 12.19 mins., purity, 92 %. Detection at 300 nm.

Synthesis of *4-[2-(tritylsulfanyl)ethyl]pyridin*e (**5.13**).

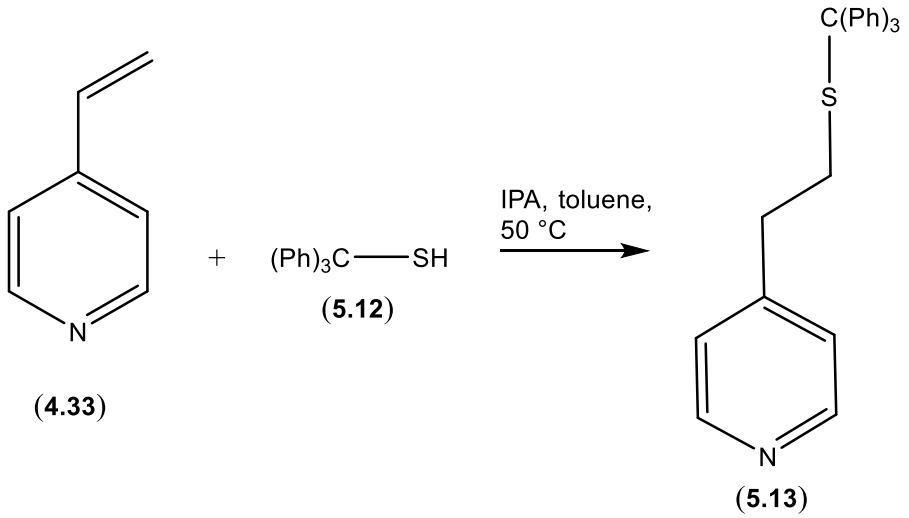

(**4.33**) (**5.12**) (**5.13**)

4-Vinyl pyridine (**4.33**, 150 mg, 1.43 mmol) was dissolved in 2-propanol (6 mL) and toluene (3 mL). Tritylthiol (**5.12**, 1.1 eq., 434 mg, 1.57 mmol) was added to the stirring solution and the reaction was heated from room temperature to 50 °C. The temperature was maintained for 4 hours. The reaction was concentrated and the crude was purified by silica gel chromatography (10 % EtOAc/petroleum ether → 100 % EtOAc) to yield **5.13** as a white solid (430 mg, 79 %). ^{1}H NMR, $CDCl_3$, 400 MHz: δ 8.43 (d, 2H, H-2 & H-6, *J* = 5.8 Hz), 7.41-7.20 (m, 15H, 3 x Ar-*H*), 6.90 (d, 2H, H-3 & H-5, *J* = 5.8 Hz), 2.55-2.50 (m, 2H, CCH_2CH_2S), 2.46-2.42 (m, 2H, CCH_2CH_2S). ^{13}C NMR, $CDCl_3$, 100 MHz: δ 149.6 (C-2 & C-6), 149.1 (C-4), 144.6 (3 x *ipso* Ar-*C*), 129.5, 127.9, 126.7 (3 x *para* Ar-*C*), 123.8 (C-3 & C-5), 66.9 ($SC(C)_3$), 34.5 (CCH_2CH_2S), 32.1 (CCH_2CH_2S). ESI-MS: Expected for $C_{26}H_{23}N_1Na_1S_1$ ($M+Na^+$) = *m/z* 404.1449. Found: *m/z* 404.1464. Infrared (KBr): 3067, 1601 cm^{-1}. HPLC: column: Waters Symmetry Shield RP_8 (100 x 4.60 mm), gradient: (0.5 mL/min) 5 % MeCN in water → 100 % MeCN over 20 minutes, retention time, 19.98 mins., purity, 95.8 %. Detection at 280 nm.

Synthesis of *N-acetyl-S-[(2E,Z)-2-hydroxyimino-2-(pyridin-4-yl)ethyl]-L-cysteinate* (**5.15**).

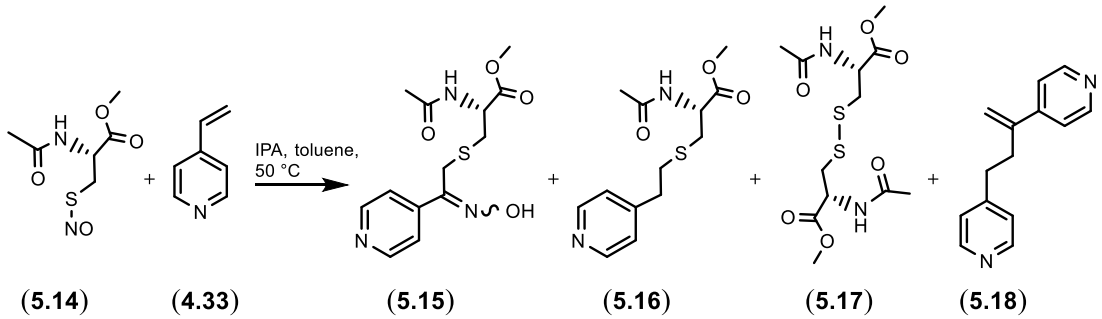

(**5.14**) (**4.33**) (**5.15**) (**5.16**) (**5.17**) (**5.18**)

4-VP (**4.33**, 500 mg, 4.76 mmol) was dissolved in 2-propanol (3 mL) and toluene (1.5 mL). *N*-acetyl-*S*-nitroso-L-cysteinate (**5.14**, 5 eq., 196 mg, 0.951 mmol) was added to the stirring solution and the reaction was heated from room temperature to 50 °C and maintained at this temperature for 4 hours. The reaction was concentrated and the crude was purified by silica gel chromatography (10 % EtOAc/petroleum ether → 100 % EtOAc) to yield **5.15** as a white amorphous solid (127.3 mg, 43 %). ^{1}H NMR, acetone-d_6, 400 MHz: δ 11.24 (s, 1H, NO*H*), 8.59 (d, 2H, H-2 & H-6, *J* = 5.3 Hz), 7.67 dd, 2H, H-3 & H-5, *J* = 1.7 & 5.3 Hz), 4.79 (m, 1H, CH_2CHCO_2), 4.09 (d, 1H, SC*H*HCNOH, *J* = 13.3 Hz), 3.86 (d, 1H, SCH*H*CNOH, *J* = 13.3 Hz), 3.69 (s, 3H, CO_2CH_3), 3.03 (dd, 1H, SC*H*HCHNH, *J* = 5.1 & 13.8 Hz), 2.83 (1H, SCH*H*CHNH), 1.93 (s, 3H, NHCOC*H*$_3$). ^{13}C NMR, acetone-d_6, 125 MHz: δ 172.8 ($NHCOCH_3$), 170.8 ($CHCO_2CH_3$), 153.9 (C*C*NOH), 151.6 (C-2 & C-6), 143.8 (C-4), 122.07 (C-3 & C-5), 53.6 (CH_2CHCO_2), 53.2 (CO_2CH_3), 35.4 (SCH_2CH), 24.6 (SCH_2CNOH), 23.4 ($NHCOCH_3$). ESI-MS: Expected for $C_{13}H_{18}N_3O_4S_1$ ($M+H^+$) = *m/z* 312.1013. Found: *m/z* 312.1017. IR (KBr): 3261, 1741, 1655, 967 cm^{-1}. HPLC: column: Phenomenex Luna-C18 (250 x 4.60 mm), gradient (0.7 mL/min) 100 % water → 9:1 (MeCN:water) over 20 minutes, purity 92 %. Detection at 300 nm. Also isolated was dimethyl N,N'-diacetyl-L-cystinate (**5.17**) as a white solid (174.5 mg, 52 %). Experimental data was consistent with that reported in the literature [200]. ^{1}H NMR, CD_3OD, 400 MHz: δ 4.76 (dd, 1H, CH_2CHCO_2, *J* = 5.0 & 8.6 Hz), 3.77 (s, 3H, H-5), 3.28 (dd, 1H, SC*H*HCH, *J*

= 5.0 & 14.0 Hz), 3.00 (dd, SCH*H*CH, *J* = 8.6 & 14.0 Hz), 2.02 (s, 3H, NHCOC*H*$_3$), ^{13}C NMR, CD_3OD, 100 MHz: δ 173.3 (NH*C*OCH$_3$), 172.4 (CH*C*O$_2$), 53.0 (CH$_2$*C*HCO$_2$ & CO$_2$*C*H$_3$), 40.5 (S*C*H$_2$CH), 22.4 (NHCO*C*H$_3$). ESI-MS: Expected for $C_{12}H_{21}N_2O_6S_2$ ($M+H^+$)= *m/z* 353.0836. Found: *m/z* 353.0856. Methyl N-acetyl-S-[2-(pyridin-4-yl)ethyl]-L-cysteinate (**5.16**) was identified in the mass spectrum of the crude reaction: ESI-MS: Expected for $C_{13}H_{19}N_2O_3S_1$ ($M+H^+$) = *m/z* 283.1111. Found: *m/z* 283.1110. Also isolated was 6 mg of 4,4'-but-1-ene-2,4-diyldipyridine (**5.18**) as a transparent oil (6 mg, yield: 3 %). ^{1}H NMR, CD_3OD, 400 MHz: δ 8.50 (dd, 2H, 2 x Ar-*H*, *J* = 1.7 & 4.6 Hz), 8.39 (dd, 2H, 2 x Ar-*H*, *J* = 1.6 & 4.6 Hz), 7.50 (dd, 2H, 2 x Ar-*H*, *J* = 1.7 & 4.6 Hz), 7.27 (dd, 2H, 2 x Ar-*H*, *J* = 1.6 & 4.6 Hz), 5.58 (s, 1H, CH$_2$CC*H*H), 5.28 (s, 1H, CH$_2$CCH*H*), 2.93 (m, 2H, CH$_2$C*H*$_2$CCH$_2$), 2.84 (m, 2H, CC*H*$_2$CH$_2$CCH$_2$). ^{13}C NMR, CD_3OD, 100 MHz: δ 153.22 (Ar-*C*), 150.52 (Ar-*C*), 150.40 (Ar-*C*), 149.87 (2 x Ar-*C*), 146.19 (Ar-*C*), 125.75 (Ar-*C*), 122.58 (Ar-*C*), 117.77 (CH$_2$C*C*H$_2$), 35.63 (CH$_2$*C*H$_2$CCH$_2$), 34.63 (C*C*H$_2$CH$_2$C). ESI-MS: Expected for $C_{14}H_{15}N_2$ ($M+H^+$) = *m/z* 211.1230. Found: *m/z* 211.1253. HPLC: column: Waters Symmetry Shield RP$_8$ (100 x 4.60 mm), gradient: (0.5 mL/min) 5 % MeCN in water $\rightarrow$ 100 % MeCN over 20 minutes, retention time, 14.49 mins., purity, 91.1 %. Detection at 280 nm.

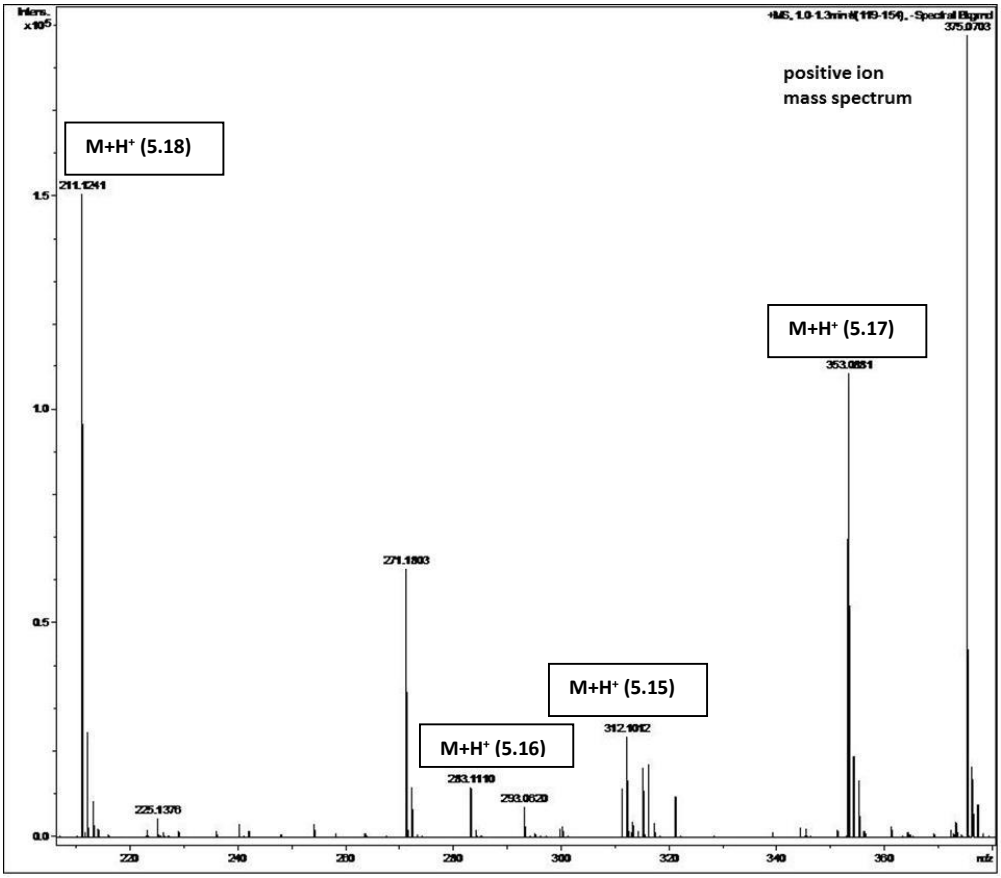

Mass spectrum of reaction from synthesis of *N-acetyl-S-[(2E,Z)-2-hydroxyimino-2-(pyridin-4-yl)ethyl]-L-cysteinate* (**5.15**).

Synthesis of *N-[(2E,Z)-2-(hydroxyimino)-3-(tritylsulfanyl)propyl]acetamide* (**5.21**).

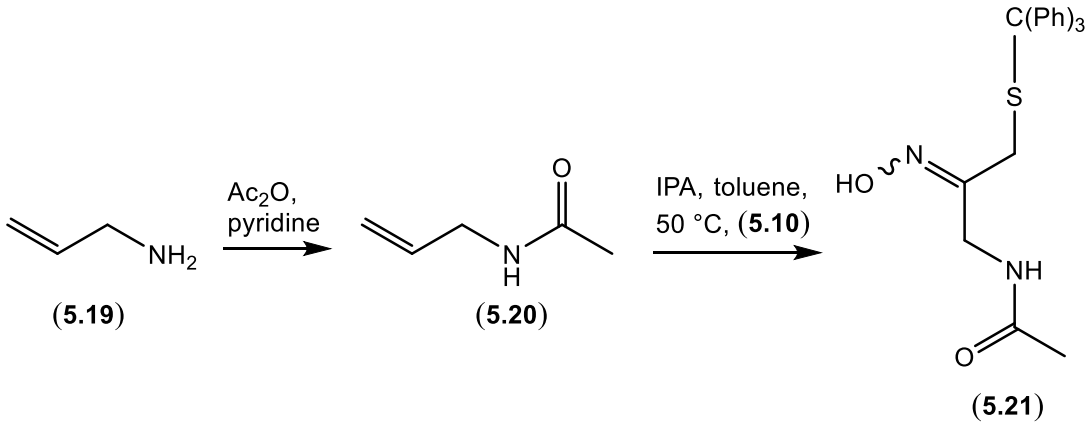

Allylamine (**5.19**, 0.40 g, 7.0 mmol) was dissolved in dry pyridine (10 mL). Acetic anhydride (2 eq., 1.32 mL, 14.0 mmol) was slowly added and the reaction was stirred under N_2 for 6 hours. The reaction was cooled in an ice bath and MeOH (2 mL) was slowly added. The reaction was concentrated and co-evaporated with toluene (2 x 20 mL). The crude was purified by silica gel chromatography (10 % EtOAc/petroleum ether → 70 % EtOAc) to yield N-allylacetamide (**5.20**) as a clear oil (0.58 g, 84 %). The experimental is consistent with that reported in the literature [201]. ^{1}H NMR, 400 MHz ($CDCl_3$): δ 6.26 (br. s, 1H), 5.82-5.72 (m, 1H), 5.15-5.04 (m, 2H), 3.82-3.78 (m, 2H), 1.95 (s, 3H). ^{13}NMR, 100 MHz ($CDCl_3$): δ 170.1, 134.2, 116.1, 42.0, 23.0. ESI-MS: Expected for $C_5H_{10}N_1O_1$ ($M+H^+$)= *m/z* 100.0757. Found: *m/z* 100.0756. N-Allylacetamide (**5.20**, 0.10 g, 1.8 mmol) was dissolved in 2-propanol (2 mL) and toluene (1 mL). Comound **5.10** (0.11 g, 0.35 mmol) was added to the reaction was subsequently heated from room temperature to 50 °C. This temperature was maintained for 4 hours. The crude was analysed by HRMS which confirmed the presence of the oxime product **5.21**. ESI-MS: Expected for $C_{24}H_{24}N_2Na_1O_2S_1$ ($M+Na^+$) = *m/z* 427.1451. Found *m/z* 427.1435. The reaction was concentrated and the residue was purified by silica gel chromatography (10 % EtOAc/petroleum ether → 10 % MeOH/EtOAc) but the product could not be isolated.

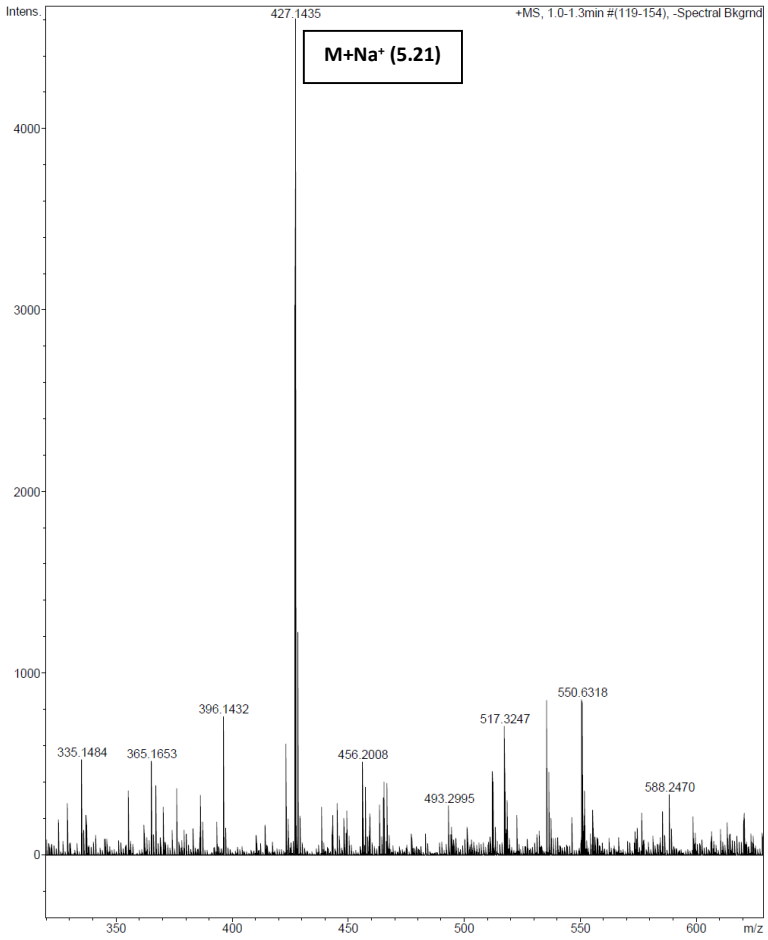

Mass spectrum of synthesis of *N-[(2E,Z)-2-(hydroxyimino)-3-(tritylsulfanyl)propyl]acetamide* (**5.21**).

Synthesis of D-Biotin allylamide (**5.23**) and *methyl N-acetyl-S-[(2Z)-2-(hydroxyimino)-3-({5-[(3aS,4S,6aR)-2-oxohexahydro-1H-thieno[3,4-d]imidazol-4-yl]pentanoyl}amino)propyl]-L-cysteinate* (**5.25**).

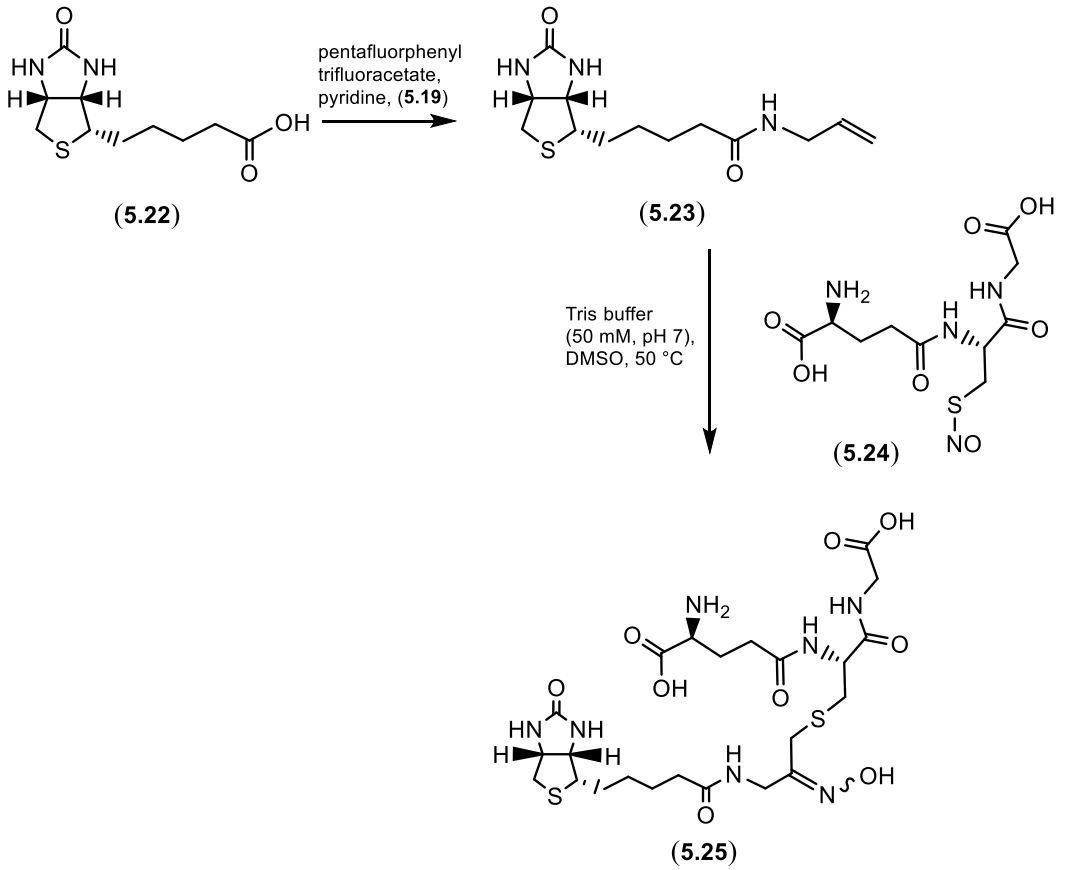

Pentafluorophenyl trifluoroacetate (1.4 eq., 0.200 mL, 1.15 mmol) was added to a stirred solution of D-biotin (**5.22**, 0.20 g, 0.819 mmol) in pyridine (3 mL) and the mixture stirred at room temperature for 1 hour. Allylamine (**5.19**, 2 eq., 0.12 mL, 1.64 mmol) was then added to the mixture and stirring continued for a further 30 minutes. The mixture was concentrated and purified by silica gel chromatography (100 % EtOAc $\rightarrow$ 15 % MeOH/CH_2Cl_2) to give **5.23** as a white amorphous powder (225 mg, 97 %). Spectral data was consistant with that reported in the literature [202]. ^{1}H NMR, CD_3OD, 400 MHz: δ 8.12 (s, 1H, NH), 5.91 (m, 1H), 5.24 (dd, 1H, *J* = 1.6 & 17.2 Hz), 5.16 (dd, 1H, *J* = 1.6 & 10.3 Hz), 4.56 (dd, 1H, *J* = 5.0 & 7.8 Hz), 4.37 (dd, 1H, *J* = 4.5 & 7.8 Hz), 3.86 (m, 2H), 3.28 (m, 1H), 3.0 (dd, 1H, *J* = 5.0 & 12.7 Hz), 2.78 (d, 1H, *J* = 12.7 Hz), 2.30 (t, 2H, *J* = 7.4 Hz), 1.86-1.62 (m, 4H), 1.56-1.48 (m, 2H).

^{13}C NMR, 100 MHz, (CD_3OD): δ 175.9, 166.2, 135.6, 116.2, 63.4, 61.7, 57.0, 42.7, 41.1, 36.8, 29.8, 29.5, 26.9. Infrared (KBr): 3294, 1698 cm^{-1}. ESI-HRMS: Expected for $C_{13}H_{22}N_3O_2S_1$ ($M+H^+$) = *m/z* 284.1427. Found: *m/z* 284.1426. SNO-glutathione (**5.24**, 20.0 mg, 0.0595 mmol) was dissolved in Tris buffer (2 mL, 50 mM, pH = 7). A solution of **5.23** (3 eq., 51.0 mg, 0.180 mmol) in DMSO (0.5 mL) was added to the buffered solution of **5.24**. The reaction was heated from room temperature to 50 °C and held at this temperature for 4 hours. The reaction was analysed by HRMS which confirmed the presence of the oxime product **5.25**. ESI-MS: Expected for $C_{23}H_{38}N_7O_9S_2$ ($M+H^+$) = *m/z* 620.2167. Found: *m/z* 620.2146.

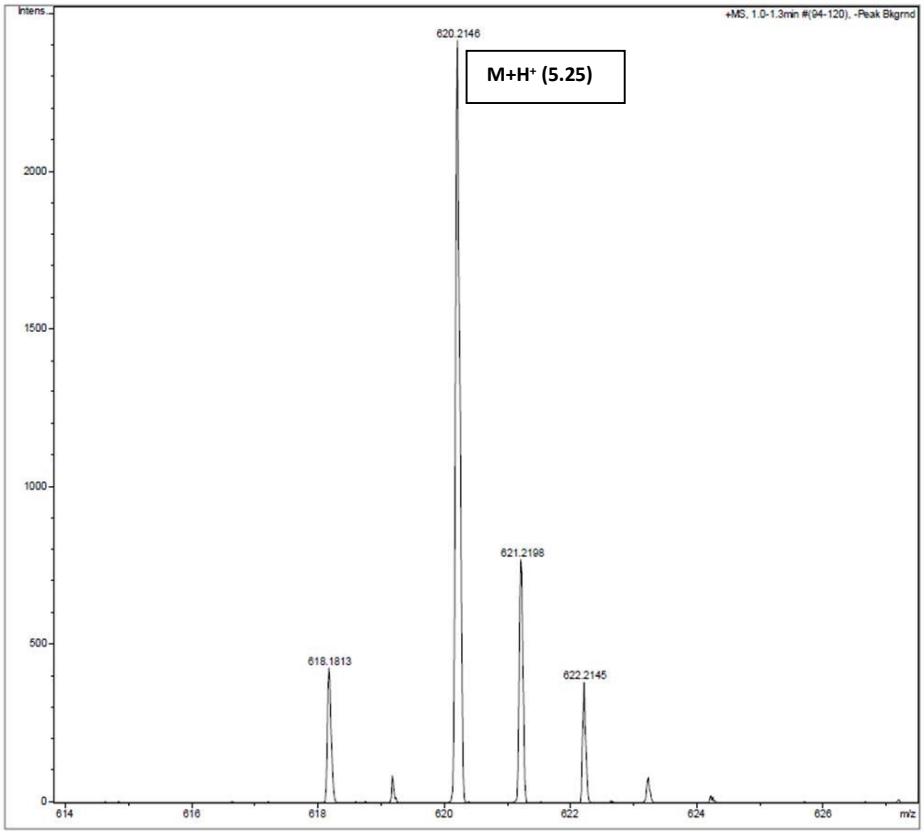

Mass spectrum for synthesis of *methyl N-acetyl-S-[(2Z)-2-(hydroxyimino)-3-({5-[(3aS,4S,6aR)-2-oxohexahydro-1H-thieno[3,4-d]imidazol-4-yl]pentanoyl}amino)propyl]-L-cysteinate* (**5.25**).

Synthesis of 6-({5-[(3aS,4S,6aR)-2-oxohexahydro-1H-thieno[3,4-d]imidazol-4-yl]pentanoyl}amino)-N-(prop-2-en-1-yl)hexanamide (**5.26**).

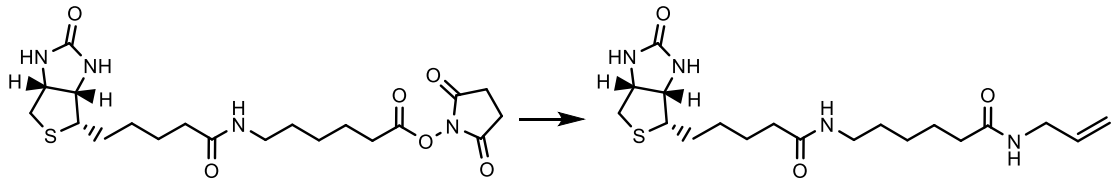

(**5.29**) (**5.26**)

Triethylamine (2 eq., 28.2 μL, 0.202 mmol) and allyl amine (4 eq., 30.4 μL, 0.405 mmol) were added to a stirred solution of succinimidyl-D-biotinamide hexonate (**5.29**,46.0 mg, 0.101 mmol) in dichloromethane (2 mL). The reaction was stirred for 1.5 hours at room temperature and then concentrated. The crude was purified by silica gel chromatography: 100 % EtOAc → 15 % MeOH/CH_2Cl_2) to yield **5.26** as a white amorphous powder (36 mg, 90 %). Spectral data was consistant with that reported in the literature [202]. ^{1}H NMR, 400 MHz, CD_3OD: δ 5.89 (m, 1H), 5.23 (dd, 1H, *J* = 1.6 & 17.2 Hz), 5.16 (dd, 1H, 1.6 & 10.3 Hz), 4.56 (dd, 1H, *J* = 5.0 & 7.8 Hz), 4.37 (dd, 1H, *J* = 4.5 & 7.8 Hz), 3.85 (m, 2H), 3.30-3.21 (m, 3H), 2.99 (dd, 1H, *J* = 5.0 & 12.7 Hz), 2.77 (d, 1H, *J* = 12.7 Hz), 2.27 (m, 4H), 1.85-1.35 (m, 12H). ^{13}C NMR, 100 MHz, CD_3OD: δ 176.0, 175.9, 166.1, 135.7, 116.2, 63.4, 61.7, 57.0, 42.7, 41.1, 40.2, 37.0, 36.9, 30.2, 29.8, 29.5, 27.6, 27.0, 26.7. Infrared (KBr): 1710, 1641 cm^{-1}. ESI-HRMS: Expected for $C_{19}H_{33}N_4O_3S_1$ ($M+H^+$) = *m/z* 397.2268. Found: *m/z* 397.2272.

Synthesis of *6-({5-[(3aS,4S,6aR)-2-oxohexahydro-1H-thieno[3,4-d]imidazol-4-yl]pentanoyl}amino)-N-[6-oxo-6-(prop-2-en-1-ylamino)hexyl]hexanamide* (**5.27**).

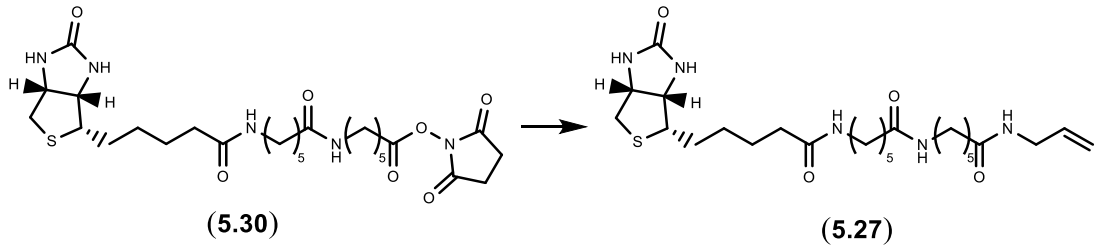

(**5.30**) (**5.27**)

Allylamine (10 eq., 66.1 µL, 0.881 mmol) was added to a stirred solution of D-biotinamidohexanoyl-6-amino-hexanoic acid *N*-hydroxysuccinimide ester (**5.30**, 50 mg, 0.0881 mmol) in DMF (3 mL). The mixture was stirred for 3 hours and then concentrated. The crude was purified by silica gel chromatography (100 % EtOAc $\rightarrow$ 15 % MeOH/CH_2Cl_2) to yield **5.27** as a white amorphous powder (34 mg, 76 %). ^{1}H NMR, 400 MHz, CD_3OD: δ 5.88 (m, 1H), 5.23 (dd, 1H, *J* = 1.5 & 17.2 Hz), 5.15 (dd, 1H, *J* = 1.5 & 10.3 Hz), 4.55 (dd, 1H, *J* = 5.0 & 7.7 Hz), 4.37 (dd, 1H, *J* = 4.5 & 7.7 Hz), 3.84 (m, 2H), 3.29-3.20 (m, 5H), 2.99 (dd, 1H, *J* = 4.9 & 12.7 Hz), 2.76 (d, 1H, *J* = 12.7 Hz), 2.30-2.22 (m, 6H), 1.85-1.46 (m, 19H). ^{13}C NMR, 100 MHz, CD_3OD: δ 176.1, 176.0, 175.9, 166.1, 135.6, 116.1, 63.4, 61.7, 57.0, 42.7, 41.1, 40.2, 37.0, 36.9, 36.8, 30.1, 29.8, 29.5, 27.6, 26.9, 26.7, 26.6. Infrared (KBr): 3298, 1706, 1636 cm^{-1}. ESI-HRMS, Expected for $C_{25}H_{44}N_5O_4S$ ($M+H^+$) = *m/z* 510.3109. Found: *m/z* 510.3111. HPLC: column: Phenomenex Luna-NH_2 (250 x 4.60 mm, 5 micron) column, gradient (0.5 mL/min) 100 % water $\rightarrow$ 9:1 (acetonitrile:water) over 20 minutes, retention time, 2.87 mins., purity, 98.7 %. Detection at 220 nm.

Synthesis of D-biotin propylamide (**5.28**).

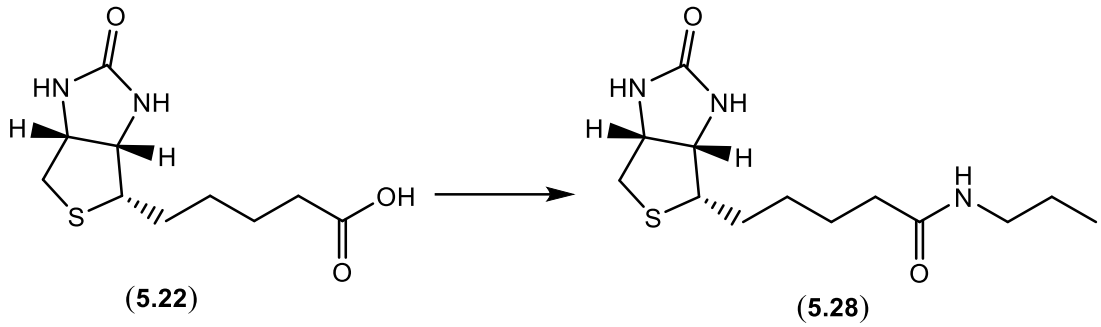

Pentafluorophenyl trifluoroacetate (1.5 eq., 211 μL, 1.16 mmol) was added to a stirred solution of D-biotin (**5.22**, 200 mg, 0.819 mmol) in pyridine (3 mL). The solution was stirred at room temperature for 1 hour, then propylamine (4 eq., 269 μL, 3.28 mmol) was added and the reaction was stirred for a further 60 minutes. The reaction was concentrated and purified by silica gel chromatography (100 % EtOAc → 15 % MeOH/CH_2Cl_2) to yield **5.28** as a white amorphous powder (217 mg, 93 %). Spectral data was consistant with that reported in the literature [203]. ^{1}H NMR, CD_3OD, 400 MHz: δ 4.55 (dd, 1H, *J* = 5.0 & 7.8 Hz), 4.36 (dd, 1H, *J* = 4.5 & 7.8 Hz), 3.27 (m, 1H), 3.18 (t, 2H, *J* = 7.2 Hz), 2.99 (dd, 1H, *J* = 5.0 & 12.8 Hz), 2.76 (d, 1H, *J* = 12.8 Hz), 2.26 (t, 2H, *J* = 7.3 Hz), 1.84-1.46 (m, 8H), 0.98 (t, 3H, *J* = 7.3 Hz). ^{13}C NMR, CD_3OD, 100 MHz: δ 176.0, 166.1, 63.4, 61.7, 57.0, 42.2, 41.1, 36.9, 29.8, 29.5, 27.0, 23.7, 11.7. Infrared (KBr): 1710 cm^{-1}. ESI-HRMS: Expected for $C_{13}H_{24}N_3O_2S_1$ ($M+H^+$) = *m/z* 286.1584. Found: *m/z* 286.1584.

Preparation of *S*-nitrosated BSA and Western blot analysis of allylamide functionalisation.

Commercial bovine serum albumin (BSA, 2 mg/mL) was incubated with DEA NONOate solution (1 mM) in light limited conditions for 20 minutes, where all reactions were performed in physiological salt solutions containing NaCl (130 mM), KCl (5 mM), $CaCl_2$ (1.5 mM), $MgCl_2$, $NaHCO_3$ (1 mM), KH_2PO_4 (1.5 mM), Hepes (25 mM), glucose (10 mM) (pH 7.3 with NaOH). Control samples were left untreated

without addition of DEA NONOate. Control and *S*-nitrosated BSA samples were incubated individually with either 450 µM of compounds **5.23**, **5.26**, **5.27** and **5.28** for 15 minutes at 60 ˚C under limited light conditions. For detection of protein biotinylation, 80 ng per protein sample were resolved alongside pre-biotinylated SDS-PAGE standard markers (Biorad, Hertfordshire, UK) as a positive control. Proteins were resolved using 4-12 % BIS-TRIS gradient gel and transferred to nitrocellulose membranes. Membranes were blocked with 5 % BSA and biotinylated proteins detected using neutravidin HRP. After washing steps, bound neutravidin HRP was detected by the ECL detection system (Amersham, GE Healthcare).

LC-MS analysis of *S*-nitrosated BSA functionalized with compound **5.27**.

A sample of *S*-nitrosated BSA (120 µL, 2 mg/mL) was incubated with a solution of **5.27** (5 µL, 10 mM) for 15 minutes at 37 °C. Peptic digestion of labelled BSA was then performed by addition of pepsin (50 µL, 0.3 mg/mL) in digestion buffer (1M NaH_2PO_4, pH = 2) and incubated for 2 hours at 37 °C. Biotinylated peptides were then separated using Captavidin biotin-binding agarose suspension. The digestion mixture was diluted in 0.5 mL of biotin-binding buffer (50 mM citrate phosphate buffer, pH 4) and applied to Captavidin resin. Biotinylated peptides were purified under standard conditions and eluted using 1 mL of elution buffer (50 mM sodium carbonate-HCl buffer, pH = 10). The eluent was then analysed by ES-LC-MS. In each of the MS experiments, the peptic digest was loaded onto a C-18 column (LC Packing, 100 Å pepMap, 1 mm × 150 mm) equilibrated with solvent A (solvent A: 0.05 % trifluoroacetic acid and 2 % acetonitrile in water). Elution of the peptides was accomplished using a gradient (0 % $\rightarrow$ 60 %) of solvent B over 60 min followed by 85 % solvent B over 20 min (solvent B: 0.045 % trifluoroacetic acid and 80 % acetonitrile in water). Solvents were pumped at a constant flow rate of 50 µL/min. Spectra were recorded in the single quadrupole scan mode (LC–MS), the quadrupole mass analyser was scanned over a mass-to-charge ratio (*m/z*) range of 100–2200 Da with a step size of 0.5 Da and a dwell time of 1.5 ms per step. The ion source voltage (ISV) was set at 5.5 kV and the orifice energy (OR) was 45 V.

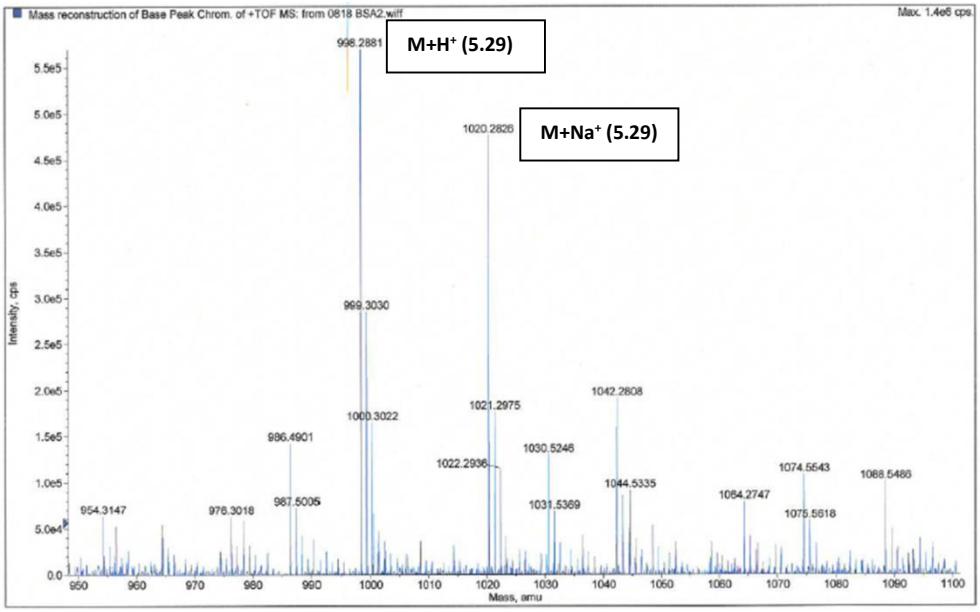

Mass spectrum of BSA functionalised with **5.27.**

Chapter 7: References

1. Means, G.E. and R.E. Feeney, *Chemical Modifications of Proteins: History and Applications.* Bioconjugate Chemistry, 1990. **1**(1): p. 2-12.

2. Glenny A. T. and Hopkins, B.E., *Diphtheria toxin as an immunizing agent.* British Journal of Experimental Pathology, 1923. **4**: p. 283-8.

3. Olcott, H.S. and H. Fraenkelconrat, *Specific Group Reagents for Proteins.* Chemical Reviews, 1947. **41**(1): p. 151-197.

4. Walsh, C.T., *Posttranslational Modification of Proteins: Expanding Nature's Inventory*. 2006: Roberts and Company Publishers.

5. Veronese, F.M. and G. Pasut, *PEGylation, successful approach to drug delivery.* Drug Discov Today, 2005. **10**(21): p. 1451-8.

6. Wang, L., W.J. Zhao, and W.H. Tan, *Bioconjugated Silica Nanoparticles: Development and Applications.* Nano Research, 2008. **1**(2): p. 99-115.

7. Kubler-Kielb, J. and V. Pozsgay, *A New Method for Conjugation of Carbohydrates to Proteins Using an Aminooxy-Thiol Heterobifunctional Linker.* The Journal of Organic Chemistry, 2005. **70**(17): p. 6987-6990.

8. Tyagarajan, K., E. Pretzer, and J.E. Wiktorowicz, *Thiol-reactive dyes for fluorescence labeling of proteomic samples.* Electrophoresis, 2003. **24**(14): p. 2348-2358.

9. Wenska, M., et al., *An activated triple bond linker enables 'click' attachment of peptides to oligonucleotides on solid support.* Nucleic Acids Research, 2011. **39**(20): p. 9047-9059.

10. de Araújo, A.D., et al., *Diels-Alder Ligation and Surface Immobilization of Proteins.* Angewandte Chemie International Edition, 2006. **45**(2): p. 296-301.

11. Qin, P.Z.F. and A.M. Pyle, *Site-specific labeling of RNA with fluorophores and other structural probes.* Methods-a Companion to Methods in Enzymology, 1999. **18**(1): p. 60-70.

12. Schaeffer, P.M. and N.E. Dixon, *Synthesis and Applications of Covalent Protein-DNA Conjugates.* Australian Journal of Chemistry, 2009. **62**(10): p. 1328-1332.

13. Panowski, S., et al., *Site-specific antibody drug conjugates for cancer therapy.* mAbs, 2014. **6**(1): p. 34-45.

14. Trail, P., *Antibody Drug Conjugates as Cancer Therapeutics.* Antibodies, 2013. **2**(1): p. 113-129.

15. Klein, D.L., *Pneumococcal conjugate vaccines: review and update.* Microb Drug Resist, 1995. **1**(1): p. 49-58.

16. Pollard, A.J., K.P. Perrett, and P.C. Beverley, *Maintaining protection against invasive bacteria with protein–polysaccharide conjugate vaccines.* Nature Reviews Immunology, 2009. **9**(3): p. 213-220.

17. Chalker, J.M., et al., *Chemical Modification of Proteins at Cysteine: Opportunities in Chemistry and Biology.* Chemistry - An Asian Journal, 2009. **4**(5): p. 630-640.

18. Hansen, R.E. and J.R. Winther, *An introduction to methods for analyzing thiols and disulfides: Reactions, reagents, and practical considerations.* Anal Biochem, 2009. **394**(2): p. 147-58.

19. Ban, H., J. Gavrilyuk, and C.F. Barbas, *Tyrosine Bioconjugation through Aqueous Ene-Type Reactions: A Click-Like Reaction for Tyrosine.* Journal of the American Chemical Society, 2010. **132**(5): p. 1523-1525.

20. Haun, M. and S. Wasi, *Biotinylated antibodies bound to streptavidin beads: a versatile solid matrix for immunoassays.* Anal Biochem, 1990. **191**(2): p. 337-42.

21. Dong, Y., K.S. Phillips, and Q. Cheng, *Immunosensing of Staphylococcus enterotoxin B (SEB) in milk with PDMS microfluidic systems using reinforced supported bilayer membranes (r-SBMs).* Lab on a Chip, 2006. **6**(5): p. 675-681.

22. [cited 2014 September 02]; Available from: http://www.piercenet.com/method/overview-elisa.

23. [cited 2014 September 18]; Available from: http://www.fda.gov/MedicalDevices/ProductsandMedicalProcedures/DeviceApprovalsandClearances/Recently-ApprovedDevices/ucm082556.htm.

24. Arney, A. and K.M. Bennett, *Molecular Diagnostics of Human Papillomavirus.* Laboratory Medicine, 2010. **41**(9): p. 523-530.

25. Jasanoff, A., *MRI contrast agents for functional molecular imaging of brain activity.* Current Opinion in Neurobiology, 2007. **17**(5): p. 593-600.

26. Koyama, T., et al., *Evaluation of selective tumor detection by clinical magnetic resonance imaging using antibody-conjugated superparamagnetic iron oxide.* Journal of Controlled Release, 2012. **159**(3): p. 413-418.

27. Townsend, D.W., *Physical principles and technology of clinical PET imaging.* Annals Academy of Medicine Singapore, 2004. **33**(2): p. 133-145.

28. Treglia, G. and M. Salsano, *PET imaging using radiolabelled antibodies: future direction in tumor diagnosis and correlate applications.* Research and Reports in Nuclear Medicine, 2013: p. 9.

29. [cited 2014 September 15]; Available from: http://ghr.nlm.nih.gov/condition/adenosine-deaminase-deficiency.

30. [cited 2014 September 15]; Available from http://www.drugabuse.gov/publications/teaching-packets/understanding-drug-abuse-addiction/section-ii/2-positron-emission-tomography-pet-scan-person-us.

31. Pollok, B.A. and R. Heim, *Using GFP in FRET-based applications.* Trends in Cell Biology, 1999. **9**(2): p. 57-60.

32. Zhang, C.-Y., et al., *Single-quantum-dot-based DNA nanosensor.* Nature Materials, 2005. **4**(11): p. 826-831.

33. Keppler, A., et al., *Labeling of fusion proteins with synthetic fluorophores in live cells.* Proceedings of the National Academy of Sciences of the United States of America, 2004. **101**(27): p. 9955-9959.

34. [cited 2014 December 03]; Available from: http://www.tankonyvtar.hu/en/tartalom/tamop425/0011_1A_Proteinbiotech_en_book/ch07.html.

35. Abuchowski, A., et al., *Alteration of immunological properties of bovine serum albumin by covalent attachment of polyethylene glycol.* J Biol Chem, 1977. **252**(11): p. 3578-81.

36. Abuchowski, A., et al., *Effect of covalent attachment of polyethylene glycol on immunogenicity and circulating life of bovine liver catalase.* J Biol Chem, 1977. **252**(11): p. 3582-6.

37. Yang, T., *PEGylation-Successful Approach for Therapeutic Protein Conjugation.* Modern Chemistry & Applications, 2013. **01**(04).

38. Fishburn, C.S., *The pharmacology of PEGylation: Balancing PD with PK to generate novel therapeutics.* Journal of Pharmaceutical Sciences, 2008. **97**(10): p. 4167-4183.

39. Li, H. and M. d'Anjou, *Pharmacological significance of glycosylation in therapeutic proteins.* Current Opinion in Biotechnology, 2009. **20**(6): p. 678-684.

40. Walsh, G., *Post-translational modifications of protein biopharmaceuticals.* Drug Discovery Today, 2010. **15**(17-18): p. 773-780.

41. Farkas, P. and S. Bystricky, *Chemical conjugation of biomacromolecules: A mini-review.* Chemical Papers, 2010. **64**(6): p. 683-695.

42. Peri, F., *Clustered carbohydrates in synthetic vaccines.* Chemical Society Reviews, 2013. **42**(11): p. 4543.

43. Lee, C.H., et al., *Preparation and characterization of an immunogenic meningococcal group A conjugate vaccine for use in Africa.* Vaccine, 2009. **27**(5): p. 726-732.

44. [cited 2015 March 28]; Available from: https://www.neb.com/~/media/NebUs/Page%20Images/Applications/Glycobiology/L1_Glycosylation.jpg?device=modal.

45. Rohrer, T., *Consideration for the safe and effective manufacturing of antibody drug conjugates.* Chimica Oggi-Chemistry Today, 2012. **30**(5): p. 76-79.

46. Kitson, S.L., et al., *Antibody-Drug Conjugates (ADCs) - Biotherapeutic bullets.* Chimica Oggi-Chemistry Today, 2013. **31**(4): p. 29-35.

47. [cited 2014 September]; Available from: http://www.nbe-therapeutics.com/template/smac_technology_mediated_generation_of_adcs.php.

48. [cited 2014 September 29]; Available from: http://www.everybody.co.nz/page-49c3fe4a-1a06-4571-b6ab-e365e6c3b681.aspx.

49. Cazet, A., et al., *Consequences of the expression of sialylated antigens in breast cancer.* Carbohydrate Research, 2010. **345**(10): p. 1377-1383.

50. Guo, Z.a.W., Q, *Recent development in carbohydrate-based cancer vaccines.* Current Opinion in Chemical Biology, 2009. **13**: p. 608-617.

51. Livingston, P.O., S.L. Zhang, and K.O. Lloyd, *Carbohydrate vaccines that induce antibodies against cancer .1. Rationale.* Cancer Immunology Immunotherapy, 1997. **45**(1): p. 1-9.

52. Zeichner, S.B., *The failed Theratope vaccine: 10 years later.* J Am Osteopath Assoc, 2012. **112**(8): p. 482-3.

53. Miles, D., et al., *Phase III Multicenter Clinical Trial of the Sialyl-TN (STn)-Keyhole Limpet Hemocyanin (KLH) Vaccine for Metastatic Breast Cancer.* The Oncologist, 2011. **16**(8): p. 1092-1100.

54. Goldblatt, D., *Conjugate vaccines.* Clinical and Experimental Immunology, 2000. **119**(1): p. 1-3.

55. Whitney, C.G., et al., *Decline in invasive pneumococcal disease after the introduction of protein-polysaccharide conjugate vaccine.* New England Journal of Medicine, 2003. **348**(18): p. 1737-1746.

56. Trotter, C.L., et al., *Optimising the use of conjugate vaccines to prevent disease caused by Haemophilus influenzae type b, Neisseria meningitidis and Streptococcus pneumoniae.* Vaccine, 2008. **26**(35): p. 4434-4445.

57. Dawson, P.E., et al., *Synthesis of Proteins by Native Chemical Ligation.* Science, 1994. **266**(5186): p. 776-779.

58. Wood, R.J., et al., *Optimized Conjugation of a Fluorescent Label to Proteins via Intein-Mediated Activation and Ligation.* Bioconjugate Chemistry, 2004. **15**(2): p. 366-372.

59. Rohde, H. and O. Seitz, *Invited reviewligation-Desulfurization: A powerful combination in the synthesis of peptides and glycopeptides.* Biopolymers, 2010. **94**(4): p. 551-559.

60. Staudinger, H. and J. Meyer, *Über neue organische Phosphorverbindungen III. Phosphinmethylenderivate und Phosphinimine.* Helvetica Chimica Acta, 1919. **2**(1): p. 635-646.

61. Saxon, E. and C.R. Bertozzi, *Cell surface engineering by a modified Staudinger reaction.* Science, 2000. **287**(5460): p. 2007-10.

62. Kohn, M. and R. Breinbauer, *The Staudinger ligation-a gift to chemical biology.* Angew Chem Int Ed Engl, 2004. **43**(24): p. 3106-16.

63. Kalia, J. and R.T. Raines, *Advances in Bioconjugation.* Curr Org Chem, 2010. **14**(2): p. 138-147.

64. Avci, F.Y., et al., *Isolation of carbohydrate-specific CD4(+) T cell clones from mice after stimulation by two model glycoconjugate vaccines.* Nature Protocols, 2012. **7**(12): p. 2180-2192.

65. Melnyk, O., et al., *Peptide Arrays for Highly Sensitive and Specific Antibody-Binding Fluorescence Assays.* Bioconjugate Chemistry, 2002. **13**(4): p. 713-720.

66. Falsey, J.R., et al., *Peptide and small molecule microarray for high throughput cell adhesion and functional assays.* Bioconjug Chem, 2001. **12**(3): p. 346-53.

67. Hein, C.D., X.-M. Liu, and D. Wang, *Click Chemistry, A Powerful Tool for Pharmaceutical Sciences.* Pharmaceutical Research, 2008. **25**(10): p. 2216-2230.

68. Nwe, K. and M.W. Brechbiel, *Growing applications of "click chemistry" for bioconjugation in contemporary biomedical research.* Cancer Biother Radiopharm, 2009. **24**(3): p. 289-302.

69. Houseman, B.T., et al., *Peptide chips for the quantitative evaluation of protein kinase activity.* Nat Biotechnol, 2002. **20**(3): p. 270-4.

70. Pozsgay, V., N.E. Vieira, and A. Yergey, *A Method for Bioconjugation of Carbohydrates Using Diels–Alder Cycloaddition.* Organic Letters, 2002. **4**(19): p. 3191-3194.

71. Cremers, C.M. and U. Jakob, *Oxidant sensing by reversible disulfide bond formation.* J Biol Chem, 2013. **288**(37): p. 26489-96.

72. Miseta, A. and P. Csutora, *Relationship between the occurrence of cysteine in proteins and the complexity of organisms.* Mol Biol Evol, 2000. **17**(8): p. 1232-9.

73. Rzychon, M., D. Chmiel, and J. Stec-Niemczyk, *Modes of inhibition of cysteine proteases.* Acta Biochimica Polonica, 2004. **51**(4): p. 861-873.

74. Fass, D., *Disulfide Bonding in Protein Biophysics.* Annual Review of Biophysics, Vol 41, 2012. **41**: p. 63-79.

75. Carter, P., *Site-Directed Mutagenesis.* Biochemical Journal, 1986. **237**(1): p. 1-7.

76. Tiwari, D.K., et al., *Synthesis and Characterization of Anti-HER2 Antibody Conjugated CdSe/CdZnS Quantum Dots for Fluorescence Imaging of Breast Cancer Cells.* Sensors, 2009. **9**(11): p. 9332-9354.

77. Ji, T., et al., *Increased Sensitivity in Antigen Detection with Fluorescent Latex Nanosphere−IgG Antibody Conjugates.* Bioconjugate Chemistry, 2010. **21**(3): p. 427-435.

78. [cited 2014 April 29]; Available from: http://hamptonresearch.com/product_detail.aspx?cid=4&sid=47&pid=47.

79. [cited 2014 October 13]; Available from: http://www.piercenet.com/product/tcep-hcl.

80. Getz, E.B., et al., *A comparison between the sulfhydryl reductants tris(2-carboxyethyl)phosphine and dithiothreitol for use in protein biochemistry.* Anal Biochem, 1999. **273**(1): p. 73-80.

81. Sechi, S. and B.T. Chait, *Modification of cysteine residues by alkylation. A tool in peptide mapping and protein identification.* Analytical Chemistry, 1998. **70**(24): p. 5150-5158.

82. [cited 2014 October 7]; Available from: http://www.fda.gov/Drugs/GuidanceComplianceRegulatoryInformation/Guidances/ucm122883.htm.

83. Hermanson, G.T., *Bioconjugate techniques*. 1996, San Diego: Academic Press. xxv, 785 p.

84. Morales-Sanfrutos, J., et al., *Vinyl sulfone: a versatile function for simple bioconjugation and immobilization.* Organic & Biomolecular Chemistry, 2010. **8**(3): p. 667.

85. *http://www.sigmaaldrich.com/catalog/product/sigma/s3401?lang=en&region=GB*. [cited 2014 September 19].

86. Shapira, E. and R. Arnon, *Cleavage of One Specific Disulfide Bond in Papain.* Journal of Biological Chemistry, 1969. **244**(4): p. 1026-&.

87. Thomas, M. and A.M. Klibanov, *Conjugation to gold nanoparticles enhances polyethylenimine's transfer of plasmid DNA into mammalian cells.* Proceedings of the National Academy of Sciences of the United States of America, 2003. **100**(16): p. 9138-9143.

88. Kim, Y.G., et al., *Efficient site-specific Labeling of proteins via cysteines.* Bioconjugate Chemistry, 2008. **19**(3): p. 786-791.

89. Yoshitake, S., et al., *Conjugation of Glucose-Oxidase from Aspergillus-Niger and Rabbit Antibodies Using N-Hydroxysuccinimide Ester of N-(4-Carboxycyclohexylmethyl)-Maleimide.* European Journal of Biochemistry, 1979. **101**(2): p. 395-399.

90. de Weers, O., et al., *Application of cystamine and N,N'-Bis(glycyl)cystamine as linkers in polysaccharide-protein conjugation.* Bioconjug Chem, 1998. **9**(3): p. 309-15.

91. Cleland, W.W., *Dithiothreitol New Protective Reagent for Sh Groups.* Biochemistry, 1964. **3**(4): p. 480-&.

92. Ruegg, U.T. and J. Rudinger, *Reductive cleavage of cystine disulfides with tributylphosphine.* Methods Enzymol, 1977. **47**: p. 111-6.

93. http://www.interchim.fr/ft/0/054721.pdf. [cited 2014 October 13].

94. Bell, S.J., et al., *Enhanced Circulating Half-Life and Antitumor Activity of a Site-Specific Pegylated Interferon-α Protein Therapeutic.* Bioconjugate Chemistry, 2008. **19**(1): p. 299-305.

95. Nobs, L., et al., *Surface modification of poly(lactic acid) nanoparticles by covalent attachment of thiol groups by means of three methods.* Int J Pharm, 2003. **250**(2): p. 327-37.

96. Kafi, K., et al., *Maleimide conjugation markedly enhances the immunogenicity of both human and murine idiotype-KLH vaccines.* Molecular Immunology, 2009. **46**(3): p. 448-456.

97. Schönberg, A., Chemische Berichte, 1935. **68**: p. 163-164.

98. Levison, M.E., A.S. Josephson, and D.M. Kirschenbaum, *Reduction of biological substances by water-soluble phosphines: gamma-globulin (IgG).* Experientia, 1969. **25**(2): p. 126-7.

99. Streuli, C.A., *Determination of Basicity of Substituted Phosphines by Nonaqueous Titrimetry.* Analytical Chemistry, 1960. **32**(8): p. 985-987.

100. Maclaren, J.A., *Quantitative Reduction and Alkylation of Wool.* Textile Research Journal, 1971. **41**(8): p. 713-&.

101. Kirley, T.L., *Determination of 3 Disulfide Bonds and One Free Sulfhydryl in the Beta-Subunit of (Na,K)-Atpase.* Journal of Biological Chemistry, 1989. **264**(13): p. 7185-7192.

102. Krijt, J., M. Vackova, and V. Kozich, *Measurement of homocysteine and other aminothiols in plasma: Advantages of using tris(2-carboxyethyl)phosphine as reductant compared with tri-n-butylphosphine.* Clinical Chemistry, 2001. **47**(10): p. 1821-1828.

103. http://www.bio-rad.com/en-uk/sku/163-2101-tributylphosphine-tbp. [cited 2014 May 28].

104. http://www.sigmaaldrich.com/catalog/product/aldrich/247049?lang=en&region=GB. [cited 2014 May 28].

105. Burns, J.A., et al., *Selective Reduction of Disulfides by Tris(2-Carboxyethyl)Phosphine.* Journal of Organic Chemistry, 1991. **56**(8): p. 2648-2650.

106. Han, J.C. and G.Y. Han, *A procedure for quantitative determination of tris(2-carboxyethyl)phosphine, an odorless reducing agent more stable and effective than dithiothreitol.* Anal Biochem, 1994. **220**(1): p. 5-10.

107. Krężel, A., et al., *Coordination Properties of Tris(2-carboxyethyl)phosphine, a Newly Introduced Thiol Reductant, and Its Oxide.* Inorg Chem, 2003. **42**(6): p. 1994-2003.

108. Cumnock, K., et al., *Trisulfide Modification Impacts the Reduction Step in Antibody-Drug Conjugation Process.* Bioconjugate Chemistry, 2013. **24**(7): p. 1154-1160.

109. Shafer, D.E., J.K. Inman, and A. Lees, *Reaction of tris(2-carboxyethyl)phosphine (TCEP) with maleimide and alpha-haloacyl groups: Anomalous elution of TCEP by gel filtration.* Analytical Biochemistry, 2000. **282**(1): p. 161-164.

110. Santarino, I.B., S.C.B. Oliveira, and A.M. Oliveira-Brett, *Protein reducing agents dithiothreitol and tris(2-carboxyethyl)phosphine anodic oxidation.* Electrochemistry Communications, 2012. **23**: p. 114-117.

111. Wang, Z., et al., *Desulfurization of cysteine-containing peptides resulting from sample preparation for protein characterization by mass spectrometry.* Rapid Communications in Mass Spectrometry, 2010. **24**(3): p. 267-275.

112. Liu, P., et al., *A tris (2-carboxyethyl) phosphine (TCEP) related cleavage on cysteine-containing proteins.* Journal of the American Society for Mass Spectrometry, 2010. **21**(5): p. 837-844.

113. Rhee, S.S. and D.H. Burke, *Tris(2-carboxyethyl)phosphine stabilization of RNA: comparison with dithiothreitol for use with nucleic acid and thiophosphoryl chemistry.* Analytical Biochemistry, 2004. **325**(1): p. 137-143.

114. Greenland, W.E. and P.J. Blower, *Water-soluble phosphines for direct labeling of peptides with technetium and rhenium: insights from electrospray mass spectrometry.* Bioconjug Chem, 2005. **16**(4): p. 939-48.

115. Bergendahl, V., et al., *On-column tris(2-carboxyethyl)phosphine reduction and IC5-maleimide labeling during purification of a RpoC fragment on a nickel–nitrilotriacetic acid Column.* Analytical Biochemistry, 2002. **307**(2): p. 368-374.

116. http://www.sigmaaldrich.com/catalog/product/aldrich/777854?lang=en&region=GB. [cited 2014 September 19].

117. Moiseev, D.V. and B.R. James, *Air-stability of aqueous solutions of (HOCH2)3P and (HOCH2CH2CH2)3P.* Inorganica Chimica Acta, 2011. **379**(1): p. 23-27.

118. Cline, D.J., et al., *New Water-Soluble Phosphines as Reductants of Peptide and Protein Disulfide Bonds: Reactivity and Membrane Permeability†.* Biochemistry, 2004. **43**(48): p. 15195-15203.

119. Švagera, Z., et al., *Study of disulfide reduction and alkyl chloroformate derivatization of plasma sulfur amino acids using gas chromatography–mass spectrometry.* Anal Bioanal Chem, 2012. **402**(9): p. 2953-2963.

120. http://hamptonresearch.com/product_detail.aspx?cid=4&sid=47&pid=47. [cited 2014 April 27].

121. http://www.piercenet.com/product/tcep-hcl. [cited 2014 October 13].

122. Espuelas, S., et al., *Effect of synthetic lipopeptides formulated in liposomes on the maturation of human dendritic cells.* Molecular Immunology, 2005. **42**(6): p. 721-729.

123. Kiesewetter, D.O., et al., *Radiolabeling of HER2-specific Affibody® molecule with F-18.* Journal of Fluorine Chemistry, 2008. **129**(9): p. 799-806.

124. Sánchez, A., E. Pedroso, and A. Grandas, *Oligonucleotide cyclization: the thiol-maleimide reaction revisited.* Chemical Communications, 2013. **49**(3): p. 309.

125. Maret, B., et al., *Reduction with tris(2-carboxyethyl)phosphine (TCEP) enables the use of an S-sulphonate protecting group for thiol-mediated bioconjugation.* RSC Advances, 2014. **4**(15): p. 7725.

126. Hedaya, E., Theodoro, S., *The preparation and reactions of stable phosphorus ylides derived from maleic anhydrides, maleimides or isomaleimides.* Tetrahedron, 1968. **24**: p. 2241-2254.

127. Giri, V.S., et al., *First Triphenylphosphine PromotedReduction of Maleimides to Succinimides.* Synthesis, 2003(10): p. 1549-1552.

128. Thomas, L.C. and Chittend.Ra, *Characteristic Infra-Red Absorption Frequencies of Organophosphorus Compounds .V. Phosphorus-Carbon Bonds.* Spectrochimica Acta, 1965. **21**(11): p. 1905-&.

129. Morpurgo, M., et al., *Preparation of characterization of poly(ethylene glycol) vinyl sulfone.* Bioconjug Chem, 1996. **7**(3): p. 363-8.

130. Cross, A.D. and R.A. Jones, *An introduction to practical infra-red spectroscopy*. 3ed. ed. 1969.

131. Cox, A.D., et al., *Investigating the candidacy of LPS-based glycoconjugates to prevent invasive meningococcal disease: chemical strategies to prepare glycoconjugates with good carbohydrate loading.* Glycoconjugate Journal, 2010. **27**(4): p. 401-417.

132. Nagorny, P., et al., *On the Emerging Role of Chemistry in the Fashioning of Biologics: Synthesis of a Bidomainal Fucosyl GM1-Based Vaccine for the Treatment of Small Cell Lung Cancer.* The Journal of Organic Chemistry, 2009. **74**(15): p. 5157-5162.

133. Ni, J., et al., *Toward a Carbohydrate-Based HIV-1 Vaccine: Synthesis and Immunological Studies of Oligomannose-Containing Glycoconjugates.* Bioconjugate Chemistry, 2006. **17**(2): p. 493-500.

134. Huang, Y.L., et al., *Carbohydrate-based vaccines with a glycolipid adjuvant for breast cancer.* Proceedings of the National Academy of Sciences, 2013. **110**(7): p. 2517-2522.

135. *http://www.cdc.gov/vaccines/pubs/pinkbook/downloads/pneumo.pdf*. [cited 2014 October 09].

136. Shriver-Lake, L.C., S.H. North, and C. Rowe Taitt, *Loss of cationic peptides with agarose gel-immobilized tris[2-carboxyethyl]phosphine (TCEP).* Biotechniques, 2013. **55**(6): p. 292-4.

137. Nepomniaschiy, N., et al., *Switch Peptide via Staudinger Reaction.* Organic Letters, 2008. **10**(22): p. 5243-5246.

138. Faucher, A.-M. and C. Grand-Maître, *tris(2-Carboxyethyl)phosphine (TCEP) for the Reduction of Sulfoxides, Sulfonylchlorides,N-Oxides, and Azides.* Synthetic Communications, 2003. **33**(20): p. 3503-3511.

139. Taddei, M., S. Ferrini, and E. Cini, *Synthetic Applications of 2-(Azidomethyl)allyltrimethylsilane.* Synlett, 2013. **24**(04): p. 491-495.

140. Sebastiano, R., et al., *A new deuterated alkylating agent for quantitative proteomics.* Rapid Communications in Mass Spectrometry, 2003. **17**(21): p. 2380-2386.

141. Lindorff-Larsen, K. and J.R. Winther, *Thiol alkylation below neutral pH.* Anal Biochem, 2000. **286**(2): p. 308-10.

142. *TOXNET Toxicology Data Network. http://toxnet.nlm.nih.gov/cgi-bin/sis/search/a?dbs+hsdb:@term+@DOCNO+1509. Accessed 22 July 2014.*

143. *http://www.reaxys.com*.

144. Ma, F.-H., et al., *Kinetic Assay of the Michael Addition-Like Thiol-Ene Reaction and Insight into Protein Bioconjugation.* Chemistry - An Asian Journal, 2014: p. n/a-n/a.

145. Jones, R.C., et al., *Supported palladium catalysis using a heteroleptic 2-methylthiomethylpyridine–N,S–donor motif for Mizoroki–Heck and Suzuki–Miyaura coupling, including continuous organic monolith in capillary microscale flow-through mode.* Tetrahedron, 2009. **65**(36): p. 7474-7481.

146. McKean, D.R., et al., *Synthesis of functionalized styrenes via palladium-catalyzed coupling of aryl bromides with vinyl tin reagents.* The Journal of Organic Chemistry, 1987. **52**(3): p. 422-424.

147. Liu, Z., et al., *A Zn2+Fluorescent Sensor Derived from 2-(Pyridin-2-yl)benzoimidazole with Ratiometric Sensing Potential.* Organic Letters, 2009. **11**(4): p. 795-798.

148. Carlsen, P.H.J., et al., *A greatly improved procedure for ruthenium tetroxide catalyzed oxidations of organic compounds.* The Journal of Organic Chemistry, 1981. **46**(19): p. 3936-3938.

149. *Gonzalez, J. et al. Inhibitors of Hepatitis C virus RNA-dependent RNA polymerase, and compositions and treatments using the same. WO 2006/018725 A1. 23.02.2006. United States Patent Application Publication.*

150. Familoni, O.B., et al., *The Baylis?Hillman approach to quinoline derivatives.* Organic & Biomolecular Chemistry, 2006. **4**(21): p. 3960.

151. *Bonnert, R. et al., NOVEL BENZOTHIAZOLONE DERIVATIVES, WO 2007/018461 A1, 15.02.2007.*

152. Maclaren, J.A., *Quantitative Reduction and Alkylation of Wool.* Textile Research Journal, 1971. **41**: p. 713.

153. Seth, D. and J.S. Stamler, *The SNO-proteome: causation and classifications.* Current Opinion in Chemical Biology, 2011. **15**(1): p. 129-136.

154. Ainscough, E.W. and A.M. Brodie, *Nitric-Oxide - Some Old and New Perspectives.* Journal of Chemical Education, 1995. **72**(8): p. 686-692.

155. Groves, J.T. and C.C. Wang, *Nitric oxide synthase: models and mechanisms.* Curr Opin Chem Biol, 2000. **4**(6): p. 687-95.

156. SoRelle, R., *Nobel Prize awarded to scientists for nitric oxide discoveries.* Circulation, 1998. **98**(22): p. 2365-2366.

157. Kroncke, K.D., K. Fehsel, and V. Kolb-Bachofen, *Nitric oxide: cytotoxicity versus cytoprotection--how, why, when, and where?* Nitric Oxide, 1997. **1**(2): p. 107-20.

158. Antosova, M., *Nitric oxide—important messenger in human body.* Open Journal of Molecular and Integrative Physiology, 2012. **02**(03): p. 98-106.

159. Berridge, M.J., *Cell Signalling Biology*.

160. Ng, E.S.M. and P. Kubes, *The physiology of S-nitrosothiols: carrier molecules for nitric oxide.* Canadian Journal of Physiology and Pharmacology, 2003. **81**(8): p. 759-764.

161. Schmidt, H.H., F. Hofmann, and J.P. Stasch, *Handbook of Experimental Pharmacology 191. cGMP: generators, effectors and therapeutic implications. Preface.* Handb Exp Pharmacol, 2009(191): p. v-vi.

162. Marozkina, N.V. and B. Gaston, *S-Nitrosylation signaling regulates cellular protein interactions.* Biochim Biophys Acta, 2012. **1820**(6): p. 722-9.

163. Davis, K.L., et al., *Novel effects of nitric oxide.* Annual Review of Pharmacology and Toxicology, 2001. **41**: p. 203-236.

164. Schrammel, A., *S-nitrosation of glutathione by nitric oxide, peroxynitrite, and •NO/O2•−.* Free Radical Biology and Medicine, 2003. **34**(8): p. 1078-1088.

165. Smith, B.C. and M.A. Marletta, *Mechanisms of S-nitrosothiol formation and selectivity in nitric oxide signaling.* Current Opinion in Chemical Biology, 2012. **16**(5-6): p. 498-506.

166. Grisham, M.B., D. Jourd'Heuil, and D.A. Wink, *Nitric oxide. I. Physiological chemistry of nitric oxide and its metabolites:implications in inflammation.* Am J Physiol, 1999. **276**(2 Pt 1): p. G315-21.

167. Hess, D.T., et al., *Protein S-nitrosylation: purview and parameters.* Nature Reviews Molecular Cell Biology, 2005. **6**(2): p. 150-166.

168. Chan, N.-L., P.H. Rogers, and A. Arnone, *Crystal Structure of the S-Nitroso Form of Liganded Human Hemoglobin†,‡.* Biochemistry, 1998. **37**(47): p. 16459-16464.

169. Weichsel, A., J.L. Brailey, and W.R. Montfort, *BuriedS-Nitrosocysteine Revealed in Crystal Structures of Human Thioredoxin†,‡.* Biochemistry, 2007. **46**(5): p. 1219-1227.

170. Kaneko, R. and Y. Wada, *Decomposition of protein nitrosothiolsin matrix-assisted laser desorption/ionization and electrospray ionization mass spectrometry.* Journal of Mass Spectrometry, 2003. **38**(5): p. 526-530.

171. Gow, A.J., *Basal and Stimulated Protein S-Nitrosylation in Multiple Cell Types and Tissues.* Journal of Biological Chemistry, 2002. **277**(12): p. 9637-9640.

172. Boullerne, A.I., et al., *Indirect evidence for nitric oxide involvement in multiple sclerosis by characterization of circulating antibodies directed against conjugated S-nitrosocysteine.* J Neuroimmunol, 1995. **60**(1-2): p. 117-24.

173. Foster, M.W., *Methodologies for the characterization, identification and quantification of S-nitrosylated proteins.* Biochimica et Biophysica Acta (BBA) - General Subjects, 2012. **1820**(6): p. 675-683.

174. Jaffrey, S.R., et al., *Protein S-nitrosylation: a physiological signal for neuronal nitric oxide.* Nat Cell Biol, 2001. **3**(2): p. 193-7.

175. Diers, A.R., A. Keszler, and N. Hogg, *Detection of S-nitrosothiols.* Biochimica et Biophysica Acta (BBA) - General Subjects, 2014. **1840**(2): p. 892-900.

176. Martínez-Ruiz, A. and S. Lamas, *Detection and Identification of S-Nitrosylated Proteins in Endothelial Cells.* 2005. **396**: p. 131-139.

177. Forrester, M.T., et al., *Detection of protein S-nitrosylation with the biotin-switch technique.* Free Radic Biol Med, 2009. **46**(2): p. 119-26.

178. Zhang, Y., et al., *Characterization and application of the biotin-switch assay for the identification of S-nitrosated proteins.* Free Radical Biology and Medicine, 2005. **38**(7): p. 874-881.

179. Wang, X., et al., *Copper dependence of the biotin switch assay: Modified assay for measuring cellular and blood nitrosated proteins.* Free Radical Biology and Medicine, 2008. **44**(7): p. 1362-1372.

180. Giustarini, D., et al., *Is ascorbate able to reduce disulfide bridges? A cautionary note.* Nitric Oxide, 2008. **19**(3): p. 252-258.

181. Huang, B. and C. Chen, *An ascorbate-dependent artifact that interferes with the interpretation of the biotin switch assay.* Free Radical Biology and Medicine, 2006. **41**(4): p. 562-567.

182. Chen, Y.J., W.C. Ching, and Y.P. Lin, *Methods for detection and characterization of protein S-nitrosylation.* Methods-a Companion to Methods in Enzymology, 2013. **62**(2): p. 138-50.

183. Wang, H. and M. Xian, *Fast Reductive Ligation ofS-Nitrosothiols.* Angewandte Chemie International Edition, 2008. **47**(35): p. 6598-6601.

184. Zhang, J., et al., *Reductive Ligation Mediated One-Step Disulfide Formation ofS-Nitrosothiols.* Organic Letters, 2010. **12**(18): p. 4208-4211.

185. Cavero, M., W.B. Motherwell, and P. Potier, *Studies on the intermolecular free radical addition of thionitrites to alkenes: a convenient method for the preparation of alpha-tritylthio oximes and related derivatives.* Tetrahedron Letters, 2001. **42**(26): p. 4377-4379.

186. Stamler, J.S., et al., *Nitric-Oxide Circulates in Mammalian Plasma Primarily as an S-Nitroso Adduct of Serum-Albumin.* Proceedings of the National Academy of Sciences of the United States of America, 1992. **89**(16): p. 7674-7677.

187. Gibson, J., *Collaborative work at the University of Bath, Department of Pharmacy and Pharmacology.* 2012.

188. He, S.-M., *Collaborative work at the University of British Columbia, Department of Chemistry.* 2012.

189. Krivec, M., et al., *A Way to Avoid Using Precious Metals: The Application of High-Surface Activated Carbon for the Synthesis of Isoindoles via the Diels–Alder Reaction of 2H-Pyran-2-ones.* The Journal of Organic Chemistry, 2012. **77**(6): p. 2857-2864.

190. Chudzik, S.J.e.a., *COATINGS FOR MEDICAL ARTICLES INCLUDING NATURAL BIODEGRADABLE POLYSACCHARIDES, US 2005/0255142 A l*. 17/11/2005: United States Patent Application Publication.

191. Bonger, K.M., et al., *Synthesis and evaluation of homo-bivalent GnRHR ligands.* Bioorganic & Medicinal Chemistry, 2007. **15**(14): p. 4841-4856.

192. Wen, W.-H., et al., *Synergistic Effect of Zanamivir−Porphyrin Conjugates on Inhibition of Neuraminidase and Inactivation of Influenza Virus.* Journal of Medicinal Chemistry, 2009. **52**(15): p. 4903-4910.

193. Jones, G., et al., *Triazolopyridines .18. Nucleophilic substitution reactions on triazolopyridines; A new route to 2,2'-bipyridines.* Tetrahedron, 1997. **53**(24): p. 8257-8268.

194. GmbH, A.C.S. 05/09/2014]; Available from: http://akoscompounds.de/catalogue/akossamplesretrieval.php?IDNUMBERS=AKOS015909967.

195. *Hong Kong Chemhere* 05/09/2014]; Available from: http://hkchemhere.com/?navTab=1

196. *Ryan Scientific Intermediate and Building Block Compounds*. 05/09/2014]; Available from: https://ryansci.com/products/4933443/view.

197. Bolli, M.H., et al., *Novel S1P1Receptor Agonists − Part 3: From Thiophenes to Pyridines.* Journal of Medicinal Chemistry, 2014. **57**(1): p. 110-130.

198. Ross, A.J., et al., *Parasite glycoconjugates. Part 11. Preparation of phosphodisaccharide synthetic probes, substrate analogues for the elongating alpha-D-mannopyranosylphosphate transferase in the Leishmania.* Journal of the Chemical Society-Perkin Transactions 1, 2001(1): p. 72-81.

199. Cheng, H., et al., *Synthesis and enzyme-specific activation of carbohydrate-geldanamycin conjugates with potent anticancer activity.* J Med Chem, 2005. **48**(2): p. 645-52.

200. Wang, H., J. Zhang, and M. Xian, *Facile formation of dehydroalanine from S-nitrosocysteines.* J Am Chem Soc, 2009. **131**(37): p. 13238-9.

201. Prediger, P.c., et al., *Substrate-Directable Heck Reactions with Arenediazonium Salts. The Regio- and Stereoselective Arylation of Allylamine Derivatives and Applications in the Synthesis of Naftifine and Abamines.* The Journal of Organic Chemistry, 2011. **76**(19): p. 7737-7749.

202. Weinrich, D., et al., *Preparation of Biomolecule Microstructures and Microarrays by Thiol-ene Photoimmobilization.* ChemBioChem, 2010. **11**(2): p. 235-247.

203. Crisp, G.T. and J. Gore, *Biotin derivatives as gelators of organic solvents.* Synthetic Communications, 1997. **27**(13): p. 2203-2215.

Appendix 1: THPP Reduction of α,β-Unsaturated Dicarbonyl Substrates

A1.0) Introduction

The rapid and mild conditions that resulted in the reduction of N-ethyl maleimide to N-ethyl succinimide by THPP, described previously in **Chapter 2**, prompted an investigation into the scope for THPP-mediated reduction of α,β-unsaturated dicarbonyl substrates. There are a number of methods available for reduction of 1,4-dicarbonyl substrates, including hydrogenation reactions using metal catalysts such as Pd [1-3], Ru [4] or $SnCl_2$/HCl [5], however, trisubstituted phosphines could offer an alternative method. Tributylphosphine and diethylphenylphosphine have been previously reported to reduce *trans*-dibenzoylethylene to 1,2-benzoylethane [6]. The reactions, however, required pre-forming the ylide intermediate in an anhydrous organic solvent, followed by a hydrolysis reaction by addition of water. The anhydrous organic solvents are probably required to dissolve the hydrophobic phosphines and also to prevent oxidation of the phosphines to phosphine oxides. Triphenylphosphine has been utilised to reduce maleimide to succinimide, although refluxing in an organic solvent was required [7]. The phosphorus containing Woollins reagent has also been reported to reduce α,β-unsaturated diketones [8]. THPP was investigated as a reagent for the mild reduction of α,β-unsaturated dicarbonyl substrates.

A1.1) Reduction of α,β-Unsaturated Diesters and Diketones by THPP

It was envisaged to investigate the potential of the water soluble THPP to rapidly reduce α,β-unsaturated diesters and diketones at room temperature and in an aqueous environment, with addition of minimal organic solvent (THF) to ensure dissolution of the 1,4-dicarbonyl substrates.

A selection of α,β-unsaturated dicarbonyl substrates were investigated and successfully reduced by THPP (**Figure A1.1**) at ambient temperature and complete within an hour. Reduction reactions were successful on unsaturated 1,4-diester and 1,4-diketo substrates and also reduced both *E* and *Z* isomers in very good yield.

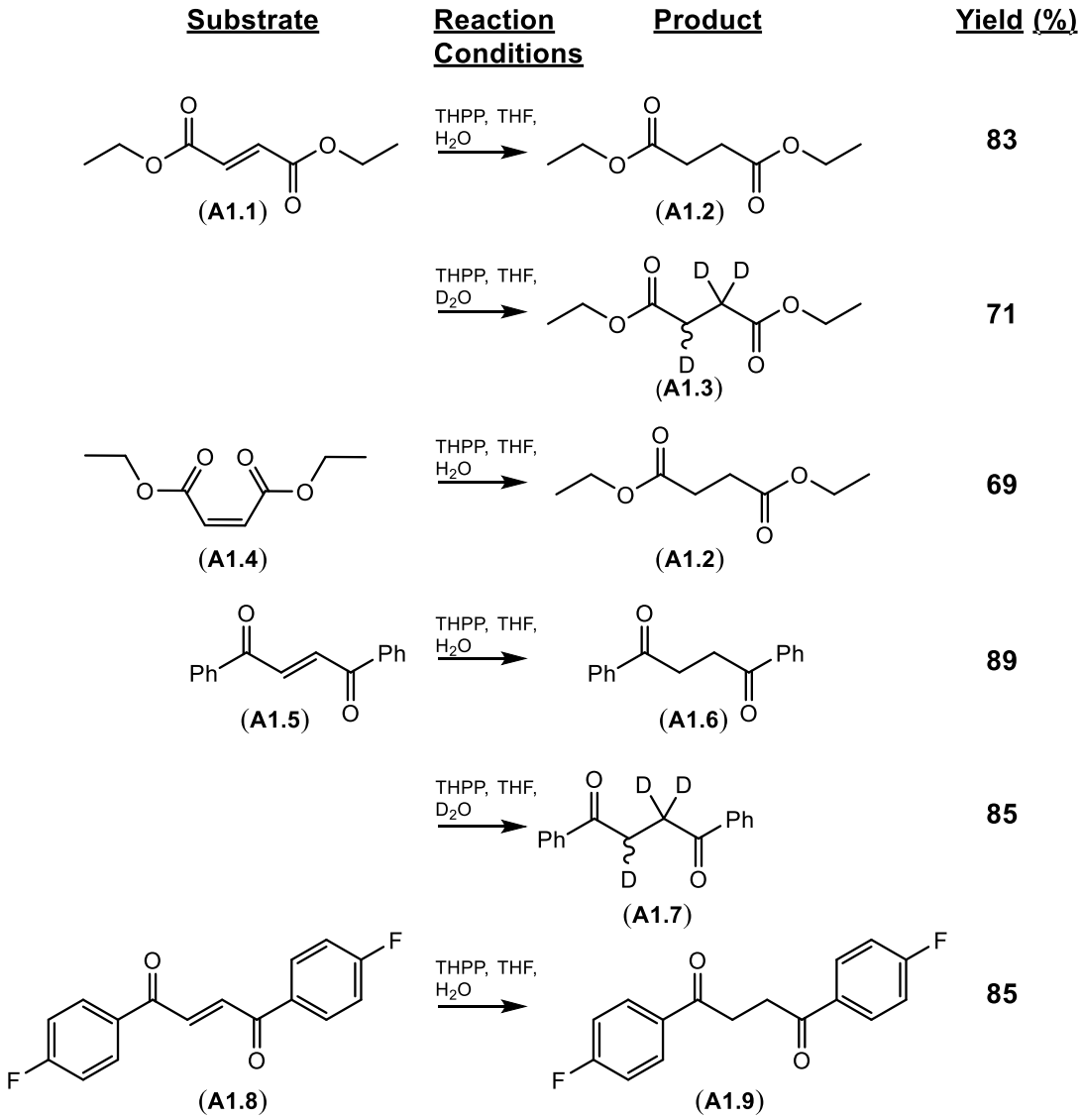

Figure A1.1: Reduction of α,β-unsaturated diesters and diketones by THPP.

Reduction reactions were also performed in deuterium oxide on a selection of substrates and consistently resulted in the incorporation of 3 deuterium atoms during saturation of the alkene (**A1.3** & **A1.7**). The characterisation of the deuterated products indicated the reduction occurred through a similar mechanism

of reduction to that proposed for N-ethyl maleimide in **Chapter 2**. A general mechanism for reduction is illustrated in **Figure A1.2**.

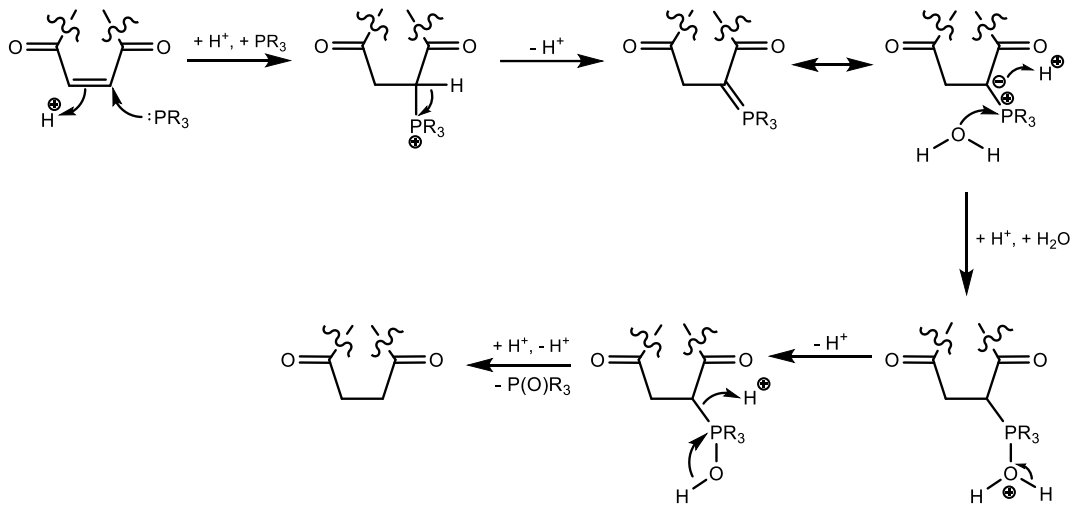

Figure A1.2: Mechanism of reduction of α,β-unsaturated diesters and diketones by THPP.

A1.2) Conclusion

THPP has been proven to be a rapid and efficient reducing agent for α,β-unsaturated dicarbonyl substrates under very mild, aqueous conditions. The method is convenient as the reduced product can be isolated in high yield through a simple extraction with diethyl ether, while the phosphine or phosphine oxide remains in the aqueous phase.

Experimental

Synthesis of diethyl butanedioate (**A1.2**).

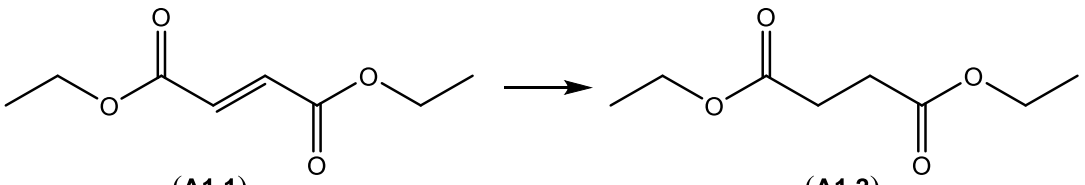

(**A1.1**) (**A1.2**)

Diethyl fumarate (**A1.1**, 0.10 g, 0.581 mmol) was dissolved in THF/water (2:8, 4.5 mL). A solution of THPP (**2.7**, 1 eq., 0.12 g, 0.581 mmol) was prepared in water (0.5 mL) and added slowly to the rapidly stirring solution. The reaction was left to stir for 30 minutes at room temperature. The reaction was diluted with 50 mL of diethyl ether and extracted with water (30 mL). The aqueous layer was extracted with diethyl ether (2 x 30 mL). The organic extraction layer were combined and dried over $MgSO_4$. The mixture was filtered and the organic solution was concentrated. The residue was purified by silica gel chromatography (CH_2Cl_2 $\rightarrow$ 2 % acetone/CH_2Cl_2) to yield **A1.2** as a clear oil (84.0 mg, 83 %). Spectral data consistent with data from commercial source [9]. ^{1}H NMR, $CDCl_3$, 400 MHz: δ 4.12 (q, 4 H, *J* = 7.2 Hz), 2.59 (s, 4H), 1.23 (t, 6H, *J* = 7.2 Hz). ^{13}C NMR, $CDCl_3$, 100 MHz: δ 172.3, 60.6, 29.1, 14.1. ESI-HRMS: Expected for $C_8H_{14}Na_1O_4$ ($M+Na^+$) = *m/z* 197.0790. Found: *m/z* 197.0785.

Synthesis of *diethyl-2-dideutero-(3R,S)-deutero butanedioate* (**A1.3**).

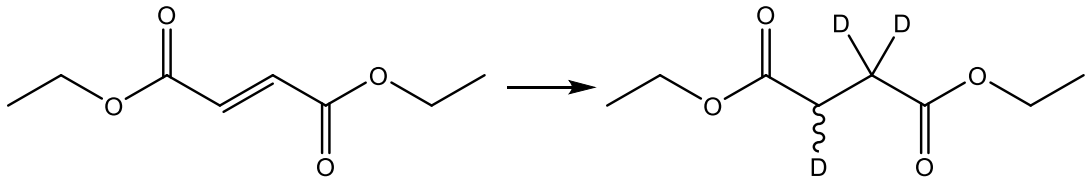

(**A1.1**) (**A1.3**)

Diethyl fumarate (**A1.1**, 0.10 g, 0.581 mmol) was dissolved in THF/deuterium oxide (2:8, 4.5 mL). A solution of THPP (**2.7**, 1 eq., 0.12 g, 0.581 mmol) was prepared in deuterium oxide (0.5 mL) and added slowly to the rapidly stirring solution. The reaction was left to stir for 30 minutes at room temperature. The reaction was extracted with 50 mL of diethyl ether. The aqueous layer was extracted with diethyl ether (2 x 30 mL). The organic extraction layer were combined and dried over $MgSO_4$. The mixture was filtered and the organic solution was concentrated. The residue was purified by silica gel chromatography ($CH_2Cl_2 \rightarrow$ 2 % acetone/CH_2Cl_2) to yield **A1.3** as a clear oil (82.6 mg, 71 %). ^{1}H NMR, $CDCl_3$, 400 MHz: δ 4.07 (q, 4H, *J* = 7.1 Hz), 2.51 (s, 1H), 1.18 (t, 6H, *J* = 7.1 Hz). ^{13}C NMR, $CDCl_3$, 100 MHz: δ 172.14, 60.43, 28.52 (m), 13.96. ESI-HRMS: Expected for $C_8H_{11}D_3Na_1O_4$ ($M+Na^+$) = 200.0973. Found: 200.0972. Infrared (thin film): 1738 cm^{-1}. HPLC: column: Phenomenex Luna-C18 (250 x 4.60 mm), gradient (0.7 mL/min) 100 % water $\rightarrow$ 9:1 (acetonitrile:water) over 20 minutes, retention time: 18.40 mins., purity: 90.4 %. Detection at 225 nm.

Synthesis of diethyl butanedioate **(A1.2)**.

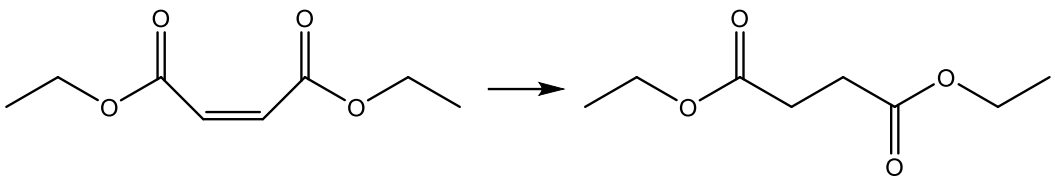

(**A1.4**) (**A1.2**)

Diethyl maleate (**A1.4**, 0.11 g, 0.621 mmol) was dissolved in THF/water (2:8, 4.5 mL). A solution of THPP (**2.7**, 1 eq., 0.13 g, 0.620 mmol) was prepared in water (0.5 mL) and added slowly to the rapidly stirring solution. The reaction was left to stir for 30 minutes at room temperature. The reaction was diluted with 50 mL of diethyl ether and extracted with water (30 mL). The aqueous layer was extracted with diethyl ether (2 x 30 mL). The organic extraction layer were combined and dried over $MgSO_4$. The mixture was filtered and the organic solution was concentrated. The residue was purified by silica gel chromatography (CH_2Cl_2 $\rightarrow$ 2 % acetone/CH_2Cl_2) to yield **A1.2** as a clear oil (75.0 mg, 69 %).

Synthesis of 1,4-diphenylbutane-1,4-dione (**A1.6**).

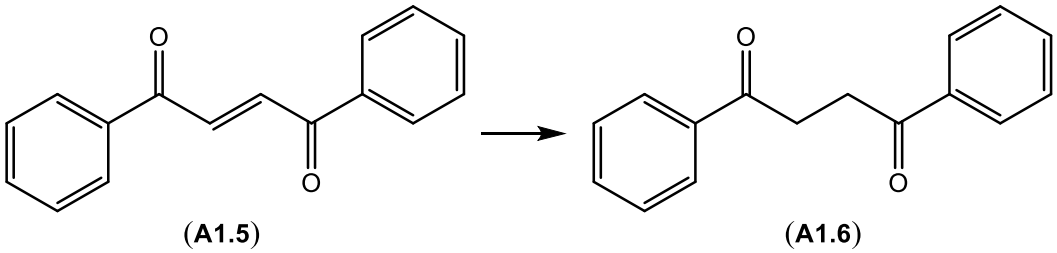

(**A1.5**) (**A1.6**)

Trans-1,4-diphenyl-2-butene-1,4-dione (**A1.5**, 0.17 mg, 0.731 mmol) was dissolved in THF/water (2:8, 4.5 mL). A solution of THPP (**2.7**, 1 eq., 0.15 g, 0.731 mmol) was prepared in water (0.5 mL) and added slowly to the rapidly stirring solution. The reaction was left to stir for 30 minutes at room temperature. The reaction was diluted with 50 mL of diethyl ether and extracted with water (30 mL). The aqueous layer was extracted with diethyl ether (2 x 30 mL). The organic extraction layer were combined and dried over $MgSO_4$. The mixture was filtered and the organic solution was concentrated. The residue was purified by silica gel chromatography (10 % CH_2Cl_2/Petroleum ether $\rightarrow$ 100 % CH_2Cl_2) to yield **A1.6** as a white solid (155 mg, 89 %). NMR data consistent with literature [10]. ^{1}H NMR, $CDCl_3$, 400 MHz: δ 8.06-8.03 (m, 4H), 7.60-7.56 (m, 2H), 7.50-7.46 (m, 4H), 3.47 (s, 4H). ^{13}C NMR, $CDCl_3$, 100 MHz: δ 198.6, 136.7, 133.1, 128.6, 128.1, 32.5. ESI-HRMS: Expected for $C_{16}H_{14}Na_1O_2$ ($M+Na^+$) = 261.0891. Found 261.0930.

Synthesis of *1,4-diphenyl-2-dideutero-(3R,S)-deutero butane-1,4-dione* (**A1.7**).

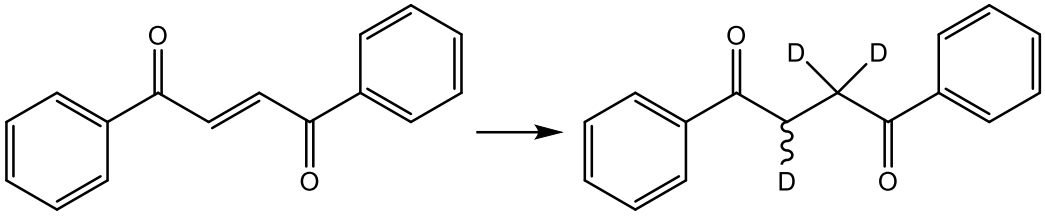

(**A1.5**) (**A1.7**)

Trans-1,4-diphenyl-2-butene-1,4-dione (**A1.5**, 0.11 mg, 0.466 mmol) was dissolved in THF/water (2:8, 4.5 ml). A solution of THPP (**2.7**, 1 eq., 96.8 mg, 0.466 mmol) was prepared in water (0.5 mL) and added slowly to the rapidly stirring solution. The reaction was left to stir for 30 minutes at room temperature. The reaction was diluted with 50 mL of diethyl ether and extracted with water (30 mL). The aqueous layer was extracted with diethyl ether (2 x 30 mL). The organic extraction layer were combined and dried over $MgSO_4$. The mixture was filtered and the organic solution was concentrated. The residue was purified by silica gel chromatography (5 % EtOAc/Petroleum ether $\rightarrow$ 40 % EtOAc/Petroleum ether) to yield **A1.7** as a white solid (95.5 mg, 85 %). ^{1}H NMR, $CDCl_3$, 400 MHz: δ 8.04-7.46 (m, 10H, Ar-H), 3.43 (br. s, 1H). ^{13}C NMR, $CDCl_3$, 100 MHz: δ 198.8 & 198.7 (2 x C=O), 136.7, 133.1, 128.6, 128.1, 32.2. ESI-HRMS: Expected for $C_{16}H_{11}D_3Na_1O_2$ ($M+Na^+$) = *m/z* 264.1074. Found: *m/z* 264.1099. Infrared (thin film): 1676, 1451 cm^{-1}. HPLC: column: Waters Symmetry Shield RP_8 (100 x 4.60 mm), gradient elution: (0.5 mL/min) 5 % MeCN in water $\rightarrow$ 100 % MeCN over 20 minutes, retention time, 17.19 mins., purity: 95.2 %. Detection at 280 nm.

Synthesis of 1,4-bis(4-fluorophenyl)butane-1,4-dione (**A1.9**).

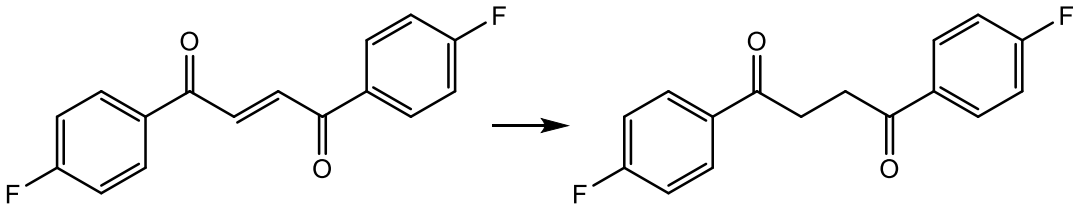

(**A1.8**) (**A1.9**)

Trans-1,4-(4-fluorophenyl)-2-butene-1,4-dione (**A1.8**, 0.13 g, 0.478 mmol) was dissolved in THF/water (2:8, 4.5 mL). A solution of THPP (**2.7**, 1 eq., 96.8 mg, 0.478 mmol) was prepared in water (0.5 mL) and added slowly to the rapidly stirring solution. The reaction was left to stir for 30 minutes at room temperature. The reaction was diluted with 50 mL of diethyl ether and extracted with water (30 mL). The aqueous layer was extracted with diethyl ether (2 x 30 mL). The organic extraction layer were combined and dried over $MgSO_4$. The mixture was filtered and the organic solution was concentrated. The residue was purified by silica gel chromatography (5 % EtOAc/Petroleum ether $\rightarrow$ 40 % EtOAc/Petroleum ether) to yield **A1.9** as a white solid (0.11 g, 85 %). NMR data consistent with literature [10]. ^{1}H NMR, $CDCl_3$, 400 MHz: δ 8.08-8.04 (m, 4H), 7.17-7.12 (m, 4H), 3.42 (s, 4H). ^{13}C NMR, $CDCl_3$, 100 MHz: δ 196.98 (2C), 165.81 (d, 2C, *J* = 254.72 Hz), 133.10 (d, 2C, *J* = 3.01 Hz), 130.73 (d, 4C, *J* = 9.31 Hz), 115.69 (d, 4C, *J* = 21.87 Hz), 32.39 (2C). ^{19}F NMR, $CDCl_3$, 470 MHz: δ -105.10. ESI-HRMS: Expected for $C_{16}H_{12}F_2Na_1O_2$ ($M+Na^+$) = m/z 297.0703. Found: m/z 297.0708.

References

1. Chang, F., et al., *Highly efficient solvent-free catalytic hydrogenation of solid alkenes and nitro-aromatics using Pd nanoparticles entrapped in aluminum oxy-hydroxide.* Tetrahedron Letters, 2010. **51**(32): p. 4250-4252.

2. M, L.K., P. T, and M. S.V, *Layered double hydroxides supported nano palladium: An efficient catalyst for the chemoselective hydrogenation of olefinic bonds.* Journal of Molecular Catalysis A: Chemical, 2012. **365**: p. 115-119.

3. Oyamada, H., T. Naito, and S. Kobayashi, *Continuous flow hydrogenation using polysilane-supported palladium/alumina hybrid catalysts.* Beilstein Journal of Organic Chemistry, 2011. **7**: p. 735-739.

4. Mercadante, M.A., et al., *Continuous Flow Hydrogenation Using an On-Demand Gas Delivery Reactor.* Organic Process Research & Development, 2012. **16**(5): p. 1064-1068.

5. Kotani, S., et al., *A Tertiary Amine as A Hydride Donor: Trichlorosilyl Triflate-mediated Conjugate Reduction of Unsaturated Ketones.* Organic Letters, 2011. **13**(15): p. 3968-3971.

6. Ramirez, F., O.P. Madan, and C.P. Smith, *Reaction of Trivalent Phosphorus Compounds with Alpha,Beta-Unsaturated Ketones - Reaction of Amino Alkyl and Aryl Phosphines with Trans-Dibenzoylethylene 31p Nuclear Magnetic Resonance.* Tetrahedron, 1966. **22**(2): p. 567-&.

7. Giri, V.S., et al., *First Triphenylphosphine PromotedReduction of Maleimides to Succinimides.* Synthesis, 2003(10): p. 1549-1552.

8. Jaisankar, P., M. Mandal, and S. Chatterjee, *Woollins Reagent: A Chemoselective Reducing Agent for 1,4-Enediones and 1,4-Ynediones to Saturated 1,4-Diones.* Synlett, 2012. **23**(18): p. 2615-2618.

9. [cited 2014 October 20]; Available from: http://www.sigmaaldrich.com/spectra/fnmr/FNMR000370.PDF.

10. Peppe, C. and R. Pavão das Chagas, *Indium(I) Bromide-Mediated Reductive Coupling of α,α-Dichloroketones to 1-Aryl-butane-1,4-diones.* Synlett, 2004(7): p. 1187-1190.

Appendix 2: Reaction of a TCEP-Maleimide Ylene Adduct with Selectfluor®

A2.0) Introduction

Chapter 2 describes the reaction of TCEP (**2.6**) with maleimide functionalised ligands **2.8** & **2.11**, resulting in ylene adducts of TCEP and maleimide (**2.9** & **2.12**). The ylene adduct **2.9** was subsequently incubated with glutathione (**2.21**) to investigate the potential reaction of the nucleophilic thiol of **2.21** with **2.9**. The reaction was performed at pH = 4, 7 and 8 and monitored by either NMR spectroscopy or mass spectrometry. No reaction between **2.9** and **2.21** was detected. The stability of **2.9** towards nucleophilic attack by a thiol over a wide pH range suggested that TCEP should be removed from the reaction before attempting a bioconjugation reaction utilising a thiol alkylation reagent based on maleimide.

The potential reaction of **2.9** with an electrophilic reagent was subsequently investigated since the ylene adduct **2.9** resembles an ylide intermediate utilised in the Wittig reaction for the synthesis of alkene derivatives.

A2.1) Reaction of 2.9 with Selectfluor®

The reaction of the ylene **2.9** with an electrophile was investigated by incubating **2.9** with selectflour®, a source of electrophilic fluorine (**Figure A2.1**). Purification of the reaction by silica gel chromatography yielded a racemic mixture of (3*R*)-1-ethyl-3-fluoropyrrolidine-2,5-dione (**A2.1**) and (3*S*)-1-ethyl-3-fluoropyrrolidine-2,5-dione (**A2.2**).

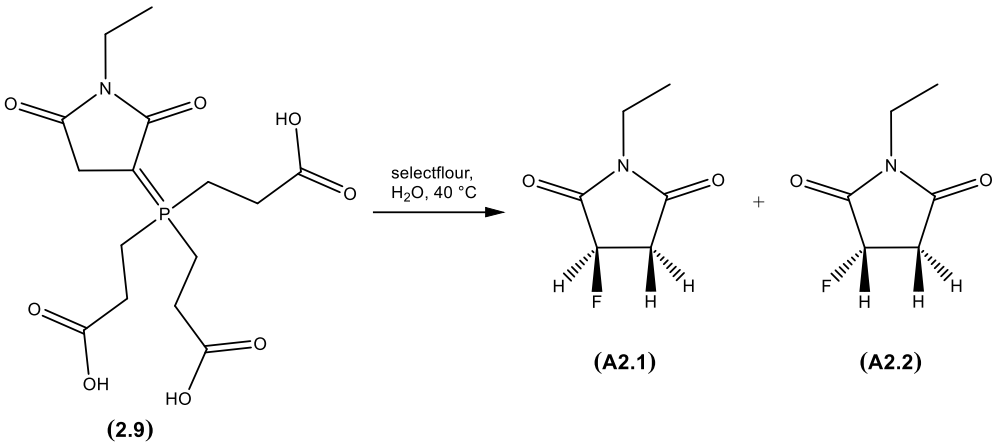

Figure A2.1: Reaction of **2.9** with Selectfluor®

A1.2) Conclusion

The ylene **2.9** reacted with Selectfluor® to yield a racemate of **A2.1** and **A2.2**. The isolation and characterisation of **A2.1** and **A2.2** suggested that **2.9** is capable of reacting with electrophilic reagents analogous to ylide derivatives, which react with electrophilic substrates in a Wittig reaction. The reaction of **2.9** with electrophilic Selectfluor® provided further evidence for **2.9** existing as an ylene derivative, which was suggested in Chapter 2.

Experimental

Synthesis of (3*R*)-1-ethyl-3-fluoropyrrolidine-2,5-dione (**A2.1**) and (3*S*)-1-ethyl-3-fluoropyrrolidine-2,5-dione (**A2.2**)

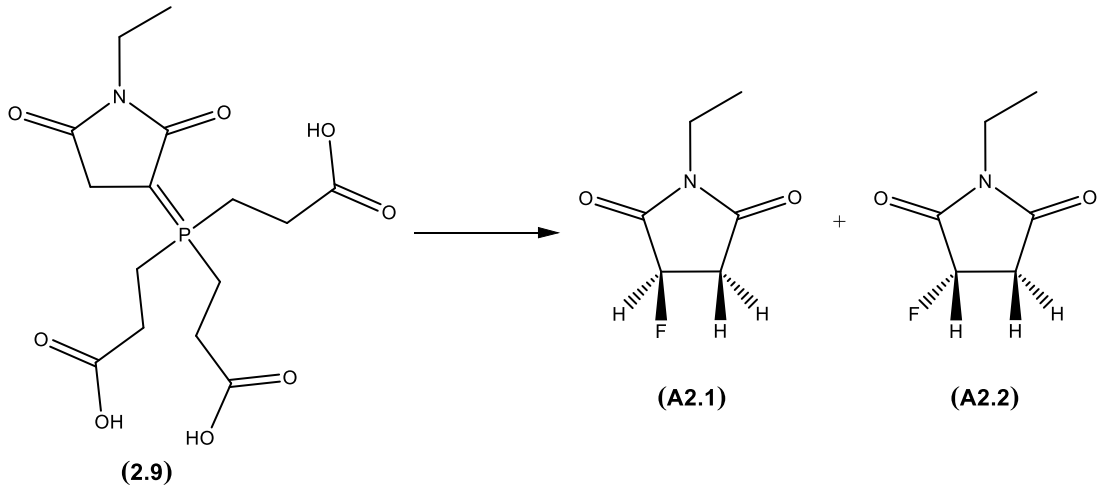

The ylene **2.9** (46 mg, 0.123 mmol) was dissolved in water (3 mL). Selectfluor (5 eq., 217.1 mg, 0.615 mmol) was added and the reaction was stirred at 40 °C for 6 hours. The reaction was extracted with Et_2O (3 x 15 mL). The organic layer was dried ($MgSO_4$), filtered and concentrated. The crude was purified by silica gel chromatography (10 % EtOAc/petroleum ether – 50 % EtOAc/petroleum ether) to yield racemic **A2.1** and **A2.2** as a transparent oil (6mg, 33.7 %). ^{1}H NMR, $CDCl_3$, 500 MHz: δ 5.31 (ddd, 1H, COCF*H*CH_2, *J* = 3.8, 8.1 & 51.5 Hz), 3.62 (q, 2H, NC*H*$_2$$CH_3$, *J* = 7.2 Hz), 3.13 (ddd, 1H, CFHC*H*HCO, *J* = 8.1, 12.4 & 18.6 Hz), 2.87 (ddd, 1H, CFHCH*H*CO, *J* = 3.8, 18.6 & 45.0 Hz), 1.21 (t, 3H, NCH_2C*H*$_3$, *J* = 7.2 Hz). ^{13}C NMR, $CDCl_3$, 125 MHz: 172.2 (d, *J* = 5.3 Hz), 171.90 (d, *J* = 20.1 Hz), 84.36 (d, *J* = 188.7 Hz), 35.91 (d, *J* = 21.6 Hz), 34.11, 12.84. ^{19}F NMR, $CDCl_3$, 470.5 MHz: δ -190.2 (dddd, *J* = 12.2, 26.1 & 52 Hz). Infrared (NaCl disc): 1716.1, 1129.8, 1034.3 cm^{-1}.